ATLAS OF GALAXIES

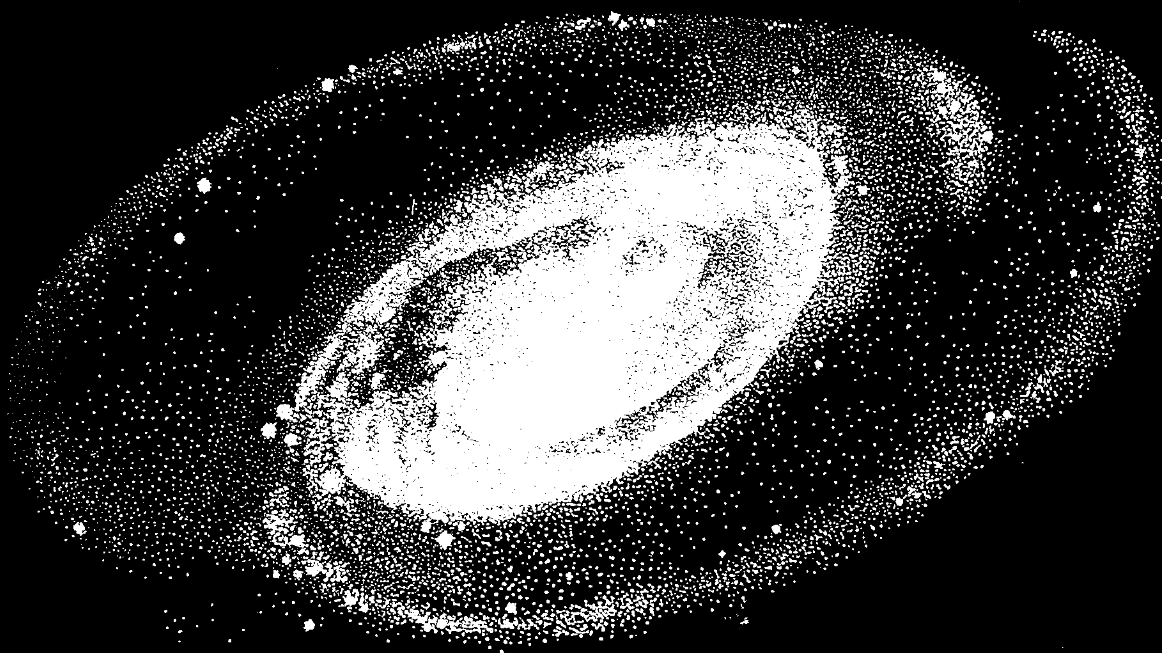

USEFUL FOR MEASURING THE COSMOLOGICAL DISTANCE SCALE

NASA

ATLAS OF GALAXIES

USEFUL FOR MEASURING THE COSMOLOGICAL DISTANCE SCALE

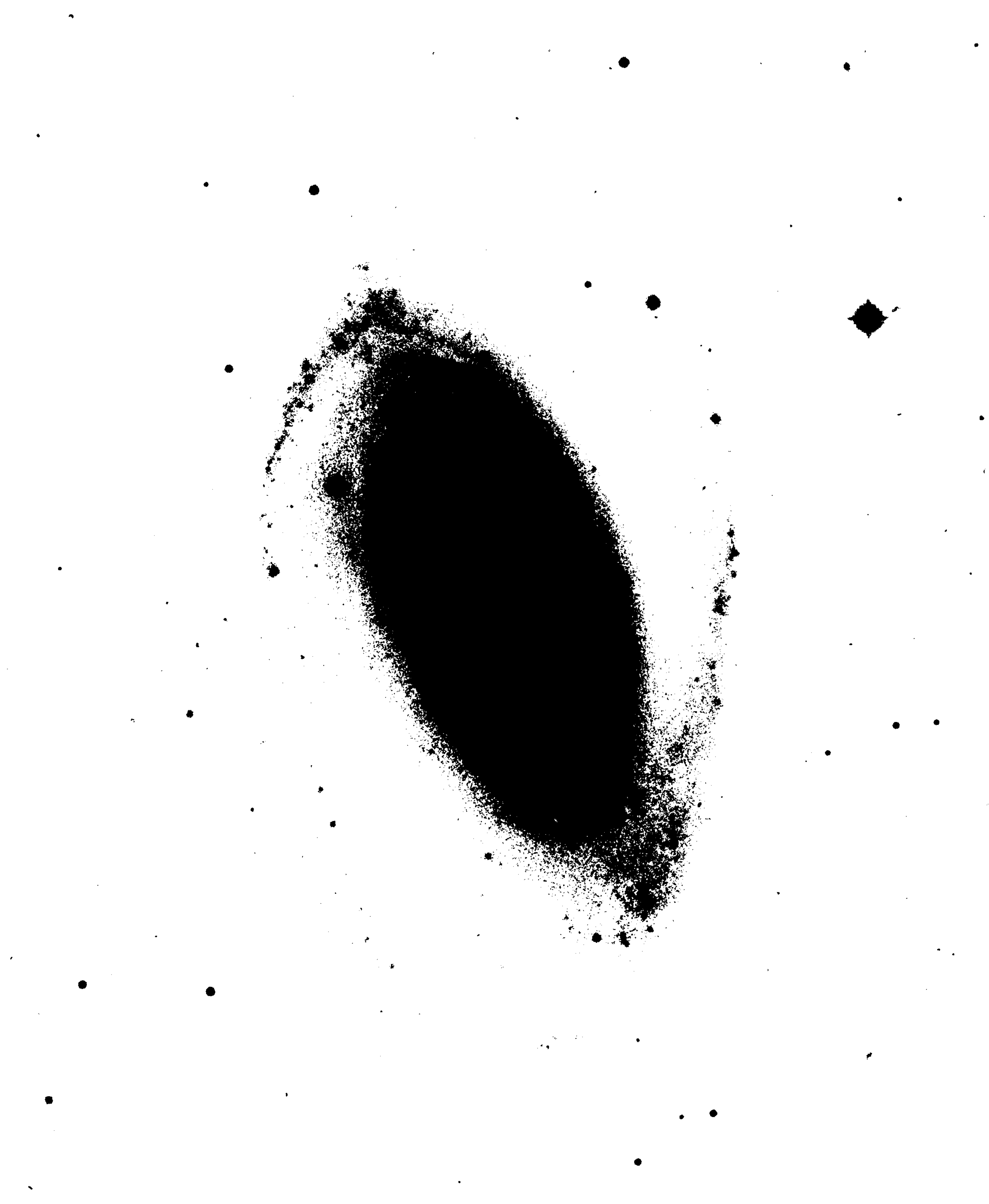

NASA SP-496

ATLAS OF GALAXIES

USEFUL FOR MEASURING THE COSMOLOGICAL DISTANCE SCALE

Allan Sandage

Space Telescope Science Institute
Baltimore, Maryland

and

Department of Physics and Astronomy,
The Johns Hopkins University
Baltimore, Maryland

and

John Bedke

Computer Sciences Corporation
Space Telescope Science Institute
Baltimore, Maryland

NASA Scientific and Technical Information Division 1988
National Aeronautics and Space Administration
Washington, DC

Library of Congress Cataloging-in-Publication Data

Sandage, Allan.
Atlas of galaxies useful for measuring the cosomological distance scale.

(NASA SP ; 496)
Bibliography: p.
1. Cosmological distances—Measurement. 2. Galaxies—Atlases. 3. Hubble Space Telescope.
I. Bedke, John. II. Title. III. Series.
QB991.C66S36 1988 523.1'1 88-600056

For sale by the Superintendent of Documents, U.S. Government Printing Office, Washington, DC 20402

PREFACE

A critical first step in determining distances to galaxies is to measure some property (e.g., size or luminosity) of primary objects such as stars of specific types, H II regions, and supernovae remnants that are resolved out of the general galaxy stellar content. Very few galaxies are suitable for study at such high resolution because of intense disk background light, excessive crowding by contaminating images, internal obscuration due to dust, high inclination angles, or great distance. Nevertheless, these few galaxies with accurately measurable primary distances are required to calibrate secondary distance indicators which have greater range.

If telescope time is to be optimized, it is important to know which galaxies are suitable for specific resolution studies. No atlas of galaxy photographs at a scale adequate for resolution of stellar content exists that is complete for the bright galaxy sample [e.g.; for the Shapley-Ames (1932) list, augmented with listings in the *Second Reference Catalog* (*RC2*) (de Vaucouleurs, de Vaucouleurs, and Corwin, 1977); and the Uppsala Nilson (1973) catalogs]. Before large telescopes became more generally available (~ 1970), knowledge about which galaxies would be adequate candidates for the cosmic distance scale problem rested with only those few observers who had enjoyed continued access to the large reflectors at only a few observatories and who had acquired an encyclopedic knowledge (i.e., Keeler, Curtis, Baade, Hubble, Mayall, Humason, de Vaucouleurs, Vorontsov-Vel'yaminov, and very few others).

With the completion of the Mount Wilson/Palomar/Las Campanas survey of bright galaxies in 1985, excellent large-scale photographs of the complete Shapley-Ames sample were on hand. Most of the galaxies useful for the distance scale calibration are in this collection. The last phases of this particular survey project were sponsored by the National Aeronautics and Space Administration (NASA) when the need became evident to adequately illustrate a large body of the galaxy sample for detailed planning of the targets for the Hubble Space Telescope (HST), particularly for the key project on the distance scale.

In this atlas of photographs of 322 galaxies we have included the majority of all Shapley-Ames bright galaxies, plus cluster members in the Virgo Cluster core, that might be usefully resolved with HST. Because of crowding and high background-disk surface brightness, the choice of field position is crucial for programs involving resolution of particular galaxies into individual stars. The purpose of this atlas is to facilitate this choice. Enough information is given herein (coordinates of the galaxy center and the scale of the photograph) to allow optimum placement of the HST wide-field planetary camera format of ~ 150 arc-seconds on a side.

Most of the photographs herein were obtained between 1949 and 1985. The principal telescopes that we used are the Hale 200-inch reflector of the then Mount Wilson and Palomar Observatories (later the Hale Observatories), and the du Pont 100-inch reflector at the Las Campanas Observatory, Chile. The Hale and the du Pont telescopes have the same focal length, each giving a scale of 11 arc-seconds per millimeter at the normal photographic focal plane. Because of the focal-length equality, each telescope has the same limiting magnitude (in equal seeing conditions) when used in the photographic mode. However, the required exposure for the du Pont 100-inch telescope is of course four times that of the Hale reflector. This limiting magnitude is B ≈ 23.4 for 0.8 arc-second seeing (full width at half maximum) when using photographic detection with 20-μm grain size on Eastman Kodak 103a0-type emulsion (blue).

The photographic reproductions have been made here to emphasize the *outer* spiral regions. These are the most likely targets for Cepheid searches. It should be remembered that the nonlinear nature of the photographic process gives false impressions of intensity ratios. No surface brightness (SB) features that are fainter than SB ~ 23 mag/□″ are probably shown in these reproductions. The apparent edges of the galaxies become visible to the eye at about this SB, which is the SB of the night sky air glow. The Holmberg radius, defined at SB = 26 mag/□″, is ~2.5 times this *visible* disk radius. The *old exponential disk* which underlies the young spiral pattern is the structure that reaches to these very large Holmberg radii. This radius limit will often extend beyond the edges of the photographs shown in this atlas. The point is that there is light at these large radii of which the observer should be aware.

The images obtained with HST will have ~10 times the resolution of these photographs. To assess the crowding problem in galaxies at ~10 times the distance of M33 and, for comparison, at 10 times again the larger distance of M101, we have included the best seeing photographs of M33 and M101 in our collection. These galaxies are shown in Panels 1 and 12. The M33 plate was taken by Francois Schwiezer with the Carnegie 60-inch reflector at Palomar Mountain. The M101 image is from the Baade 200-inch plate illustrated on page 27 of *The Hubble Atlas of Galaxies* [Sandage, 1961].

The ease of detection of Cepheids in the inter-arm region of the outer south-proceeding arm of M33 can be seen from the Cepheid finding chart of M33, Field 25, given in Sandage and Carlson [1983] (Figure 1). The Cepheid chart for M101 is from Cook, Aaronson, and Illingworth [1986]. Comparison of these detailed photographs with Panels 1 and 12 given in this atlas will illustrate what the crowding problem will be like on the HST frames at ~ 10 times the M33 distance and 10 times again the M101 distance, but with 10 times the angular resolution of Panels 1 and 2 (i.e., at ~0.1 arc-seconds). This comparison will thereby show the constraints that should be placed on the chosen target regions for HST.

ACKNOWLEDGMENTS

The final stages of the photographic work were done at the Space Telescope Science Institute (ST ScI) photolab under contract with Computer Sciences Corporation. We are particularly grateful for the technical expertise of Carl Schuetz and Stuart Simpson at ST ScI, whose efforts resulted in the atlas photographs contained herein.

CONTENTS

Atlas of Galaxies Useful for Measuring the Cosmological Distance Scale

The Need for Determining Galaxy Distances

The most central problem in observational cosmology concerns distances to galaxies. Our knowledge of the formation and subsequent development of the Universe depends on the outcome of various tests of cosmological models, each of which depends in some way on knowledge of distances. Several of these tests depend on only *relative* distances. These include the following relations:

- The way the galaxy number-counts increase with redshift z [i.e., the N(z) relation]
- How the angular diameters of "standard" galaxies vary with redshift [i.e., $\theta(z)$]
- A direct measure of the deceleration of the expansion over time, made by using the m(z) relation between the apparent magnitude m and redshift z

Each of these relations depends on the spatial flatness parameter q_0, related to the Riemannian space-time radius of curvature R by

$$\frac{kc^2}{R^2} = H_0^2(2q_0 - 1)$$

where H_0 is the Hubble expansion rate, c is the velocity of light, and k is the sign of the spatial curvature. (k = +1 for a closed curved space, 0 for flat Euclidean space, and -1 for open curved space.) Clearly if $q_0 = 1/2$, then the curvature kc^2/R^2 equals zero, meaning that the space-time is flat. In each of the three tests we attempt to find $N(z, q_0)$, $\theta(z, q_0)$, and $m(z, q_0)$, where the redshift z is the relative wavelength shift in the spectra of the galaxies which mark the space.

However, the most crucial of the tests is a comparison of the several relevant time scales given by the natural processes in the Universe. To determine the expansion-rate time scale, we need *absolute* distances to galaxies. In this test the time given by the inverse Hubble constant, $H_0^{-1} = r/cz$, is compared with independent knowledge of the time since the Creation. Knowledge of this time is obtained either from age dating of the galaxy made by using star clusters, or from nucleochronological ages of the first heavy chemical elements, believed to have been made in the first stars. From this comparison of time scales we can calculate the deceleration of the expansion directly, thereby giving the geometry of space-time from which the spatial curvature is obtained straightaway.

The outcome of the test is fundamental to our understanding of the early stages of creation of matter out of energy through the connection between high-energy particle physics and the astronomical Universe, given by the Grand Unification Theory. The possibility of an experimental solution to the problem depends on the accuracy with which we can measure cosmological distances.

Measurement of the distances to galaxies that are remote enough to define the global Hubble expansion rate is one of the principal reasons for the construction of the Hubble Space Telescope (HST). The increase by a factor of ~10 in the angular resolution over that which can be achieved from the ground and the increased grasp to magnitude V = 26 for isolated stellar objects are the two factors needed to solve the distance scale problem. Resolution into stars of a large number of galaxies is possible with HST.

The only fundamental methods known to measure such distances are based on photometric properties of *distance indicators*. It has taken the larger part of the past half century to identify and calibrate these indicators and to test how accurately each performs as a "standard candle." A measure of the accuracy that can be attained in the distance measurements is the dispersion, $\sigma(M)$, in absolute magnitude M of a particular distance indicator.

Many indicators have been proposed, few have been chosen. Each must be calibrated in an absolute sense. This means that their intrinsic luminosity must be known in say *ergs per second at the source*. If we measure their apparent luminosity (the flux) in *ergs per second per square centimeter at the Earth*, the distance follows directly.

It is this calibration process that divides the indicator groups into primary and secondary methods. Primary indicators are those whose properties are understood well enough to determine if second or third parameters are involved in the physics that fixes their absolute luminosities. Secondary indicators are those that are calibrated through the use of the primary indicators in those galaxies that contain both.

The Primary Distance Indicator

The only primary indicator upon which all astronomers currently agree is the Cepheid class of pulsating variable stars. The absolute luminosities of these stars are determined by the period of pulsation and a second parameter that measures position in the instability strip of the Hertzsprung-Russell diagram. This parameter can either be temperature or amplitude at a given period.

The dispersion of the Cepheid $M(P, T_e)$ relation is believed to be as small as $\sigma(M)|_{P,T_e} \lesssim 0.1$ mag (i.e., ~ ±10% in luminosity) at a given period and temperature, nearly independent of chemical composition. If the *absolute calibration* of $M(P, T_e)$ can indeed be achieved to this same precision, we would have photometric distances accurate to $\delta r/r \sim \pm 5\%$ to any given galaxy, assuming the apparent brightness, the periods, and the temperatures of its Cepheids can be measured well enough.

The brightest Cepheids are known to reach $\langle M_v \rangle \sim -7$ at mean light or $M_v \sim -6.5$ at minimum light [Sandage and Tammann, 1968 (Figures 1 and 5); 1969 (Figures 4 and 5)]. The discovery of Cepheids in galaxies for which resolution to apparent magnitude V = 25 can be achieved (i.e., in very low disk surface-brightness regions with small crowding) would permit distances to be determined to moduli of m - M ≈ 25 + 6.5 = 31.5 if we require the Cepheids to not disappear below the detection at any part of their pulsation cycles. From log r = 0.2 (m - M + 5), this modulus corresponds to a distance of ~20 Mpc, which is a distance range, at best, to only the Virgo Cluster core (assumed to be at m - M = 31.7). This distance is not nearly far enough to carry the distance scale into the unperturbed expansion field necessary to find the *global* value of H_0. Therefore, secondary indicators with larger distance grasps must be used to carry the scale outward. *These secondary indicators, however, must first be calibrated by using Cepheids in galaxies that are close enough to contain well-observed Cepheids.* As just mentioned, such galaxies must have distance moduli smaller than m - M ≈ 31.5. This distance corresponds to recession velocities smaller than ~1200 km/s.

Secondary Distance Indicators

Brightest Stars

The most promising of the *secondary* distance indicators are the brightest resolved red and blue supergiants in galaxies more massive than M33 (NGC 598). It is believed that the brightest *blue* stars in galaxies such as M33, NGC 2403, M81, and M101 are in a critical physical state in which the radiation pressure on their photospheres nearly balances the gravitational pressure (force per unit area): they are at their Eddington limit, brighter than which they cannot exist because radiation pressure would levitate their atmospheres. Because such stars can be readily identified (being blue irregular variables), and because they appear to form a well-defined upper luminosity that is independent of the size of the parent galaxy (provided that the parent is brighter than $M_B \approx -19$) [Sandage and Carlson, 1985 (Figures 8 and 9)], they are candidates for secondary standard candles. Their absolute blue magnitudes—based on the Cepheid distances to the four calibrating galaxies M33, NGC 2403, M81, and M101—are $M_B = -10.0 \pm 0.1\sigma$. Such stars can probably be detected only to B = 24 apparent magnitude, due to crowding by neighboring stars in the associations. The distance range over which they should be discoverable is then m - M = 34 or r = 60 Mpc, which is 3 times the Cepheid range.

The brightest *red* supergiants (RSG) are also potential candidates for good secondary indicators, although their physics is not understood as well as the Eddington-limited blue main sequence stars. These red stars have moved on evolutionary tracks in the Hertzsprung-Russell diagram from the bright blue main sequence into the red supergiant region. However, it is not clear that there is a critical physical phenomenon that limits their maximum luminosity, as appears to be the case with the *blue* stars. The empirical facts suggest that M_v (max) for the RSG becomes brighter as the mass of the parent galaxy increases. The reason for the correction would, of course, be statistical because the luminosity distribution would not have a sharp upper bound cutoff due to a critical physical process. Without such a process, stochastic sampling problems will exist causing σ(M) to be large and variable [Greggio, 1986].

Nevertheless, the absolute yellow luminosities are so bright at $M_v \approx -8.8$ for M101, decreasing to $M_v \approx -8.0$ for M33 and NGC 2403, that the brightest RSG *can* be resolved to a distance modulus of m - M = 34 in those favorable circumstances where V = 26 can be measured. This distance limit again is ~3 times more remote than the Virgo Cluster core.

A major problem remains. The calibration of $\langle M_B \rangle$ for the brightest blue stars and $\langle M_V \rangle$ for the brightest RSG must be strengthened. In this regard, the dependence of M_{max}(stars) on M(parent galaxy) must be understood for a large sample of galaxies, especially the more massive ones for which the stochastic sampling problems will be minimal.

The distance limit from the ground has been reached in M101 at m - M = 29.3. This ground-based barrier is likely to remain because there are no spiral galaxies brighter than $M_B \approx -20$ closer than m - M = 29.3 that have not already been used for the Cepheid-brightest star calibration. To increase the number of calibrators to an adequate statistical level (some 30 galaxies intrinsically brighter than M33) requires using HST to observe those giant spiral galaxies brighter than $M_{B_T} \approx -20$ beyond the M101 distance for which Cepheid distances can be measured. *Identification of the candidate galaxies is the purpose of this atlas.*

Novae and Supernovae

The brightest *normal novae* reach $M_B = -10.0$ at maximum, but there is a large variation in M_B (max) with the nova decay rate [Arp, 1956; Schmidt, 1957; McLaughlin, 1960; Rosino, 1964; van den Bergh, 1975; and Cohen and Rosenthal, 1983]. This variation makes conventional use of novae prohibitively expensive in telescope time; the decay time must be accurately measured, requiring a dedicated use of the telescope, which is impossible with HST. However, normal novae remain bright in *monochromatic Hα light* [Ford and Ciardullo, 1987] for weeks rather than days. This feature again makes novae prime candidates for secondary indicators, but the absolute Hα luminosities again must be calibrated by using galaxies of known distance, determined from the primary Cepheid indicator.

Supernovae of type Ia are believed to be excellent standard candles, powered by a phenomenon that may have precise criticality (i.e., a physical process that has a guillotine feature such as the nudging of a carbon-oxygen white dwarf over its Chandrasekhar mass limit by mass transfer from a companion). If so, supernovae may have a very small dispersion in M(max). A review of these possibilities from many viewpoints is provided in a work edited by Bartel [1985]. Distances to galaxies which have well-observed type Ia supernovae will give an empirical calibration of M_B (max) [Sandage and Tammann, 1982]. For the distance scale program to be carried forward, we must be able to identify those galaxies that are suitable for Cepheid detection. Some galaxies that *have* produced historical supernovae of type Ia are illustrated in the atlas.

ScI Galaxies as Secondary Standard Candles

Van den Bergh [1960a,b] discovered that galaxies of Hubble types Sb and Sc with well-developed arm patterns are more luminous than those with more chaotic arms. This discovery suggested that the luminosity functions of these galaxy types are narrow. Such galaxies could then be used as standard candles. The dispersion in M was indeed shown to be moderately small, from the studies of the apparent magnitude distributions in the Virgo Cluster core [Sandage, Binggeli, and Tammann, 1985] and in the general field [Sandage and Tammann, 1975].

These results confirmed an early conclusion of Hubble [1936] that $\sigma(M) = 0.8$ for high surface brightness spirals. The modern data indicate $\sigma(M) = 0.72$ mag for ScI galaxies [Sandage, 1988], a value which, although large, is small compared with the range of ~12 magnitudes for galaxies of all Hubble types. This large range was suggested by Zwicky [1957], who felt, as a result, that galaxies could not be used as distance indicators.

The difference between the conclusions of Zwicky and of Hubble concerning the use of galaxies as standard candles rests with the different categories of surface brightness among the galaxies studied by each. The galaxy types in each of their samples hardly overlap. Studies of the content of the Virgo Cluster [Sandage, Binggeli, and Tammann, 1985] showed that galaxies with high surface brightness (SB) of a given Hubble type have a luminosity function that is bounded at both the bright and the faint end. Those of low SB do not. Hubble's program was confined almost entirely to high SB systems.

Because ScI galaxies occur nearly everywhere in the general field and because they can be identified at very large distances (velocities ~10,000 km/s; $\bar{r}$ ~200 Mpc) on existing all-sky survey photographs (Palomar Observatory Sky Survey, European Southern Observatory Survey, and Scientific Research Council Survey), they are very powerful markers of the space. This distance, which is ~10 times further than the Virgo Cluster core, reaches well into the global expansion field, making ScI spirals of potentially great use in directly measuring the Hubble constant. Furthermore, many other cosmological parameters can be determined by using ScI spirals, such as the mean mass density found from the velocity perturbations about the global Hubble flow, the galaxy clustering scales, the presence of sheets and voids in the field galaxy distribution, and a measurement of biasing properties in galaxy samples cut at different flux levels.

To solve any of these problems, it is necessary to know the mean absolute magnitude $\langle M \rangle_{ScI}$ for a *volume-limited sample* of such galaxies and to know the dispersion σ(M) of the magnitude distribution of such a sample. Knowledge of σ(M) is central to the problem of correcting for observational bias. The mean absolute magnitude of any given sample that has been selected on the basis of flux limitation (i.e., to a given apparent magnitude) is different than for a sample selected to be distance limited. This bias ultimately determines the *systematic* error made in any measurement of the Hubble constant. *No amount of observational data obtained with HST will produce a correct value of H_0 unless the bias properties of the samples are understood and controlled.*

However, *if* $\langle M \rangle_{ScI}$ *were* known to ±0.2 mag accuracy for ScI galaxies in a strictly volume-limited sample, the Hubble constant could be determined to within ±10% by using known data on ScI's in the general field [Sandage, 1988]. The current calibration of $\langle M \rangle_{ScI}$ rests only on the Cepheid distances to M31, M81, and M101 (the two SbI-II galaxies being reduced to the magnitude system of the ScI's). These three calibrations do indeed form the beginning of a distance-limited sample, but they constrain the calibration only to a range of ~0.5 mag around the value $\langle M_B \rangle = -21.5 \pm 0.5\sigma$. *To improve the calibration, we need to know Cepheid distances to many well-resolved ScI galaxies. These must be chosen to form a distance-limited sample or must be correctable to such a sample from properties of the known selection criteria.* Candidates for such a list are provided in this atlas.

Rotational Velocity/Luminosity Relation

A variation of the method of distance determination invented by Öpik [1922] was developed by Tully and Fisher [1977]. The complex relation has begun to be understood over the multiple-parameter space that consists of rotational velocity (v), Hubble type (T), B-H colors, surface brightness (SB), and van den Bergh luminosity class (L). Each of these variables contributes scatter at some level to the correlation between M and v, T, SB, and L.

The absolute luminosity calibration again must be made by using galaxies whose primary distances *are already known from Cepheids*. The relation using near infrared H magnitudes currently rests on only M33, M31, NGC 2403, and M81. To increase the calibration weight and to study the intrinsic dispersion of the Tully-Fisher relation, we shall need to measure Cepheid or brightest star distances for a much larger sample of spiral galaxies in distance-limited samples than are now available from ground-based observations.

Use of the Öpik/Tully-Fisher method requires moderate inclinations of the galaxy disks to the line of sight so as to measure the maximum rotational velocities with adequate precision. The calibrating galaxies must not only be close enough to have detectable Cepheids but must have major-to-minor axial ratios of $a/b \gtrsim 1.2$ corresponding to inclination angles of greater than $\sim 35°$ (90° being edge-on).

Therefore, the calibration program calls again for an extension of the Cepheid base to a number of nearby galaxies more remote than can be studied from the ground but close enough to be within the HST capability. This Cepheid-calibrating sample must be either distance limited or properly chosen to be so corrected.

Summary of Distance Indicators

The primary indicator is the Cepheid class of variables. The secondary indicators are listed in Table 1 in the order of their $\langle M(\max)\rangle$ values. These values are uncertain enough that each needs a broad new data base of calibrating spiral galaxies to find adequately precise $\langle M\rangle$ and $\sigma(M)$ values.

The primary Cepheid indicator has a maximum magnitude of only $\langle M_B\rangle \sim -6$. This means that the calibrating galaxies, if they are to reach sufficiently large distances for the HST Hubble constant program, must meet a highly restricted set of criteria.

Selection Criteria

Resolution Limits and Stellar Crowding

The most distant galaxy in which Cepheids have been detected is M101 [Cook, Aaronson, and Illingworth, 1986]. The Cepheid distance is between the two conclusions: $m - M = 29.3$ [Sandage and Tammann, 1974] and $m - M = 29.0$ to 29.5 [Cook, Aaronson, and Illingworth, 1986]. As mentioned previously, the resolution obtained on the ground into individual brightest stars, H II regions, supernovae, and Cepheids is barely adequate in M101. At greater distances, crowding becomes serious due to lack of sufficient resolution.

Ground-based observations have typical best seeing images of ~1 arc-second, full width, half maximum (FWHM). Very few major long-range programs have attained *average* image sizes of even 0.8 arc-seconds for the bulk of their data bases.

At the distance of 7 Mpc ($m - M = 29.3$) for M101, 1 arc-second corresponds to a linear scale of 34 parsecs. The effective crowding over this scale can be estimated by inspecting high-resolution photographs of stellar associations in M33. The distance to M33 of $r \approx 0.87$ Mpc ($m - M = 24.7$) is eight times smaller than for M101. Hence, HST will give M33-like resolution at M101, and M101-like resolution at ~10 times the M101 distance, or $m - M \approx 34$. At M33 a linear scale of 34 parsecs subtends 8 arc-seconds. The level of contamination expected in M101 over a 34-parsec circle is seen by considering the effect of passing a smearing function with an 8 arc-second diameter over the photograph of M33 shown in Plate 1 of this atlas. The scale of this print is ~6 arc-seconds per millimeter. Therefore, at the distance of M101, 1 arc-second resolution is equivalent to a blur circle of 1.3 mm on this print.

Large-scale images of the association regions of M33 are shown in Humphreys and Sandage [1980] (Figures 29 and 30). Passing an 8 arc-second filter over these photographs shows that most of the brightest stars can just adequately be resolved at 8 arc-second resolution in most of the M33 associations. In particular, the three *brightest blue supergiants* (4-A, B324, and 116-B in the associations 4, 67, and 116) and the three *brightest red stars* (R254, R352, and R110) shown in the charts of Humphreys and Sandage are not severely contaminated by stars within ~2 mag of their brightness, and hence can generally be measured. Detection and measurements of selected *Cepheids* will be *more* adequate than measurements of the brightest stars, as seen by passing an 8 arc-second filter over the M33 Cepheid identification chart given by Sandage and Carlson [1983] (Figure 1). Because *all* Cepheids need not be used (only those that are uncrowded) but because *the* brightest star *must* be used to calibrate the brightest star indicator, the Cepheid program of the HST project is more reliable at this resolution than the brightest star calibration. Hence, use of the brightest star indicator must be made at higher resolution than the equivalent 8 arc-seconds at M33. At twice this resolution we can only sample ~5 times the M101 distance, or $m - M \approx 32.5$, which is ~1.5 times beyond the distance of the Virgo Cluster. This distance is slightly more than the effective range for the Cepheid detection, according to considerations of limiting magnitude previously discussed.

Limiting Magnitude

HST is expected to detect stars at $V = 26$ magnitude with a ~6% accuracy in ~1000-second exposure time. Fainter stars can be measured in correspondingly longer exposure times and/or with lower accuracy.

These numbers are for isolated point sources not embedded in background. However, stars in galaxies are generally superposed on a bright galactic disk and also often occur in confused regions containing many other stars and H II nebulosities in the young associations. The brighter is the disk contamination, the brighter will be the limit for detection of resolved stars. It is for this reason that we have used $V = 25$ for the Cepheid detection limit in previous sections.

The average disk surface-brightness of galaxies changes progressively along the Hubble sequence [Sandage 1982] (Figures 1 and 2) but with a large dispersion in surface brightness even within a given Hubble type. Galaxies with very bright disk contamination are obviously poor candidates for studies of the individual brightest stars.

Our principal criterion for the choice of galaxies to be illustrated in this atlas has been low surface brightness (as is present in many Scd, Sd, Sm, and Im types) for at least some parts of the galaxy. Further, the spiral arms should present only minimal confusion and crowding problems.

The limiting magnitude will be severely degraded in high-background fields. Only in the lowest SB regions can $V = 26$ mag be achieved. It is crucial, therefore, to choose disk regions of the candidate galaxies that have the lowest possible background. Using the *optimistic* case of $V = 26$, the distance that can be reached in the Cepheid campaign will be determined by M_V of the Cepheids at maximum light. If we require complete light curves, the limit is more stringent because the Cepheids must be brighter at their mean luminosity if they are to be observed at minimum light. The very brightest Cepheid absolute magnitude for the longest period variables is $M_v = -7.0$ [Sandage and Tammann, 1968] (Figures 1 and 5), giving a maximum distance modulus for the Cepheid candidate galaxies to be $m - M = 33$. As previously stated the more realistic expectation is, however, $V \approx 25$, $\langle M_v\rangle = -6.5$, giving at most a Cepheid range of $m - M \approx 31.5$.

Summary of Selection Criteria for the Program Galaxies

With these factors of resolution and limiting magnitude in mind, we have made a selection of candidate galaxies that should be useful in resolution studies with HST. There are three criteria:

- Low disk surface-brightness, either over most of the galaxy or over those parts where well-separated, sparse, spiral arms exist.
- Spiral arms whose associations are expected to resolve into individual stars with an effective crowding no worse than associations in M33 at ~4 arc-second resolution for brightest stars or ~8 arc-second resolution for Cepheids, appropriately scaled at increased distance to the resolution of ~0.1 arc-second of HST.

- This resolution requirement together with the apparent magnitude grasp of HST sets an upper (very liberal) distance limit of ~40 M_{pc} (m - M = 33), which translates to an unperturbed expansion redshift of ~2000 km/s.

Source of the Candidate List

Field Candidates

Photographic surveys of galaxies made by using long focal length telescopes were begun early in this century by Curtis with the Lick Observatory's 36-inch Crossely reflector and by Ritchey and Pease, using the Mount Wilson 60-inch reflector. Hubble's major Northern Hemisphere Survey made with the 100-inch Hooker reflector from 1920 to 1942 was transferred to the Palomar 200-inch Hale reflector in the 1950's by one of us (A.S.) and was completed there early in the 1980's. From 1977 to 1984, the southern survey of bright Shapley-Ames galaxies was completed with the Las Campanas 2.5-meter du Pont reflector.

Data from these complete surveys were essential before an adequately complete list of candidates could be compiled for the HST distance scale program. The small scale of the Palomar Observatory Sky Survey (POSS), European Southern Observatory (ESO), and Scientific Research Council (SRC) Schmidt all-sky plates is simply inadequate to select galaxies that satisfy the selection criteria previously described.

Our method of final selection of the Shapley-Ames [1932] galaxies that meet the three criteria was as follows. As part of the preparation to produce a more complete version of *The Hubble Atlas of Galaxies* [Sandage, 1961], in which most of the 1246 Shapley-Ames galaxies are to be illustrated, we have produced a working atlas of negative paper prints from the original plates. These have been sorted into the morphological classification bins of *A Revised Shapley-Ames Catalog of Bright Galaxies* [Sandage and Tammann, 1987] permitting easy visual comparison of all galaxies within a given Hubble type. In this way, the three criteria previously discussed could be applied by inspecting the prints and by flagging all galaxies of Hubble types Sb and later that appear to be good candidates for the HST program.

The total sample was then divided into two groups according to the degree of resolution. This approach naturally divided the sample into a near and a distant class. Many of the galaxies in the nearby group can be resolved into brightest stars from the ground and, with greater effort, by using ground-based techniques that reach B ≈ 25, resolved even into Cepheids. These galaxies should provide an excellent control on the problems of finite resolution because *comparison of results* from the HST photometry on these particular galaxies with data from ground-based measurements on the same galaxies will test the contamination directly—clearly a crucial test. A separate list of these galaxies to be observed in this way is given later, in Table 3.

The easy and the difficult galaxy groups have been separated here, being Part II and Part III of the present atlas. These panels have been published in small format as separate papers by Sandage and Bedke [1985a,b], to which reference can be made for greater explanatory detail. We reproduce these panels here in large format, renumbered and listed in Table 2 in order of NGC numbers. The listings in the *Astronomical Journal* papers are ordered by *Hubble type*. Comparison of the two listing orders, one by name and one by type, should be convenient when cross reference is made to each table.

Columns of Table 2 that require comment are as follows:

- Column 2 — Lists the atlas page number.
- Column 3 — Galaxy types from Sandage and Tammann [1987].
- Column 4 — The axial ratio a/b, useful in choosing candidate galaxies for the Öpik/Tully-Fisher calibration.
- Column 7 — The galactic latitude.
- Column 8 — The radial velocity, v_0, relative to the centroid of the Local Group, taken from column 20 of Sandage and Tammann [1987].
- Column 9 — The kinematic distance in units of the Virgo Cluster distance, after correcting for the idealized Virgocentric flow model of Kraan-Korteweg [1986].
- Column 10 — The velocity correction to be applied to v_0 for Virgocentric infall to obtain an approximation of the free expansion velocity in a Virgocentric frame [see Tammann and Sandage, 1985 for this concept], corrected for Virgo deceleration. If such a frame *were* freely expanding, albeit falling in bulk toward Hydra-Centaurus [Tammann and Sandage, 1985], $v_0 + v_g$ *would* approximate the *global* cosmological expansion rate.

It need only be emphasized that the testing of columns 9 and 10 by using *nonkinematic* distances to measure the velocity perturbations from a pure Hubble cosmological flow is one of the goals of the HST distance program. The data in columns 9 and 10 are only listed for convenience in designing an optimum program to measure the velocity perturbations induced by the local Virgo complex. Such a program would use galaxies in directions where the v_g values have maximum and minimum values, as outlined by Kraan-Korteweg [1984, 1986] and discussed in the papers that accompany the small-format edition of this atlas in Sandage and Bedke [1985 a,b].

Overlap Candidates for Ground-Based and for Parallel HST Observations

Galaxies which can be usefully resolved from the ground *and* with HST are listed in Table 3. As previously noted, parallel observations of this list will be crucial in measuring the contamination effects of finite resolution so as to interpret HST observations that are to be made in the more distant galaxies.

Virgo Cluster Members

Knowledge of the distance to the Virgo Cluster core would be an important step in establishing the global value of the Hubble constant. Because of possible local perturbations in the velocity field out to ~2 times the Virgo Cluster distance, galaxies in this distance range cannot be used directly to determine H_0 but rather can serve as the step to the Coma cluster 6 times more distant—well beyond the local velocity perturbation.

The step is made [Tammann and Sandage, 1985; Tammann, 1987; Dressler, 1987] by using relative distance measurements that give the distance *ratio* of Coma to Virgo. The absolute distance to Virgo then gives the absolute distance to Coma, after which the Hubble constant follows straightaway *from the Coma velocity-distance ratio itself, independent of the Virgo Cluster velocity*. The perturbation due to infall toward Hydra-Centaurus is less than 6%.

The capability of HST to find Cepheids in galaxies in the Virgo core is near its instrumental limit. As described in previous sections, Cepheids for which $\langle M_v \rangle \sim -6.5$ that are observed at V = 25 would reach distance moduli of m - M = 31.5. This reach is within the known range of m - M values between 30.8 and 32 that encompasses most of the literature moduli for the Virgo core, set out since the 1970's by most observers.

Brightest stars are expected to be easily resolved in the most luminous Virgo galaxies, but use of this secondary indicator is less desirable than a direct measurement using Cepheids. In any case, as these observations will be made near the telescope limit, care must be taken to use the correct values of $\langle M \rangle$ for the Cepheid and brightest star indicators so that the m - M value will be unbiased. Being near the telescope limit, the Cepheid and the chosen stars *will* originate from a flux-limited sample; hence, their $\langle M \rangle$ values *will* lie toward the upper envelope of their absolute luminosity distributions. The error caused by this situation will always give too small a distance if no bias corrections are applied. This error always propagates through the analysis to give too large a value of H_0. It is on this point that the analysis of the HST data will be most crucial. As emphasized earlier, *the power of the HST itself will not insure that a reliable value of H_0 will be found unless the selection biases of the distance indicators are accounted for.*

The best candidate galaxies for resolution in the Virgo Cluster core have been chosen from the large-scale du Pont plates made for the Virgo Cluster survey [Sandage, Binggeli, and Tammann, 1984]. A 75-galaxy candidate list in the 6° (radius) cluster core is set out in Table 4, illustrated in the final 8 panels in Part IV of the atlas.

Table 1
Properties of the Distance Indicators

Indicator	$\langle M_B \rangle$ max	$\sigma(M)$
Primary Indicator		
(1) Cepheids	-6.0	$\pm 0^m1$
Secondary Indicators		
(1) Brightest blue variables	-10.0	±0.3?
(2) Brightest red supergiants (M_V)	-8.0 to -9.0	±0.5?
(3) Normal novae	-10.0 to -7.0	±0.5?
(4) Supernovae Ia	-20.0	$\lesssim$0.3?
(5) ScI galaxies	-21.7	±0.7
(6) Öpik-TF method	-22 to -18	±0.7?

Table 2
The Atlas Field Galaxies

Name (1)	Atlas Panel (2)	Type (3)	a/b (4)	α_{50} (5)	δ_{50} (6)	b (7)	v_0 (8) km s^{-1}	x (9)	v_g (10) km s^{-1}
NGC 24	45	Sc(s)II-III	3.39	00 07 24	-25 14.6	-80.4	621	0.48	-49
NGC 45	17, 55	Scd(s)III	1.41	00 11 32	-23 27.6	-80.7	533	0.41	-45
NGC 55	45	Sc	5.01	00 12 24	-39 28.0	-75.7	115	0.09	-5
NGC 151	68	SBbc(rs)II	1.95	00 31 30	-09 58.9	-72.1	3871	3.13	-155
NGC 210	60	Sb(rs)I	1.45	00 38 04	-14 08.8	-76.5	1875	1.48	-114
NGC 247	5, 45	Sc(s)III-IV	2.69	00 44 40	-21 02.0	-83.6	227	0.17	-24
NGC 255	85	SBc(rs)II-III	1.12	00 45 16	-11 44.5	-74.3	1726	1.36	-109
NGC 289	68	SBbc(rs)I-II	1.38	00 50 17	-31 28.7	-85.9	1834	1.46	-100
NGC 300	3, 45	Sc(s)II.8	1.35	00 52 31	-37 57.4	-79.4	128	0.10	-6
NGC 428	73	Sc(s)III	1.26	01 10 23	00 42.9	-61.4	1311	1.03	-83
NGC 450	73	Sc(s)II.3	1.23	01 12 57	-01 07.6	-63.1	1911	1.52	-108
NGC 514	73	Sc(s)II	1.20	01 21 25	12 39.5	-49.2	2675	2.16	-111
NGC 578	73	Sc(s)II	1.51	01 28 05	-22 55.5	-80.1	1675	1.33	-98
NGC 598	1	Sc(s)II-III	1.58	01 31 03	30 23.9	-31.3	69	0.06	0
NGC 628	26, 45	Sc(s)I	1.07	01 34 01	15 31.6	-45.7	861	0.69	-42
NGC 672	21, 51	SBc(s)III	2.45	01 45 05	27 11.1	-33.8	647	0.54	-9
NGC 685	85	SBc(rs)II	1.02	01 45 49	-53 00.6	-62.3	1306	1.07	-35
NGC 753	73	Sc(s)I-II	1.35	01 54 46	35 40.3	-25.0	5145	4.26	-91
NGC 864	65	Sbc(r)II-III	1.29	02 12 50	05 46.2	-51.1	1707	1.37	-77
NGC 895	73	Sc(s)II.2	1.32	02 19 06	-05 45.0	-59.6	2383	1.92	-104
NGC 925	24, 51	SBc(s)II-III	1.62	02 24 18	33 21.1	-25.2	792	0.67	+8
NGC 941	86	Scd III	1.32	02 25 55	-01 22.5	-55.1	1717	1.38	-78
NGC 991	74	Sc(rs)II	1.07	02 33 03	-07 22.0	-58.2	1607	1.29	-72
NGC 1042	74	Sc(rs)I-II	1.20	02 37 56	-08 38.8	-58.2	1436	1.15	-68
NGC 1058	74	Sc(s)II-III	1.05	02 40 23	37 07.8	-20.4	746	0.65	21
NGC 1073	85	SBc(rs)II	1.07	02 41 05	01 09.9	-50.7	1318	1.07	-53
NGC 1087	74	Sc(s)III.3	1.48	02 43 52	-00 42.5	-51.6	1628	1.32	-64
NGC 1156	57	Sm IV	1.32	02 56 47	25 02.4	-29.2	558	0.48	+11
NGC 1179	85	SBc(r)II.2	1.17	03 00 21	-19 05.6	-58.8	1776	1.44	-66
NGC 1187	65	Sbc(s)II	1.23	03 00 24	-23 03.8	-60.1	1424	1.15	-55
NGC 1232	36, 74	Sc(rs)I	1.12	03 07 30	-20 46.2	-57.8	1775	1.44	-62
NGC 1249	51	SBc(s)II	1.95	03 08 35	-53 31.4	-53.4	887	0.74	-1
NGC 1288	60	Sb(r)I-II	1.07	03 15 12	-32 45.3	-58.1	4461	3.67	-104
NGC 1313	7, 51	SBc(s)III-IV	1.29	03 17 39	-66 40.7	-44.6	261	0.24	21
NGC 1337	74	Sc(s)I-II	3.31	03 25 40	-08 33.7	-48.5	1270	1.04	-32

Table 2 (Continued)

Name (1)	Atlas Panel (2)	Type (3)	a/b (4)	α_{50} (5)	δ_{50} (6)	b (7)	v_0 (8) km s^{-1}	x (9)	v_g (10) km s^{-1}
NGC 1350	Frontispiece	Sa(r)	1.78	03 29 10	-33 47.9	-55.2	1486	1.22	-34
NGC 1359	75	Sc(s)II-III	1.17	03 31 33	-19 39.5	-52.1	1972	1.62	-54
NGC 1365	42	SBbc(s)I	1.78	03 31 42	-36 18.3	-54.6	1562	1.23	-32
NGC 1425	60	Sb(r)II	2.00	03 40 10	-30 03.3	-52.6	1440	1.19	-29
NGC 1433	41	SBb(s)I-II	1.12	03 40 27	-47 22.8	-51.2	923	0.78	4
NGC 1448	75	Sc(s)II	4.47	03 42 54	-44 48.1	-51.5	1038	0.87	-3
NGC 1493	85	SBc(rs)III	1.12	03 55 54	-46 21.2	-48.9	910	0.77	7
NGC 1494	87	Scd(s)II	1.45	03 56 15	-49 03.0	-48.2	957	0.81	9
NGC 1512	41	SBb(rs)I pec	1.26	04 02 16	-43 29.2	-48.2	760	0.65	12
NGC 1518	46	Sc III	2.19	04 04 38	-21 18.7	-45.3	914	0.77	1
NGC 1532	30, 65	Sbc(s) (tides?)	3.09	04 10 09	-33 00.0	-46.6	1105	0.89	2
NGC 1566	33, 43	Sbc(s)I.2	1.23	04 18 53	-55 03.4	-43.4	1305	1.11	18
NGC 1569	58	Sm IV	1.95	04 26 05	64 44.4	11.2	144	0.15	32
NGC 1637	51	SBc(s)II.3	1.15	04 38 58	-02 57.1	-30.0	715	0.63	31
NGC 1672	39	Sb(rs)II	1.23	04 44 58	-59 19.6	-39.0	1130	0.98	37
NGC 1744	54	SBcd(s)II-III	1.66	04 57 56	-26 05.8	-35.0	639	0.57	37
NGC 1784	68	SBbc(r)II	1.48	05 03 07	-11 56.4	-28.8	2254	1.91	9
NGC 2090	46	Sc(s)II	1.91	05 45 15	-34 16.4	-27.4	755	0.69	65
NGC 2188	87	Scd III	3.24	06 08 21	-34 05.7	-22.8	555	0.53	72
NGC 2217	34	RSBa(s)	1.09	06 19 41	-27 12.5	-18.3	1434	1.28	90
NGC 2223	68	SBbc(r)I.3	1.12	06 22 31	-22 48.7	-15.8	2529	2.19	72
NGC 2280	75	Sc(s)I.2	1.74	06 42 50	-27 35.2	-13.6	1709	1.53	103
NGC 2336	69	SBbc(r)I	1.74	07 18 28	80 16.6	28.2	2424	2.18	165
NGC 2366	15, 59	SBm IV-V	2.14	07 23 37	69 19.1	28.5	281	0.25	53
NGC 2403	9, 46	Sc(s)III	1.62	07 32 03	65 42.7	29.2	299	0.25	53
NGC 2500	47	Sc(s)II.8	1.07	07 58 08	50 52.6	31.6	615	0.64	146
NGC 2541	46	Sc(s)III	1.86	08 11 02	49 13.0	33.5	646	0.68	155
NGC 2552	56	Sd(s)III	1.45	08 15 42	50 10.1	34.3	607	0.64	147
NGC 2713	65	Sbc(s)I	2.24	08 54 44	03 06.8	29.2	3690	3.30	226
NGC 2763	75	Sc(r)II	1.10	09 04 29	-15 17.9	20.8	1658	1.61	256
NGC 2776	75	Sc(rs)I	1.07	09 08 56	45 09.6	43.2	2673	2.46	247
NGC 2835	52	SBc(rs)I.2	1.45	09 15 37	-22 08.8	18.5	624	0.65	151
NGC 2841	60	Sb	2.14	09 18 35	51 11.3	44.2	714	0.75	179
NGC 2848	76	Sc(s)II	1.51	09 17 49	-16 18.8	22.7	1795	1.73	263
NGC 2903	47	Sc(s)I-II	1.91	09 29 20	21 43.2	44.5	472	0.45	62
NGC 2935	62	SBb(s)I.2	1.20	09 34 27	-20 54.2	22.6	2003	1.91	264
NGC 2942	76	Sc(s)I.3	1.23	09 36 08	34 14.0	48.4	4399	3.91	236
NGC 2967	76	Sc(rs)I-II	1.51	09 39 29	00 33.9	37.3	2065	1.38	341
NGC 2997	25, 47	Sc(s)I.3	1.26	09 43 27	-30 57.7	16.8	799	0.84	196
NGC 3001	69	SBbc(s)I-II	1.45	09 44 07	-30 12.4	17.4	2171	2.03	241
NGC 3031	16, 39	Sb(r)I-II	1.82	09 51 30	69 18.3	40.9	124	0.24	45
NGC 3041	76	Sc(s)II	1.51	09 50 23	16 54.8	47.6	1296	1.38	341
NGC 3054	69	SBbc(s)I	1.51	09 52 12	-25 28.0	22.1	1923	1.85	268
NGC 3055	76	Sc(s)II	1.58	09 52 41	04 30.4	42.2	1747	1.76	336
NGC 3079	76	Sc(s)II-III	4.47	09 58 35	55 55.4	48.4	1225	1.26	273
NGC 3109	58	Sm IV	4.07	10 00 47	-25 54.8	23.1	129	0.12	13
NGC 3124	69	SBbc(r)I	1.17	10 04 17	-18 58.3	28.8	3307	3.00	254
NGC 3147	60	Sb(s)I-II	1.12	10 12 40	73 39.0	39.5	2899	2.61	197
NGC 3184	18, 47	Sc(r)II.2	1.02	10 15 17	41 40.0	55.6	607	0.60	101
NGC 3198	77	Sc(s)I-II	2.24	10 16 53	45 48.0	54.8	702	0.73	160
NGC 3223	61	Sb(s)I-II	1.58	10 19 21	-34 01.0	19.1	2619	2.41	238
NGC 3241	61	Sb(r)II	1.32	10 22 01	-32 13.7	20.9	2584	2.39	241
NGC 3274	55	Scd III	1.91	10 29 30	27 55.6	59.2	486	0.42	11
NGC 3319	52	SBc(s)II.4	1.74	10 36 14	41 56.8	59.3	776	0.81	185
NGC 3338	65	Sbc(s)I-II	1.48	10 39 29	14 00.6	57.0	1171	1.32	398
NGC 3344	19, 66	Sbc(rs)I.2	1.07	10 40 47	25 11.1	61.2	627	0.55	19

Table 2 (Continued)

Name (1)	Atlas Panel (2)	Type (3)	a/b (4)	α_{50} (5)	δ_{50} (6)	b (7)	v_0 (8) km s^{-1}	x (9)	v_g (10) km s^{-1}
NGC 3346	85	SBc(rs)II.2	1.12	10 40 59	15 08.1	57.9	1138	1.29	396
NGC 3351	63	SBb(r)II	1.45	10 41 19	11 58.1	56.4	641	0.55	7
NGC 3359	52	SBc(s)I.8 pec	1.58	10 43 21	63 29.2	48.6	1138	1.18	259
NGC 3423	48	Sc(s)II.2	1.12	10 48 38	06 06.3	54.4	845	0.83	144
NGC 3433	66	Sbc(r)I.3	1.10	10 49 27	10 24.7	57.2	2566	2.46	353
NGC 3464	77	Sc(rs)I	1.41	10 52 15	-20 48.1	34.1	3571	3.23	263
NGC 3485	69	SBbc(s)II	1.12	10 57 24	15 06.6	61.3	1395	1.54	432
NGC 3486	20, 43	Sbc(r)I.2	1.29	10 57 42	29 14.6	65.5	636	0.55	10
NGC 3510	48	Sc (warped plane)	4.07	11 01 01	29 09.3	66.2	660	0.57	13
NGC 3511	77	Sc(s)II.8	2.40	11 00 57	-22 49.0	33.4	951	1.03	269
NGC 3513	52	SBc(s)II.2	1.20	11 01 20	-22 58.6	33.3	845	0.91	228
NGC 3521	43	Sbc(s)II	1.91	11 03 15	00 14.2	52.8	627	0.52	-7
NGC 3596	66	Sbc(r)II.2	1.02	11 12 29	15 03.5	64.4	1072	1.28	448
NGC 3614	77	Sc(r)I	1.58	11 15 34	46 01.2	63.8	2362	2.26	321
NGC 3621	48	Sc(s)II.8	1.55	11 15 50	-32 32.4	26.1	435	0.42	68
NGC 3629	77	Sc(s)II.2	1.32	11 17 52	27 14.4	69.8	1451	1.59	431
NGC 3631	66	Sbc(s)II	1.12	11 18 13	53 26.7	59.0	1238	1.31	313
NGC 3642	39	Sb(r)I	1.17	11 19 25	59 21.0	54.5	1733	1.71	297
NGC 3664	59	SBm III	1.05	11 21 51	03 36.3	58.4	1231	1.42	458
NGC 3673	61	Sb(s)I-II	1.45	11 22 44	-26 27.8	32.3	1662	1.67	325
NGC 3684	77	Sc(s)II	1.38	11 24 35	17 18.3	68.1	1065	1.30	476
NGC 3686	69	SBbc(s)II	1.26	11 25 07	17 30.0	68.3	1034	1.27	473
NGC 3705	61	Sb(r)I-II	2.19	11 27 33	09 33.2	63.8	870	0.70	-46
NGC 3726	27, 43	Sbc(rs)II	1.35	11 30 38	47 18.4	64.9	909	0.99	263
NGC 3756	78	Sc(s)I-II	1.82	11 34 05	54 34.3	59.6	1372	1.43	320
NGC 3780	78	Sc(r)II.3	1.20	11 36 38	56 33.0	58.1	2481	2.33	286
NGC 3810	78	Sc(s)II	1.38	11 38 24	11 44.9	67.2	860	0.65	-89
NGC 3887	70	SBbc(s)II-III	1.23	11 44 33	-16 34.6	43.3	915	1.00	272
NGC 3893	78	Sc(s)I.2	1.55	14 46 01	48 59.4	65.2	1026	1.12	305
NGC 3938	48	Sc(s)I	1.10	11 50 13	44 24.0	69.3	844	0.89	214
NGC 3953	70	SBbc(r)I-II	1.82	11 51 13	52 36.5	62.6	1036	1.12	295
NGC 3992	63	SBb(rs)I	1.55	11 55 01	53 39.3	61.9	1134	1.22	310
NGC 3995	78	Sc (tides)	2.40	11 55 10	32 34.3	77.3	3327	3.08	327
NGC 4041	78	Sc(s)II-III	1.05	11 59 39	62 25.0	54.0	1361	1.39	287
NGC 4051	23, 44	Sbc(r)II	1.26	12 00 37	44 48.7	70.1	746	0.74	125
NGC 4123	42	SBbc(rs)I.8	1.29	12 05 38	03 09.3	63.6	1157	1.41	517
NGC 4136	49	Sc(r)I-II	1.05	12 06 46	30 12.3	80.3	409	0.32	-35
NGC 4144	87	Scd III	3.80	12 07 28	46 44.1	69.0	316	0.27	3
NGC 4145	29, 49	Sc(s)II	1.32	12 07 30	40 09.7	74.6	1030	1.17	355
NGC 4190	58	Sm IV	1.07	12 11 13	36 54.6	77.6	231	0.18	-13
NGC 4214	59	SBm III	1.26	12 13 08	36 36.5	78.1	290	0.23	-17
NGC 4236	4, 56	SBd IV	2.69	12 14 22	69 45.0	47.3	157	0.23	38
NGC 4242	56	SBd III	1.26	12 15 01	45 53.8	70.3	564	0.51	38
NGC 4244	55	Scd	6.46	12 15 00	38 05.2	77.2	249	0.20	-14
NGC 4258	39	Sb(s)II	2.29	12 16 29	47 35.0	68.8	520	0.47	36
NGC 4303	79	Sc(s)I.2	1.10	12 19 22	04 45.1	66.3	Virgo	—	—
NGC 4304	70	SBbc(s)II	1.00	12 19 35	-33 12.4	29.0	2327	2.20	288
NGC 4321	35, 79, 91	Sc(s)I	1.12	12 20 23	16 06.0	76.9	Virgo	—	—
NGC 4394	41, 89	SBb(sr)I-II	1.10	12 23 25	18 29.4	79.3	Virgo	—	—
NGC 4395	10, 56	Sd III-IV	1.17	12 23 20	33 49.5	81.5	304	0.24	-21
NGC 4414	79	Sc(sr)II.2	1.66	12 23 57	31 29.9	83.2	702	0.56	-38
NGC 4485	87	S (tidal)	1.38	12 28 05	41 58.5	74.8	817	0.83	160
NGC 4487	49	Sc(s)II.2	1.35	12 28 30	-07 46.5	54.5	831	0.72	21
NGC 4490	87	Scd III pec	1.91	12 28 10	41 54.9	74.9	601	0.52	20
NGC 4504	49	Sc(s)II	1.45	12 29 42	-07 17.3	55.0	794	0.66	-5
NGC 4536	79, 91	Sbc(s)I-II	2.14	12 31 54	02 27.7	64.7	1646	1.78	461
NGC 4559	49	Sc(s)II	2.14	12 33 29	28 14.1	86.5	771	0.60	-56

Table 2

Table 2 (Continued)

Name (1)	Atlas Panel (2)	Type (3)	a/b (4)	α_{50} (5)	δ_{50} (6)	b (7)	v_0 (8) km s^{-1}	x (9)	v_g (10) km s^{-1}
NGC 4592	87	Scd III	3.02	12 36 45	-00 15.4	62.2	903	0.70	-70
NGC 4593	63	SBb(rs)I-II	1.29	12 37 05	-05 04.2	57.4	2505	2.42	368
NGC 4597	52	SBc(r)III:	1.95	12 37 38	-05 31.5	57.0	851	0.71	-3
NGC 4603	66	Sbc(s)I-II	1.51	12 38 11	-40 42.1	21.8	2073	1.97	267
NGC 4618	42	SBbc(rs)II.2 pec	1.15	12 39 08	41 25.6	75.8	563	0.48	8
NGC 4631	50	Sc (on edge)	4.57	12 39 41	32 48.8	84.2	606	0.48	-33
NGC 4651	79	Sc(r)I.5	1.41	12 41 13	16 40.1	79.1	Virgo	—	—
NGC 4653	79	Sc(rs)I.3	1.07	12 41 17	-00 17.2	62.2	2433	2.38	384
NGC 4656	59	Im	4.17	12 41 32	32 26.5	84.7	624	0.50	-32
NGC 4725	42	Sb/SBb(r)II	1.38	12 48 00	25 46.5	88.4	1167	1.40	496
NGC 4775	80	Sc(s)III	1.05	12 51 11	-06 21.2	56.2	1375	1.54	447
NGC 4814	61	Sb(s)I	1.32	12 53 14	58 36.9	58.8	2650	2.47	276
NGC 4861	59	SBm III	2.51	12 56 40	35 07.9	82.1	836	0.78	86
NGC 4891	70	SBbc(r)I-II	1.12	12 58 15	-13 10.9	49.4	2418	2.33	351
NGC 4899	80	Sc(s)I-II	1.66	12 58 19	-13 40.6	48.9	2437	2.35	348
NGC 4939	67	Sbc(rs)I	1.82	13 01 38	-10 04.4	52.4	2903	2.73	332
NGC 4947	67	Sbc(s)I-II pec	1.70	13 02 34	-35 04.2	27.4	2222	2.11	281
NGC 4981	70	SBbc(sr)II	1.26	13 06 13	-06 30.8	55.8	1492	1.62	432
NGC 5033	40	Sb(s)I	1.86	13 11 08	36 51.8	79.4	897	0.97	248
NGC 5054	61	Sb(s)I-II	1.62	13 14 19	-16 22.1	45.8	1524	1.60	380
NGC 5055	67	Sbc(s)II-III	1.62	13 13 35	42 17.8	74.3	550	0.48	19
NGC 5068	14, 53	SBc(s)II-III	1.10	13 16 13	-20 46.6	41.4	443	0.22	2
NGC 5085	80	Sc(r)II	1.12	13 17 33	-24 10.7	38.0	1720	1.73	338
NGC 5112	50	Sc(rs)II	1.35	13 19 41	38 59.8	76.8	998	1.12	334
NGC 5161	80	Sc(s)I	2.29	13 26 25	-32 54.9	29.0	2113	2.03	290
NGC 5194	44	Sbc(s)I-II	1.41	13 27 46	47 27.3	68.6	541	0.51	52
NGC 5204	56	Sd IV	1.58	13 27 44	58 40.7	58.0	329	0.25	26
NGC 5236	8, 53	SBc(s)II	1.10	13 34 10	-29 36.8	32.0	275	0.23	19
NGC 5247	32, 80	Sc(s)I-II	1.15	13 35 21	-17 38.1	43.6	1143	1.25	345
NGC 5248	44	Sbc(s)I-II	1.32	13 35 03	09 08.5	68.7	1049	1.28	468
NGC 5334	86	SBc(rs)II	1.32	13 50 20	-00 52.1	58.1	1237	1.40	418
NGC 5350	70	SBbc(rs)I-II	1.26	13 51 14	40 36.7	71.6	2305	2.23	337
NGC 5351	67	Sbc(rs)I.2	1.74	13 51 19	38 09.5	73.1	3663	3.33	291
NGC 5364	31, 81	Sc(r)I	1.41	13 53 42	05 15.6	63.0	1140	1.32	425
NGC 5371	62	Sb(rs)I/SBb(rs)I	1.20	13 53 33	40 42.4	71.2	2616	2.48	320
NGC 5398	53	SBc(s)II-III	2.04	13 58 27	-32 49.3	27.6	984	1.04	252
NGC 5457	12, 50	Sc(s)I	1.02	14 01 28	54 35.6	59.8	372	0.24	22
NGC 5468	81	Sc(s)I.8	1.02	14 03 58	-05 12.8	52.7	2696	2.55	331
NGC 5474	55	Scd(s)IV pec	1.07	14 03 15	53 54.0	60.2	394	0.24	21
NGC 5477	58	Sm IV	1.20	14 03 48	54 42.1	59.8	411	0.24	21
NGC 5483	71	SBbc(s)II-III	1.10	14 07 17	-43 05.3	17.2	1517	1.49	247
NGC 5494	81	Sc(s)II	1.12	14 09 29	-30 24.8	29.1	2461	2.30	271
NGC 5556	86	SBc(sr)II-III	1.15	14 17 38	-29 01.1	29.7	1163	1.22	279
NGC 5584	81	Sc(s)I.8	1.29	14 19 50	-00 09.6	54.9	1518	1.60	384
NGC 5585	13, 56	Sd(s)IV	1.48	14 18 12	56 57.5	56.5	441	0.25	28
NGC 5605	81	Sc(rs)II	1.20	14 22 25	-12 56.3	43.7	3196	2.93	283
NGC 5660	81	Sc(s)I.2	1.10	14 28 04	49 50.8	60.6	2433	2.30	296
NGC 5668	82	Sc(s)II-III	1.07	14 30 54	04 40.2	56.7	1491	1.58	381
NGC 5669	86	SBc(s)II	1.29	14 30 17	10 06.6	60.6	1304	1.43	387
NGC 5850	63	SBb(sr)I-II	1.10	15 04 35	01 44.2	48.6	2430	2.31	304
NGC 5861	82	Sc(s)II	1.70	15 06 33	-11 07.9	39.0	1725	1.71	308
NGC 5879	40	Sb(s)II	2.63	15 08 29	57 11.4	51.4	929	0.98	232
NGC 5885	37, 86	SBc(s)II	1.12	15 12 22	-09 54.0	39.0	1879	1.84	301
NGC 5905	71	SBbc(rs)I	1.26	15 14 02	55 42.1	51.6	3544	3.18	225
NGC 5921	42	SBbc(s)I-II	1.17	15 19 28	05 14.9	47.9	1428	1.48	323
NGC 5985	64	SBb(r)I	1.70	15 38 36	59 29.6	46.8	2694	2.46	225
NGC 6015	82	Sc(s)II-III	2.29	15 50 39	62 27.5	44.1	1018	1.05	222

Table 2 (Continued)

Name (1)	Atlas Panel (2)	Type (3)	a/b (4)	α_{50} (5)	δ_{50} (6)	b (7)	v_0 (8) km s^{-1}	x (9)	v_8 (10) km s^{-1}
NGC 6070	82	Sc(s)I-II	1.74	16 07 26	00 50.4	35.6	1979	1.89	260
NGC 6118	82	Sc(s)I.3	2.04	16 19 13	-02 10.1	31.5	1535	1.51	250
NGC 6217	71	RSBbc(s)II	1.15	16 35 03	78 18.0	33.4	1598	1.51	193
NGC 6384	62	Sb(r)I.2	1.41	17 29 59	07 05.8	20.8	1735	1.62	182
NGC 6643	82	Sc(s)II	1.86	18 21 14	74 32.7	28.2	1743	1.61	169
NGC 6744	22, 44	Sbc(r)II	1.51	19 05 02	-63 56.3	-26.2	663	0.61	65
NGC 6753	62	Sb(r)I	1.12	19 07 13	-57 07.7	-25.1	3001	2.55	23
NGC 6814	67	Sbc(rs)I-II	1.05	19 39 55	-10 26.6	-16.0	1643	1.42	43
NGC 6836	83	Sc(s)II-III	1.05	19 51 53	-12 49.0	—	1628	—	—
NGC 6907	71	SBbc(s)II	1.15	20 22 07	-24 58.3	-30.8	3192	2.66	-35
NGC 6946	11, 50	Sc(s)II	1.12	20 33 48	59 59.0	11.7	336	0.34	64
NGC 6951	64	Sb/SBb(rs)I.3	1.15	20 36 37	65 55.9	14.8	1710	1.54	113
NGC 7125	83	Sc(rs)I-II/SBc(s)I-II	1.48	21 45 38	-60 56.8	-44.6	2910	2.42	-41
NGC 7171	67	Sbc(r)I-II	1.58	21 58 20	-13 30.6	-47.9	2758	2.24	-95
NGC 7217	62	Sb(r)II-III	1.17	22 05 36	31 07.0	-19.7	1234	1.04	0
NGC 7329	64	SBb(r)I-II	1.48	22 36 56	-66 44.6	-45.8	3043	2.53	-39
NGC 7331	40	Sb(rs)I-II	2.69	22 34 47	34 09.5	-20.7	1114	0.94	1
NGC 7361	83	Sc II-III	3.31	22 39 31	-30 19.2	-61.6	1276	1.02	-63
NGC 7412	83	Sc(s)I-II	1.29	22 52 55	-42 54.6	-61.9	1691	1.37	-65
NGC 7418	83	Sc(rs)I.8	1.20	22 53 49	-37 17.6	-63.9	1451	1.16	-67
NGC 7421	72	SBbc(rs)II-III	1.07	22 54 06	-37 37.0	-63.8	1838	1.48	-77
NGC 7424	28, 53	Sc(rs)II.3/SBc(s)II.3	1.12	22 54 28	-41 20.4	-62.7	925	0.75	-37
NGC 7456	50	Sc(s)II-III	3.24	22 59 22	-39 50.3	-64.1	1199	0.96	-54
NGC 7479	38, 72	SBbc(s)I-II	1.26	23 02 26	12 03.1	-42.8	2630	2.13	-98
NGC 7531	44	Sbc(r)I-II	2.34	23 12 03	-43 52.4	-64.5	1607	1.30	-62
NGC 7552	64	SBb(s)I-II	1.41	23 13 25	-42 51.5	-65.2	1565	1.26	-67
NGC 7640	54	SBc(s)II:	4.27	23 19 43	40 34.2	-18.9	669	0.58	15
NGC 7678	72	SBbc(s)I-II	1.32	23 25 59	22 08.7	-36.6	3756	3.07	-109
NGC 7689	83	Sc(sr)II	1.41	23 30 34	-54 22.4	-59.4	1681	1.38	-47
NGC 7713	84	Sc(s)II-III	2.14	23 33 35	-38 13.0	-70.9	684	0.54	-38
NGC 7741	53	SBc(s)II.2	1.41	23 41 23	25 47.9	-34.4	1030	0.84	-33
NGC 7755	72	SBbc(r)/Sbc(r)I-II	1.26	23 45 15	-30 47.9	-75.7	2969	2.40	-119
NGC 7793	6, 57	Sd(s)IV	1.38	23 55 15	-32 52.1	-77.2	241	0.19	-18
IC 749	54	SBc(rs)II-III	1.17	11 56 00	43 00.8	71.0	827	0.86	189
IC 764	84	Sc(s)I.2	2.63	12 07 39	-29 27.5	32.3	1851	1.83	320
IC 1727	54	SBc(s)II-III	2.14	01 44 40	27 05.1	-33.8	662	0.54	-9
IC 1953	72	SBbc(rs)II	1.23	03 31 29	-21 38.6	-52.8	1856	1.52	-53
IC 4662	59	Im III	1.58	17 42 12	-64 37.3	-17.8	240	0.24	46
IC 5152	2, 57	Sdm IV-V	1.66	(21 59 36)	(-51 32)	-50.2	47	—	—
IC 5201	54	SBcd(s)II	2.00	22 17 55	-46 17.0	-54.9	728	0.60	-14
IC 5332	50	Sc(s)II-III	1.29	23 31 48	-36 22.6	-71.4	713	0.56	-44
NEW 1	86	SBc(s)II.2	1.12	01 02 33	-06 28.6	-68.8	1116	0.87	-82
NEW 4	84	Sc(s)II-III	1.23	12 52 39	00 23.2	63.0	1160	1.40	501
F-703	84	Sc(s)II.2	1.17	15 11 00	-15 16.7	35.2	2128	2.03	281
HA 85-1	84	Sc(s)II	1.20	05 09 25	-14 51.0	-28.6	2063	1.76	22

Table 3
Galaxies to be Observed From the Ground and in Parallel with HST

Name (1)	Atlas Panel (2)	Type (3)	a/b (4)	α_{50} (5)	δ_{50} (6)	b (7)	v_0 (8) km s^{-1}	x (9)	v_8 (10) km s^{-1}
NGC 45	17, 55	Scd(s)III	1.41	00 11 32	-23 27.6	-80.7	533	0.41	-45
NGC 55	45	Sc	5.01	00 12 24	-39 28.0	-75.7	115	0.09	-5

Table 3 (Continued)

Name (1)	Atlas Panel (2)	Type (3)	a/b (4)	α_{50} (5)	δ_{50} (6)	b (7)	v_0 (8) km s^{-1}	x (9)	v_g (10) km s^{-1}
NGC 247	5, 45	Sc(s)III-IV	2.69	00 44 40	-21 02.0	-83.6	227	0.17	-24
NGC 300	3, 45	Sc(s)II.8	1.35	00 52 31	-37 57.4	-79.4	128	0.10	-6
NGC 925	24, 51	SBc(s)II-III	1.62	02 24 18	33 21.1	-25.2	792	0.67	8
NGC 1156	57	Sm IV	1.32	02 56 47	25 02.4	-29.2	558	0.48	11
NGC 1313	7, 51	SBc(s)III-IV	1.29	03 17 39	-66 40.7	-44.6	261	0.24	21
NGC 1518	46	Sc III	2.19	04 04 38	-21 18.7	-45.3	914	0.77	1
NGC 1566	33, 43	Sbc(s)I.2	1.23	04 18 53	-55 03.4	-43.4	1305	1.11	18
NGC 2366	15, 59	SBm IV-V	2.14	07 23 37	69 19.1	28.5	281	0.25	53
NGC 2403	9, 46	Sc(s)III	1.62	07 32 03	65 42.7	29.2	299	0.25	53
NGC 2541	46	Sc(s)III	1.86	08 11 02	49 13.0	33.5	646	0.68	155
NGC 2552	56	Sd(s)III	1.45	08 15 42	50 10.1	34.3	607	0.64	147
NGC 3031	16, 39	Sb(r)I-II	1.82	09 51 30	69 18.3	40.9	124	0.24	45
NGC 3109	58	Sm IV	4.07	10 00 47	-25 54.8	23.1	129	0.12	13
NGC 3184	18, 47	Sc(r)II.2	1.02	10 15 17	41 40.0	55.6	607	0.60	101
NGC 3486	20, 43	Sbc(r)I.2	1.29	10 57 42	29 14.6	65.5	636	0.55	10
NGC 3621	48	Sc(s)II.8	1.55	11 15 50	-32 32.4	26.1	435	0.42	68
NGC 3726	27, 43	Sbc(rs)II	1.35	11 30 38	47 18.4	64.9	909	0.99	263
NGC 4214	59	SBm III	1.26	12 13 08	36 36.5	78.1	290	0.23	-17
NGC 4236	4, 56	SBd IV	2.69	12 14 22	69 45.0	47.3	157	0.23	38
NGC 4242	56	SBd III	1.26	12 15 01	45 53.8	70.3	564	0.51	38
NGC 4258	39	Sb(s)II	2.29	12 16 29	47 35.0	68.8	520	0.47	36
NGC 4395	10, 56	SdIII-IV	1.17	12 23 20	33 49.5	81.5	304	0.24	-21
NGC 4618	42	SBbc(rs)II.2 pec	1.15	12 39 08	41 25.6	75.8	563	0.48	8
NGC 4656	59	Im	4.17	12 41 32	32 26.5	84.7	624	0.50	-32
NGC 5068	14, 53	SBc(s)II-III	1.10	13 16 13	-20 46.6	41.4	443	0.22	2
NGC 5204	56	Sd IV	1.58	13 27 44	58 40.7	58.0	329	0.25	26
NGC 5474	55	Scd(s)IV pec	1.07	14 03 15	53 54.0	60.2	394	0.24	21
NGC 5477	58	Sm IV	1.20	14 03 48	54 42.1	59.8	411	0.24	21
NGC 5585	13, 56	Sd(s)IV	1.48	14 18 12	56 57.5	56.5	441	0.25	28
NGC 7424	28, 53	Sc(rs)II.3/SBc(rs)II.3	1.12	22 54 28	-41 20.4	-62.7	925	0.75	-37
NGC 7793	6, 57	Sd(s)IV	1.38	23 55 15	-32 52.1	-77.2	241	0.19	-18
IC 1727	54	SBc(s)II-III	2.14	01 44 40	27 05.1	-33.8	662	0.54	-9
IC 5152	2, 57	Sdm IV-V	1.66	(21 59 36)	(-51 32)	-50.2	47	—	—
IC 5332	50	Sc(s)II-III	1.29	23 31 48	-36 22.6	-71.4	713	0.56	-44

Table 4
The Illustrated Virgo Cluster Candidates
Chosen for Observation with HST

Atlas Panel (1)	Name (2)	α_{50} (3)	δ_{50} (4)	Type (5)	B_T (6)	M_B (7)	v (8) km s^{-1}
88	NGC 4548	12 32.92	14 46.4	SBb(rs)I-II	10.98	-20.72	486
	NGC 4571	12 34.42	14 29.8	Sc(s)II-III	11.81	-19.89	342
Excellent	7° 27	12 24.64	07 32.4	Scd(s)II	13.58	-18.12	932
	NGC 4496A	12 29.11	04 12.9	SBc III-IV	12.0:	-19.70:	1730
	NGC 4523	12 31.29	15 26.6	SBd(s)III	13.62	-18.08	262
	IC 3576	12 34.08	06 53.8	SBd IV	13.70	-18.00	1077
89	NGC 4535	12 31.80	08 28.6	SBc(s)I.3	10.51	-21.19	1961
	NGC 4178	12 10.23	11 08.8	SBc(s)II	11.89	-19.81	355
	NGC 4394	12 23.41	18 29.4	SBb(sr)I-II	11.76	-19.94	944
Good	NGC 4519	12 30.96	08 55.8	SBc(rs)II.2	12.34	-19.36	1220
	NGC 4647	12 41.02	11 51.2	Sc(rs)III	12.03	-19.67	1422
	NGC 4411A	12 23.94	09 08.9	SBc(s)II	13.42	-18.28	1277
	NGC 4411B	12 24.25	09 09.7	Sc(s)II	12.92	-18.78	1266

Table 4 (Continued)

Atlas Panel (1)	Name (2)	α_{50} (3)	δ_{50} (4)	Type (5)	B_T (6)	M_B (7)	v (8) km s^{-1}
90	NGC 4654	12 41.44	13 24.0	SBc(rs)II	11.14	-20.56	1036
	NGC 4639	12 40.35	13 31.9	SBb(r)II	12.19	-19.51	972
	A1240.2 +1332	12 40.17	13 32.4	Im III:	15.2	-16.5	-10
Good to Fair	NGC 4689	12 45.25	14 02.1	Sc(s)II.3	11.55	-20.15	1613
	NGC 4430	12 24.89	06 32.3	SBc(r)II	12.48	-19.22	1451
	IC 776	12 16.50	09 08.1	SBcd(s)III	14.01	-17.69	2467
	IC 3365	12 24.67	16 10.5	Scd(s)III	14.17	-17.53	2339
91	NGC 4321	12 20.38	16 06.0	Sc(s)I	10.11	-21.59	1568
	NGC 4536	12 31.90	02 27.7	Sc(s)I	11.01	-20.69	1809
Fair	NGC 4298	12 19.01	14 53.1	Sc(s)III	12.08	-19.62	1135
	NGC 4396	12 23.46	15 56.8	Sc(s)II	13.02	-18.68	-128
	8° 5	12 11.60	08 03.2	SBd IV	13.68	-18.02	1220
	NGC 4498	12 29.14	17 07.8	SBc(s)II	12.62	-19.08	1507
92	IC 3476	12 30.18	14 19.5	Sc(s)II.2	13.29	-18.41	-225
	NGC 4390	12 23.33	10 43.8	Sbc(s)II	13.27	-18.43	1104
Fair	NGC 4330	12 20.75	11 38.7	Sd (on-edge)	13.10	-18.60	1565
	IC 3258	12 21.20	12 45.3	Sc III-IV	13.75	-17.95	-432
	IC 3414	12 26.93	07 02.9	Sc(s)II	13.70	-18.00	528
	NGC 4633	12 40.11	14 37.8	Scd(s)	13.77	-17.93	290
93	IC 3355	12 24.30	13 27.2	SBm III	14.82	-16.88	80
	IC 3617	12 36.88	08 14.2	SBm III/BCD	14.67	-17.03	2093
	9° 49 = IC 3517	12 31.98	09 25.9	Sd IV	14.51	-17.19	439
Excellent	7° 29	12 24.94	07 55.3	Sdm III	14.85	-16.85	874
	IC 3268	12 21.57	06 53.1	Sc(s)III-IV	14.22	-17.48	728
	12° 100	12 41.65	12 23.4	Im IV	15.5	-16.2	1006
	A1231.4 +0349	12 31.37	03 49.4	Sdm III-IV	14.63	-17.07	1138
	IC 3583	12 34.21	13 32.0	Sm III	13.91	-17.79	1120
	6° 38	12 32.20	06 34.7	Sm IV	14.55	-17.15	2048
	12° 9	12 09.70	12 45.9	Sd(s)/Sm III	14.3	-17.4	-53
	IC 3059	12 12.38	13 44.2	SBd	14.23	-17.47	262
	7° 43	12 35.20	07 22.7	Sdm IV	14.54	-17.16	62
	A1221.5 +0527	12 21.50	05 27.4	SBm III?	15.06	-16.64	2048
	14° 10	12 07.48	14 38.4	Im IV	15.2	-16.5	820
94	IC 3589	12 34.50	07 12.3	SBm III	14.11	-17.59	1632
	IC 3416	12 27.04	11 04.2	Im III	14.78	-16.92	-123
Good	IC 3522	12 32.25	15 29.8	Im III-IV pec	15.2	-16.5	662
	NGC 4502	12 29.54	16 57.8	Sm III	14.57	-17.13	1623
	8° 30	12 26.02	08 54.9	Im III	14.51	-17.19	560
	8° 33	12 27.47	08 12.4	Im III-IV	14.72	-16.98	468:
	A1211.1 +1543.9	12 11.13	15 43.9	Sm III	15.0	-16.7	-129
	A1236.8 +0512.8	12 36.81	05 12.8	Im III	15.07	-16.63	1620
	IC 3049	12 11.01	14 45.5	Im III-IV	15.13	-16.57	2438
	VC 740	12 22.12	08 46.7	SBm III:	15.7	-16.0	874
	Background	12 15.64	08 36.0	(Im III)	Paper III		4314
	IC 3418	12 27.19	11 40.7	SBm IV	14.0:	-17.7:	—
	11° 6 = IC 3040	12 10.02	11 21.2	Sm III-IV	15.04	-16.66	—
	IC 3356	12 24.36	11 50.3	Sm IV	14.49	-17.21	1097
	VC 1465	12 30.38	03 38.1	Im IV	15.0:	-16.7:	734
95	A1223.1 +0226	12 23.15	02 26.0	Im IV	15.0	-16.7	1508
	14° 31	12 20.58	14 01.3	Im?	16.5	-15.2	—
Fair	IC 3475	12 30.13	13 03.0	Im IV or dE/pec	13.93	-17.77	2572
	VC 260	12 15.33	05 18.2	Im IV	15.7	-16.0	1775
	13° 29	12 16.65	13 09.7	Im IV	16.9	-14.8	2180
	A1235.1 +0850	12 35.15	08 50.0	Sm III/BCD	14.51	-17.19	1065
	10° 69	12 43.61	10 26.2	Im IV	15.8	-15.9	1500
	8° 20	12 20.25	08 11.4	Im IV-V	15.8	-15.9	—
	IC 3239	12 20.63	12 00.3	Sm III	15.2	-16.5	645
	VC 1468	12 30.41	04 51.2	Im IV	15.0	-16.7	—
	9° 4	12 12.64	09 26.1	Im IV-V	18.3	-13.4	—
	IC 3412	12 26.82	10 15.9	Im III/BCD	14.87	-16.83	762
	10° 22	12 23.14	10 51.4	Im IV, N?	15.9	-15.8	—
	11° 34	12 29.12	11 06.7	Im IV-V:	15.7:	-16.0:	—
	10° 71	12 43.73	10 28.8	Im III/BCD	15.8	-15.9	1142

References

Arp, H. C., 1956, *Astron. J.*, **61**, 15.

Bartel, N., ed., 1985, *Supernovae as Distance Indicators*, in Physics Lecture Notes 224, (Berlin: Springer-Verlag).

Cohen, J., and Rosenthal, A. J., 1983, *Astrophys. J.*, **268**, 689.

Cook, K. H., Aaronson, M. C., and Illingworth, G., 1986, *Astrophys. J. Letters*, **301**, L45.

de Vaucouleurs, G., de Vaucouleurs, A., and Corwin, H. G., 1977, *Reference Catalog of Bright Galaxies*, Second Edition, (Austin: University of Texas Press).

Dressler, A., 1987, *Astrophys. J.*, **317**, 1.

Ford, H., and Ciardullo, R., 1987, in preparation.

Greggio, L., 1986, *Astron. Astrophys.*, **160**, 111.

Hubble, E., 1936, *Astrophys. J.*, **84**, 270.

Humphreys, R. M., and Sandage, A., 1980, *Astrophys. J. Suppl. Series*, **44**, 319.

Kraan-Korteweg, R. C., 1984, in *The Virgo Cluster*, European Southern Observatory Workshop No. 20, ed. O-G. Richter and B. Binggeli, p. 397.

Kraan-Korteweg, R. C., 1986, *Astron. Astrophys. Suppl. Series*, **66**, 255.

McLaughlin, D. B., 1960, in *Stars and Stellar Systems*, Vol. 6, *Stellar Atmospheres*, ed. J. L. Greenstein (Chicago: University of Chicago Press), p. 585.

Nilson, P., 1973, *Uppsala General Catalog of Galaxies*, Uppsala Astr. Obs. Ann., Vol. 6.

Öpik, E., 1922, *Astrophys. J.*, **55**, 406.

Rosino, L., 1964, *Annal d'Astrophys.*, **27**, 498.

Sandage, A., 1961, *The Hubble Atlas of Galaxies*, Carnegie Institution of Washington Publication 618, (Washington, D.C.: Carnegie Institution of Washington).

Sandage, A., 1982, in *Kinematics and Dynamics of Galaxies*, IAU Symposium 100, ed. E. Athanassoula (Dordrecht: D. Reidel Publishing Co.).

Sandage, A., 1988, *Astrophys. J.*, in press.

Sandage, A., and Bedke, J., 1985a, *Astron. J.*, **90**, 1992.

Sandage, A., and Bedke, J., 1985b, *Astron. J.*, **90**, 2001.

Sandage, A., and Bedke, J., 1985c, *Astron. J.*, **90**, 2006.

Sandage, A., Binggeli, B., and Tammann, G. A., 1984, in *The Virgo Cluster*, European Southern Observatory Workshop No. 20, ed. O-G. Richter and B. Binggeli, p. 239.

Sandage, A., Binggeli, B., and Tammann, G. A., 1985, *Astron. J.*, **90**, 1759.

Sandage, A., and Carlson, G., 1983, *Astrophys. J. Letters*, **267**, L25.

Sandage, A., and Carlson, G., 1985, *Astron. J.*, **90**, 1464.

Sandage, A., and Tammann, G. A., 1968, *Astrophys. J.*, **151**, 531.

Sandage, A., and Tammann, G. A., 1969, *Astrophys. J.*, **157**, 683.

Sandage, A., and Tammann, G. A., 1974, *Astrophys. J.*, **194**, 223.

Sandage, A., and Tammann, G. A., 1975, *Astrophys. J.*, **197**, 265.

Sandage, A., and Tammann, G. A., 1982, *Astrophys. J.*, **256**, 339.

Sandage, A., and Tammann, G. A., 1987, *A Revised Shapley-Ames Catalog of Bright Galaxies*, Second Edition, Carnegie Institution of Washington Publication 635, (Washington, D.C.: Carnegie Institution of Washington).

Schmidt, T., 1957, *Zeitzchrift f. Astrophys.*, **41**, 182.

Shapley, H., and Ames, A., 1932, *Ann. Harv. Coll. Obs.*, **88**, No. 2.

Tammann, G. A., 1987, in *Observational Cosmology*, IAU Symposium 134, ed. A. Hewitt, G. Burbidge, and L. Z. Fang (Dordrecht: D. Reidel Publishing Co.).

Tammann, G. A., and Sandage, A., 1985, *Astrophys. J.*, **294**, 81.

Tully, R. B., and Fisher, J. R., 1977, *Astron. Astrophys.*, **54**, 661.

Van den Bergh, S., 1960a, *Astrophys. J.*, **131**, 558.

Van den Bergh, S., 1960b, *Astrophys. J.*, **131**, 215.

Van den Bergh, S., 1975, in *Stars and Stellar Systems*, Vol. 9, *Galaxies and the Universe*, ed. A. Sandage, M. Sandage, and J. Kristian (Chicago: University of Chicago Press), p. 509.

Zwicky, F., 1957, *Morphological Astronomy*, (Berlin: Springer-Verlag), pp. 220-228.

The Atlas

Part I

Single-galaxy images of 38 candidates are illustrated on panels 1-38 of the atlas. The original plates were obtained either at Las Campanas or at Palomar in seeing conditions sufficient to permit the enlargement factor given here.

The panels in Part I are arranged in order of increasing redshift. From this order, the general decrease in the resolution (per parsec) can be seen as the redshift increases. The best plates in the collection have images whose seeing disks are ~0.8 arc-seconds (FWHM). The HST resolution with the faint-object camera (FOC) and the planetary camera of the wide-field planetary camera (WFPC) is expected to be at least 10 times better than shown in the best photographs here. When the wide-field camera is used, its 0.1 arc-second pixel size *undersamples* the intrinsic resolution delivered by the telescope, thereby degrading the ultimate resolution of the instrument. It is to be emphasized that the FOC or the *planetary* camera of the WFPC are to be preferred over the *wide-field* WFPC camera when it is necessary to obtain the designed resolution of the telescope, as will usually be the case for this key distance scale program.

The scale of each reproduction is shown by the 120 arc-second markers. These scales are accurate but not precise.

The 120 arc-second scale markers define the approximate format size of the WFPC of HST. Observers wishing to choose particular parts of a given galaxy as HST targets must obtain offset coordinates of the desired image segment by noting the scale of each print and the central coordinates in Table 2.

The velocities shown in the lower right corner of each panel are the v_0 values listed in Sandage and Tammann [1987], except where occasionally updated with more accurate values.

The orientation of the images in the panels is arbitrary. Reference must be made to the POSS, ESO, and SRC sky survey prints or films to find the north and east positions. The coordinates listed in Table 2 refer to the galaxy center as given in Sandage and Tammann [1987]. The coordinate values have nominal accuracies somewhat better than 10 arc-seconds.

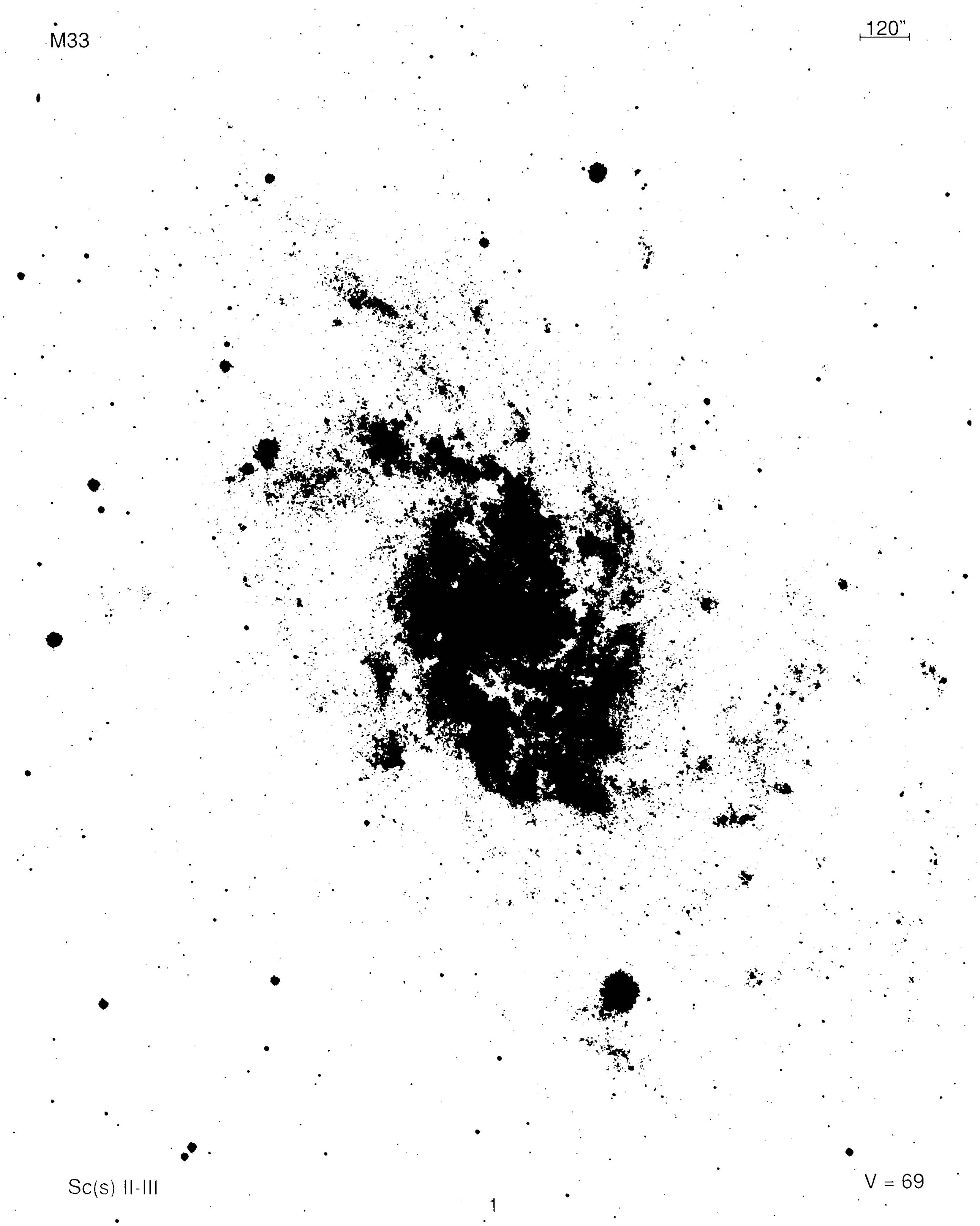
M33
120"
Sc(s) II-III
V = 69

IC 5152

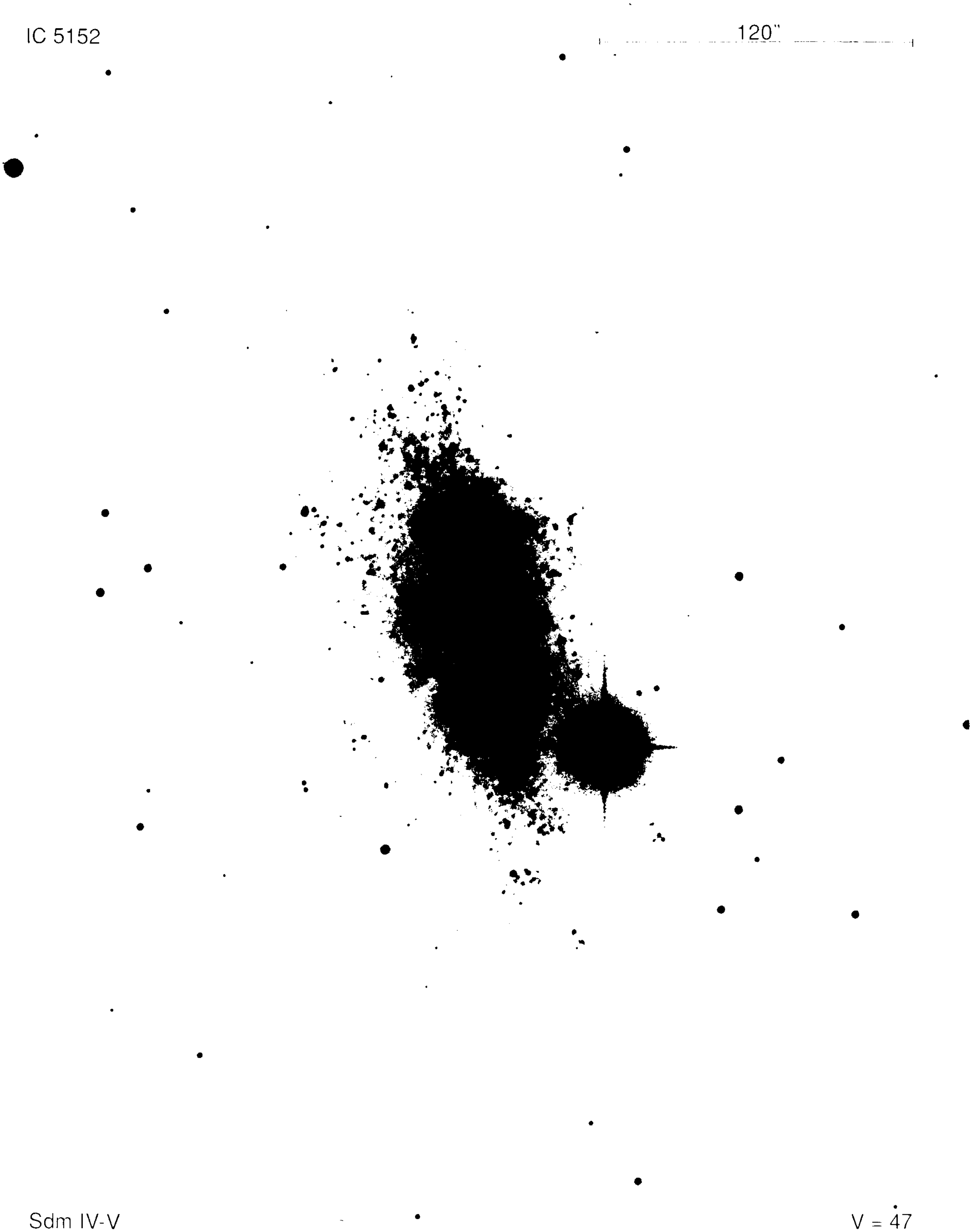

Sdm IV-V

V = 47

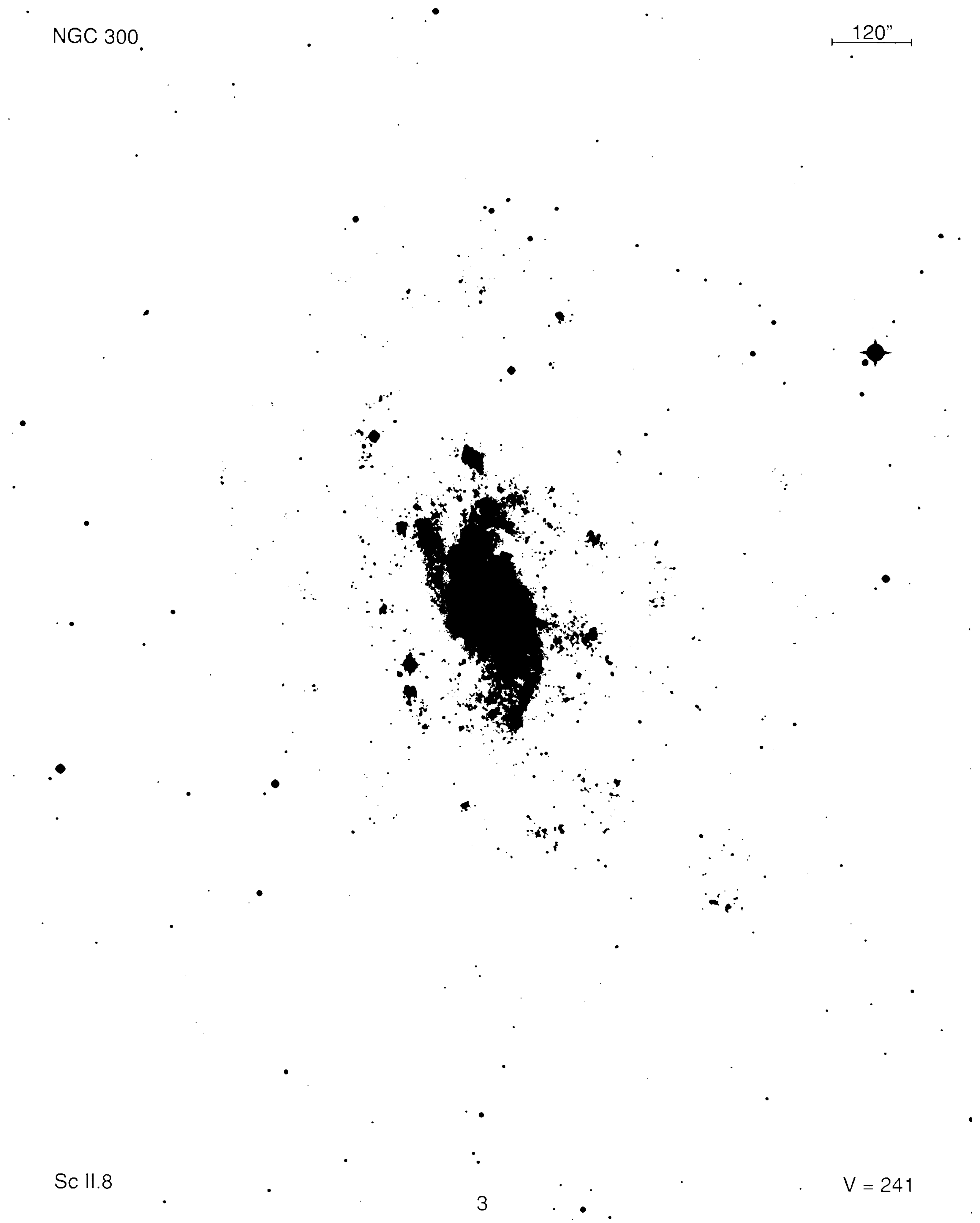
NGC 300
120"
Sc II.8
V = 241

NGC 4236

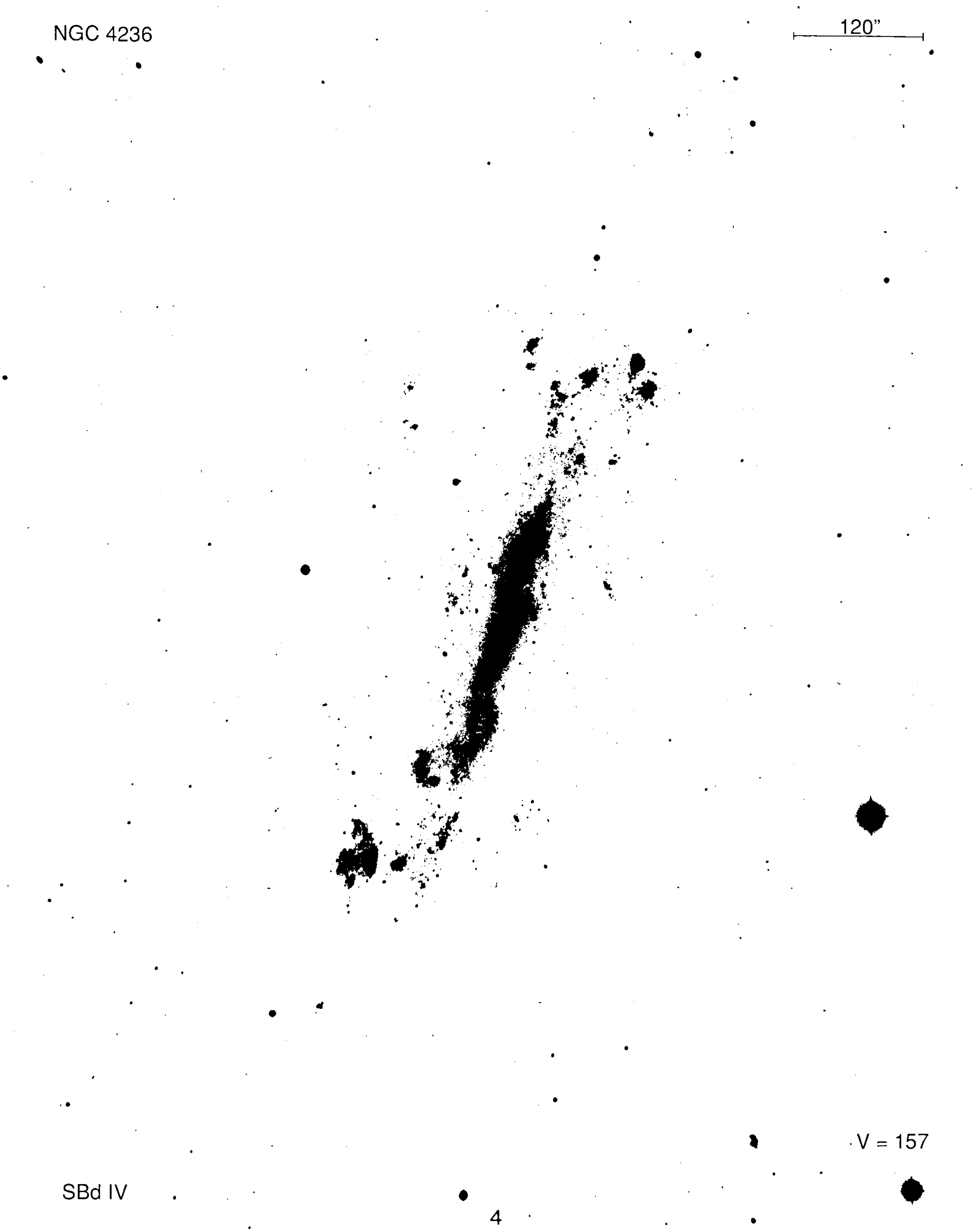

V = 157

SBd IV

NGC 247

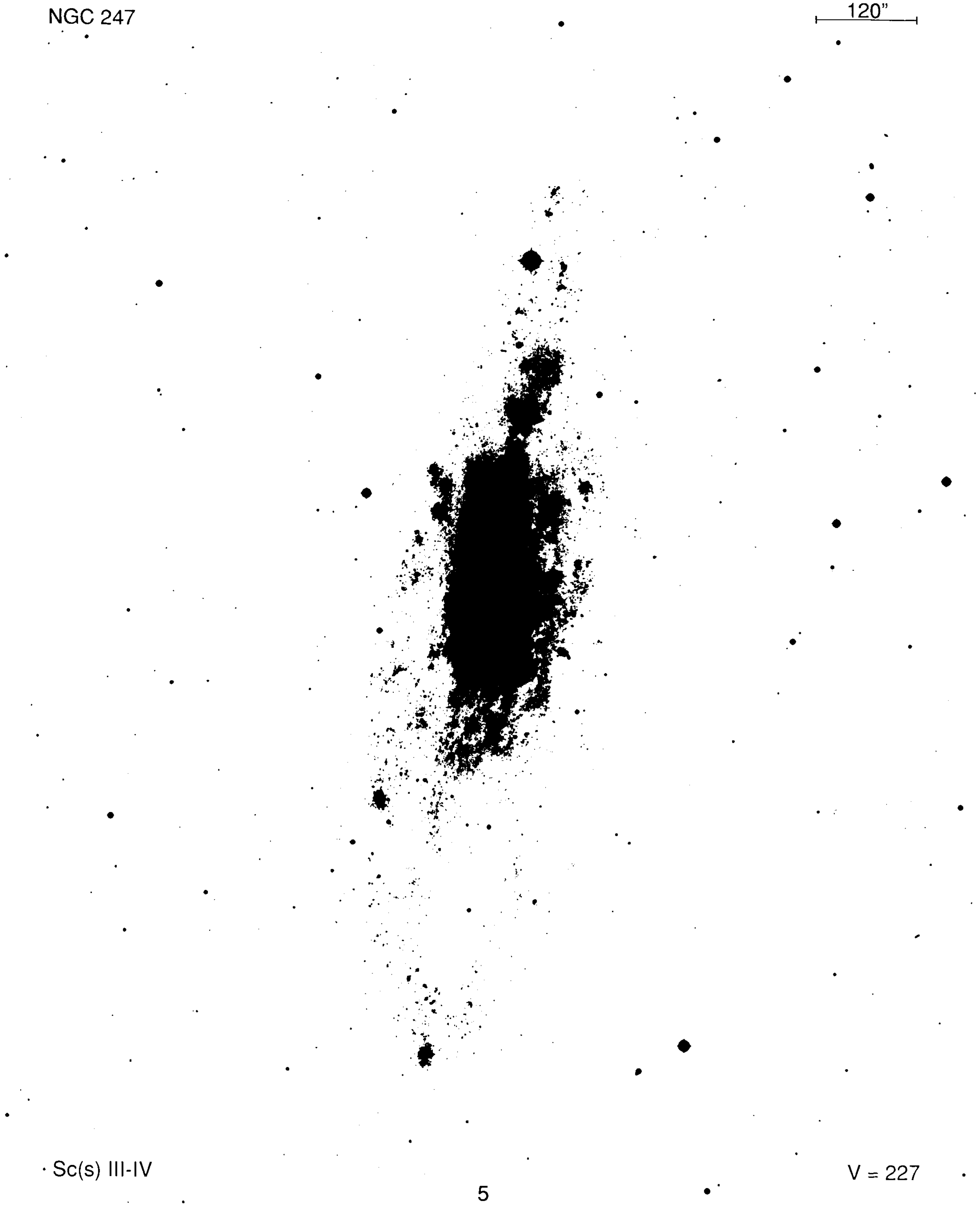

Sc(s) III-IV

V = 227

NGC 7793

120"

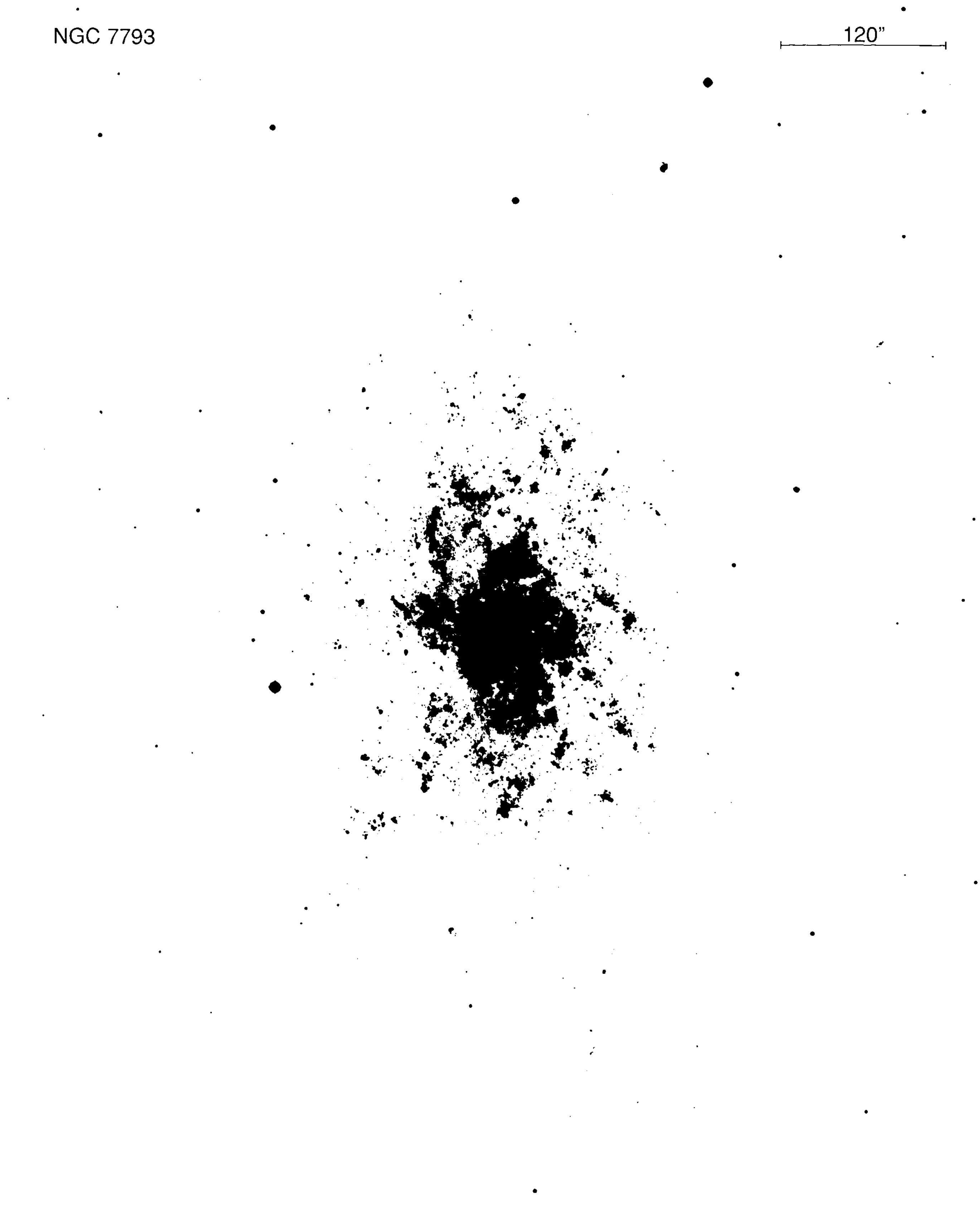

Sd(s) IV

V = 241

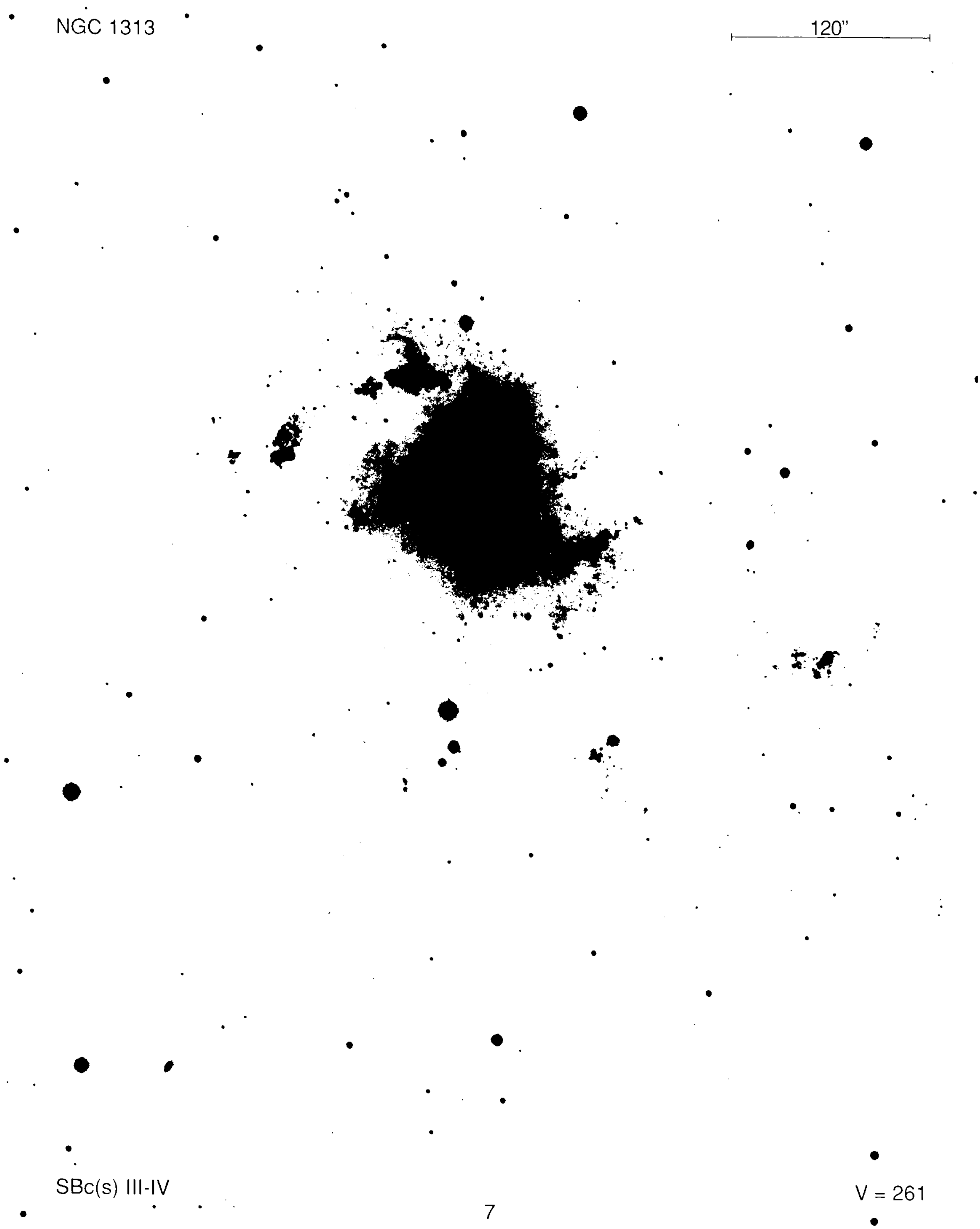

NGC 1313

SBc(s) III-IV

V = 261

NGC 5236

120"

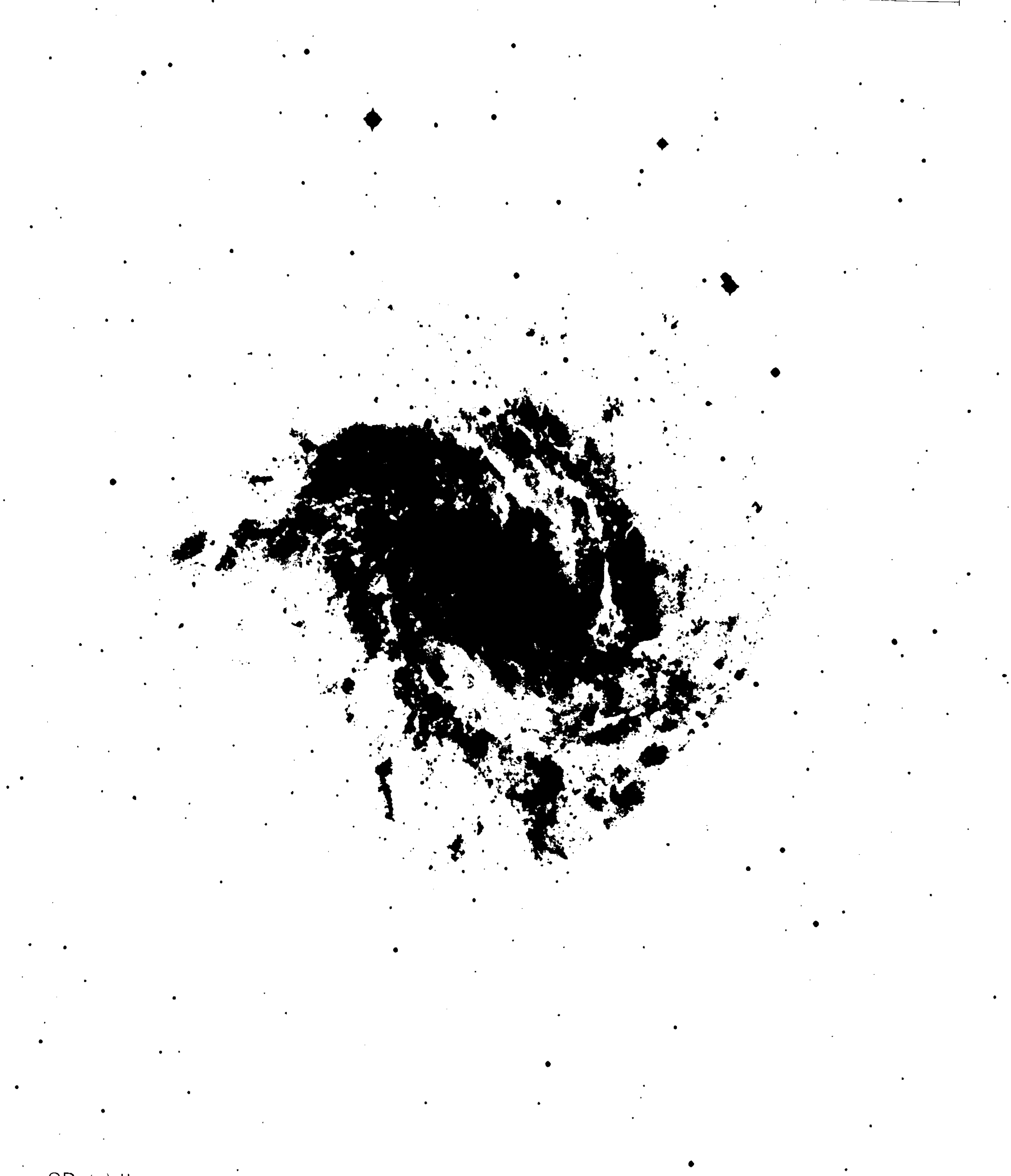

SBc(s) II

V = 275

NGC 2403

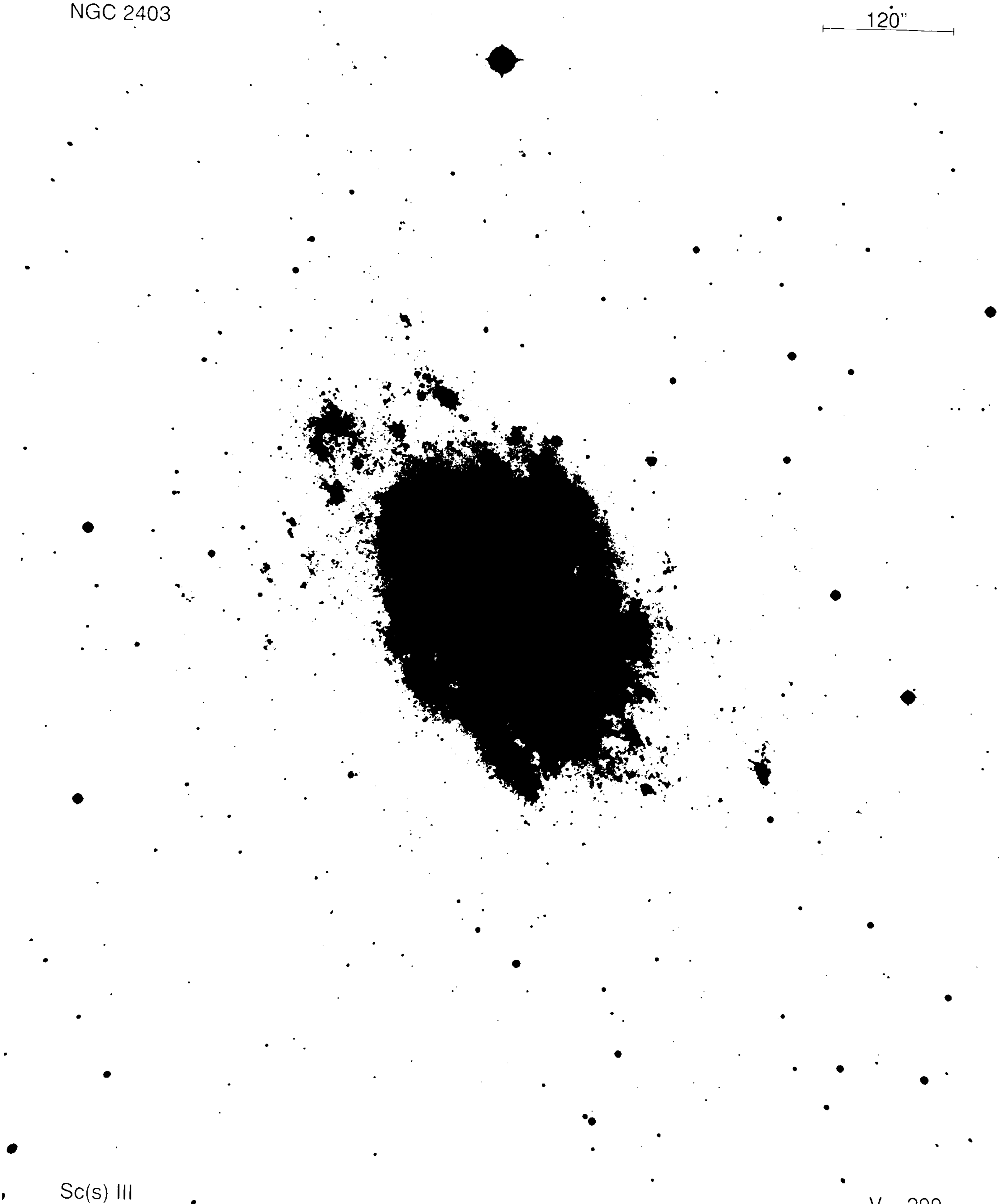

Sc(s) III

V = 299

NGC 4395

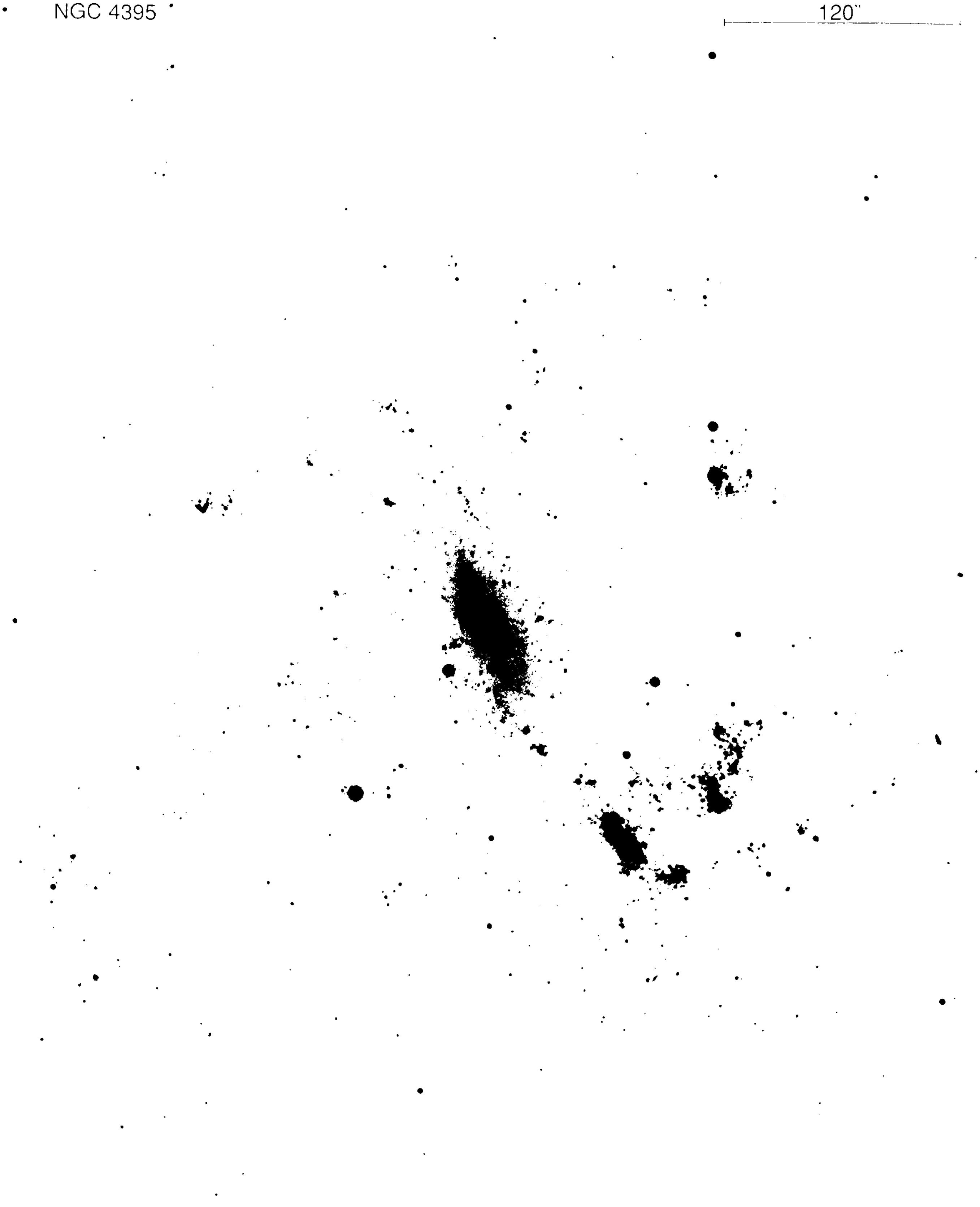

Sd III-IV

V = 304

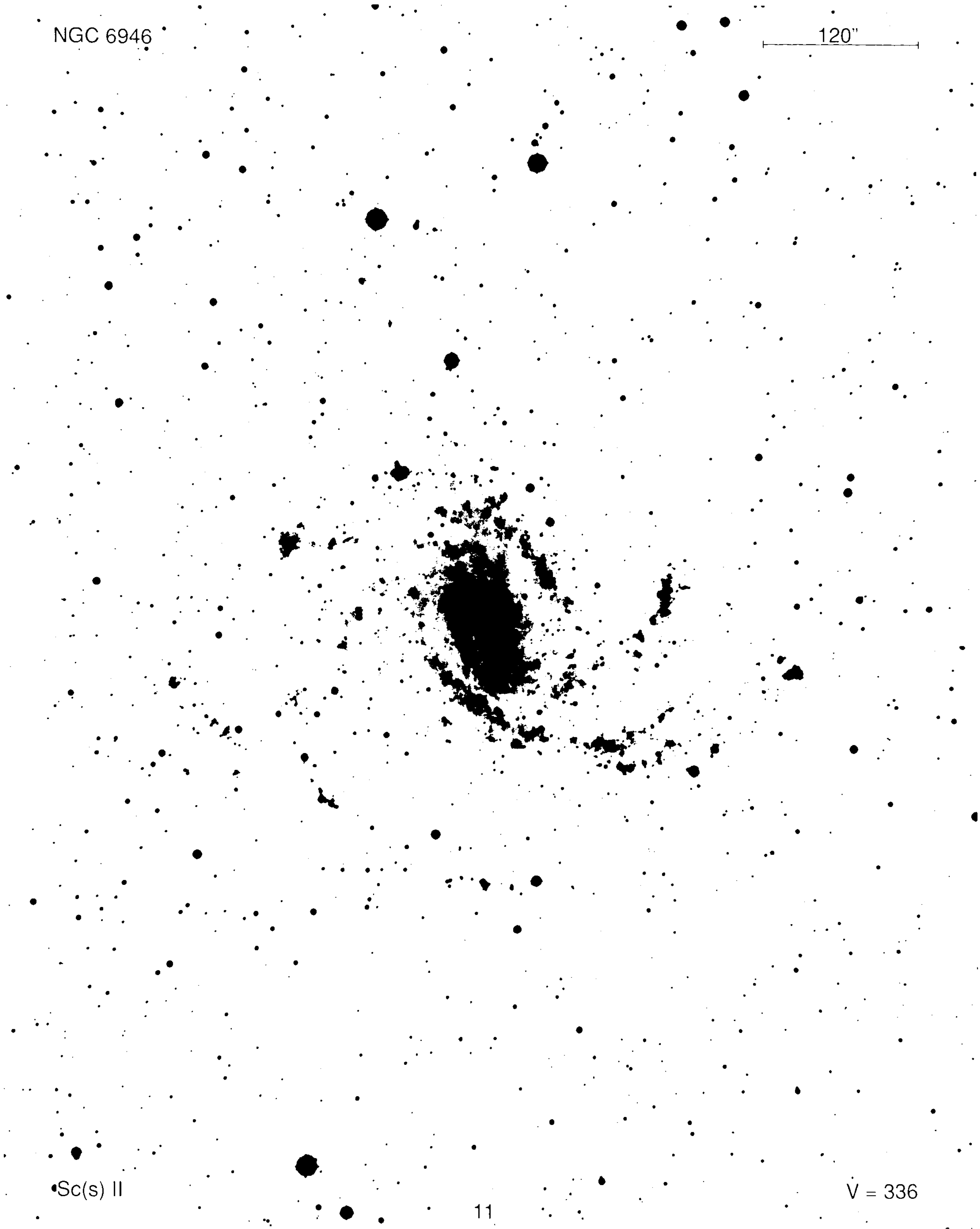
NGC 6946
120"
Sc(s) II
V = 336

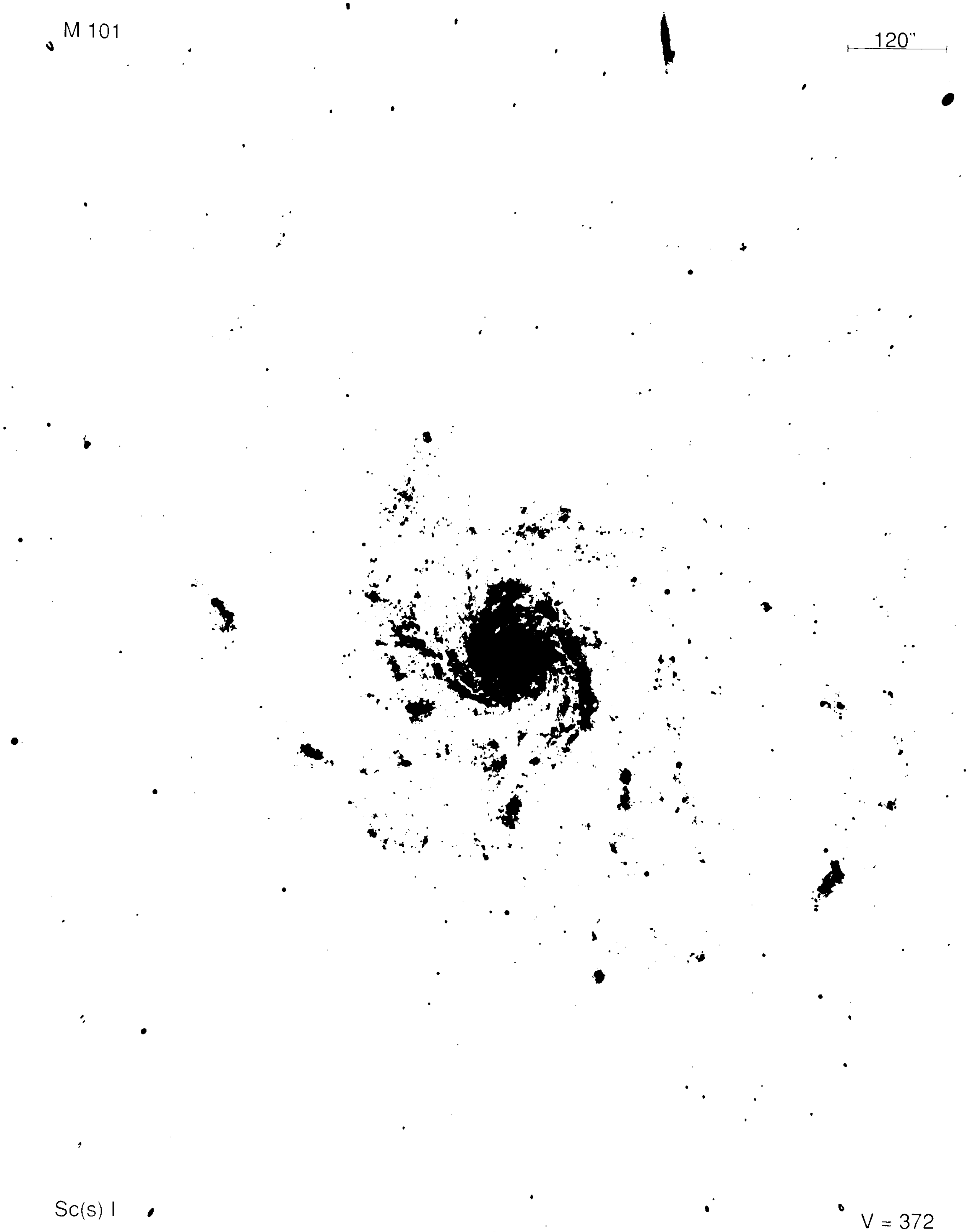
M 101
120"
Sc(s) I
V = 372

NGC 5585

Sd(s) IV

V = 441

NGC 5068

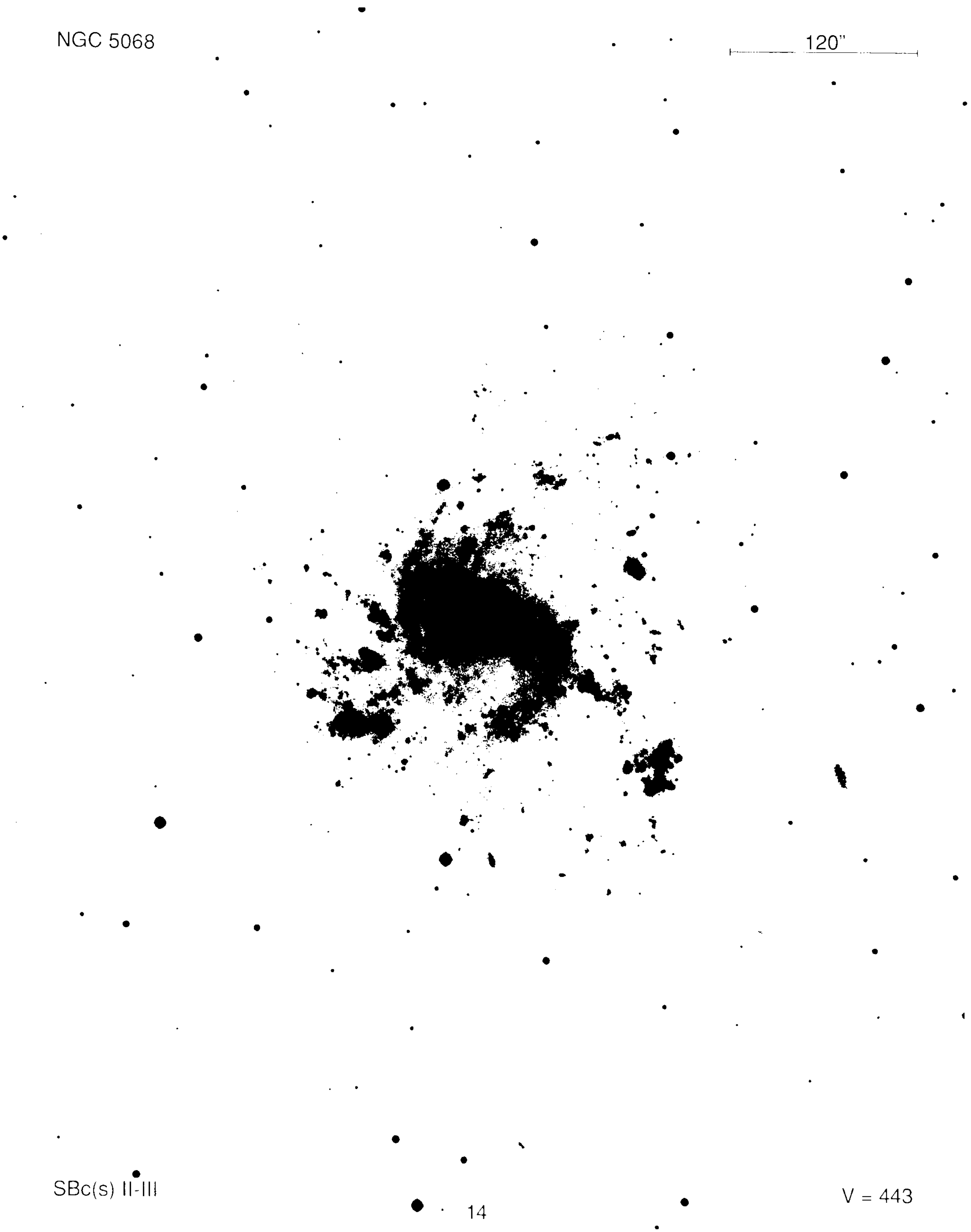

SBc(s) II-III

V = 443

NGC 2366

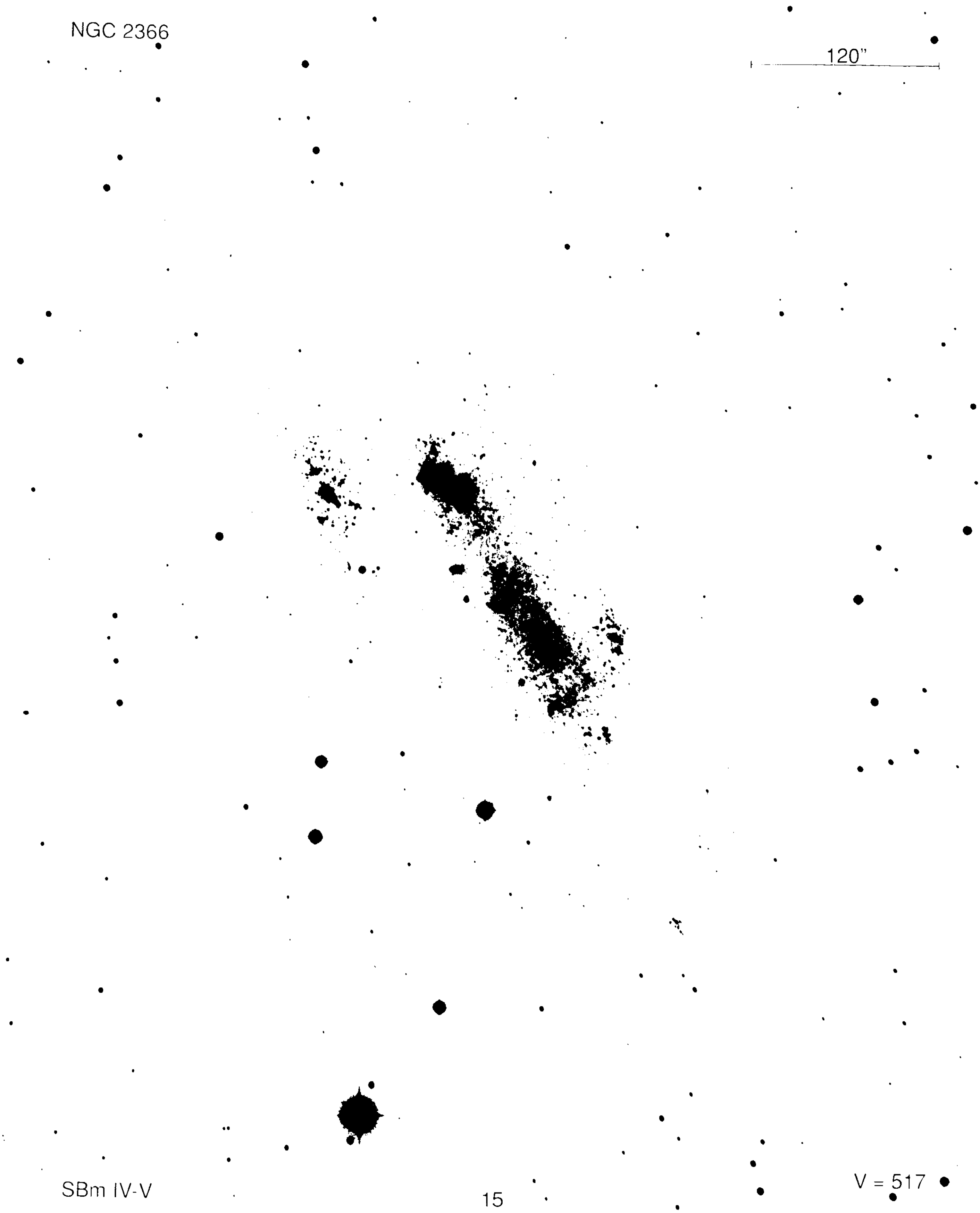

SBm IV-V

V = 517

M 81

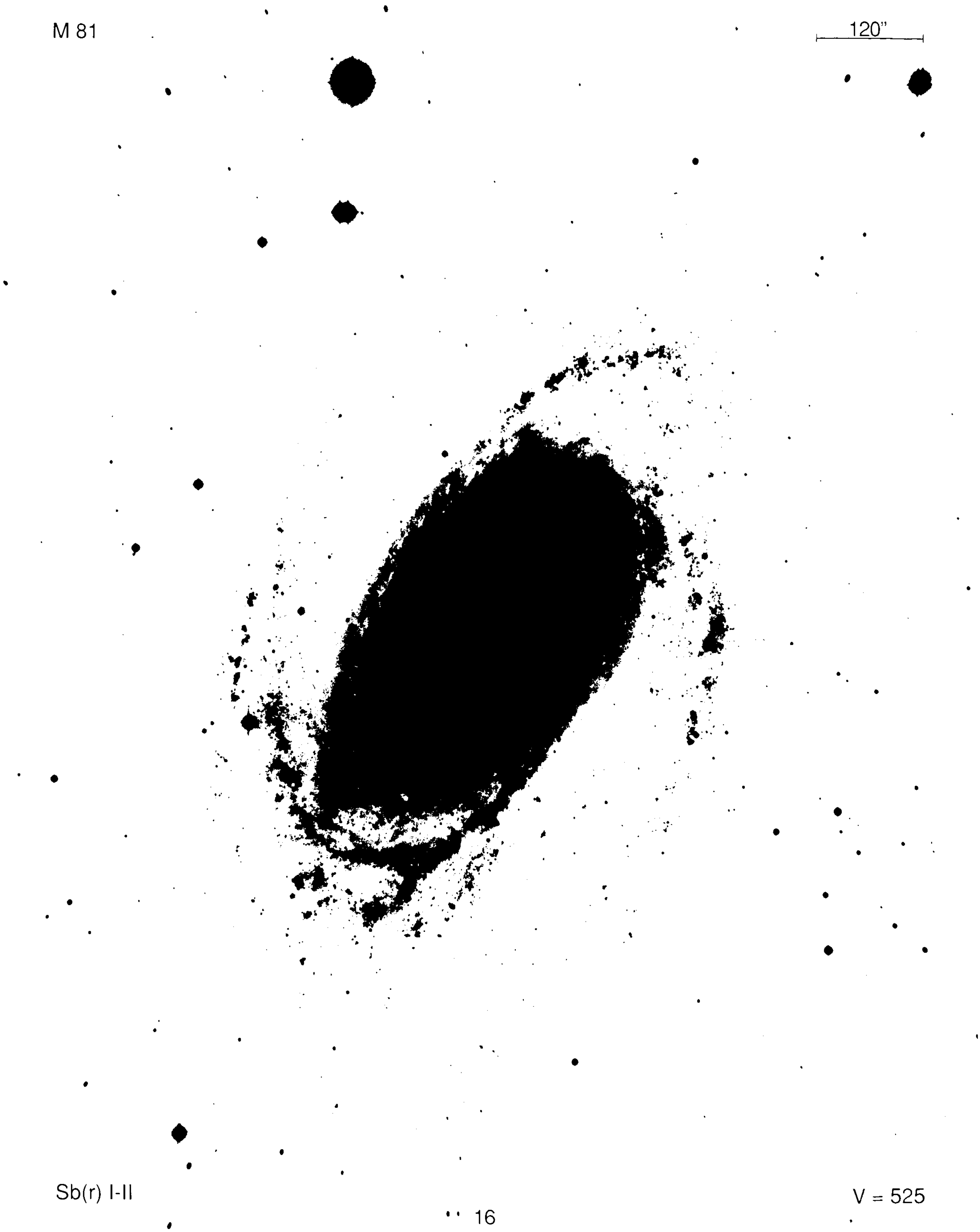

Sb(r) I-II

V = 525

N45

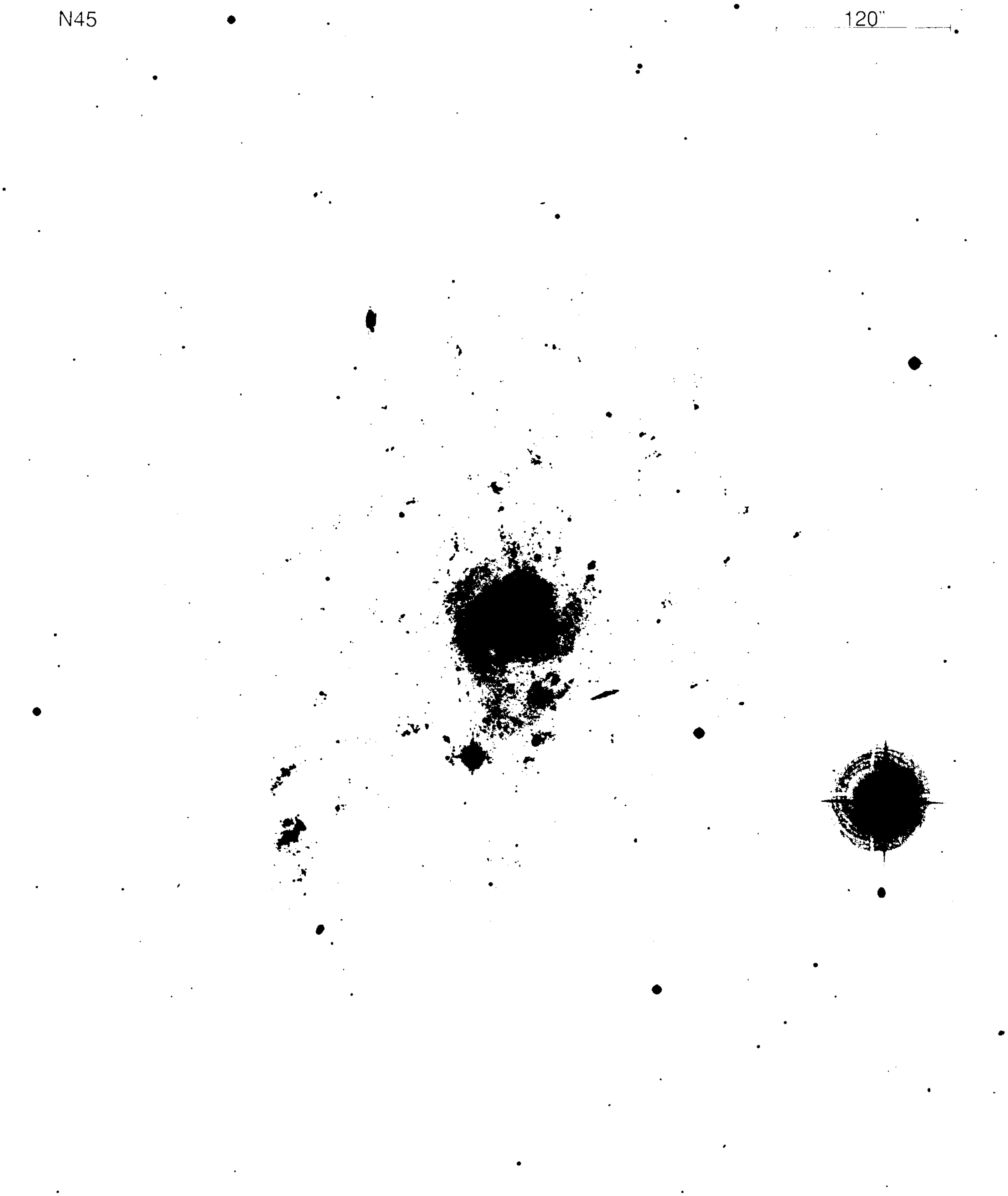

Scd(s) III

V = 533

N 3184

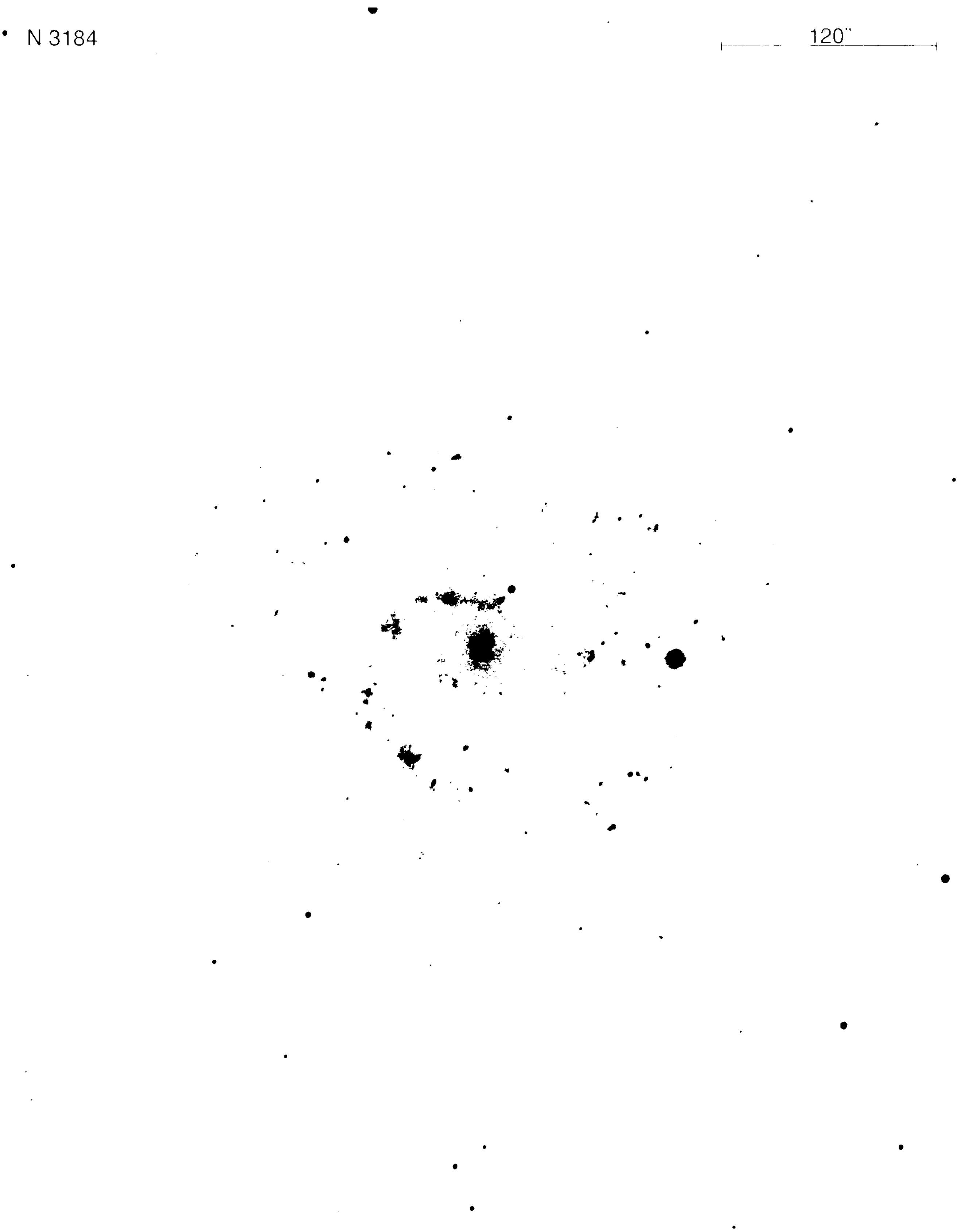

Sc(r) II.2

V = 607

NGC 3344

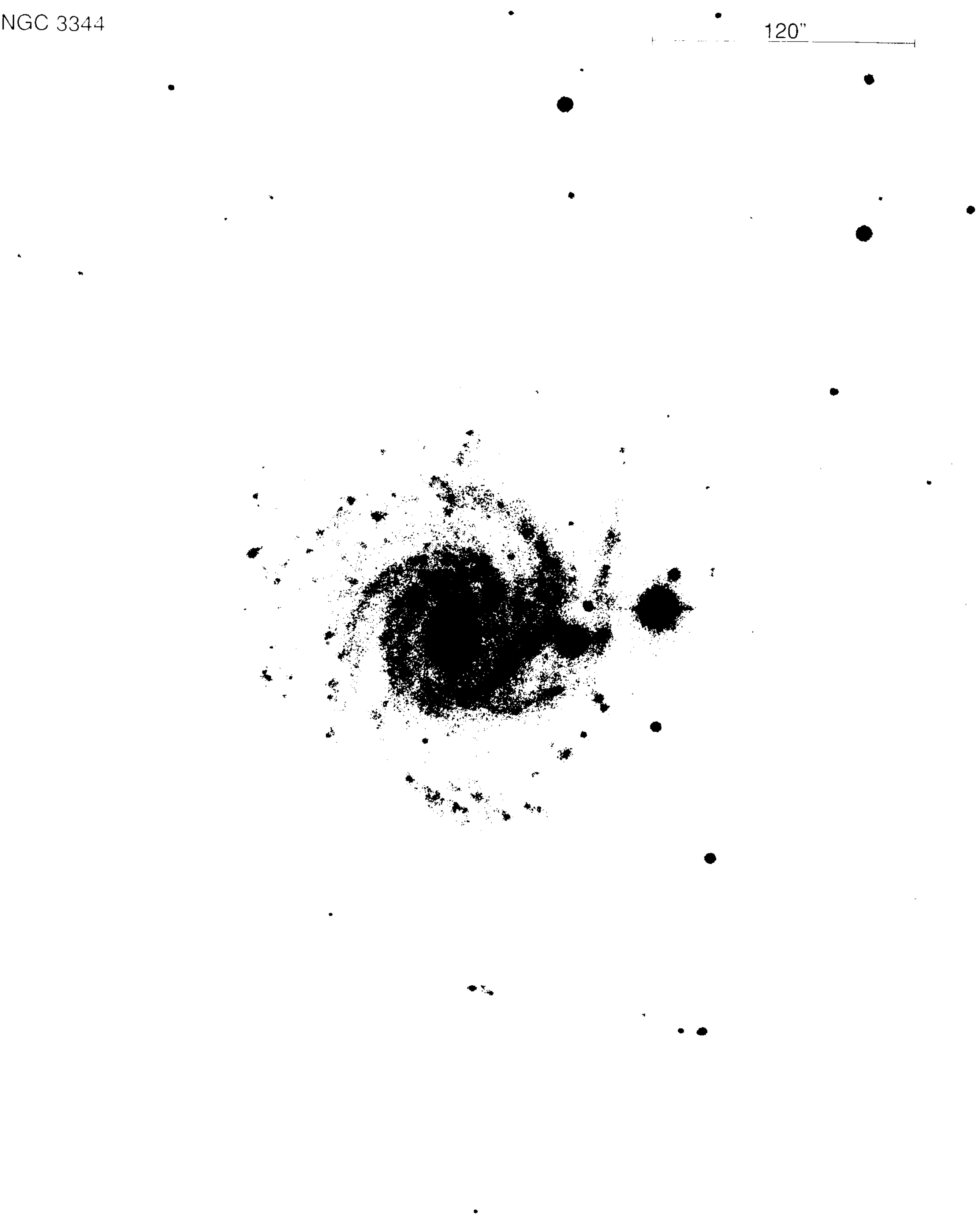

Sbc(rs) I.2

V = 627

N 3486

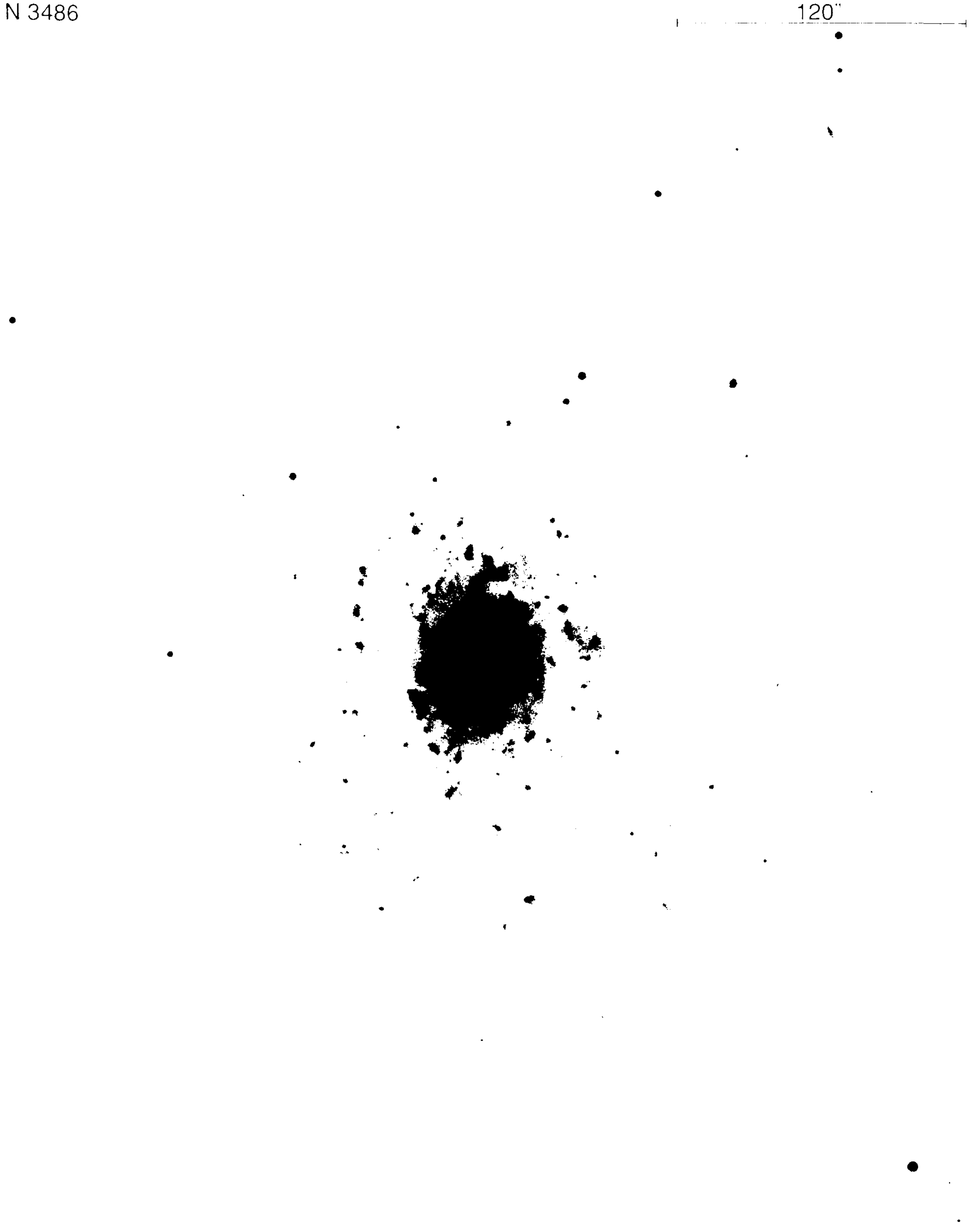

Sbc(r) I.2

V = 636

NGC 672

120"

SBc(s) III

V = 647

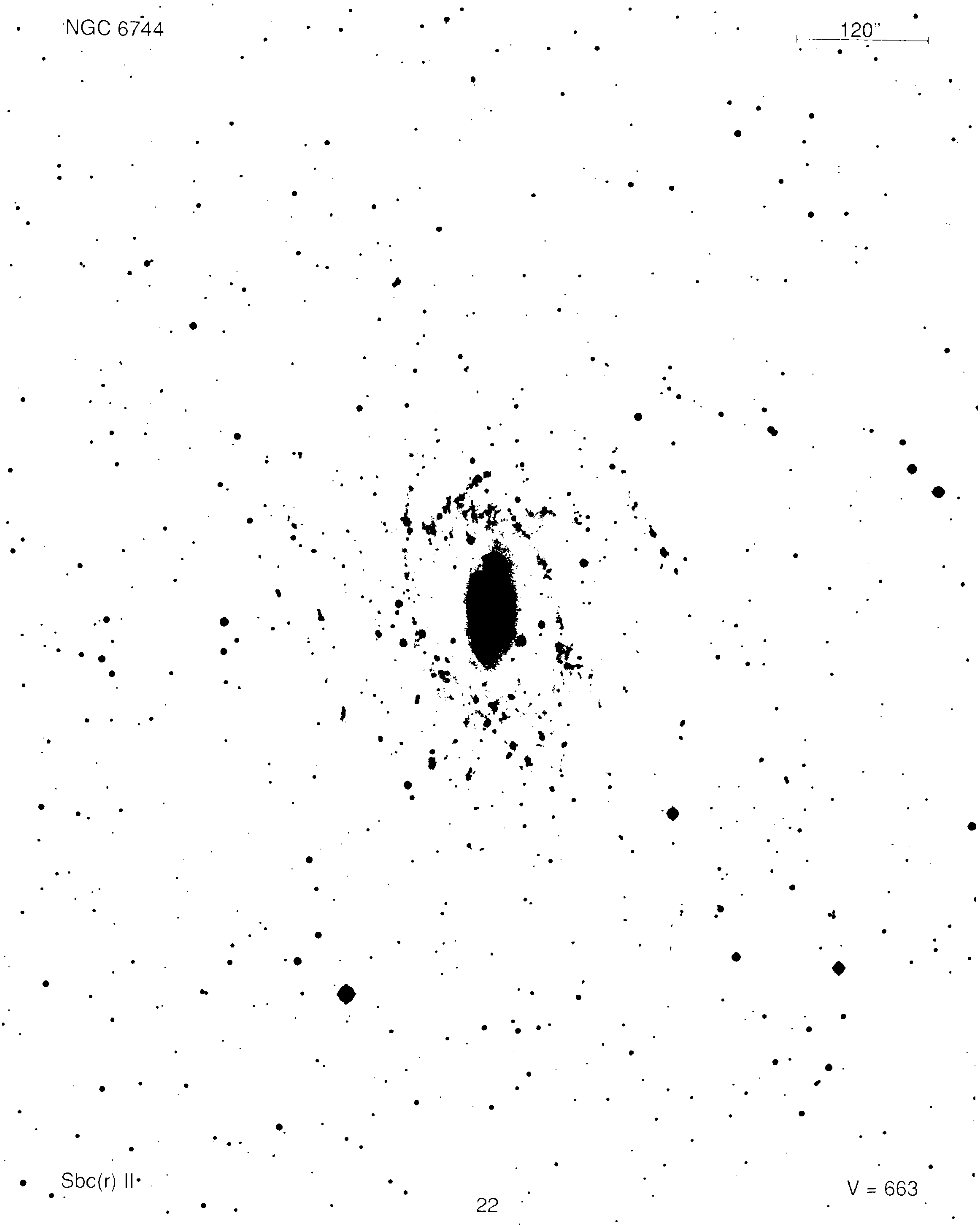
NGC 6744
120"
Sbc(r) II
V = 663

NGC 4051

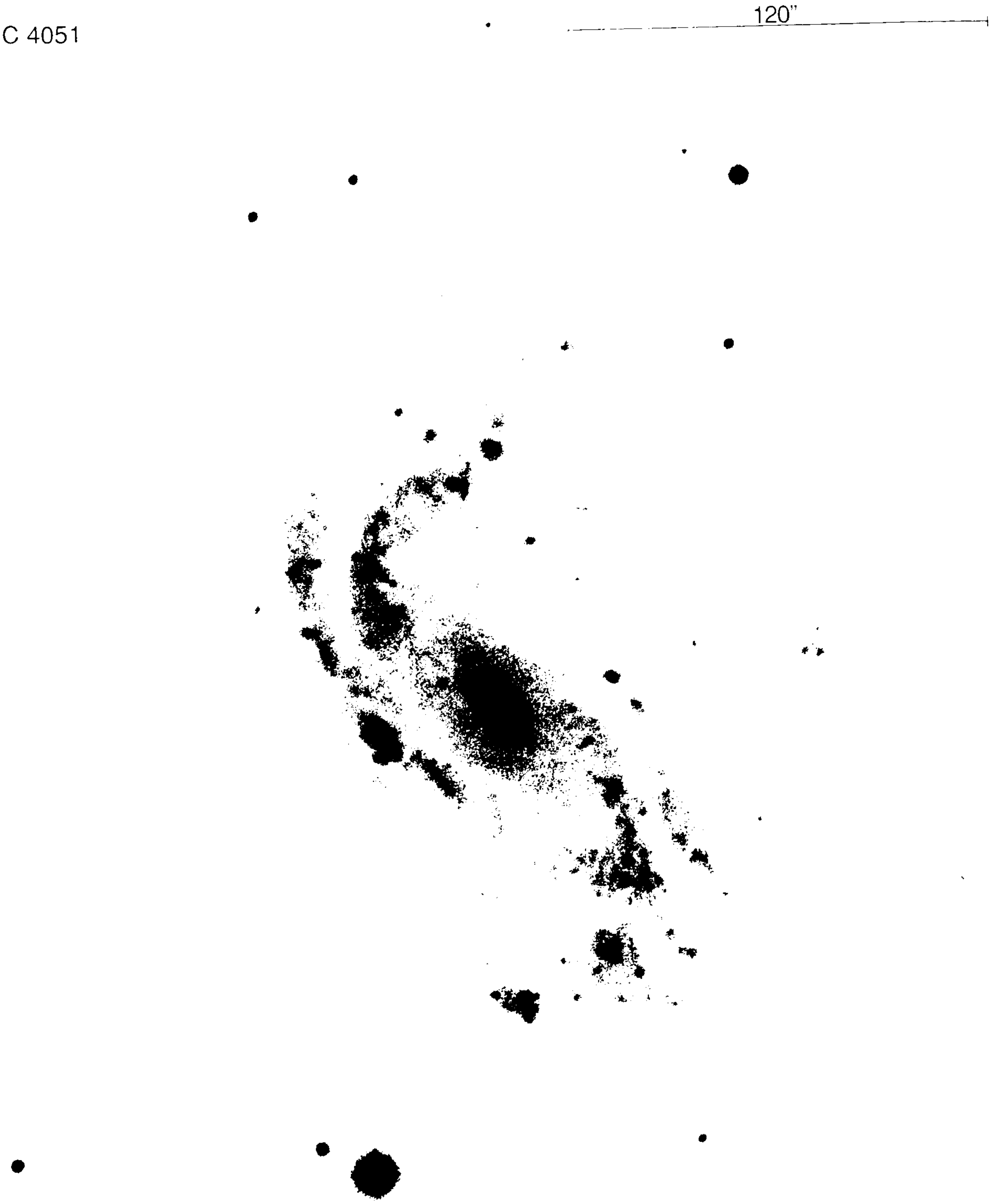

Sbc(r) II

V = 746

NGC 925

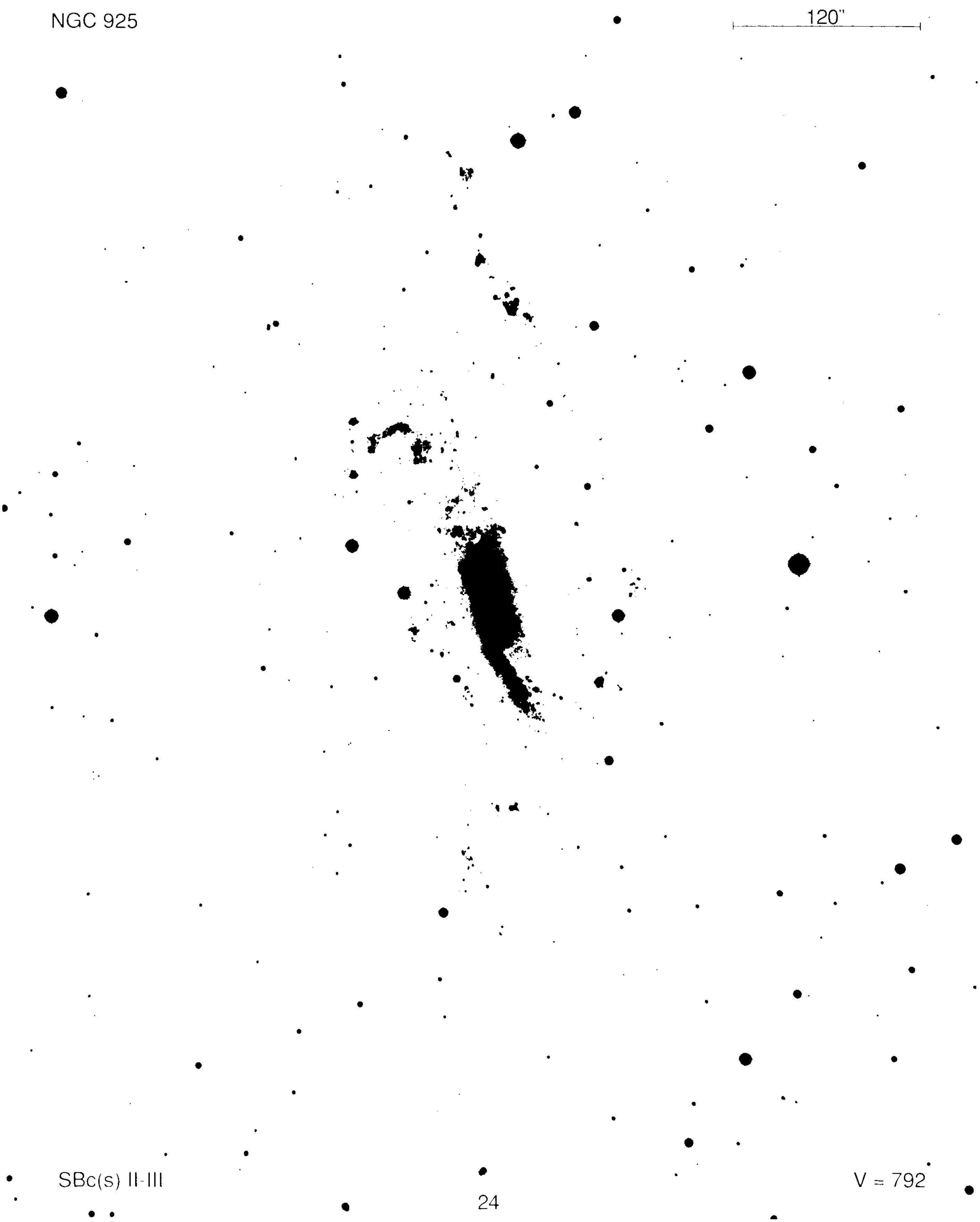

SBc(s) II-III

V = 792

NGC 2997

120"

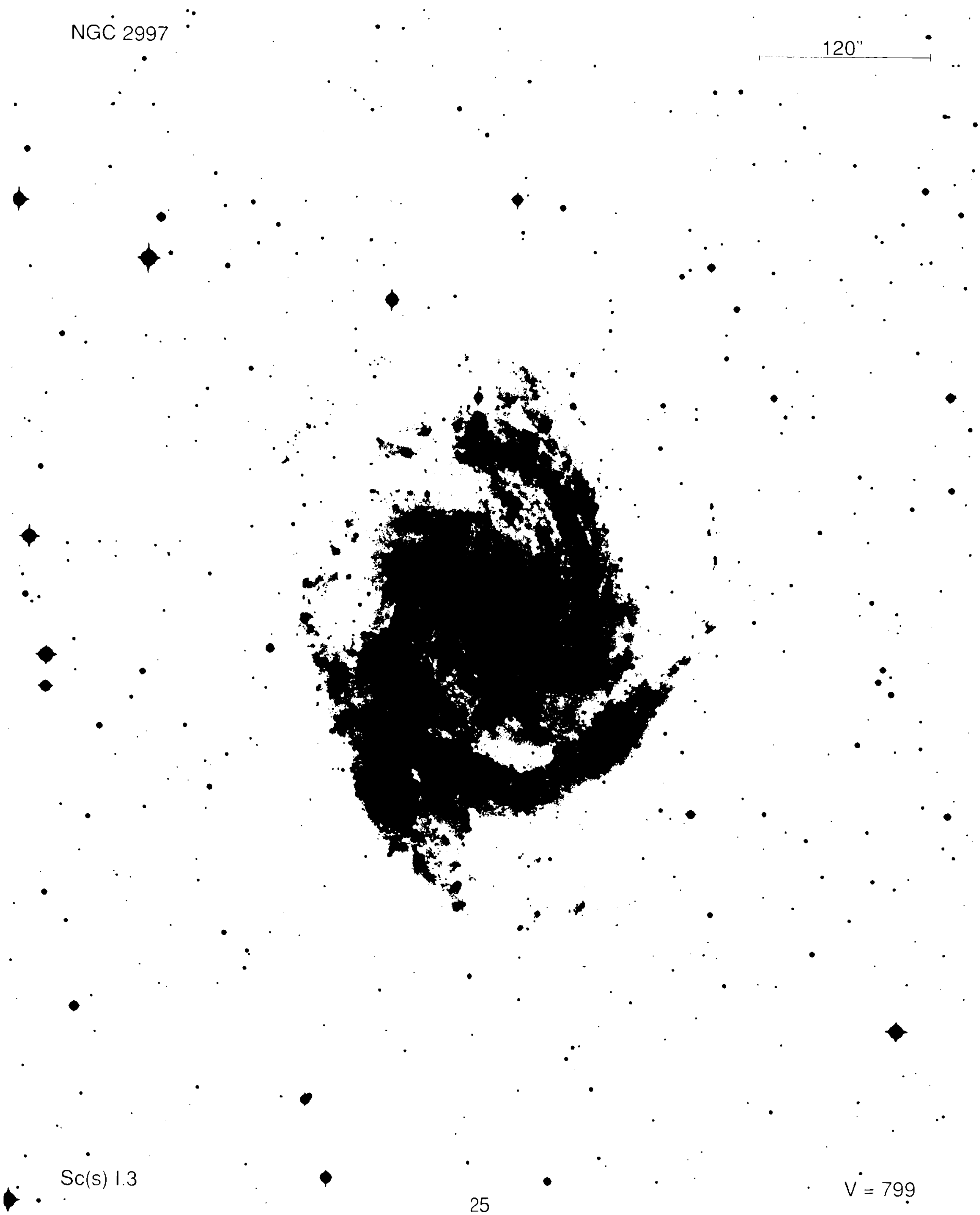

Sc(s) I.3

V = 799

NGC 628

120"

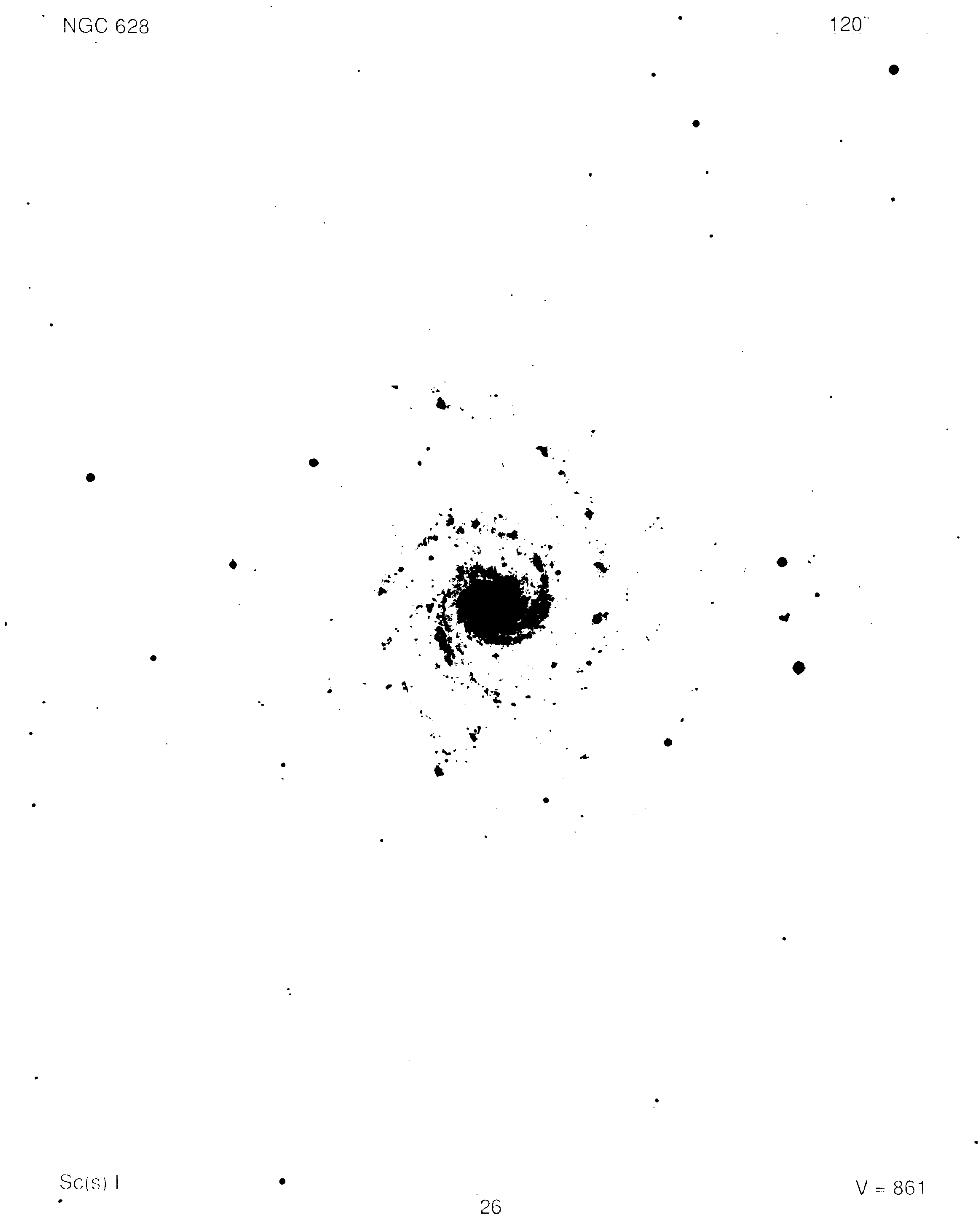

Sc(s) I

V = 861

NGC 3726

120"

Sbc(rs) II

V = 909

NGC 7424

SBc(s) II.3

V = 925

NGC 4145

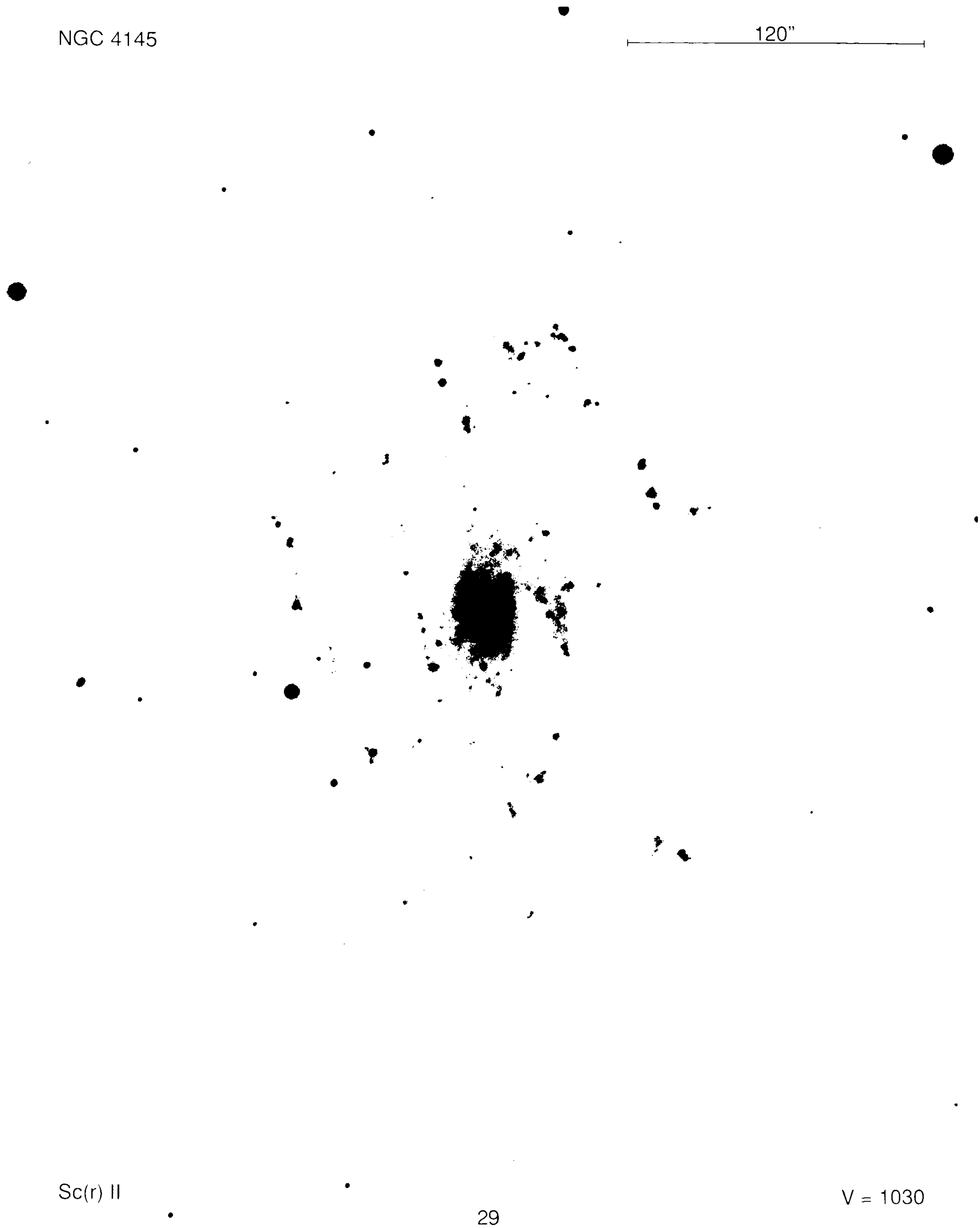

Sc(r) II

V = 1030

NGC 1531 / 32

Sbc(s) (tides?)

$V = \begin{cases} 1053 \\ 1105 \end{cases}$

NGC 5364

120"

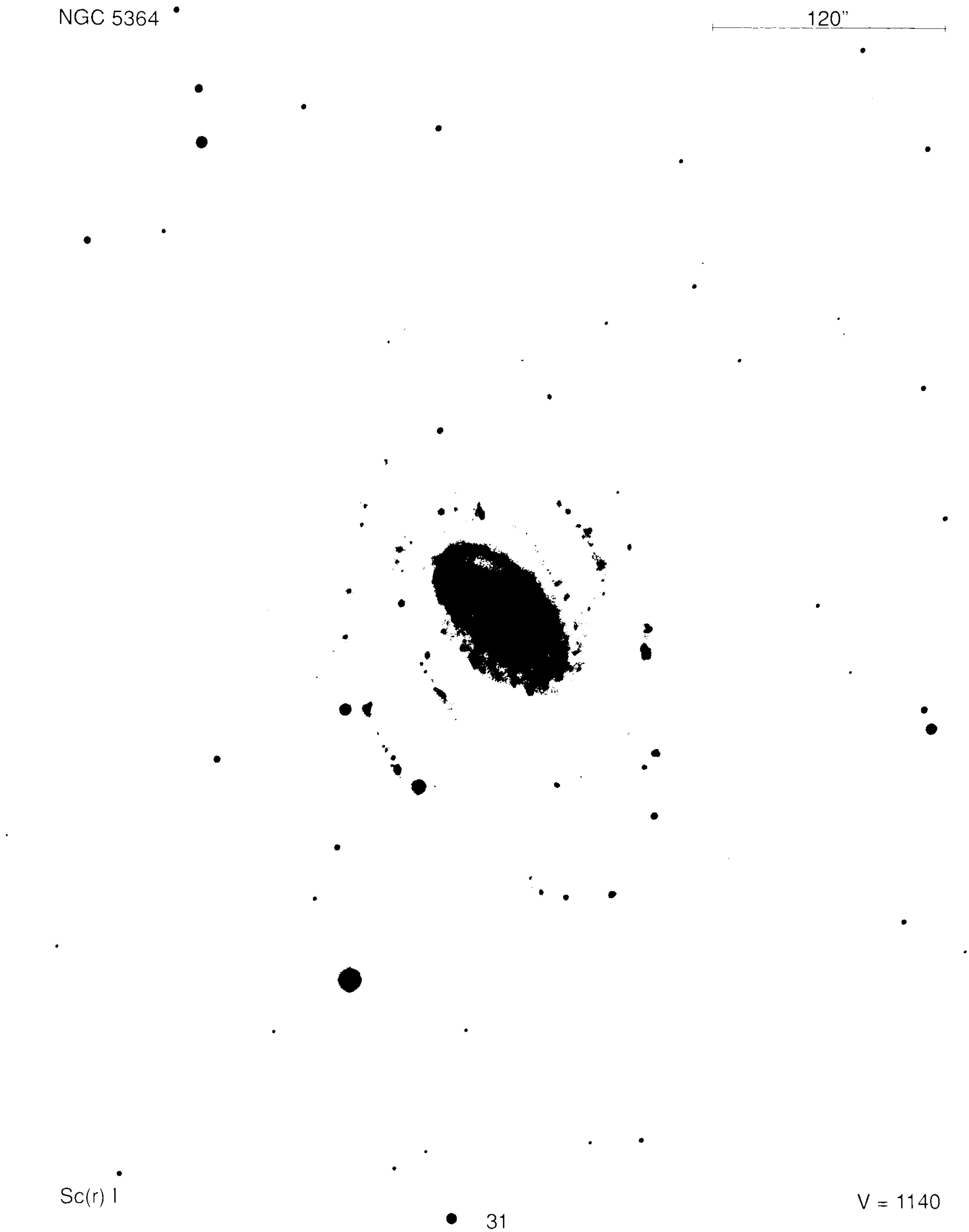

Sc(r) I

V = 1140

NGC 5247

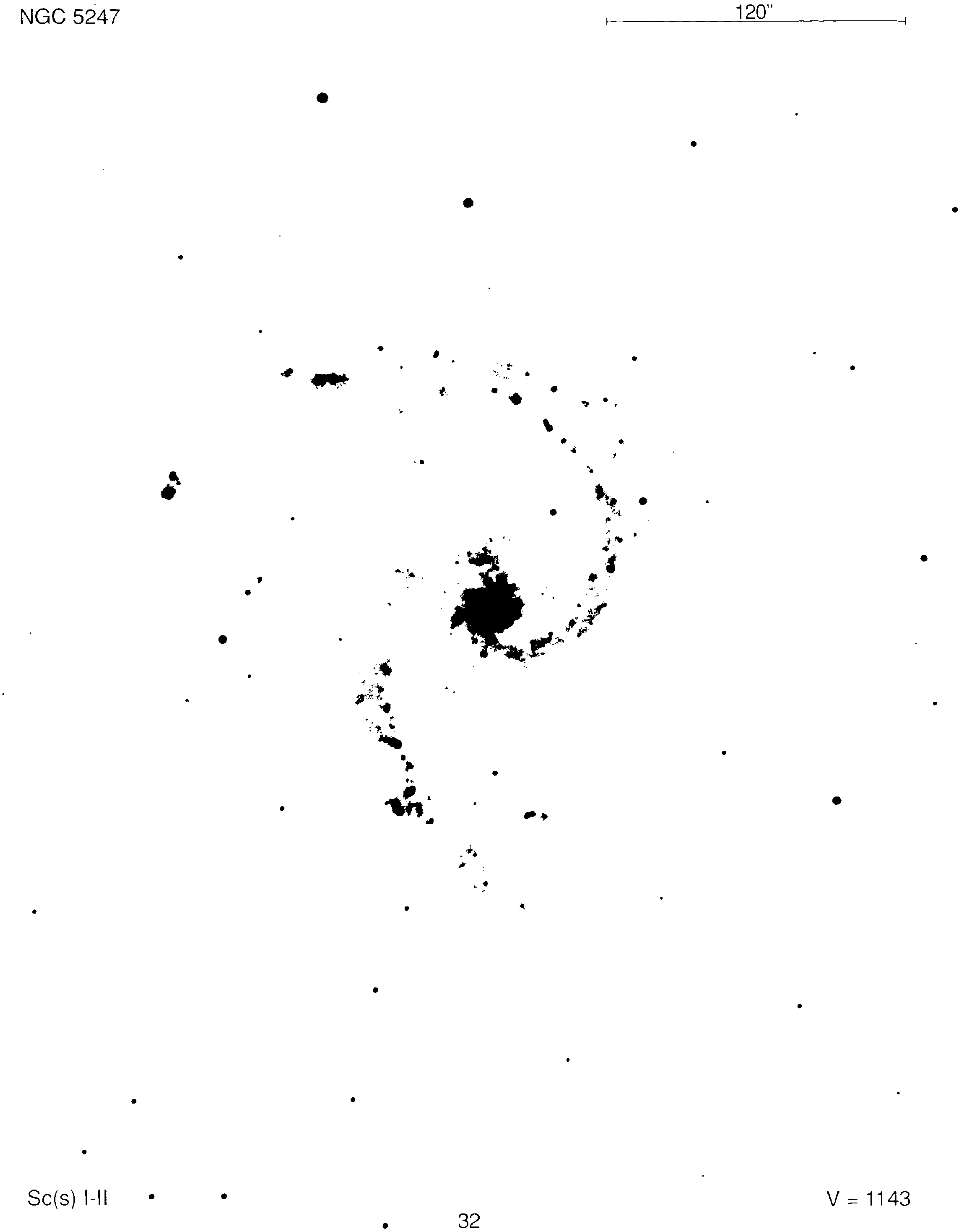

Sc(s) I-II

V = 1143

NGC 1566

120"

Sbc(s) I.2

V = 1305

NGC 2217

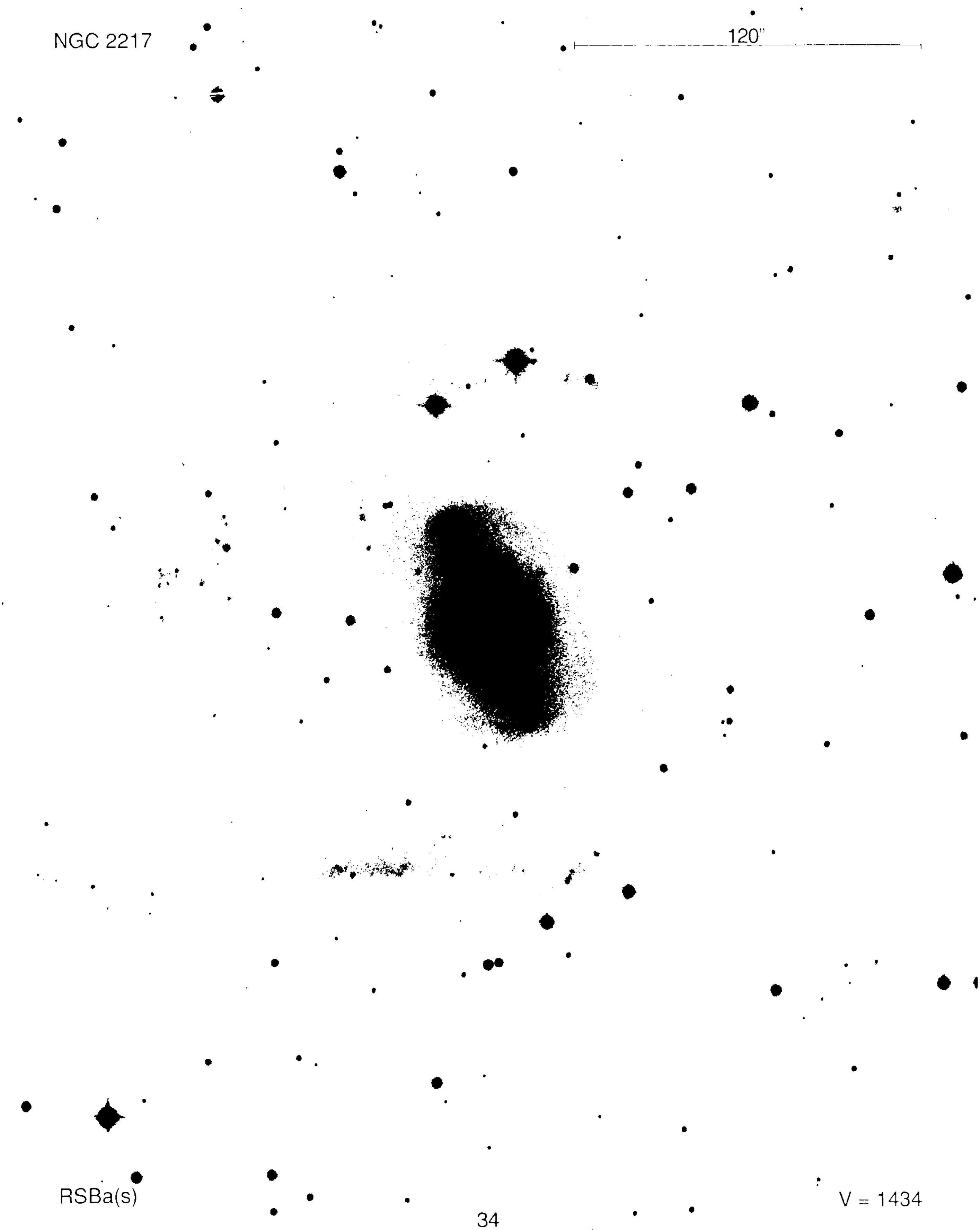

RSBa(s)

V = 1434

NGC 4321

Sc(s) I

V = 1464

NGC 1232

120"

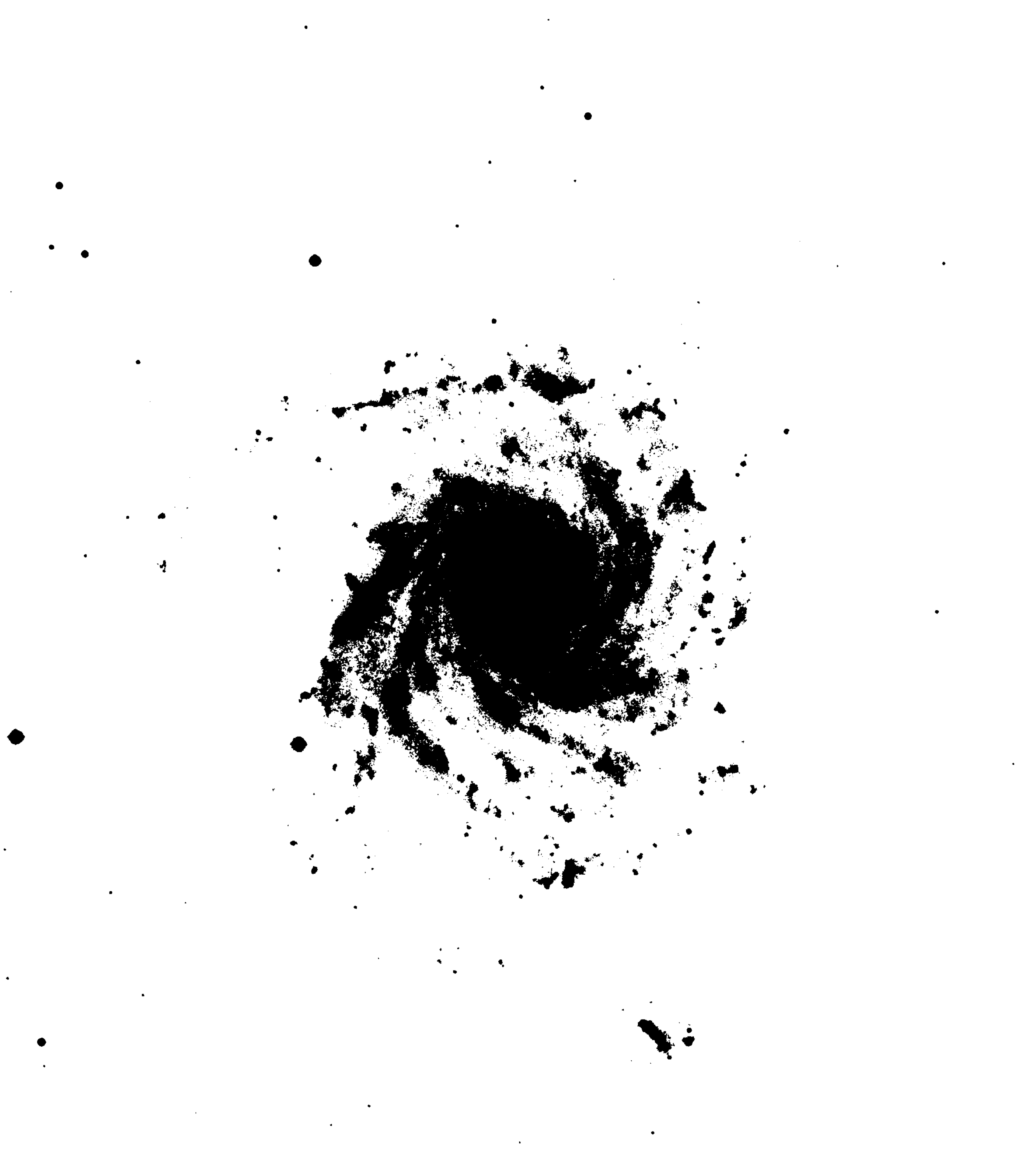

Sc(rs) I

V = 1775

Part II

The 21 panels on atlas panels 39 to 59 show those galaxies listed in Table 2 that are the most easily resolved in the sample. Some are small-scale reproductions of the enlarged images given in Part I.

The panels are arranged in order of Hubble type, and within each type, generally in order of Right Ascension. Note again that only the lowest surface brightness outer regions are expected to be useful for candidate areas of Cepheid searches because of low-resolution crowding. Photographic reproductions themselves are deceptive concerning relative surface brightness across galaxy disks. Using the darkroom art of contrast control, the photographer can vary the effective contrast of the final print to enhance faint surface brightness features for various emphases. False impressions of the true intensity ratios are the norm rather than the exception for all published photographs of galaxies. The cause is, of course, the nonlinear response of photographic density to the incident intensity. This nonlinearity offers the advantage of seeing different parts of different galaxies differently, but it includes the disadvantage that relative intensities cannot be well judged from the photographs—a crucial point in choosing HST targets.

Many of the images in this and in the next section of the atlas are shown twice, once with low contrast and once with high, thereby permitting more careful inspection of appropriate HST target areas. When two images are shown in this atlas, they often have been made from the same negative, showing the great control of the photographic contrast available in the darkroom.

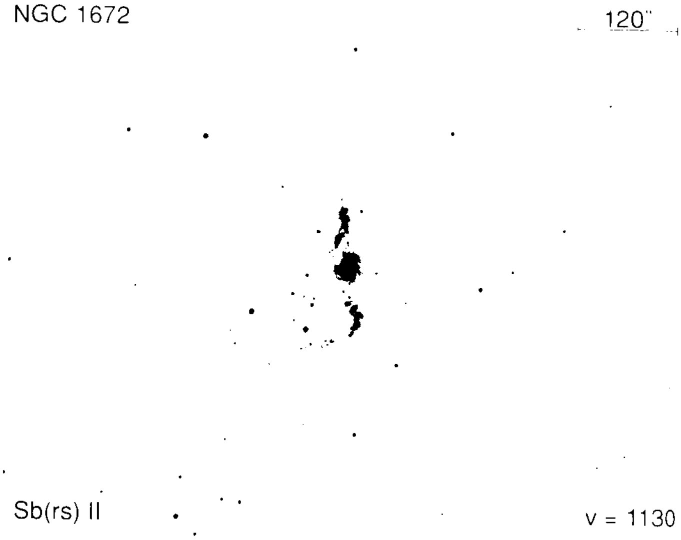
NGC 1672
120"
Sb(rs) II
v = 1130

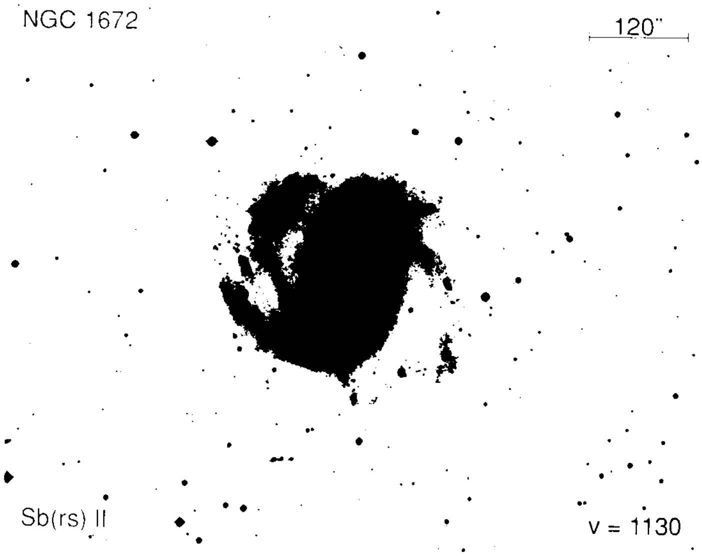
NGC 1672
120"
Sb(rs) II
v = 1130

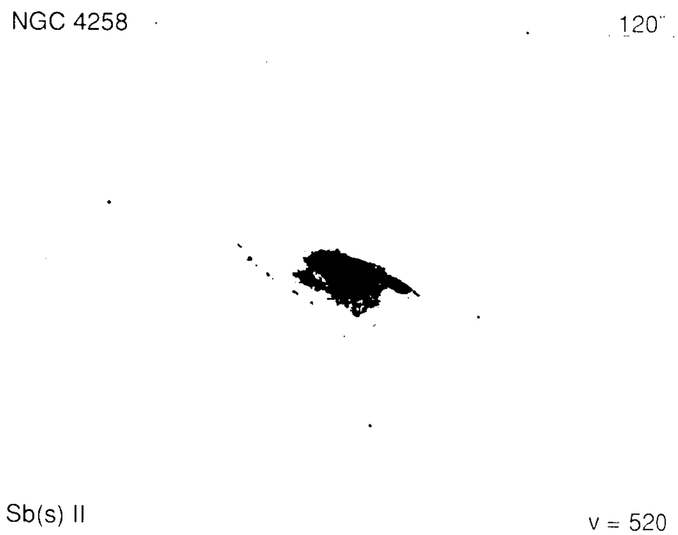
NGC 4258
120"
Sb(s) II
v = 520


NGC 4258
120"
Sb(s) II
v = 520

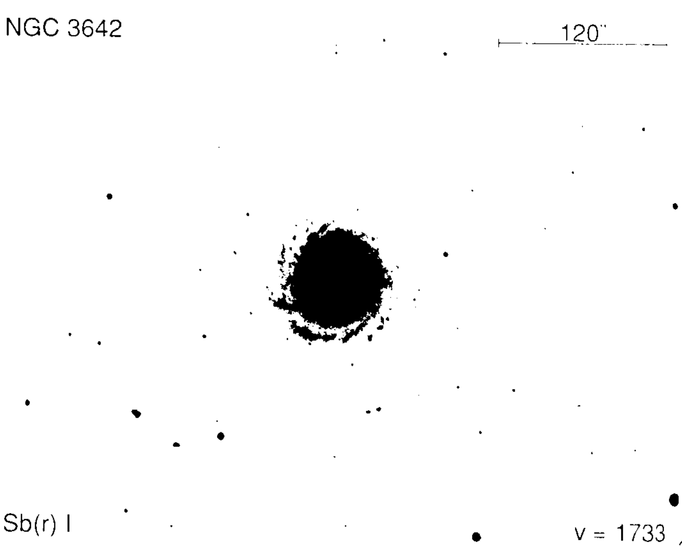
NGC 3642
120"
Sb(r) I
v = 1733

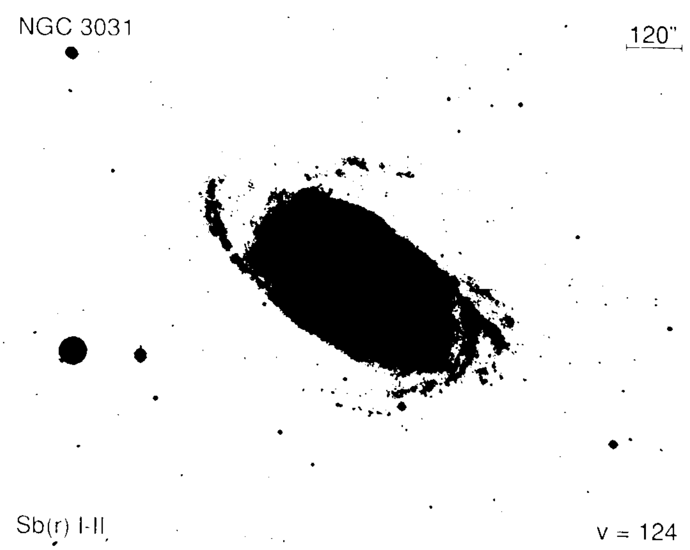
NGC 3031
120"
Sb(r) I-II
v = 124

NGC 5033 120"

Sb(s) I v = 897

NGC 5033 120"

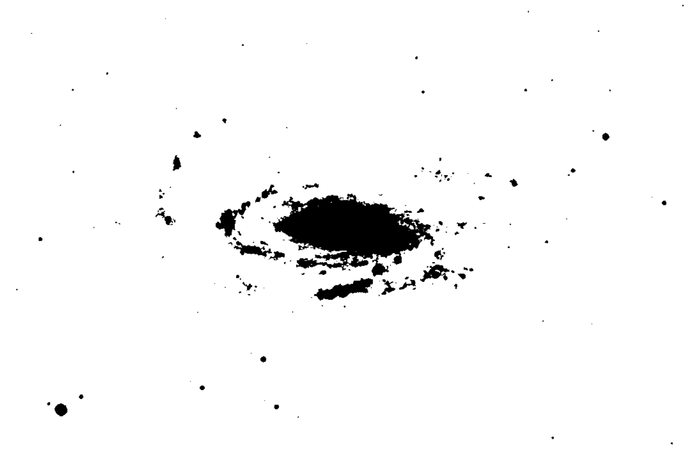

Sb(s) I v = 897

NGC 5879 120"

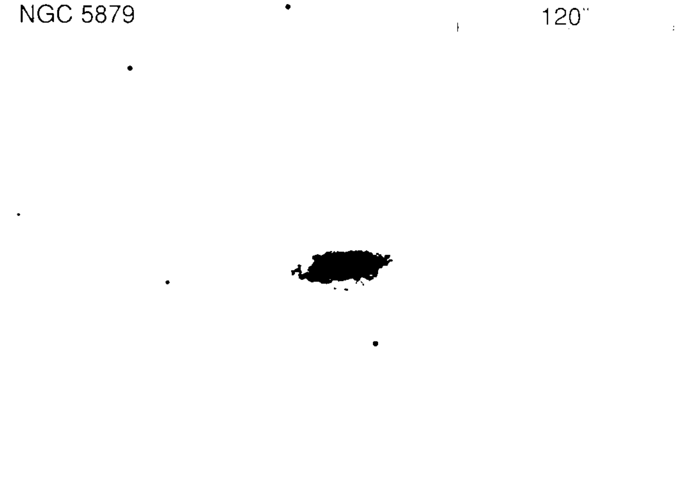

Sb(s) II v = 929

NGC 5879 120"

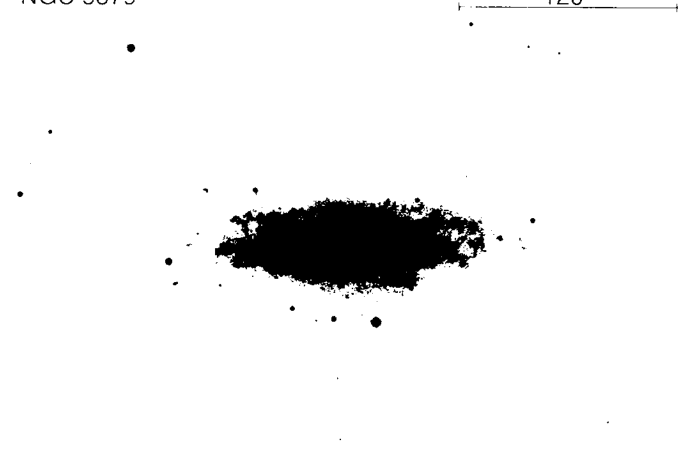

Sb(s) II v = 929

NGC 7331 120"

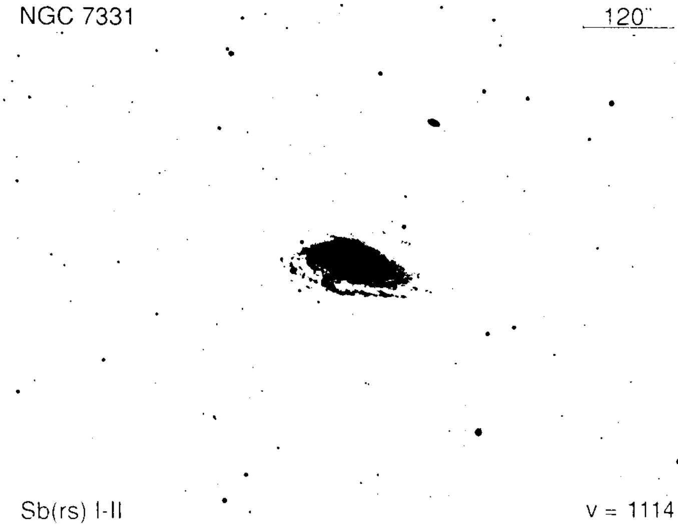

Sb(rs) I-II v = 1114

NGC 7331 120"

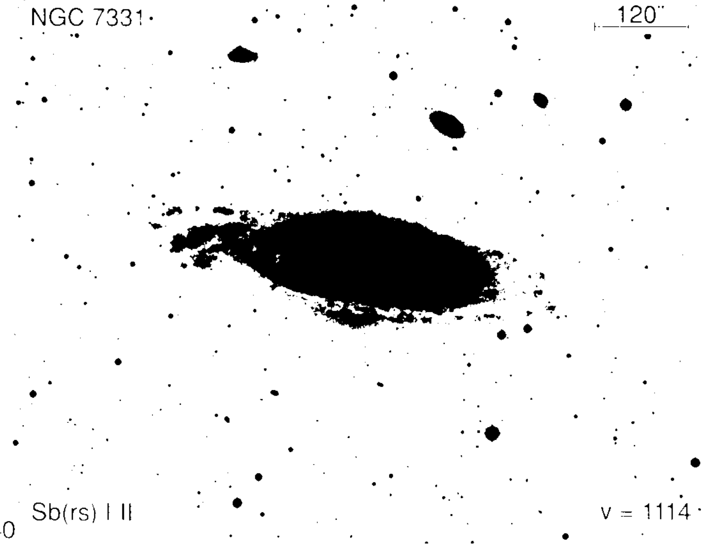

Sb(rs) I II v = 1114

NGC1433 120"

SBb(s) I-II v = 923

NGC 1433 120"

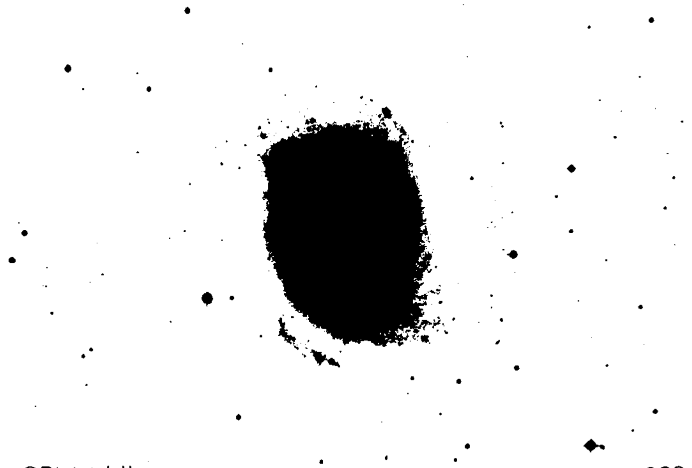

SBb(s) I-II v = 923

NGC 1512 120"

SBb(rs) I pec v = 760

NGC 1512 120"

SBb(rs) I pec v = 760

NGC 4394 120"

SBb(sr) I-II v = 853

NGC 4394 120"

SBb(s) I-II v = 853

NGC 4725 120"

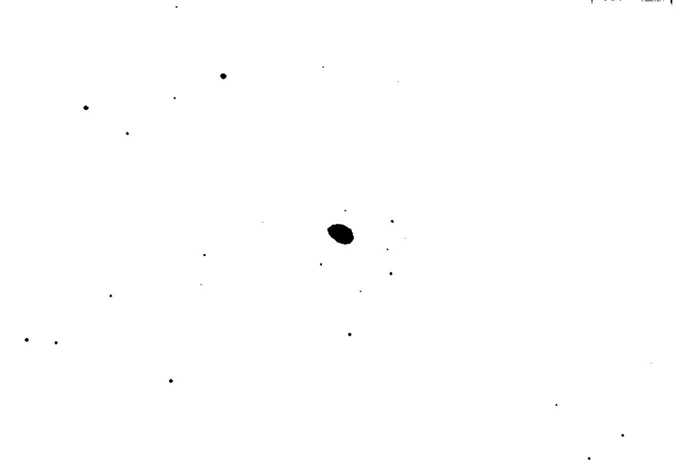

Sb/SBb(r) II v = 1167

NGC 4725 120"

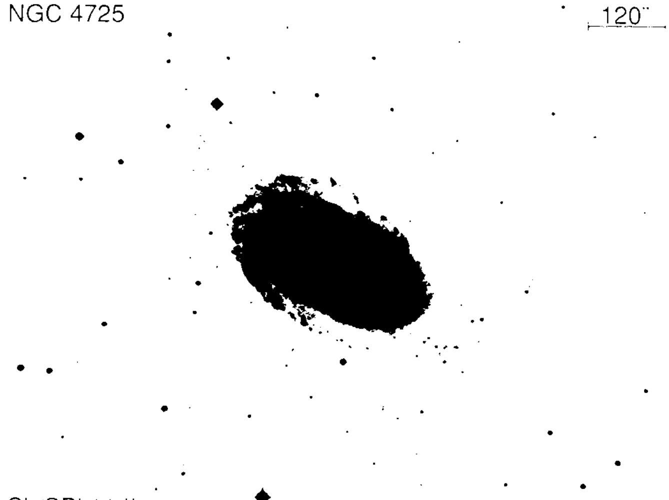

Sb/SBb(r) II v = 1167

NGC 1365 120"

SBbc(s) I v = 1562

NGC 4123 120"

SBbc(rs) I.8 v = 1157

NGC 4618 120"

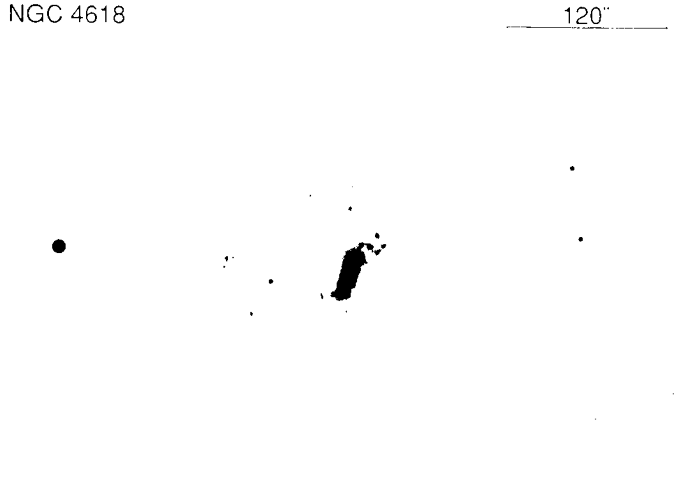

SBbc(rs) II.2 v = 563

NGC 5921 120"

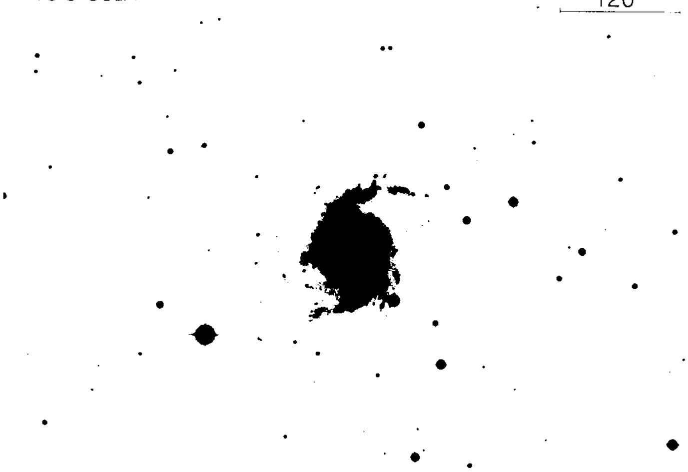

SBbc(s) I-II v = 1428

NGC 1566 120"

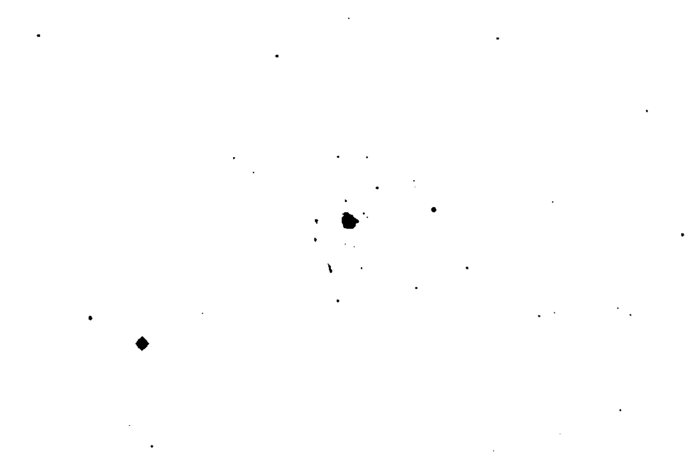

Sbc(s) I.2 v = 1305

NGC 1566 120"

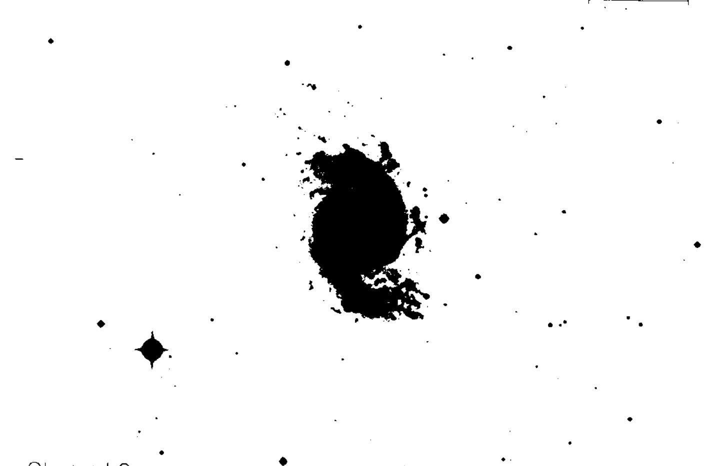

Sbc(s) I.2 v = 1305

NGC 3486 120"

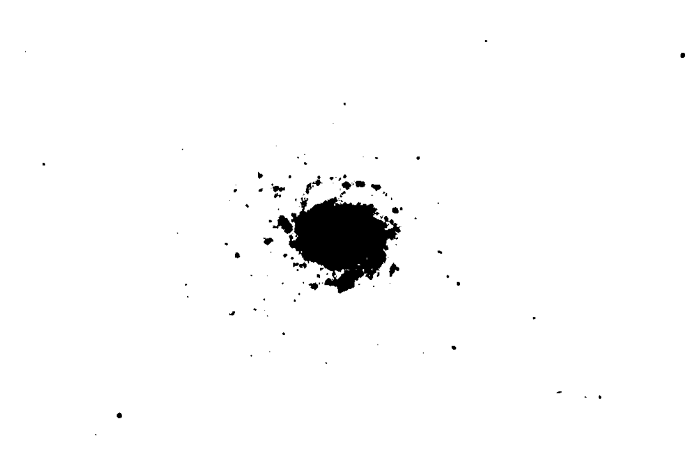

Sbc(r) I.2 v = 626

NGC 3726 120"

Sbc(rs) II v = 909

NGC 3521 120"

Sbc(s) II v = 627

NGC 3521 120"

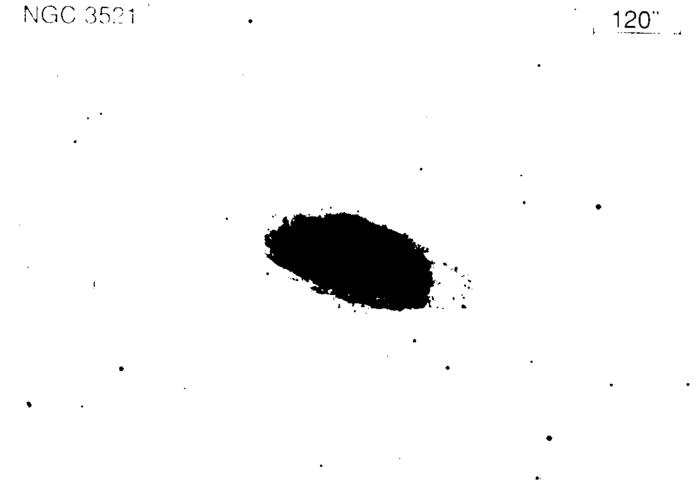

Sbc(s) II v = 627

NGC 5194/5
Hα
120"

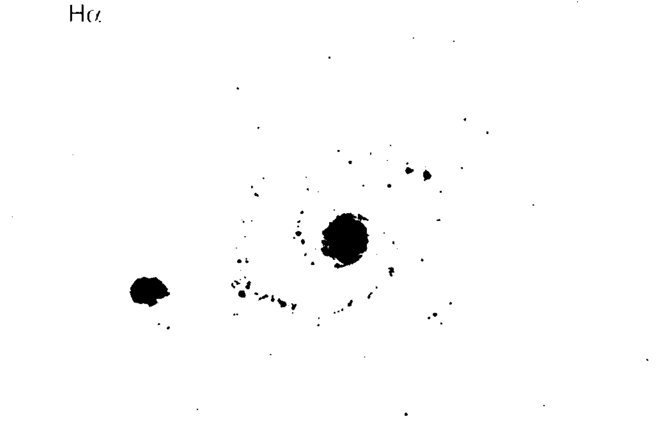

Sbc(s) I-II
v = 541

NGC 5194/5
120"

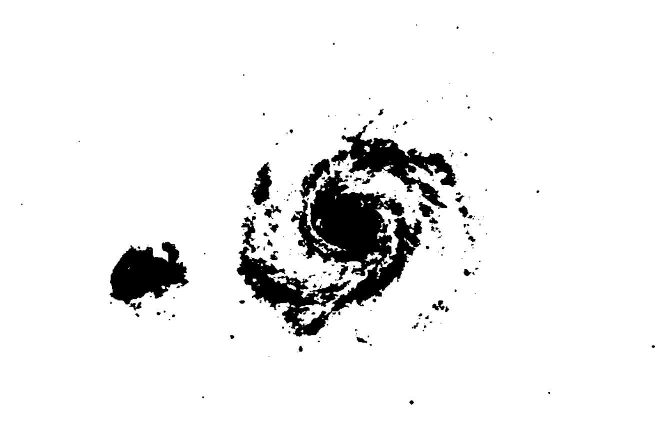

Sbc(s) I-II
v = 541

NGC 4051
120"

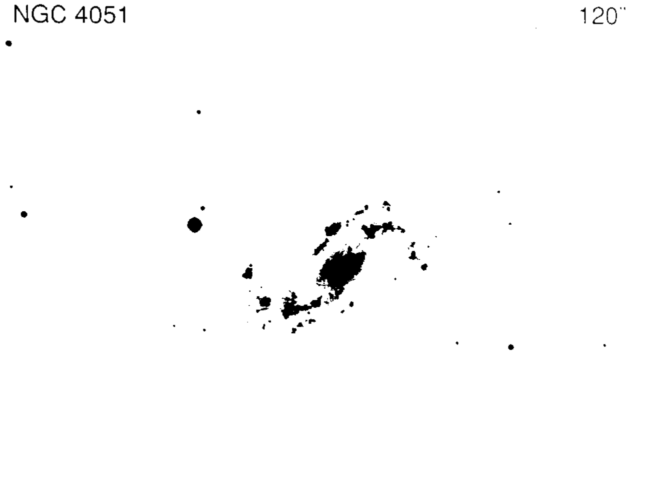

Sbc(r) II
v = 746

NGC 5248
120"

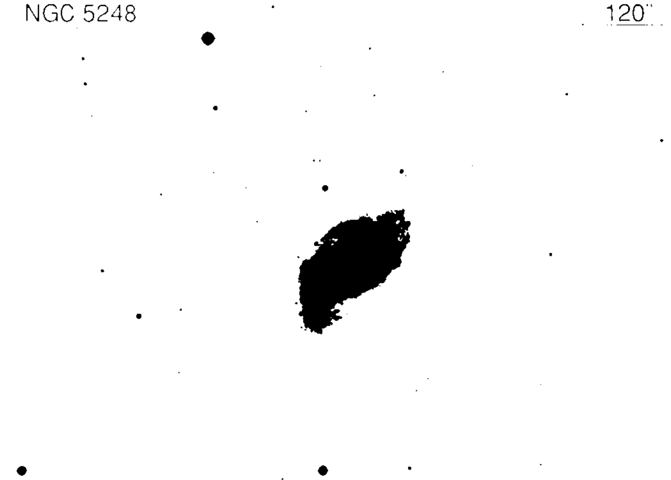

Sbc(s) I-II
v = 1049

NGC 6744
120"

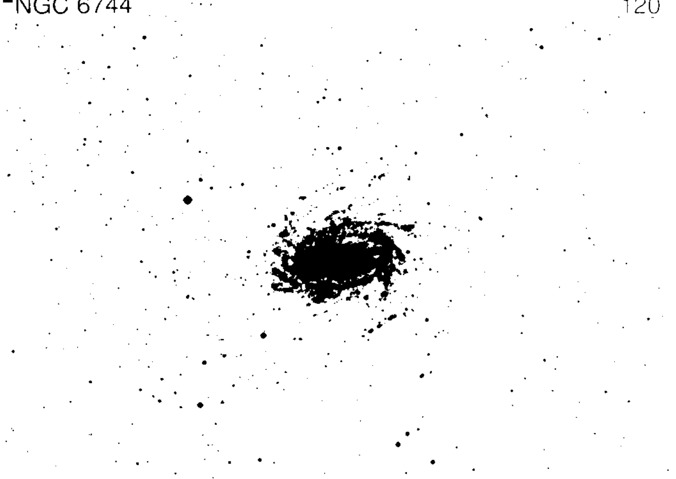

Sbc(r) II
v = 663

NGC 7531
120"

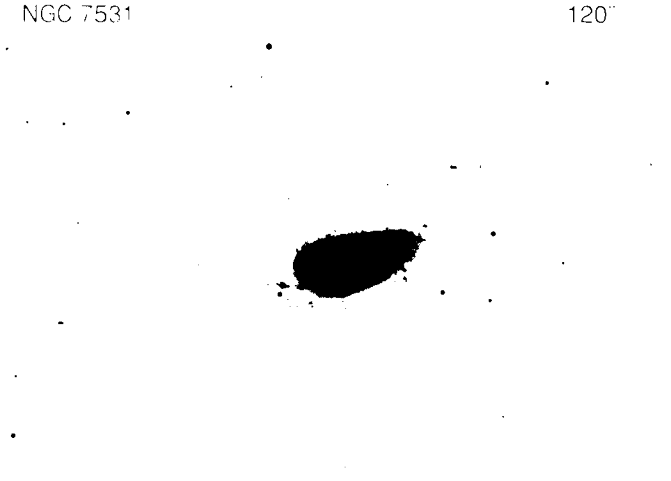

Sbc(r) I-II
v = 1607

NGC 1518 120"

Sc III v = 914

NGC 2090 120"

Sc(s) II v = 755

NGC 2403 120"

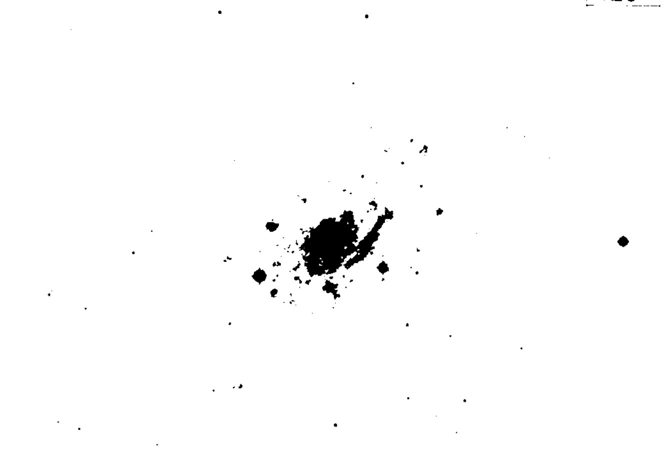

Sc(s) III v = 299

NGC 2403 120"

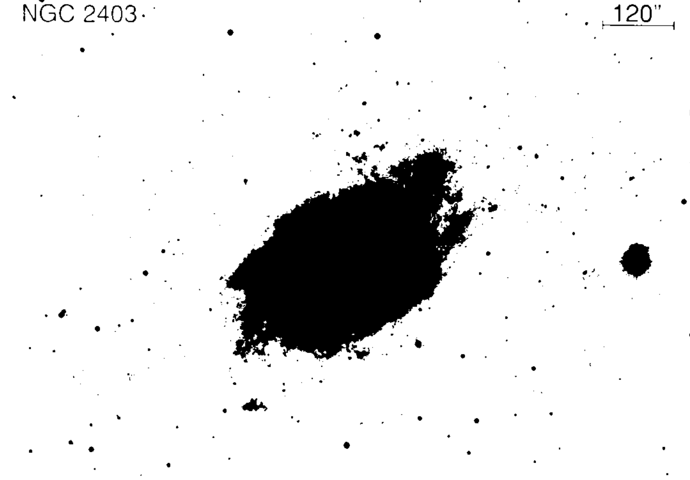

Sc(s) III v = 299

NGC 2541 120"

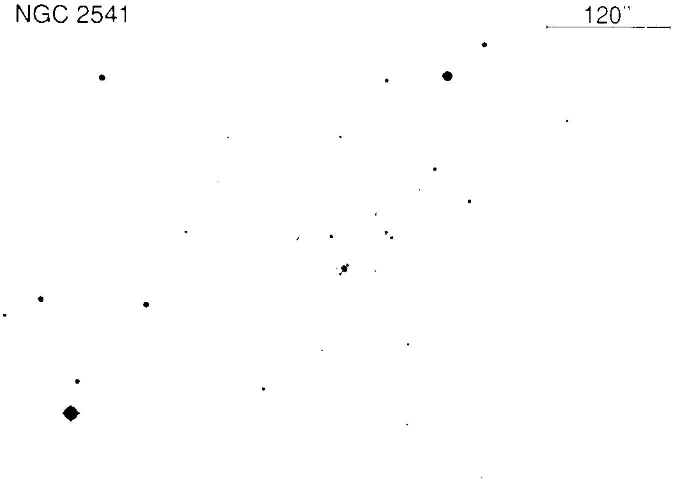

Sc(s) III v = 646

NGC 2541 120"

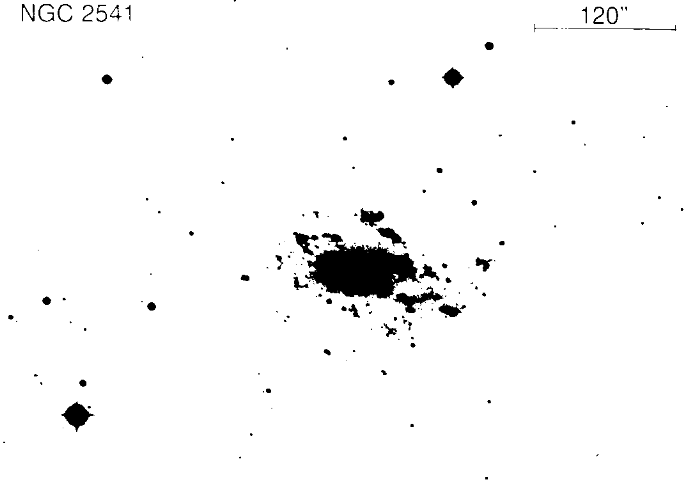

Sc(s) III v = 646

NGC 2500

120"

Sc(s) II.8

v = 615

NGC 3184

120"

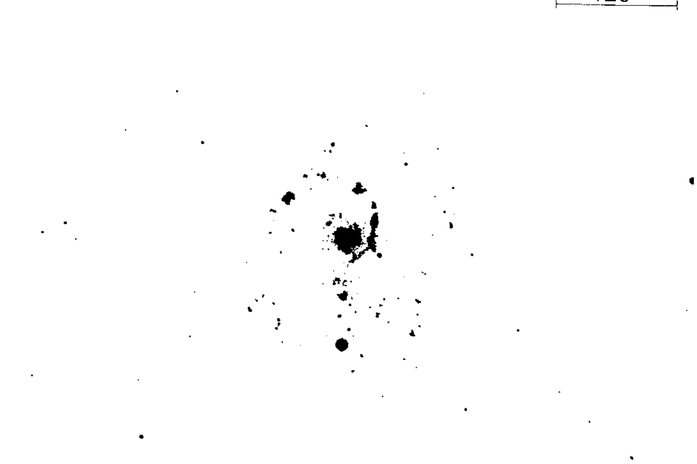

Sc(r) II.2

v = 607

NGC 2903
Hα

120"

Sc(s) I-II

v = 472

NGC 2903

120"

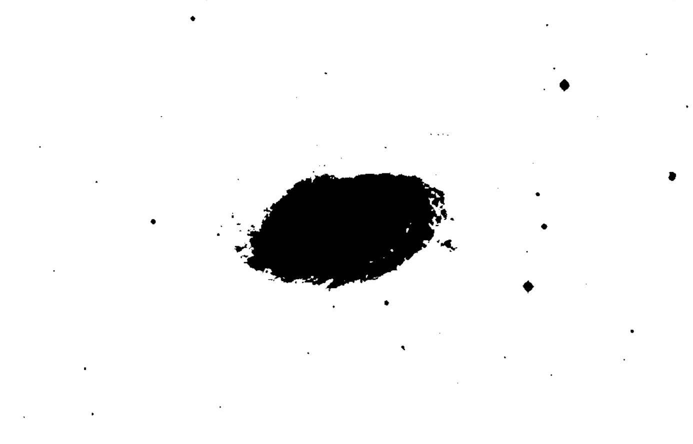

Sc(s) I-II

v = 472

NGC 2997

120"

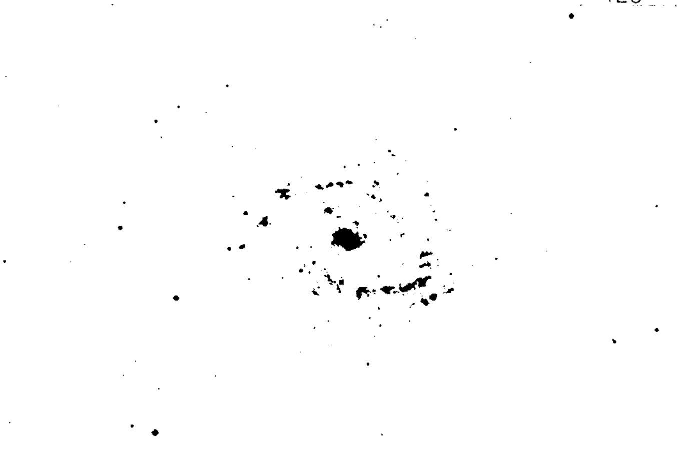

Sc(s) I.3

v = 799

NGC 2997

120"

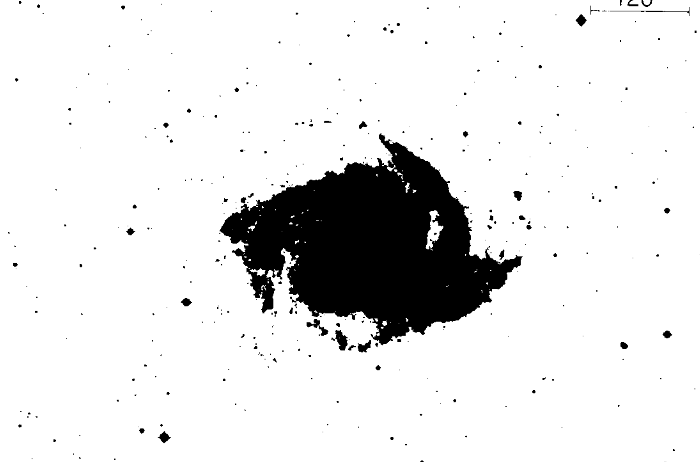

Sc(s) I.3

v = 799

NGC 3423 120"

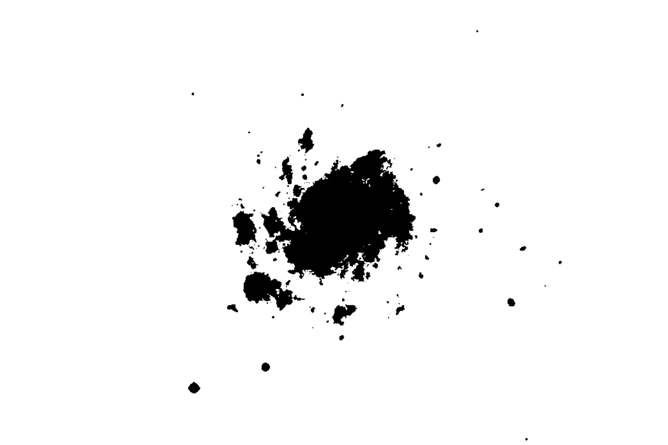

Sc(s) II.2 v = 845

NGC 3510 120"

Sc(warp) v = 660

NGC 3621 120"

Sc(s) II.8 v = 435

NGC 3621 120"

Sc(s) II.8 v = 435

NGC 3938 120"

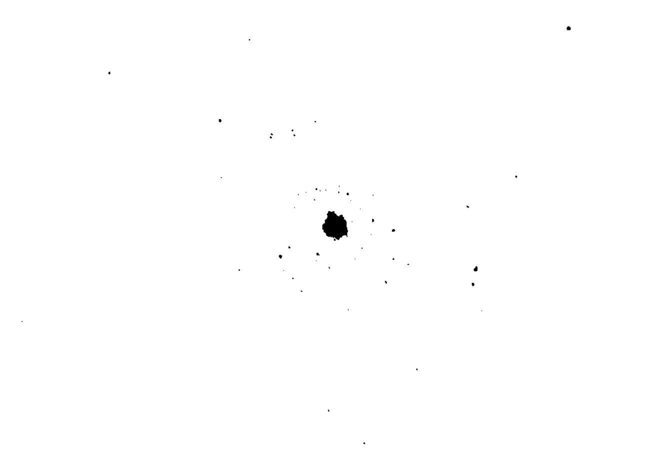

Sc(s) I v = 844

NGC 3938 120"

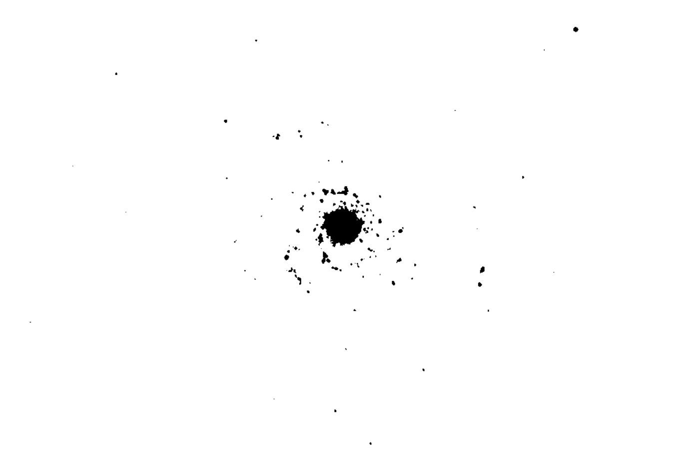

Sc(s) I v = 844

NGC 4136 120"

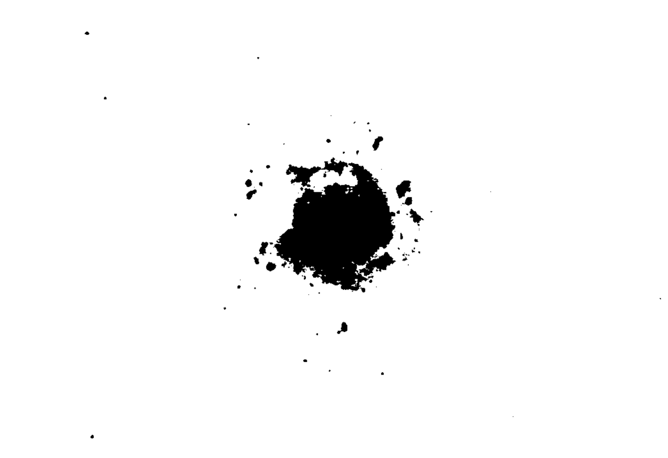

Sc(r) I-II v = 409

NGC 4145 120"

Sc(s) II v = 1030

NGC 4487 120"

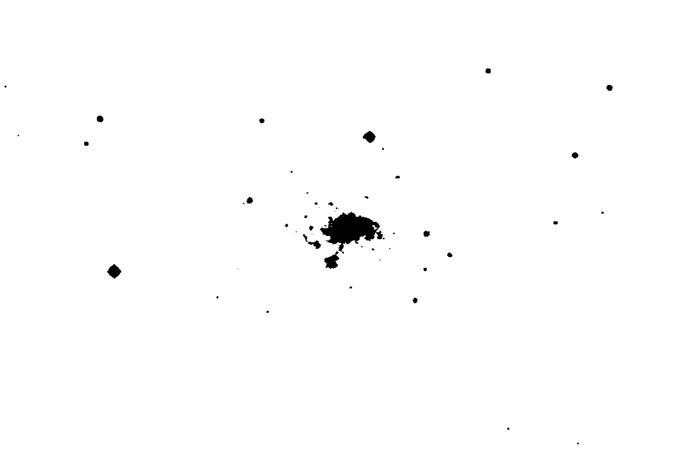

Sc(s) II.2 v = 831

NGC 4504 120"

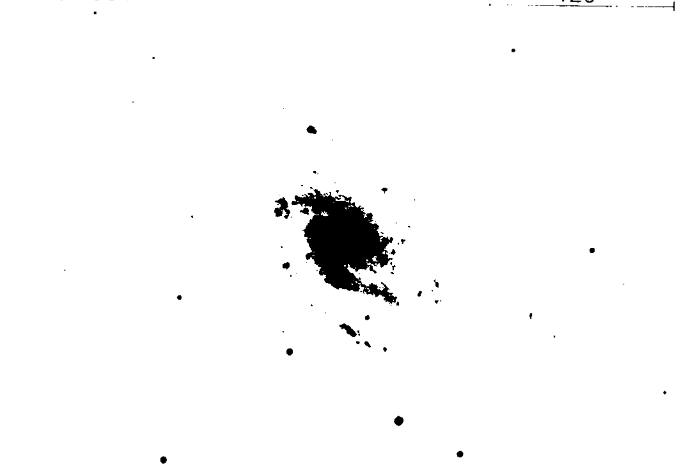

Sc(s) II v = 794

NGC 4559 120"

Sc(s) II v = 771

NGC 4559 120"

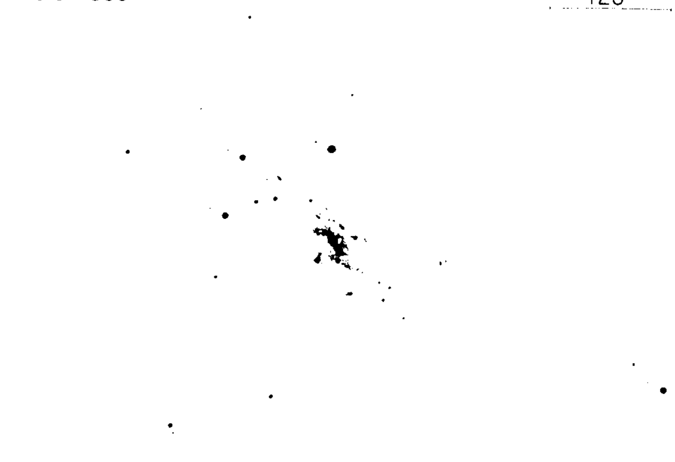

Sc(s) II v = 771

NGC 4631 120″

Sc v = 606

NGC 5112 120″

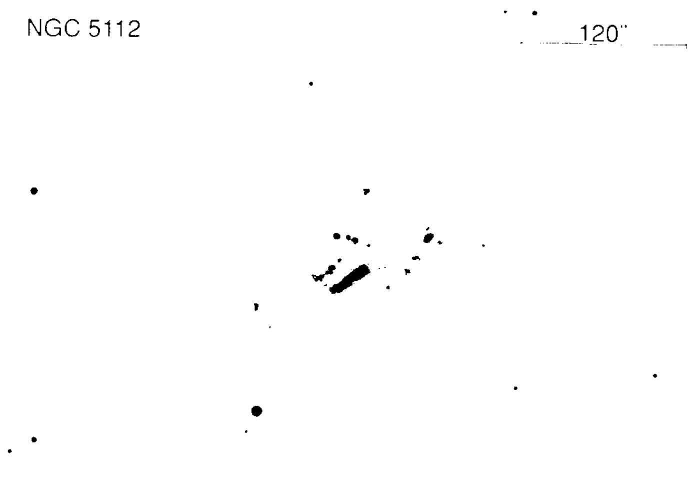

Sc(rs) II v = 998

NGC 5457 120″

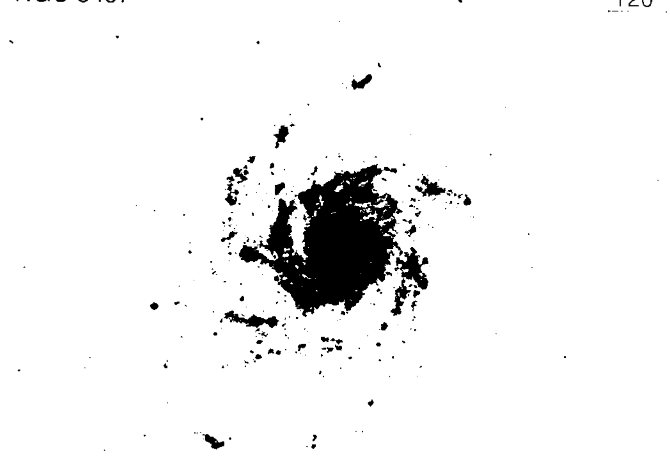

Sc(s) I v = 372

NGC 6946 120″

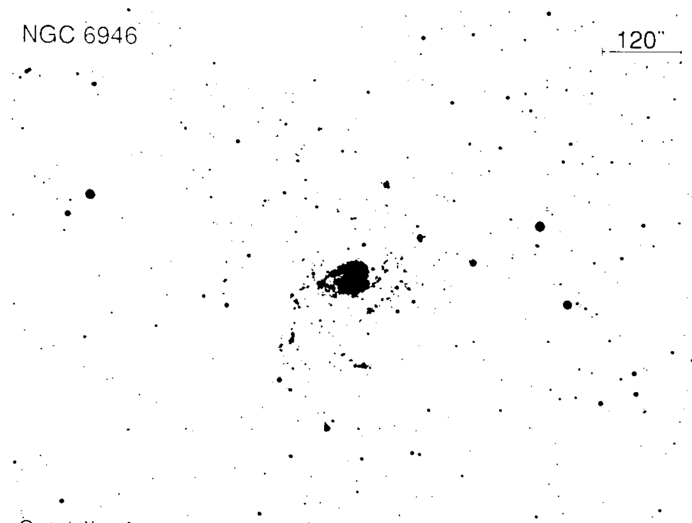

Sc(s) II v = 336

NGC 7456 120″

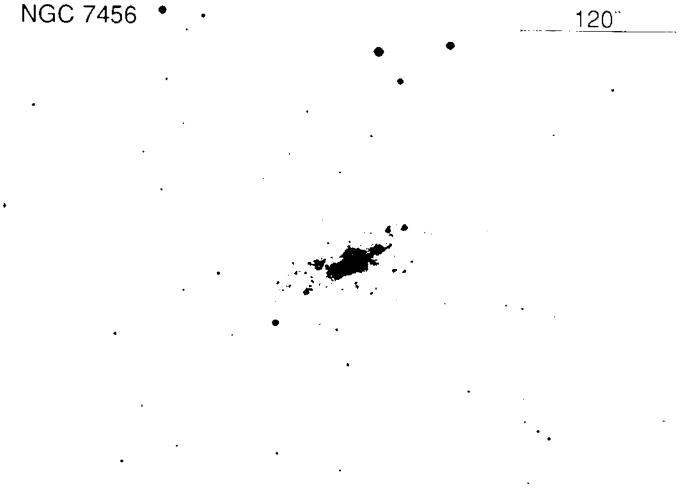

Sc(s) II-III v = 1199

IC 5332 120″

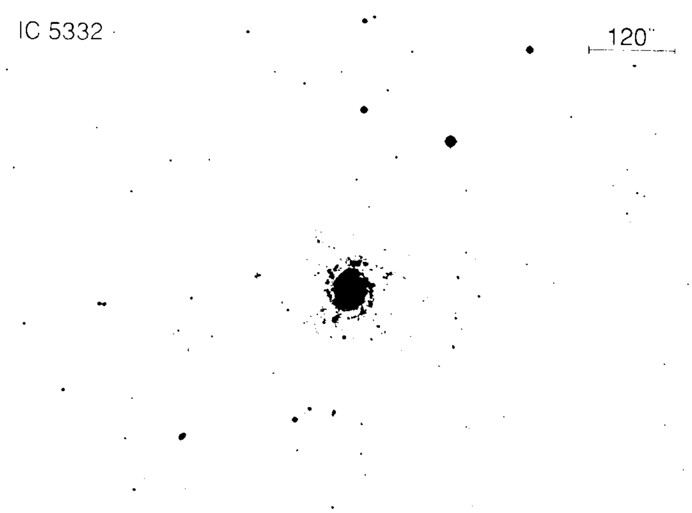

Sc(s) II-III v = 713

NGC 672 120"

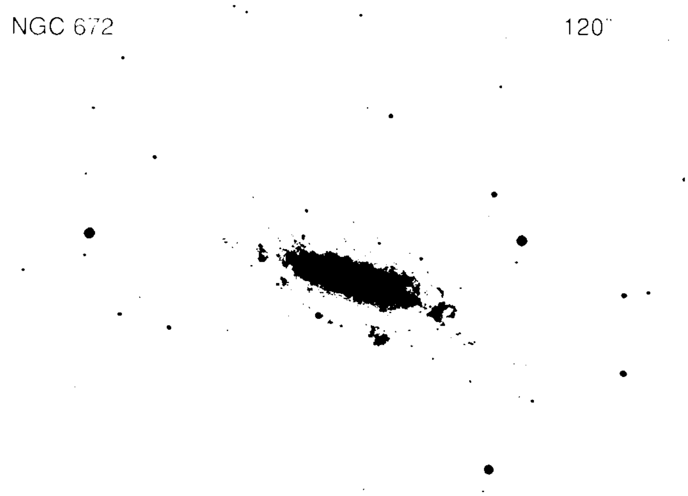

SBc(s) III v = 647

NGC 925 120"

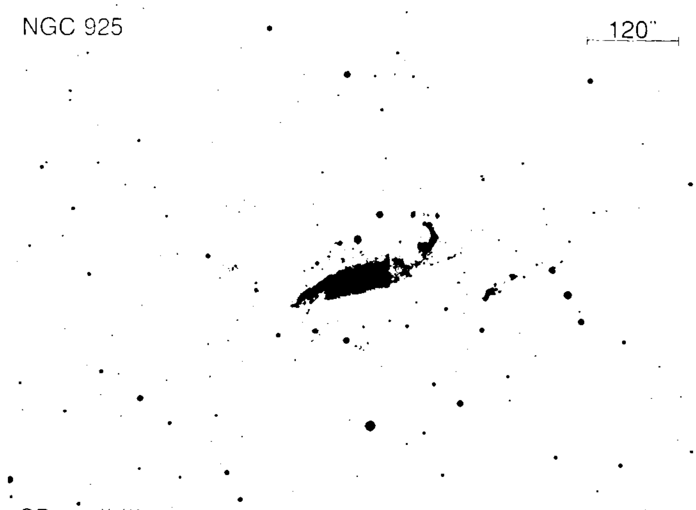

SBc(s) II-III v = 792

NGC 1249 120"

SBc(s) II v = 887

NGC 1637 120"

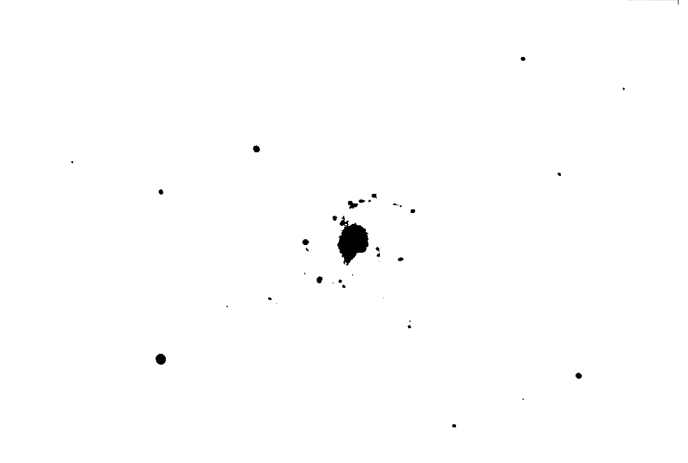

SBc(s) II.3 v = 715

NGC 1313 120"

SBc(s) II-IV v = 261

NGC 1313 120"

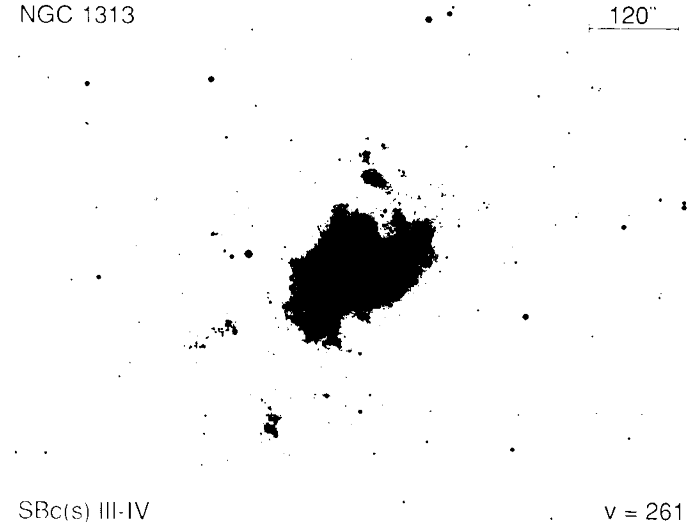

SBc(s) III-IV v = 261

NGC 2835 120"

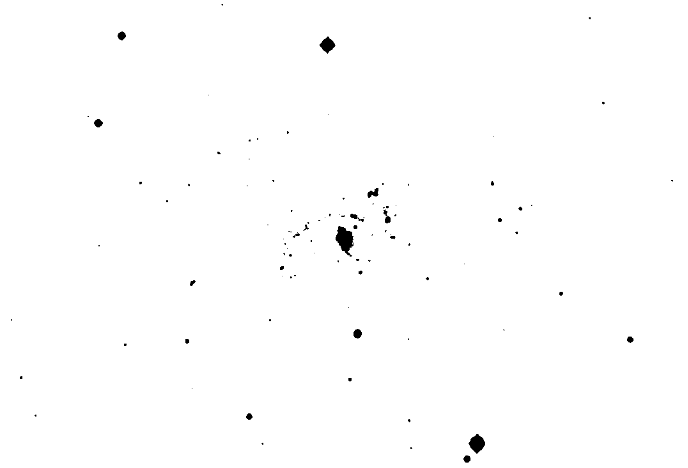

SBc(rs) I.2 v = 624

NGC 2835 120"

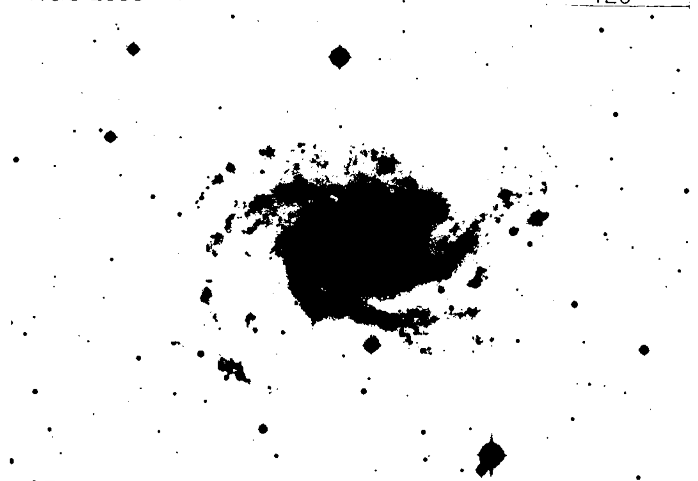

SBc(rs) I.2 v = 624

NGC 3319 120"

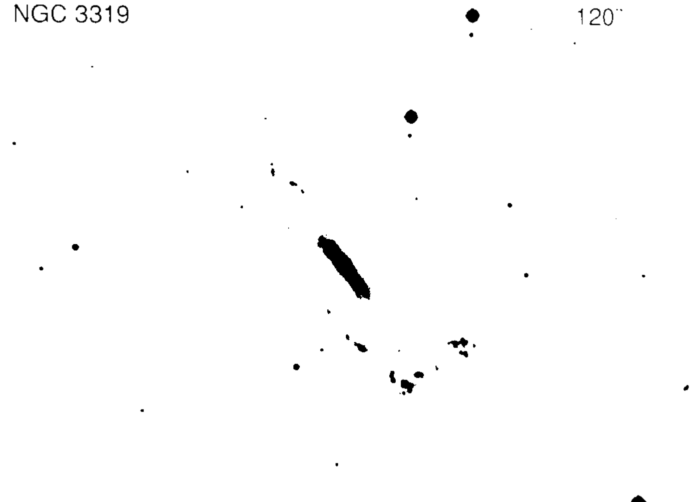

SBc(s) II.4 v = 776

NGC 3359 120"

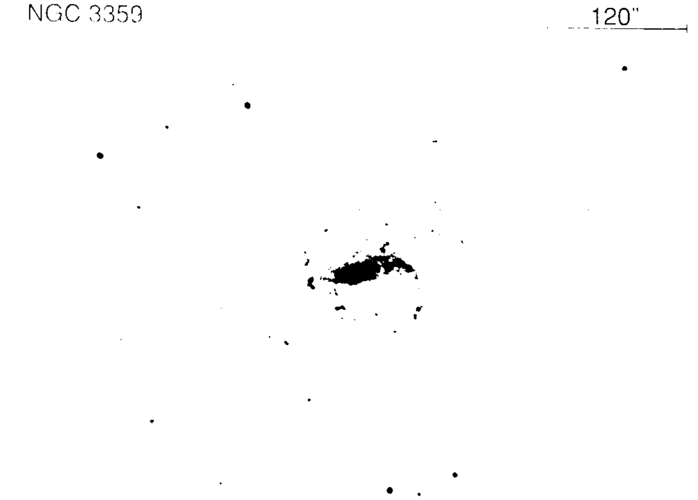

SBc(s) I.8 v = 1138

NGC 3513 120"

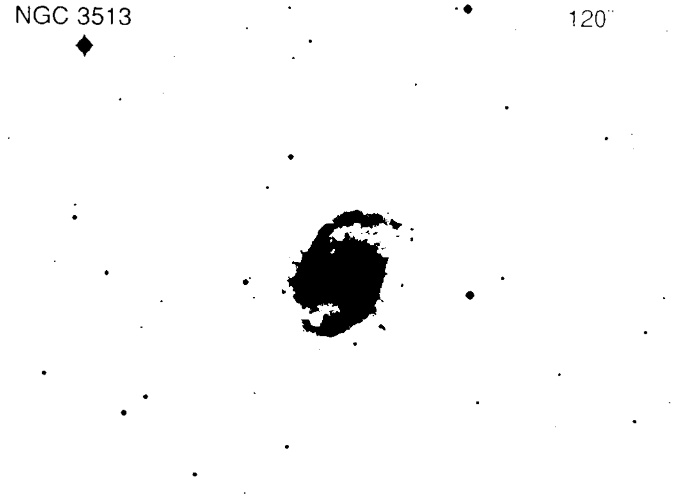

SBc(s) II.2 v = 845

NGC 4597 120"

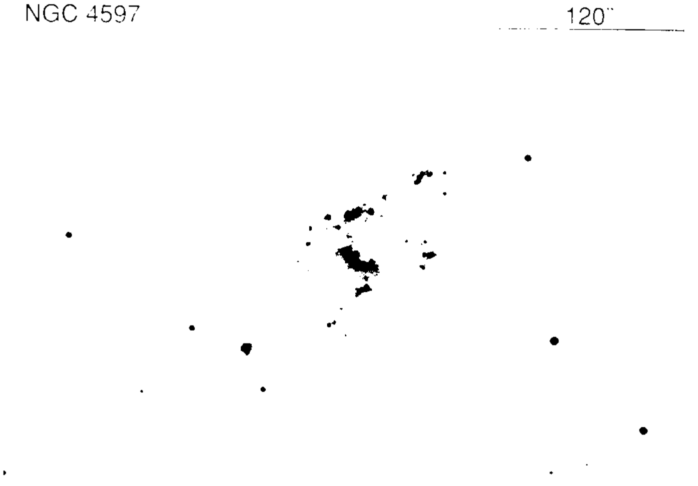

SBc(s) III: v = 851

NGC 5068 120"

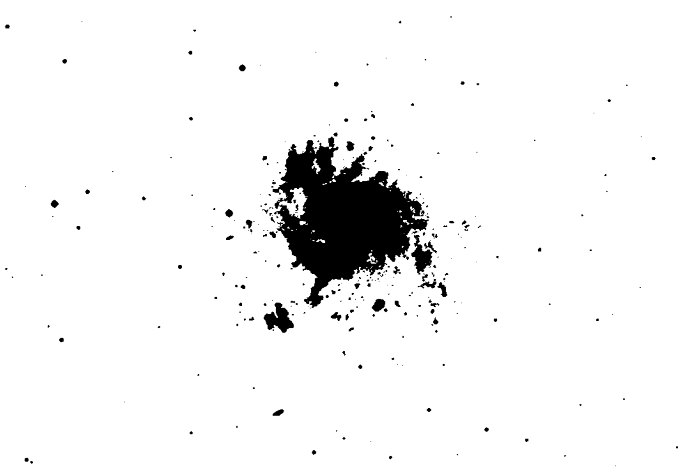

SBc(s) II-III v = 443

NGC 5398 120"

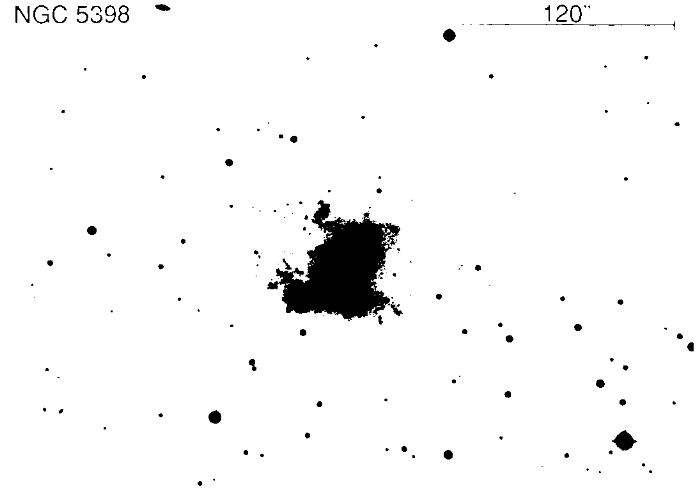

SBc(s) II-III v = 984

NGC 5236 120"

SBc(s) II v = 275

NGC 5236 120"

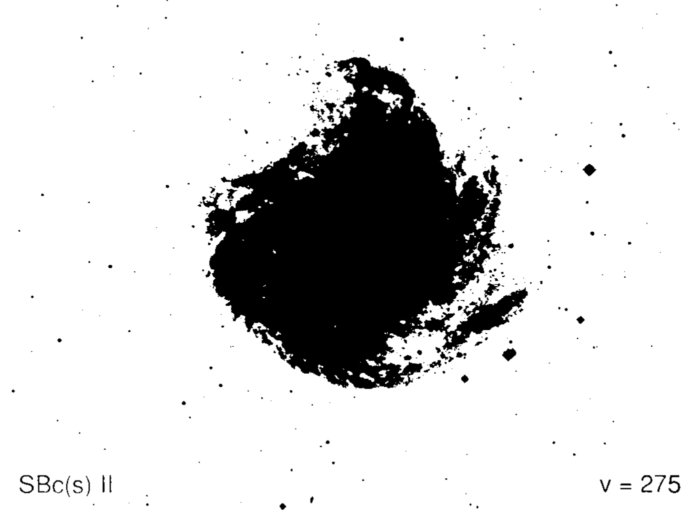

SBc(s) II v = 275

NGC 7424 120"

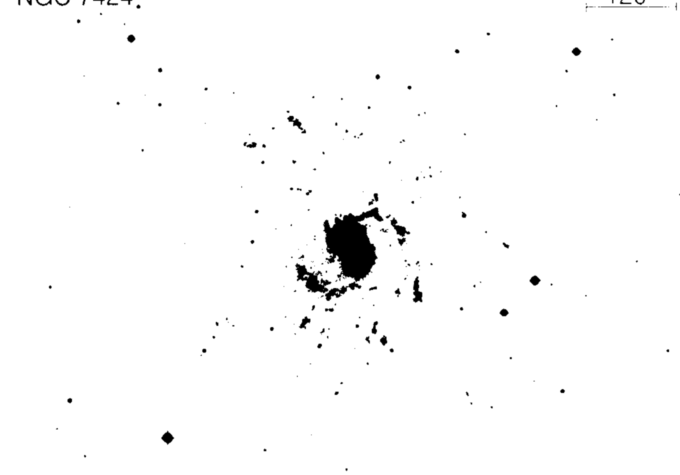

SBc(s) II.3 v = 925

NGC 7741 120"

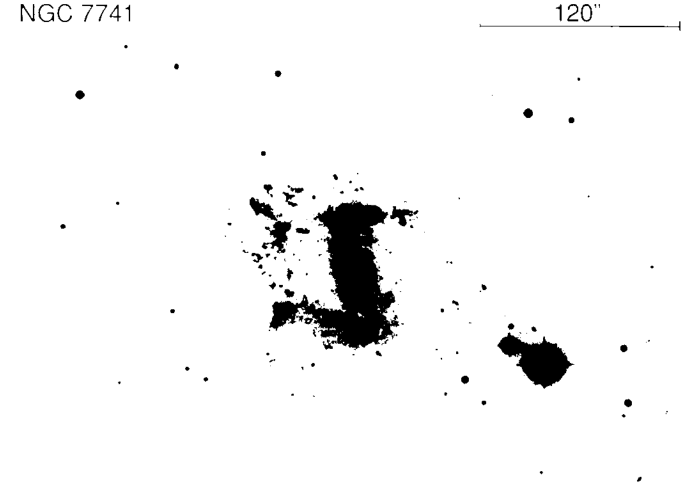

SBc(s) II.2 v = 1030

NGC 7640

120"

SBc(s) II:

v = 669

NGC 7640

120"

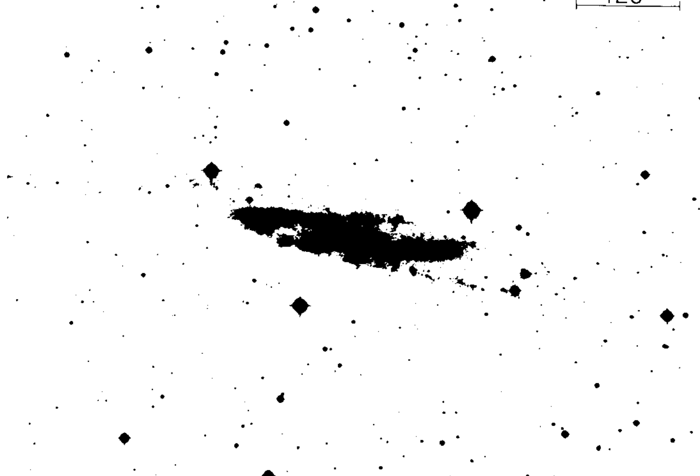

SBc(s) II:

v = 669

IC 749

120"

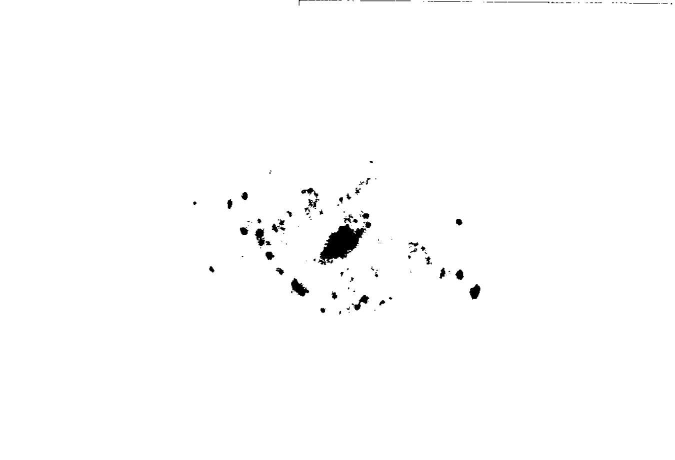

SBc(rs) II-III

v = 827

IC 1727

120"

SBc(s) II-III

v = 662

NGC 1744

120"

SBcd(s) II-III

v = 639

IC 5201

120"

SBcd(s) II

v = 728

NGC 45 120"

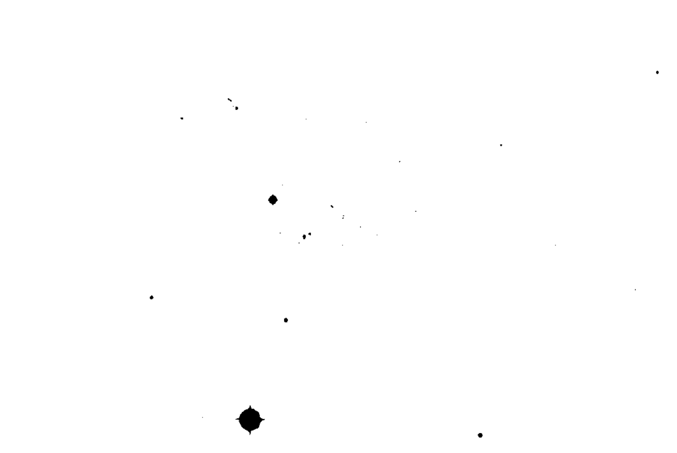

Scd(s) III v = 533

NGC 45 120"

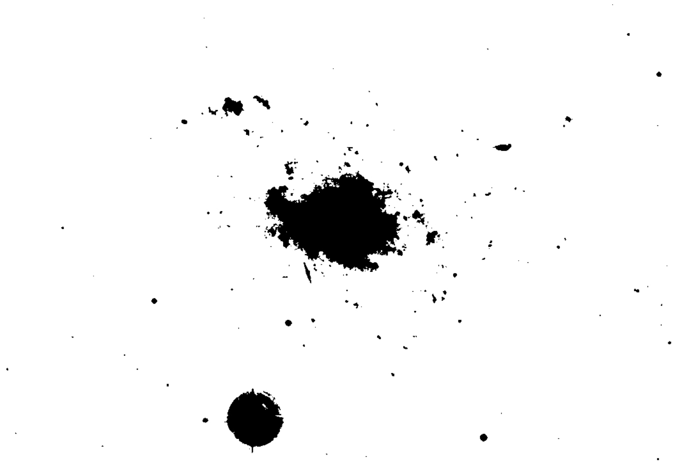

Scd(s) III v = 533

NGC 3274 120"

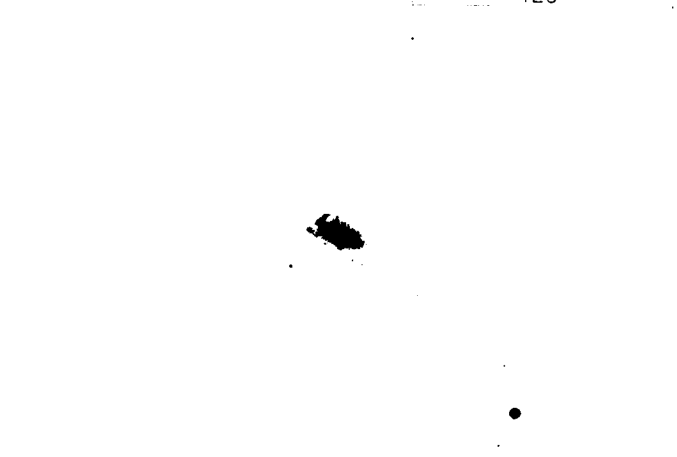

Scd III v = 486

NGC 3274 120"

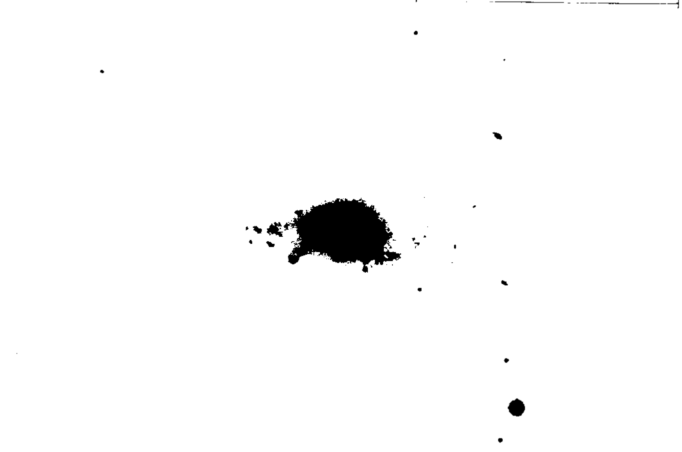

Scd III v = 486

NGC 4244 120"

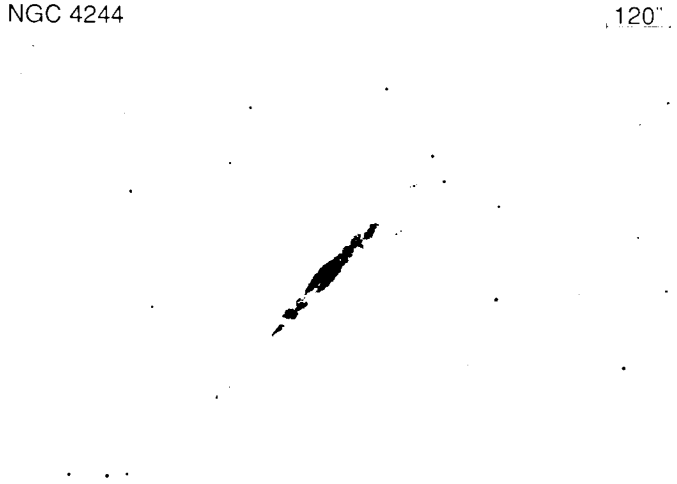

Scd v = 249

NGC 5474 120"

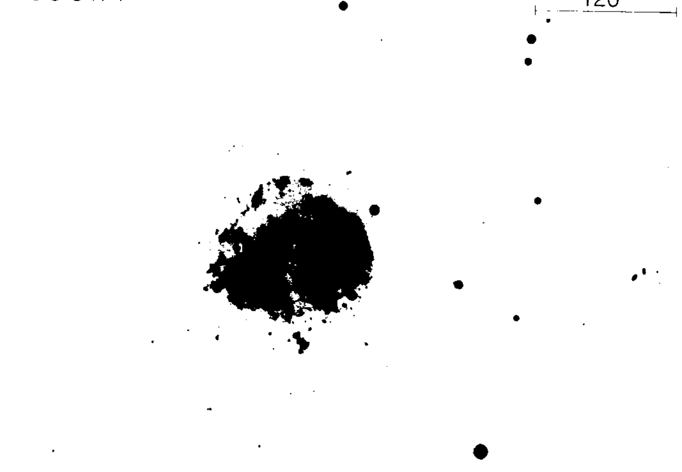

Scd(s) IV pec v = 394

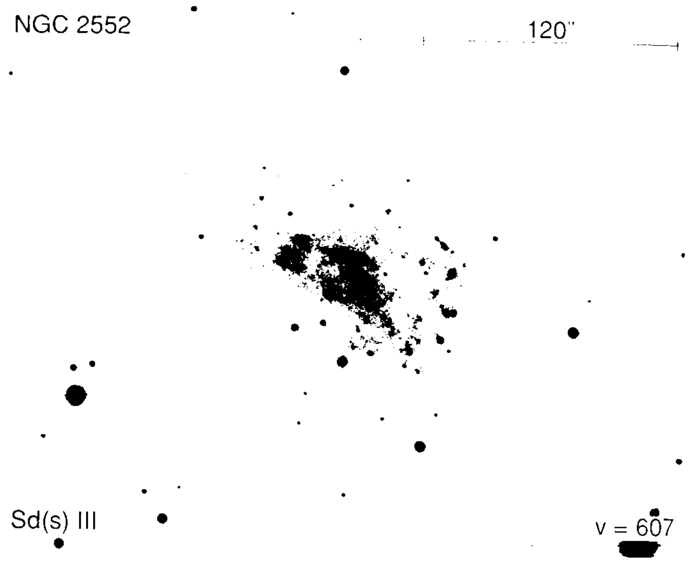
NGC 2552
120"
Sd(s) III
v = 607

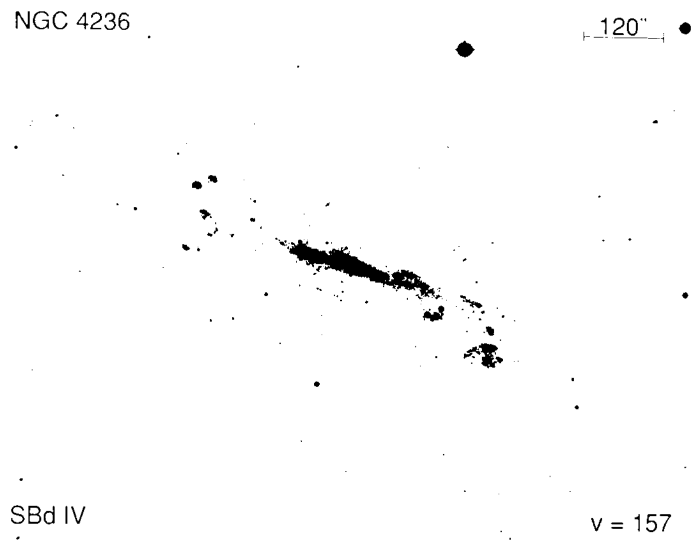
NGC 4236
120"
SBd IV
v = 157

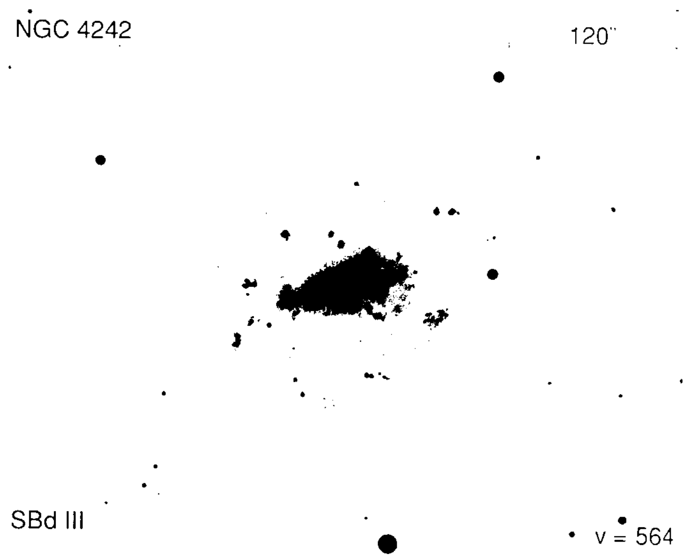
NGC 4242
120"
SBd III
v = 564

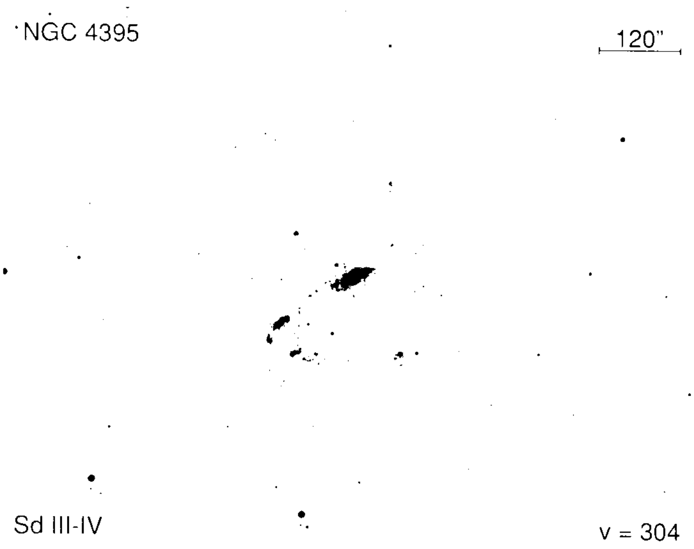
NGC 4395
120"
Sd III-IV
v = 304

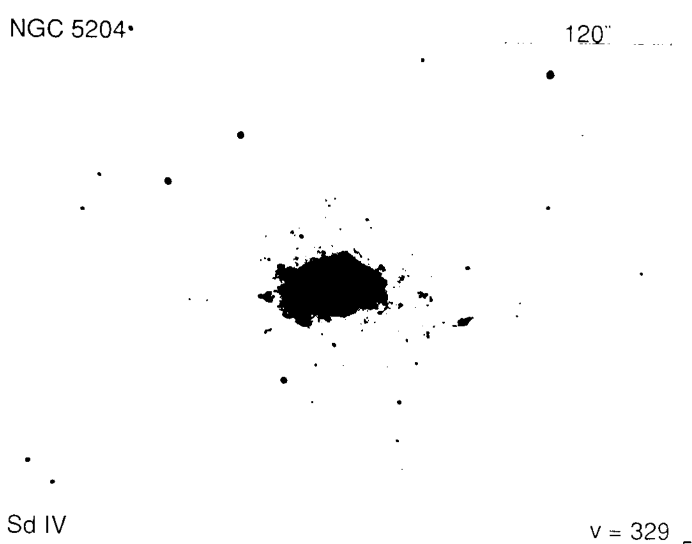
NGC 5204
120"
Sd IV
v = 329

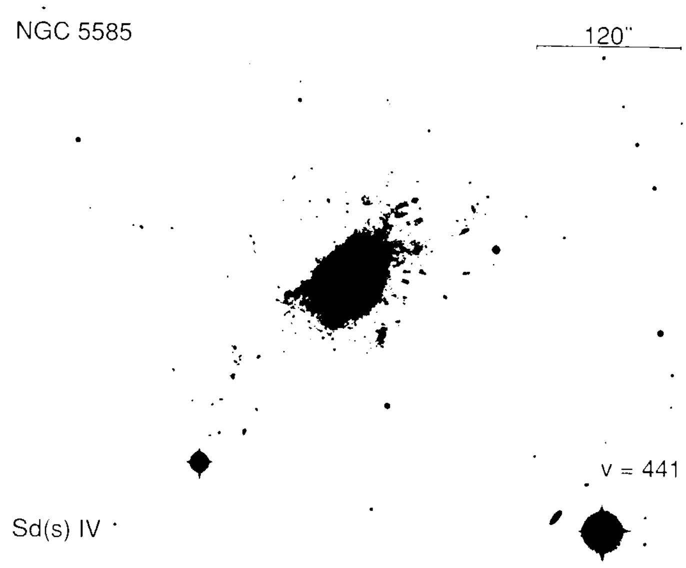
NGC 5585
120"
v = 441
Sd(s) IV

NGC 7793 120"

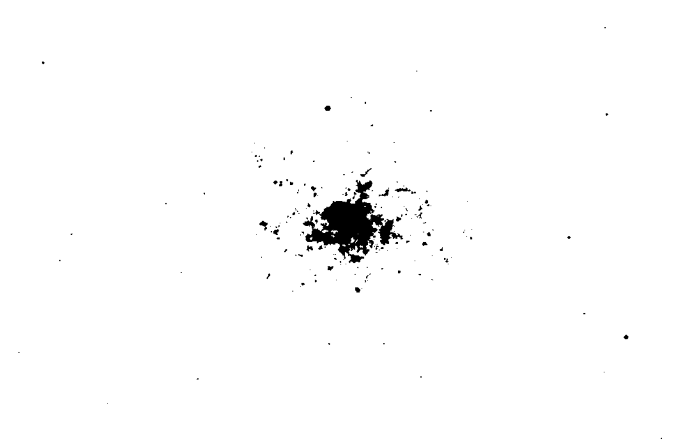

Sd(s) IV v = 241

NGC 7793 120"

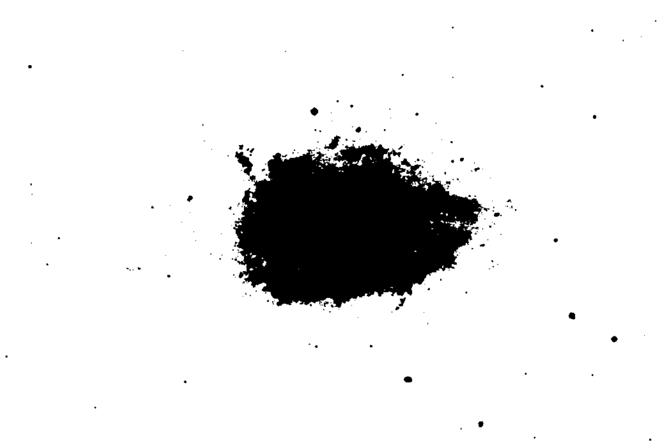

Sd(s) IV v = 241

IC 5152 120"

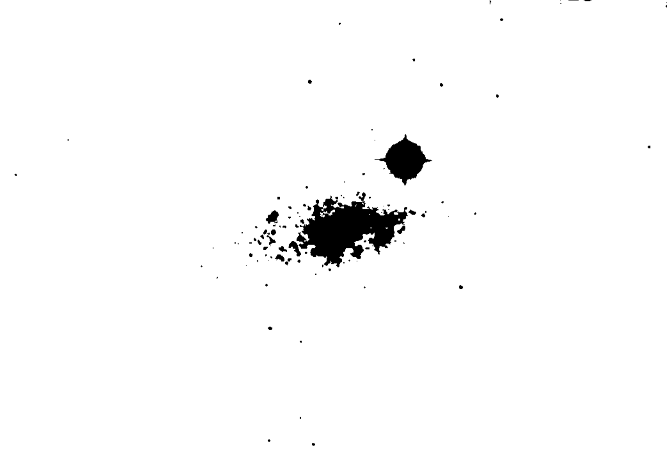

Sdm IV-V v = 47

IC 5152 120"

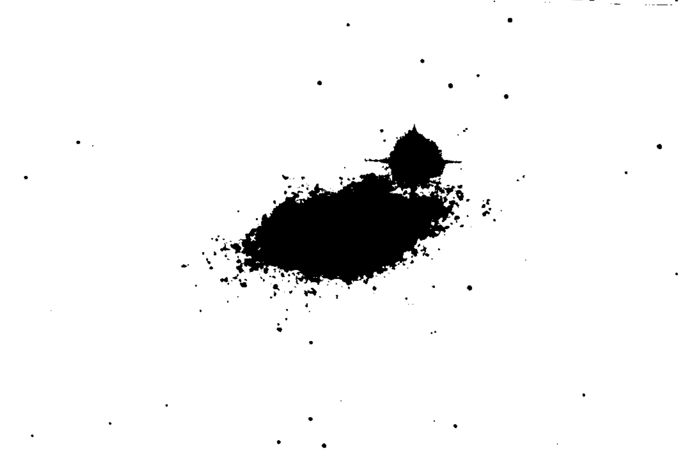

Sdm IV-V v = 47

NGC 1156 120"

Sm IV v = 558

NGC 1156 120"

Sm IV v ~ 558

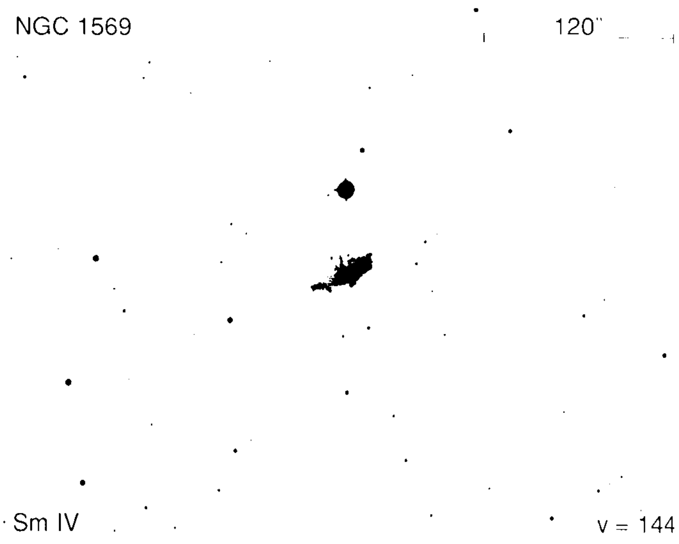
NGC 1569
120"
Sm IV
v = 144

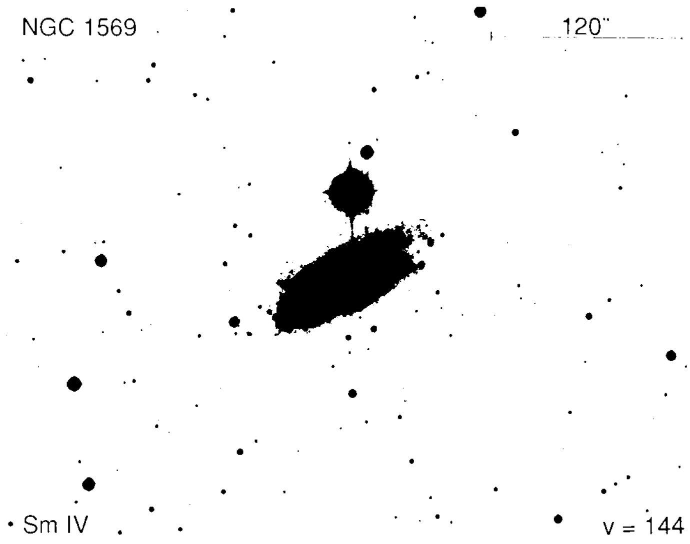
NGC 1569
120"
Sm IV
v = 144

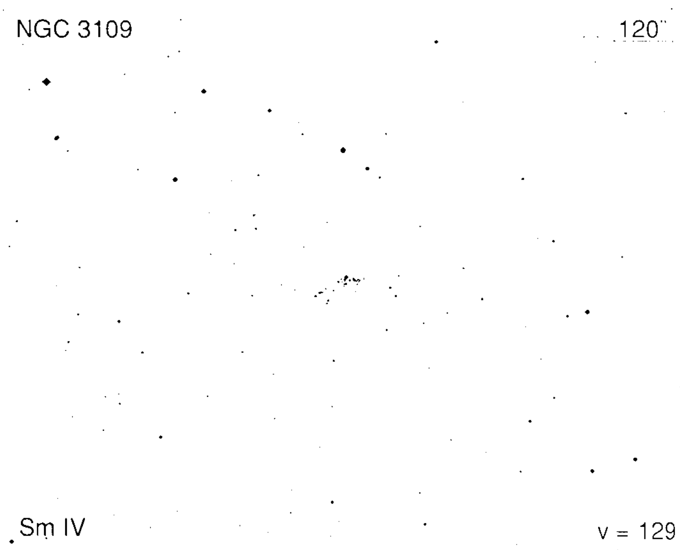
NGC 3109
120"
Sm IV
v = 129

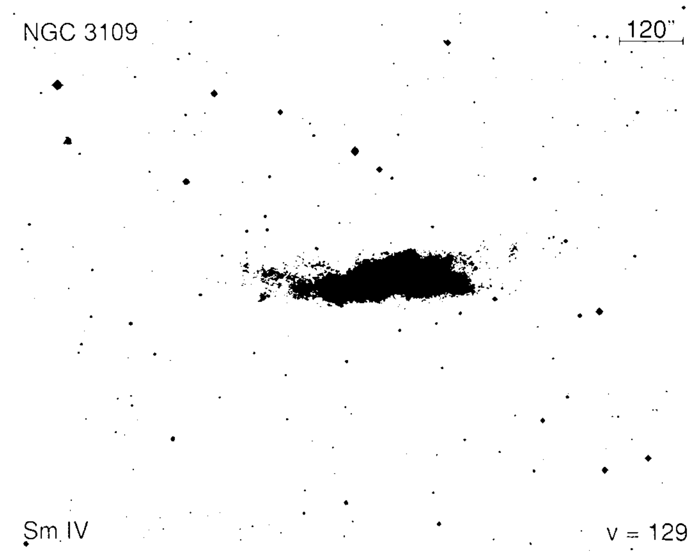
NGC 3109
120"
Sm IV
v = 129

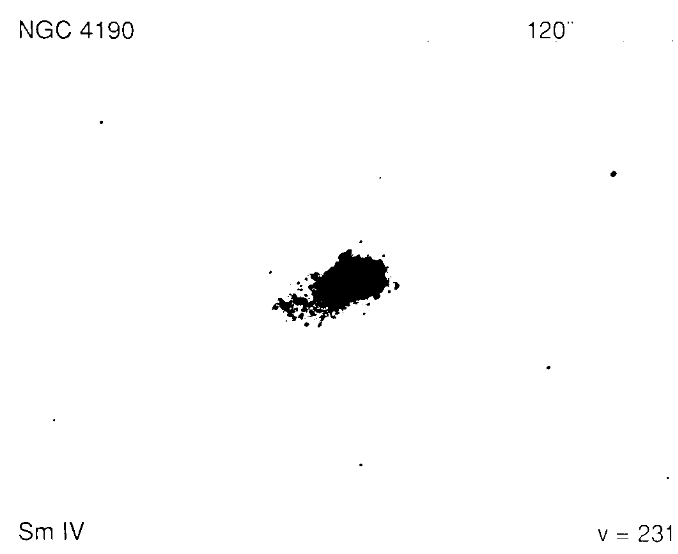
NGC 4190
120"
Sm IV
v = 231

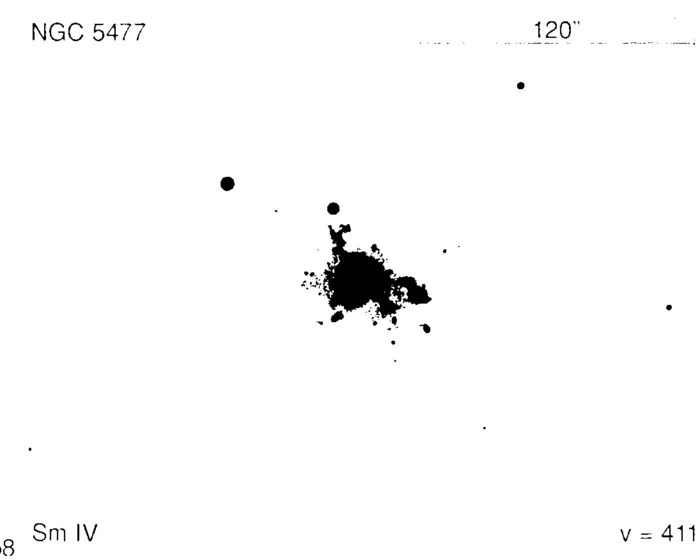
NGC 5477
120"
Sm IV
v = 411

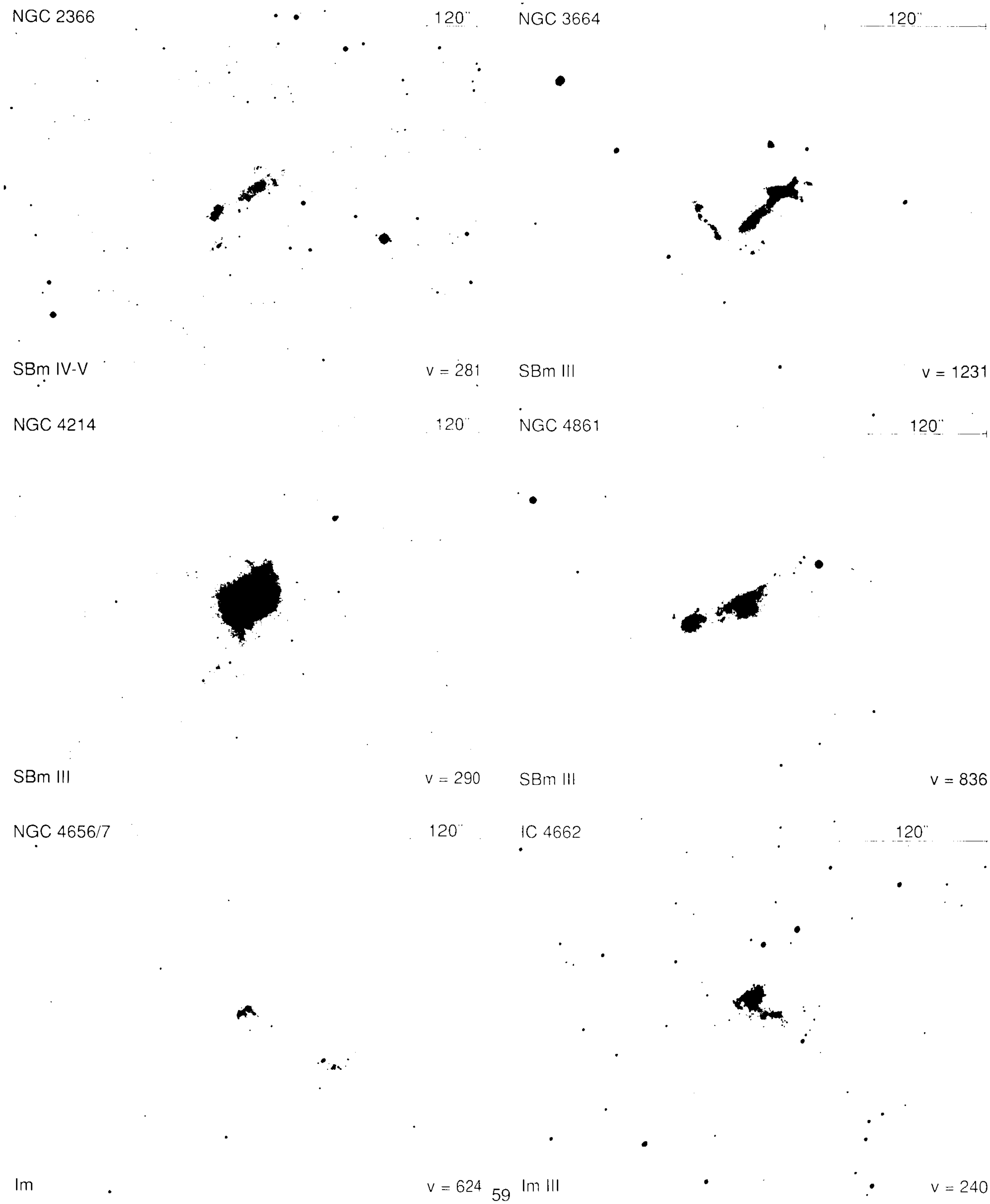
NGC 2366
120"
SBm IV-V
v = 281
NGC 3664
120"
SBm III
v = 1231
NGC 4214
120"
SBm III
v = 290
NGC 4861
120"
SBm III
v = 836
NGC 4656/7
120"
Im
v = 624
IC 4662
120"
Im III
v = 240

Part III

The 28 panels of Part III on atlas panels 60 to 87 show those galaxies listed in Table 2 that will be more difficult to resolve into Cepheids than those in Part II, but whose larger distance gives them a particularly important role in mapping the local velocity perturbation field [Sandage and Bedke, 1985a,b] (Figures 2, 3, and 4). Distances to many of these galaxies will be more easily obtained from the *brightest star* distance indicators than with Cepheids, once the brightest star <M> values are calibrated more securely by means of Cepheids in galaxies from Part II of the atlas.

NGC 210 120"

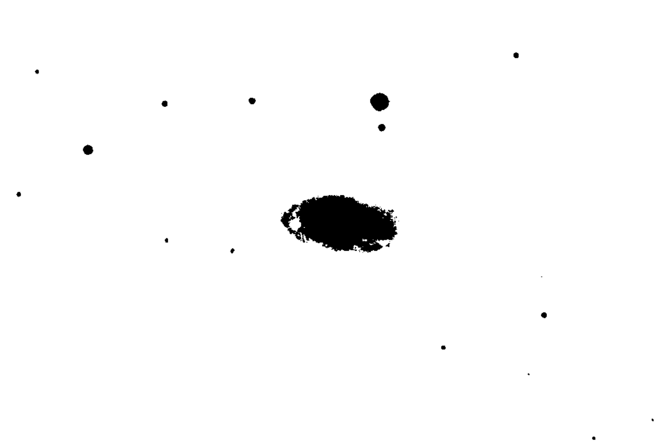

Sb(rs) I V = 1875

NGC 210 120"

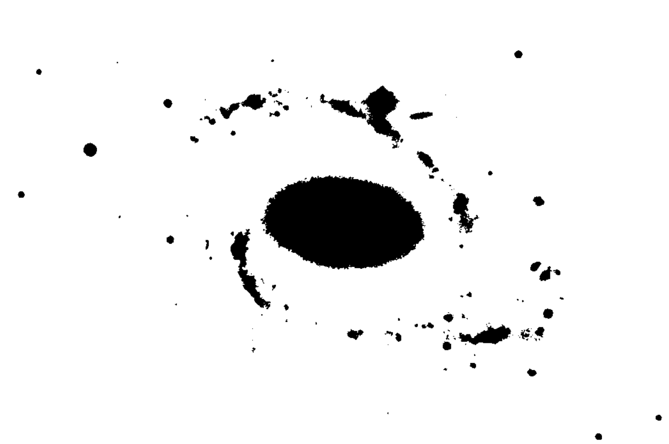

Sb(rs) I V = 1875

NGC 1288 120"

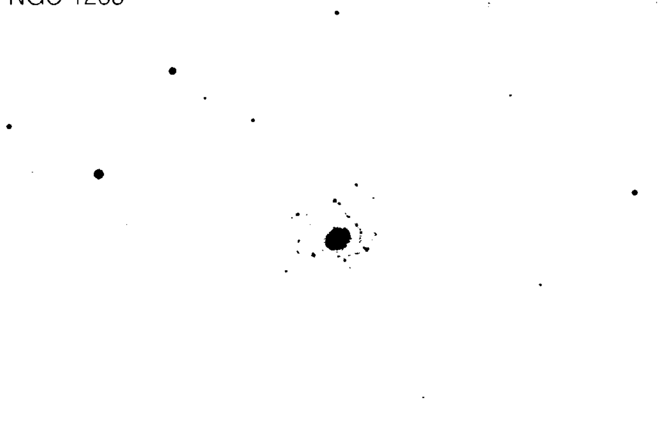

Sb(r) I-II V = 4461

NGC 1425 120"

Sb(r) II V = 1440

NGC 2841 120"

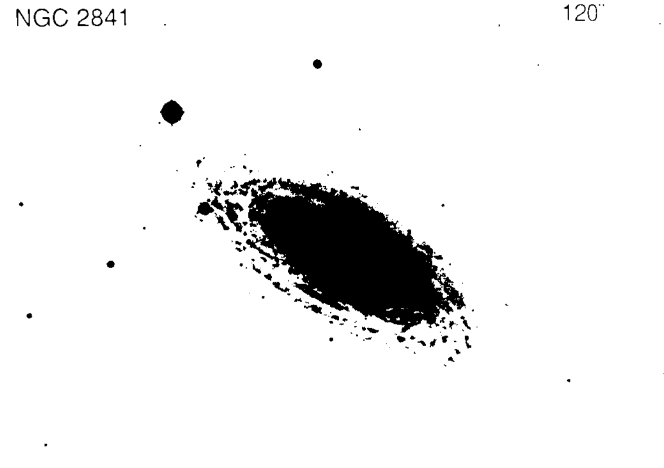

Sb V = 714

NGC 3147 120"

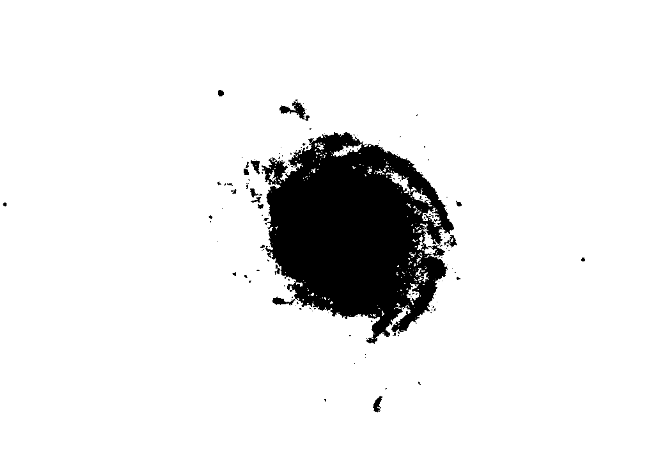

Sb(s) I-II V = 2899

NGC 3223

120"

Sb(s) I-II

V = 2619

NGC 3241

120"

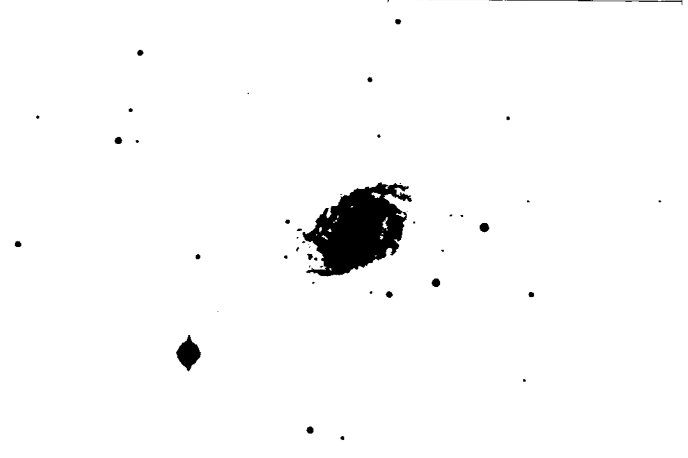

Sb(r) II

V = 2584

NGC 3673

120"

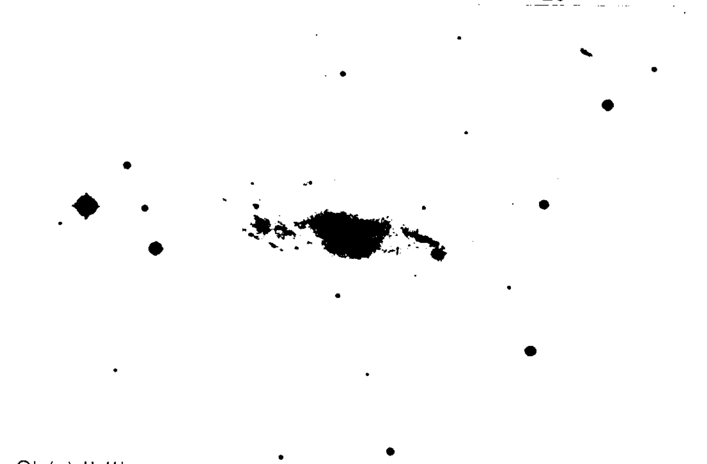

Sb(s) II-III

V = 1662

NGC 3705

120"

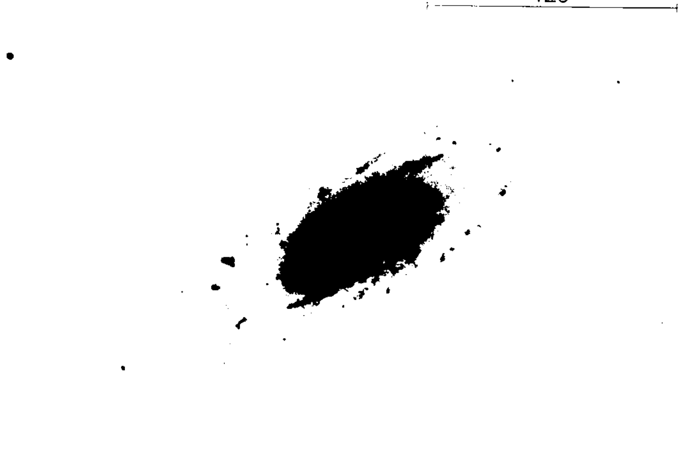

Sb(r) I-II

V = 870

NGC 4814

120"

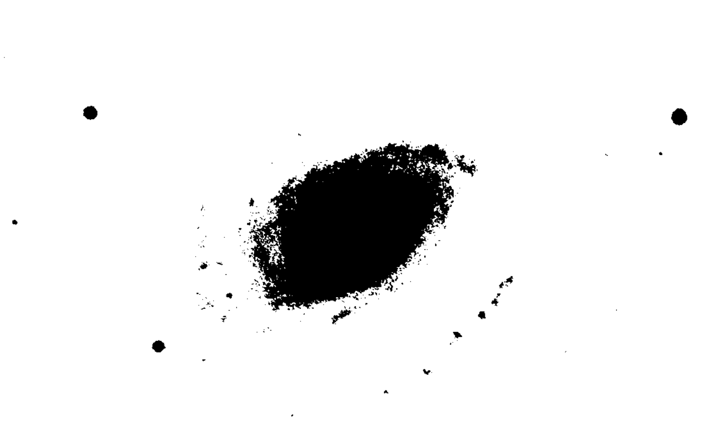

Sb(s) I

V = 2650

NGC 5054

120"

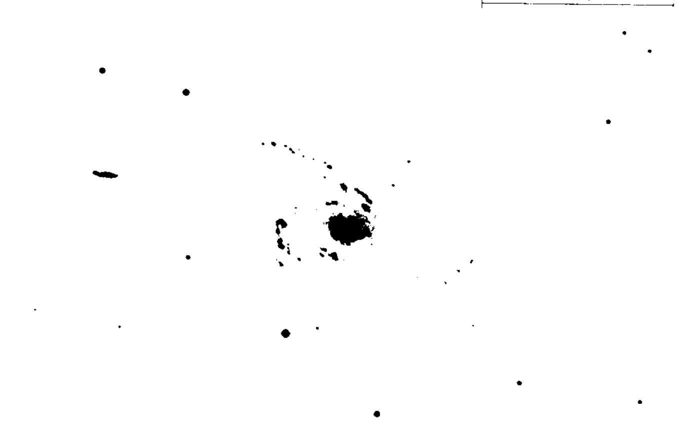

Sb(s) I-II

V = 1524

NGC 5371 120"

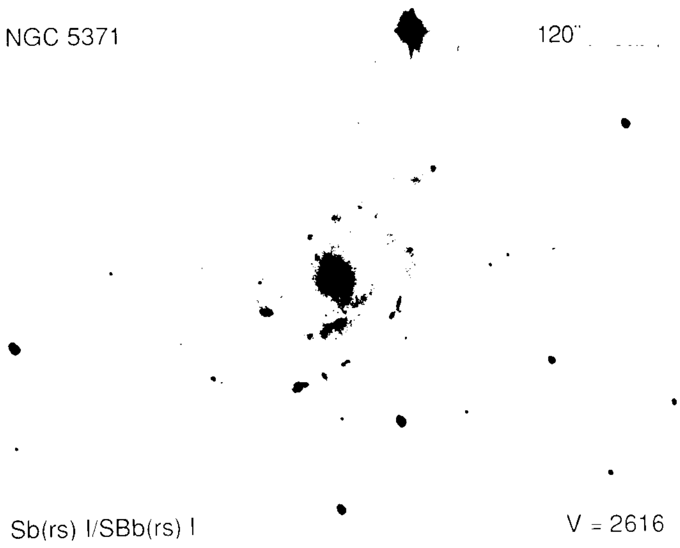

Sb(rs) I/SBb(rs) I V = 2616

NGC 6384 120"

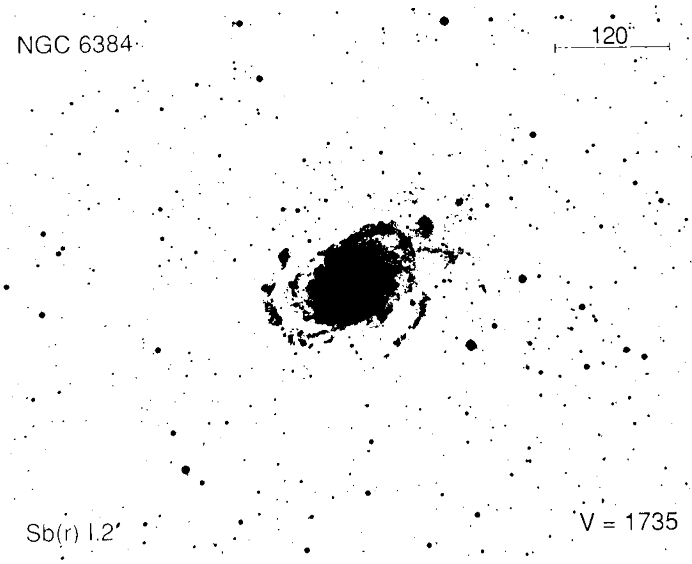

Sb(r) I.2 V = 1735

NGC 7217 120"

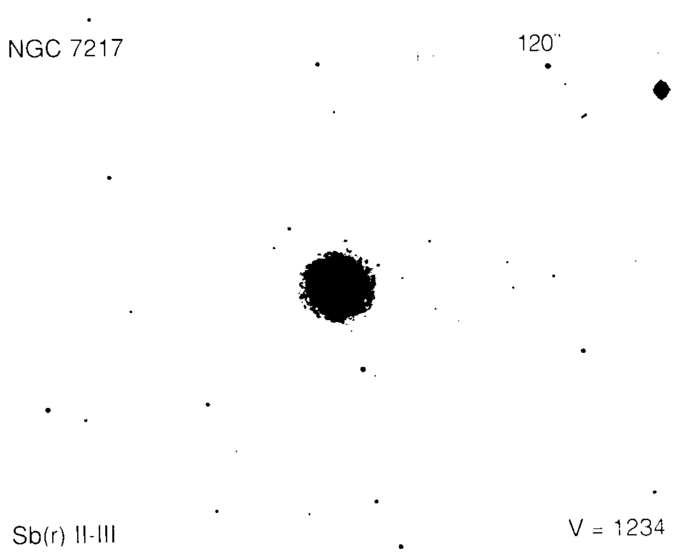

Sb(r) II-III V = 1234

NGC 7217 120"

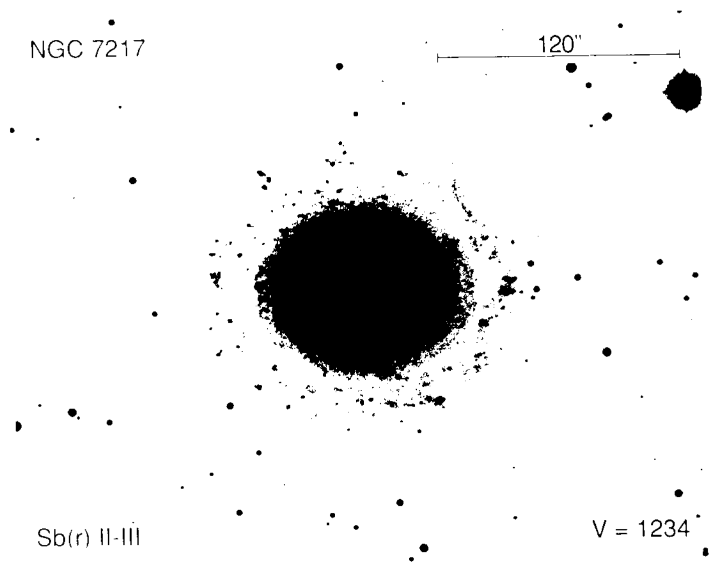

Sb(r) II-III V = 1234

NGC 6753 120"

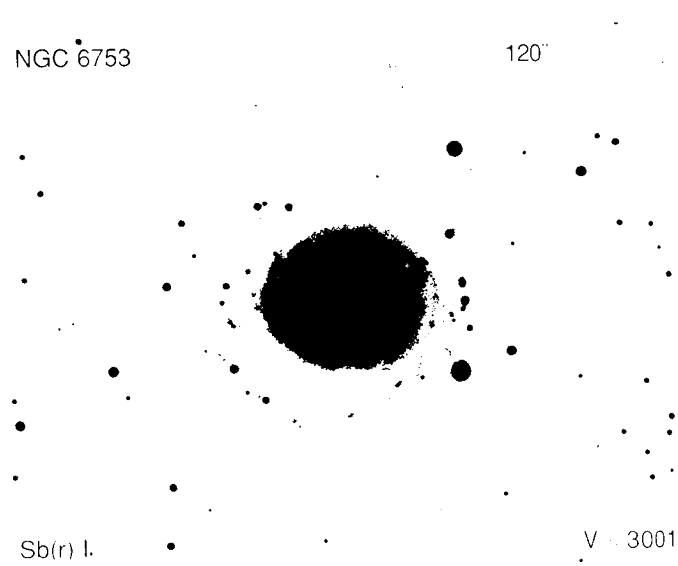

Sb(r) I. V = 3001

NGC 2935 120"

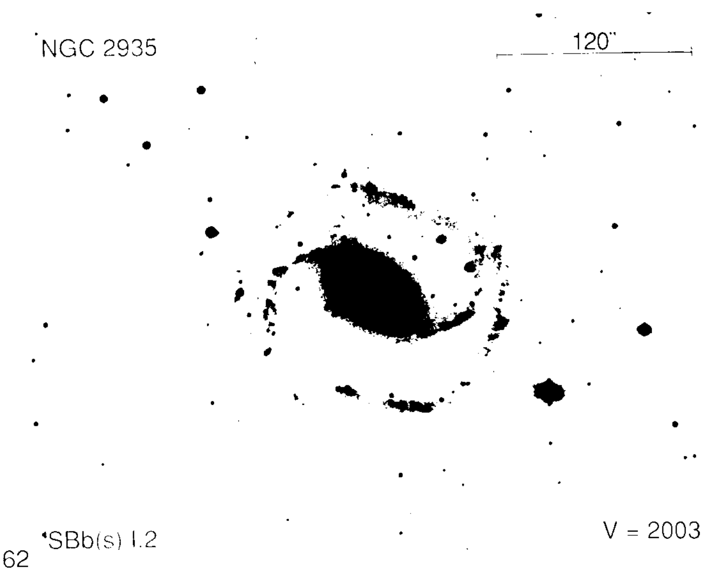

SBb(s) I.2 V = 2003

NGC 3351 120"

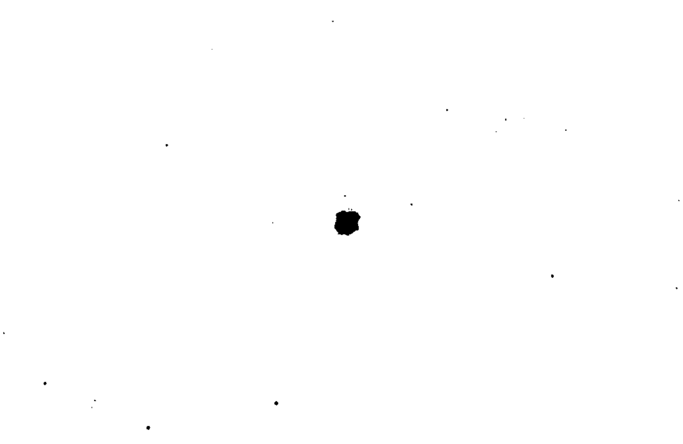

SBb(r) II V = 641

NGC 3351 120"

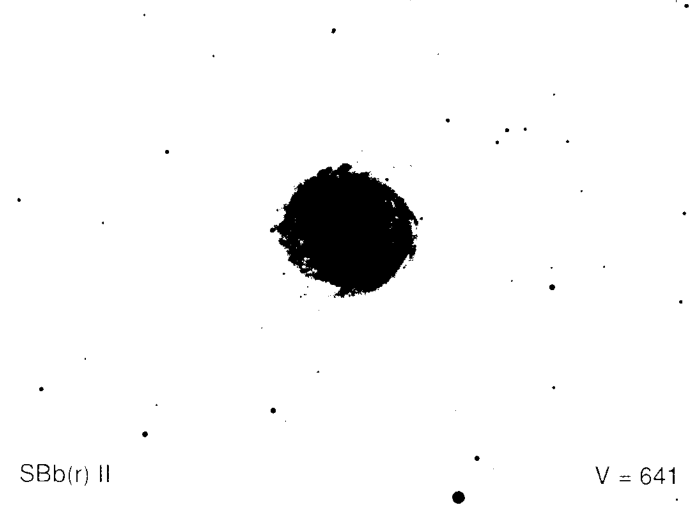

SBb(r) II V = 641

NGC 3992 120"

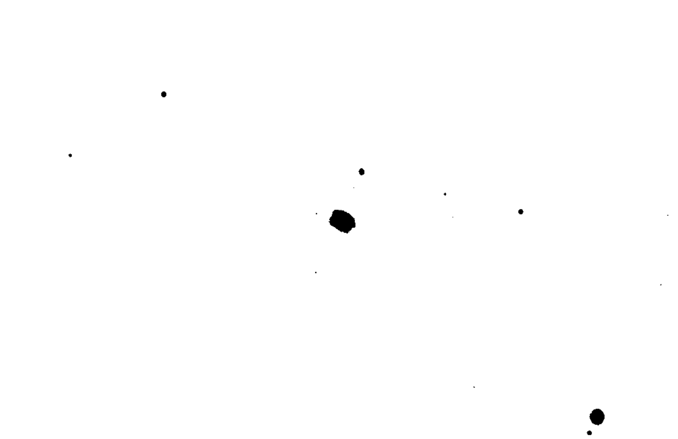

SBb(rs) I V = 1134

NGC 3992 120"

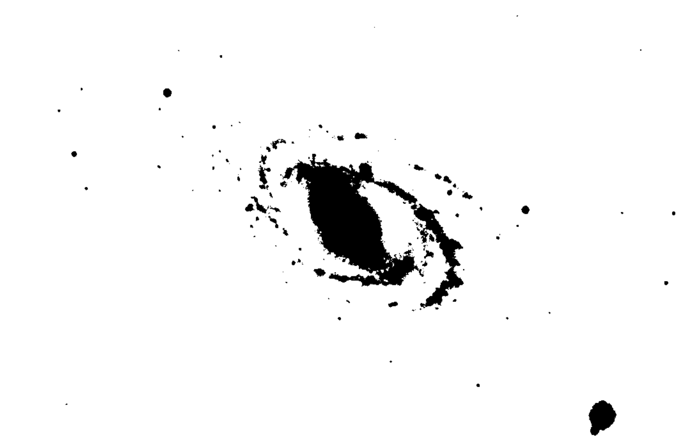

SBb(rs) I V = 1134

NGC 4593 120"

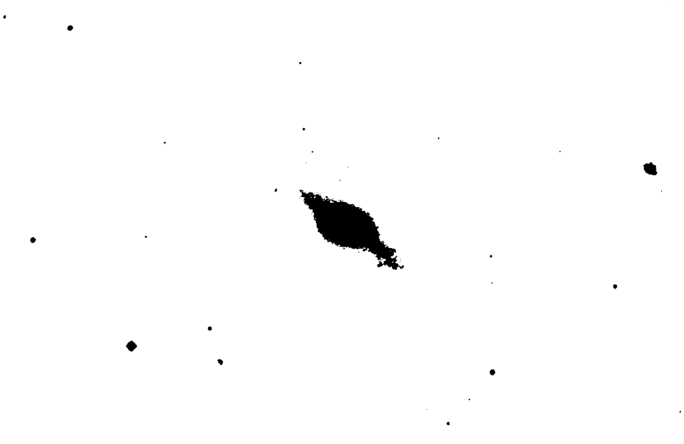

SBb(rs) I-II V = 2505

NGC 5850 120"

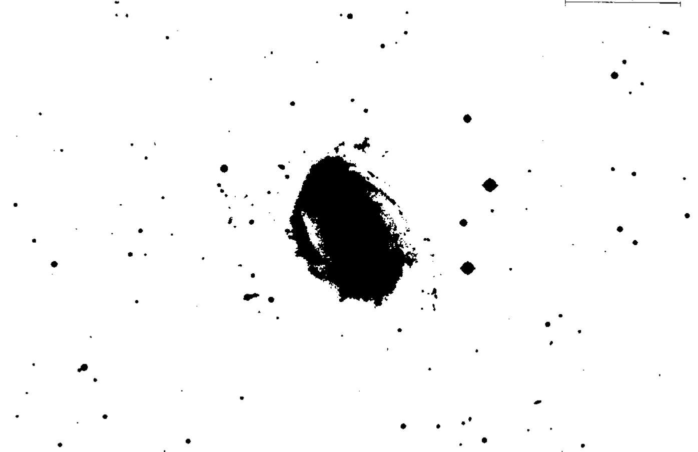

SBb(sr) I-II V = 2430

NGC 5985 120"

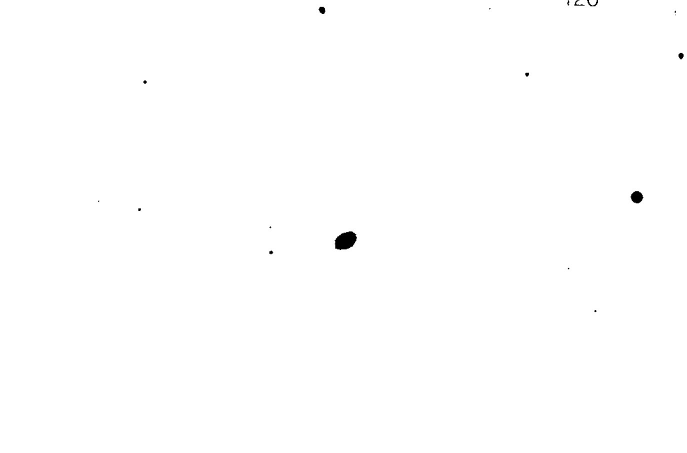

SBb(r) I V = 2694

NGC 5985 120"

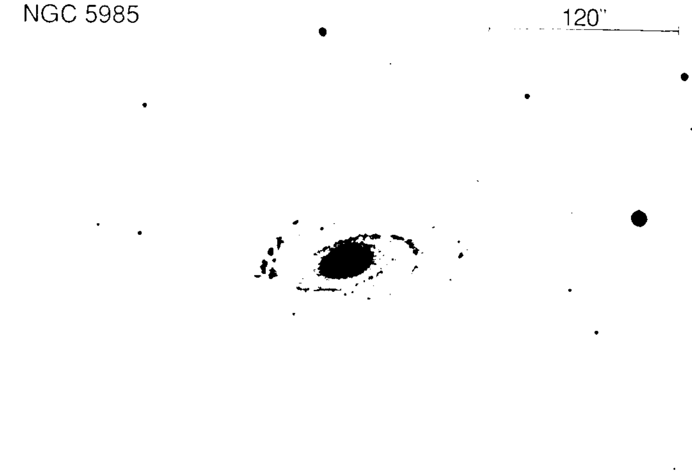

SBb(r) I V = 2694

NGC 6951 120"

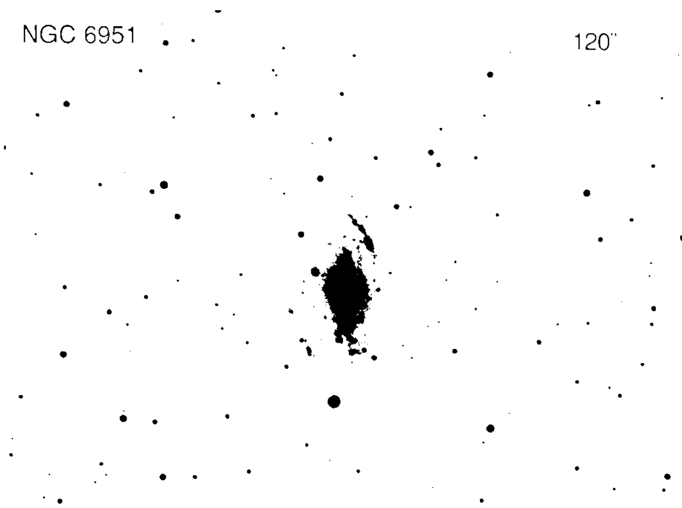

Sb/SBb(rs) I.3 V = 1710

NGC 7329 120"

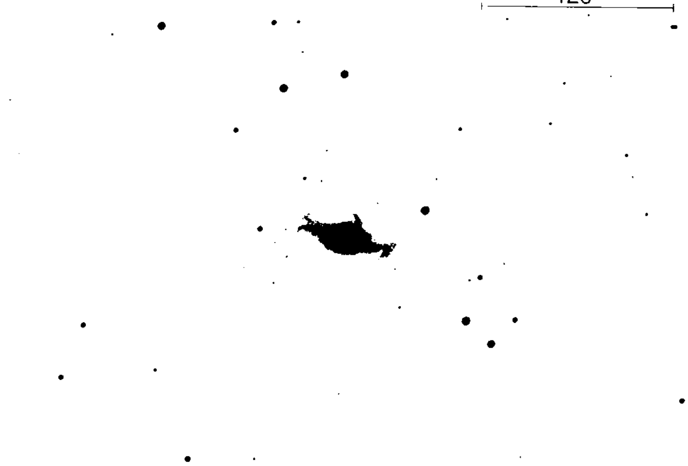

SBb(r) I-II V = 3043

NGC 7552 120"

SBb(s) I-II V = 1565

NGC 7552 120"

SBb(s) I-II V = 1565

NGC 864 120"

Sbc(r) II-III V = 1707

NGC 1531/2 120"

Sbc(s) (tides?)/Amorph V = 1105/1053

NGC 1187 120"

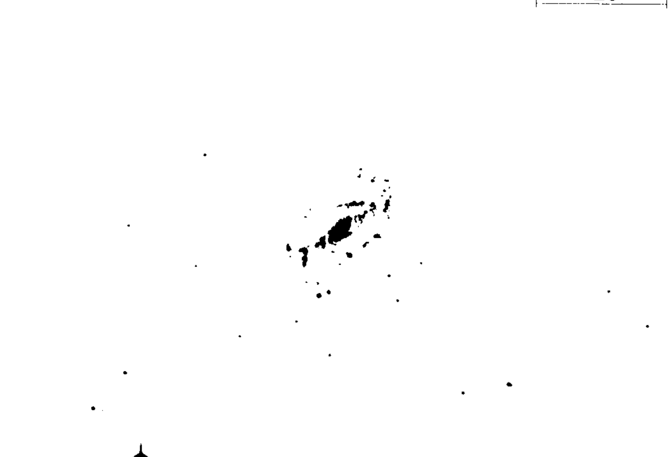

Sbc(s) II V = 1424

NGC 1187 120"

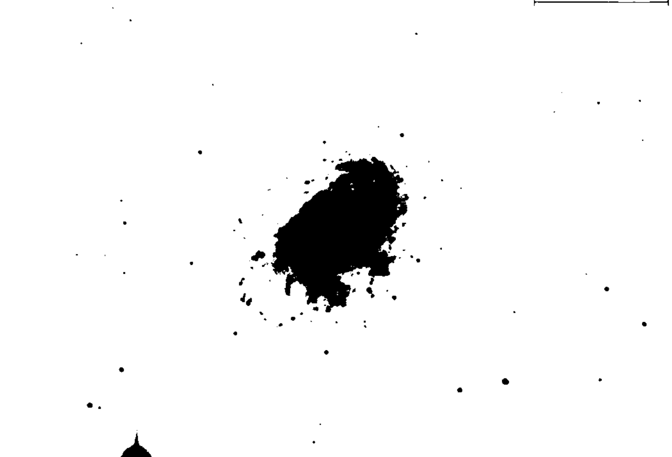

Sbc(s) II V = 1424

NGC 2713 120"

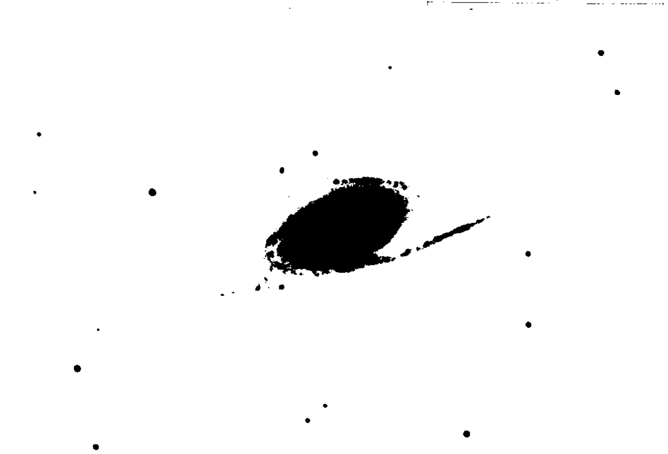

Sbc(s) I V = 3690

NGC 3338 120"

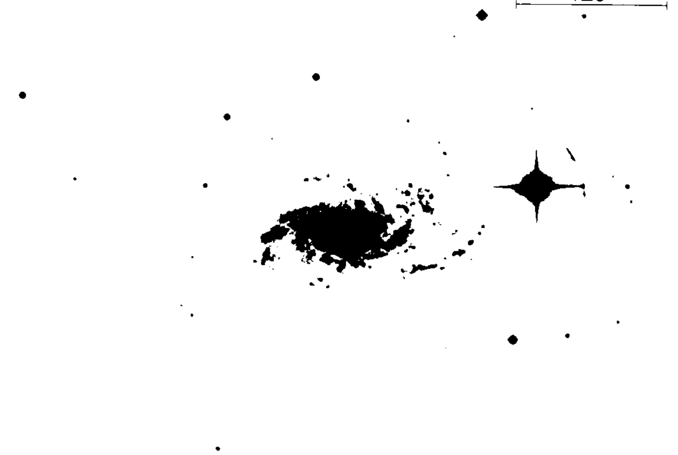

Sbc(s) I-II V = 1171

NGC 3344 120"

Sbc(rs) I.2 V = 627

NGC3433 120"

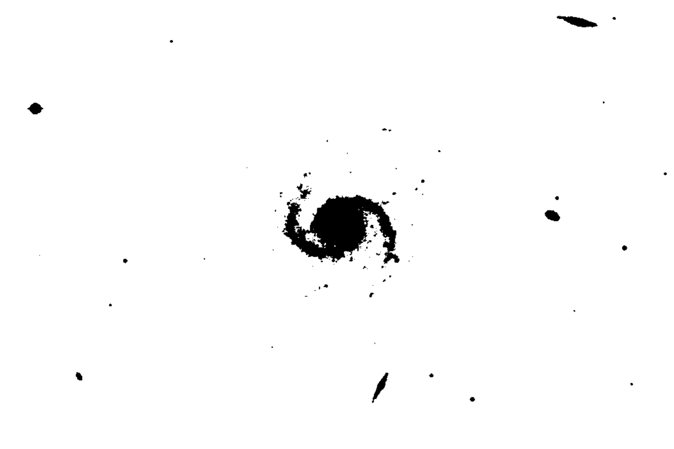

Sbc(r) I.3 V = 2566

NGC 3631 120"

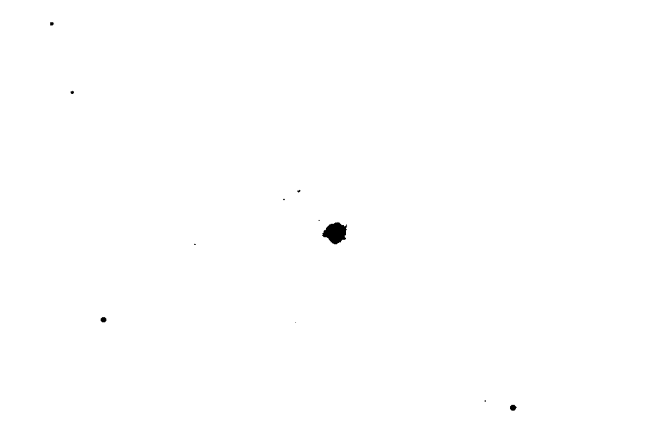

Sbc(s) II V = 1238

NGC 3631 120"

Sbc(s) II V = 1238

NGC 3596 120"

Sbc(r) II.2 V = 1072

NGC 4603 120"

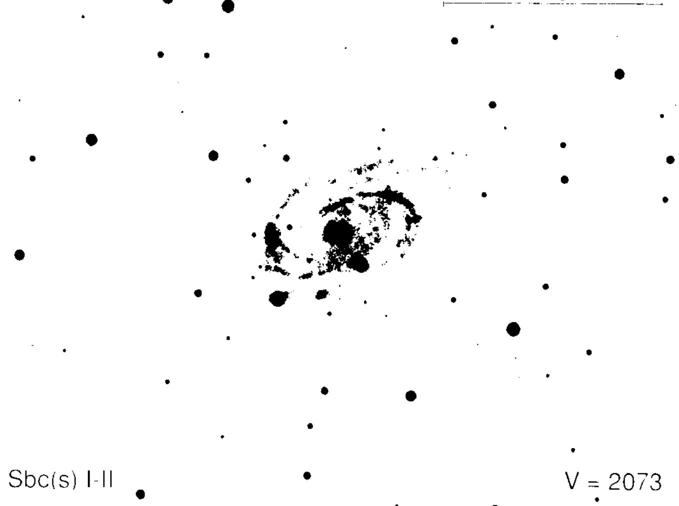

Sbc(s) I-II V = 2073

NGC 4939

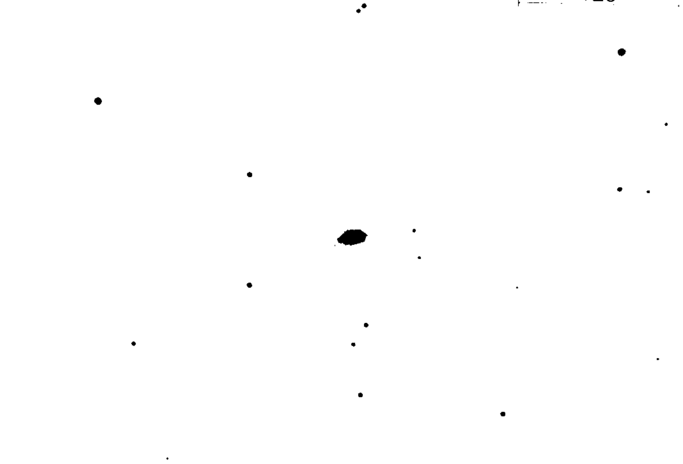

Sbc(rs) I V = 2903

NGC 4947

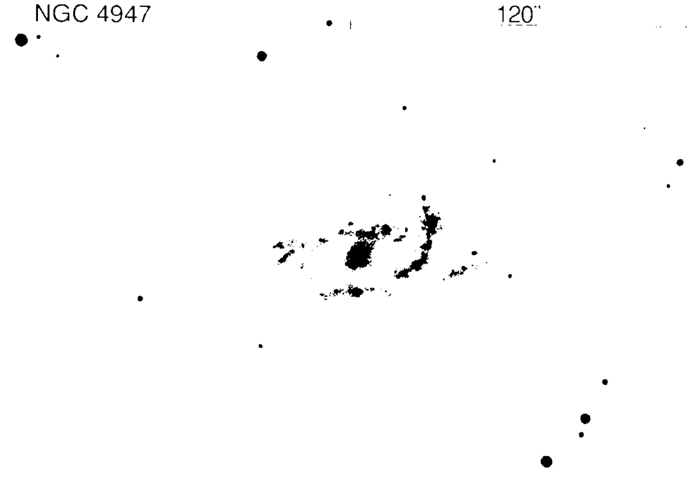

Sbc(s) I-II pec V = 2222

NGC 5055

Sbc(s) II-III V = 550

NGC 5351

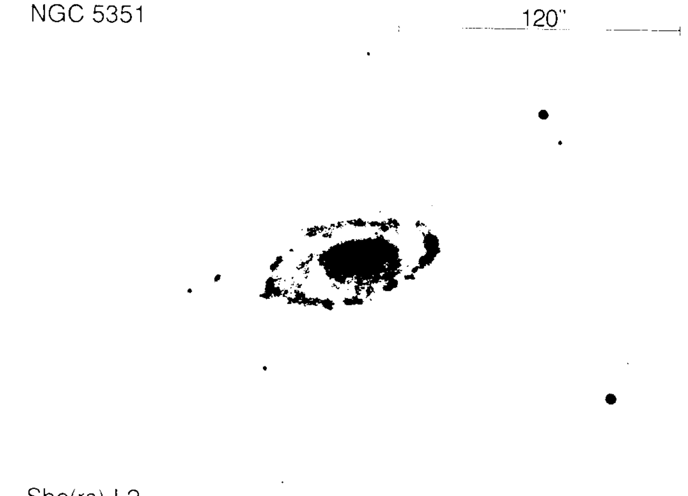

Sbc(rs) I.2 V = 3663

NGC 6814

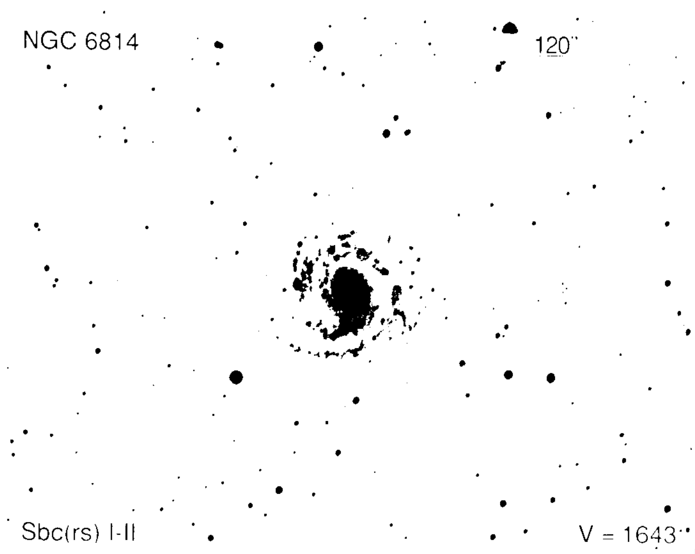

Sbc(rs) I-II V = 1643

NGC 7171

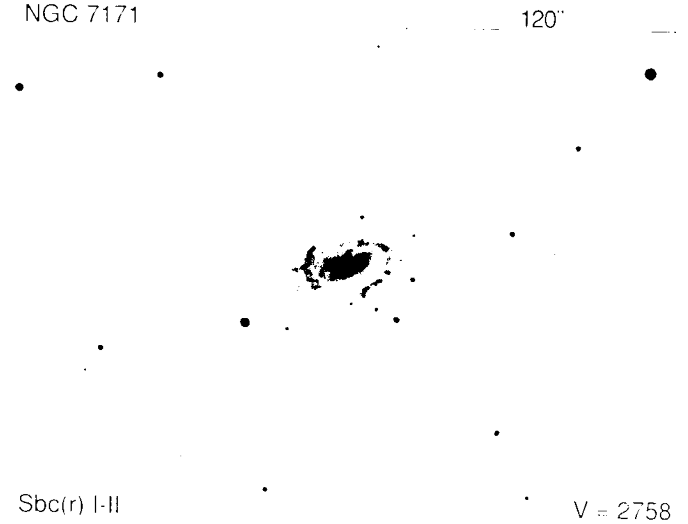

Sbc(r) I-II V = 2758

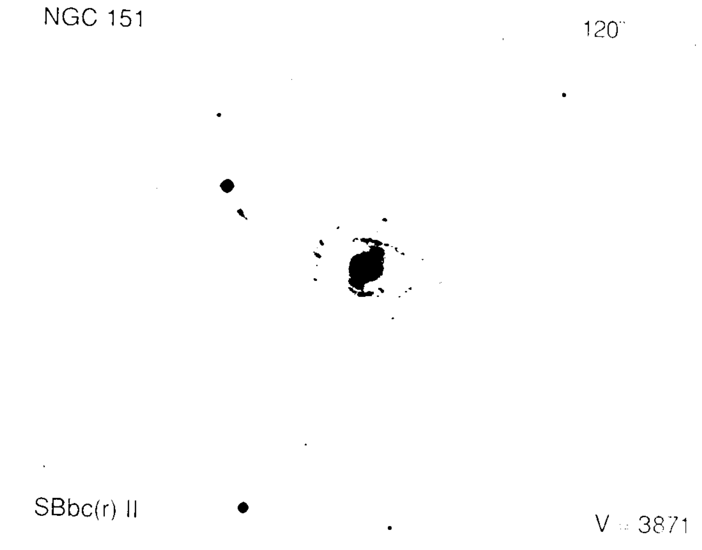
NGC 151
120"
SBbc(r) II
V = 3871

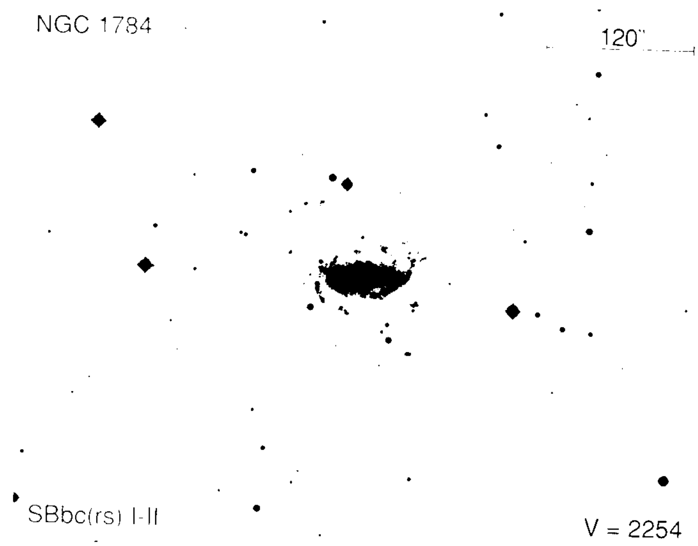
NGC 1784
120"
SBbc(rs) I-II
V = 2254

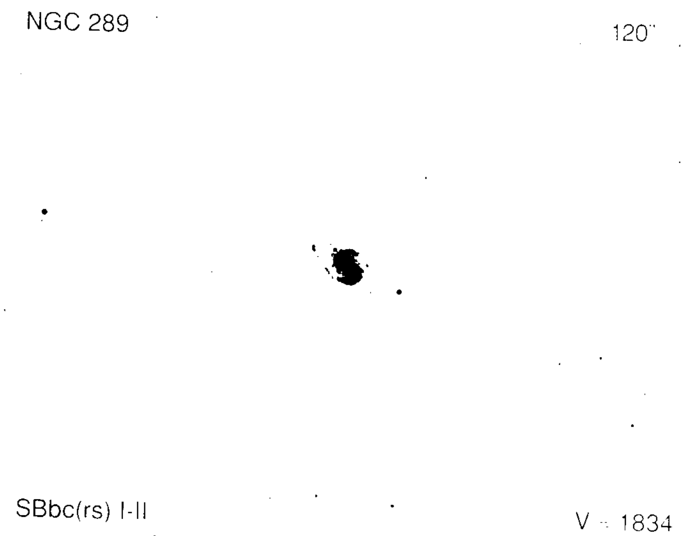
NGC 289
120"
SBbc(rs) I-II
V = 1834


NGC 289
120"
SBbc(rs) I-II
V = 1834

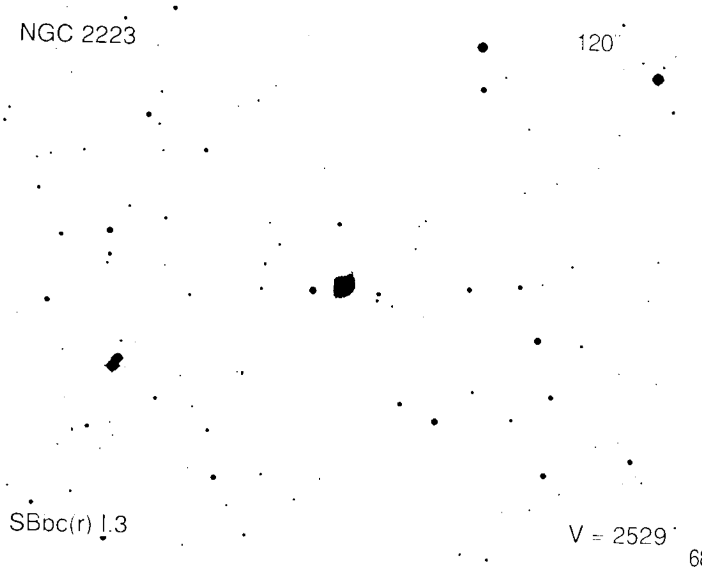
NGC 2223
120"
SBbc(r) I.3
V = 2529

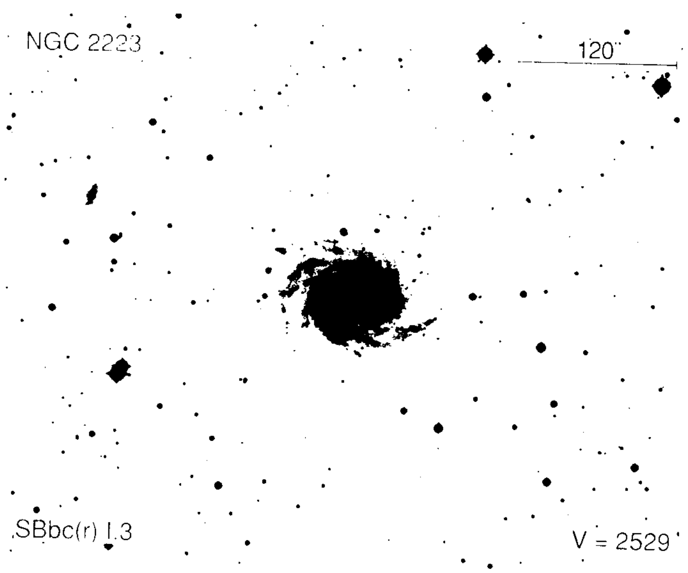
NGC 2223
120"
SBbc(r) I.3
V = 2529

NGC 2336 120"

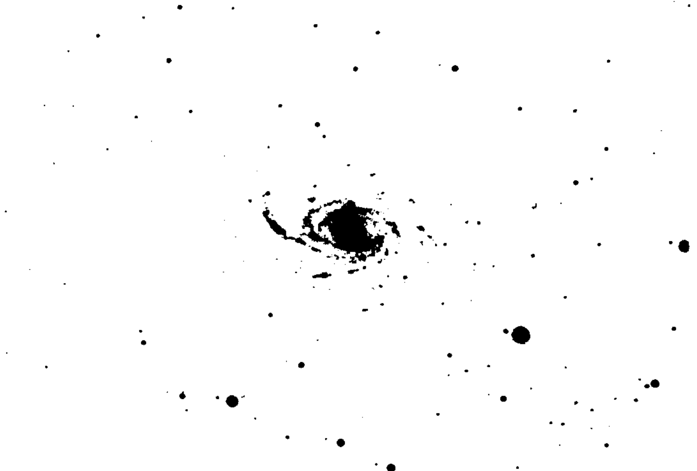

SBbc(r) I V = 2424

NGC 3001 120"

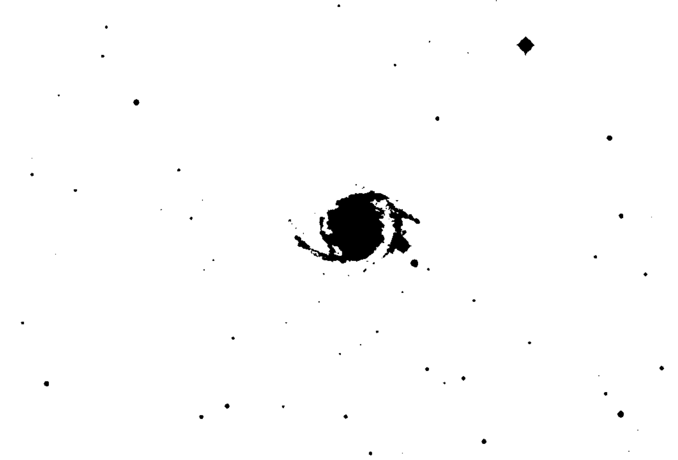

SBbc(s) I-II V = 2171

NGC 3054 120"

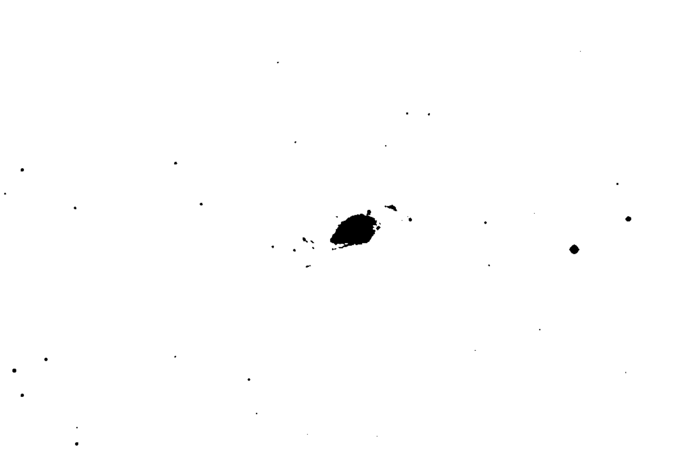

SBbc(s) I V = 1923

NGC 3124 120"

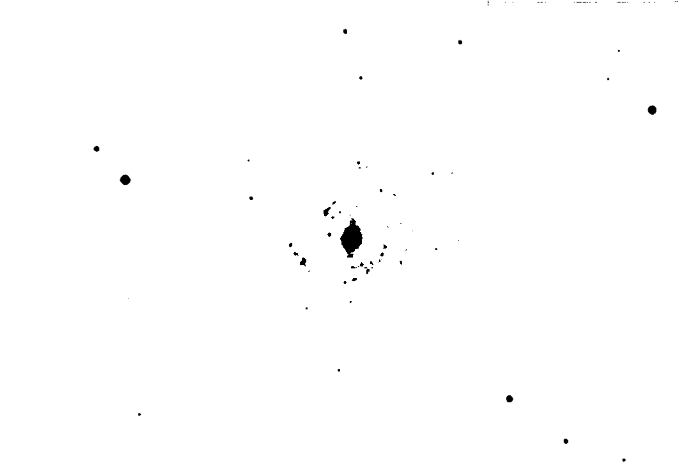

SBbc(r) I V = 3307

NGC 3485 120"

SBbc(s) II V = 1395

NGC 3686 120"

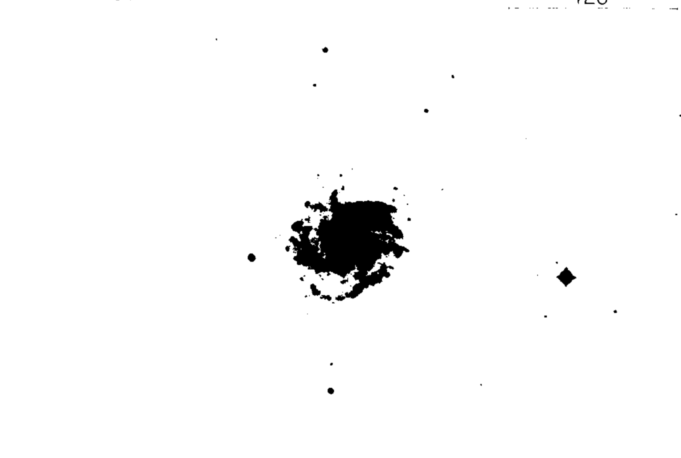

SBbc(s) II V = 1034

NGC 3887

SBbc(s) II-III

V = 915

NGC 3953

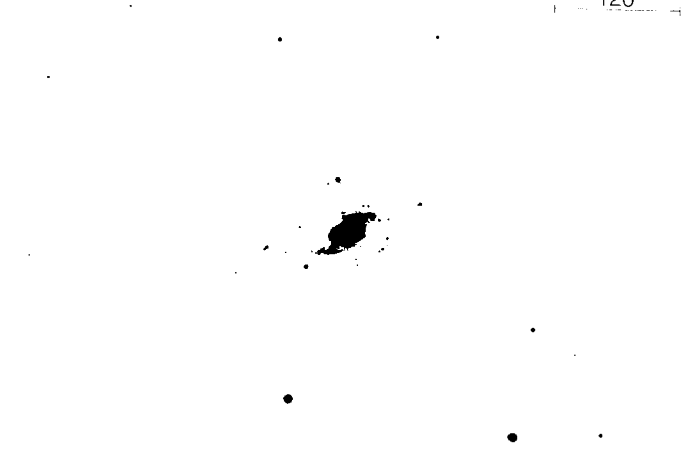

SBbc(r) I-II

V = 1036

NGC 4304

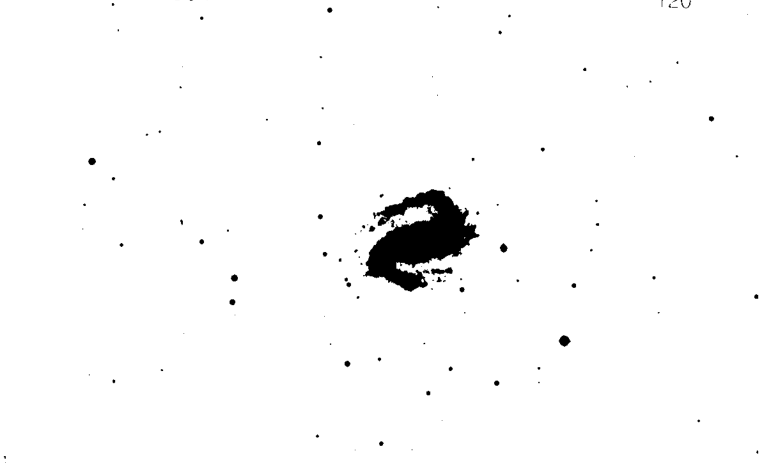

SBbc(s) II

V = 2327

NGC 4981

SBbc(r) I-II

V = 1492

NGC 4891

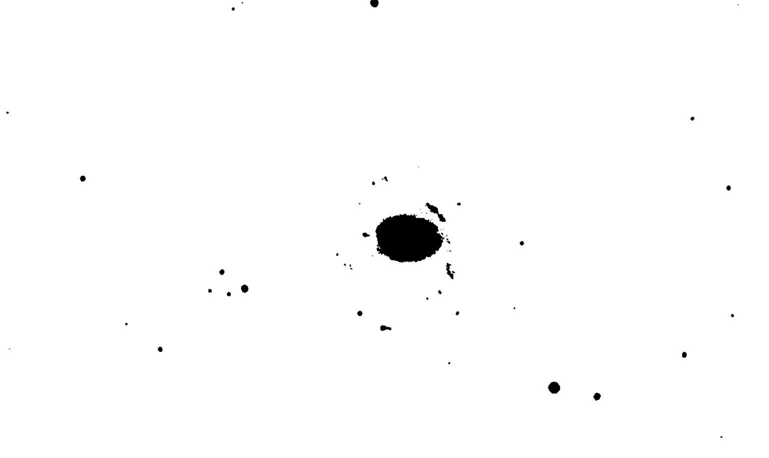

SBbc(sr) II

V = 2418

NGC 5350

SBbc(rs) I-II

V = 2305

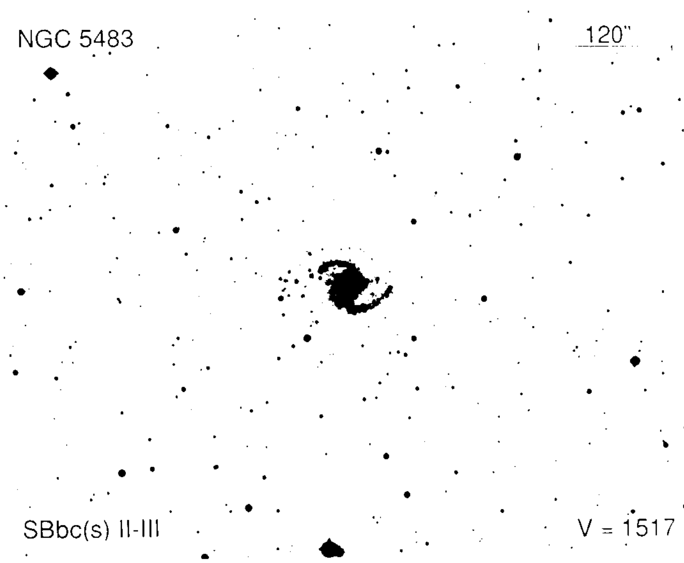
NGC 5483
120"
SBbc(s) II-III
V = 1517

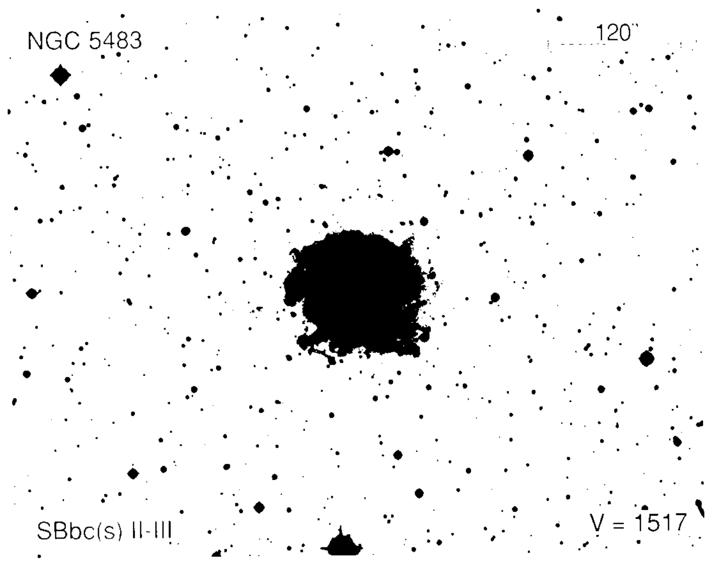
NGC 5483
120"
SBbc(s) II-III
V = 1517

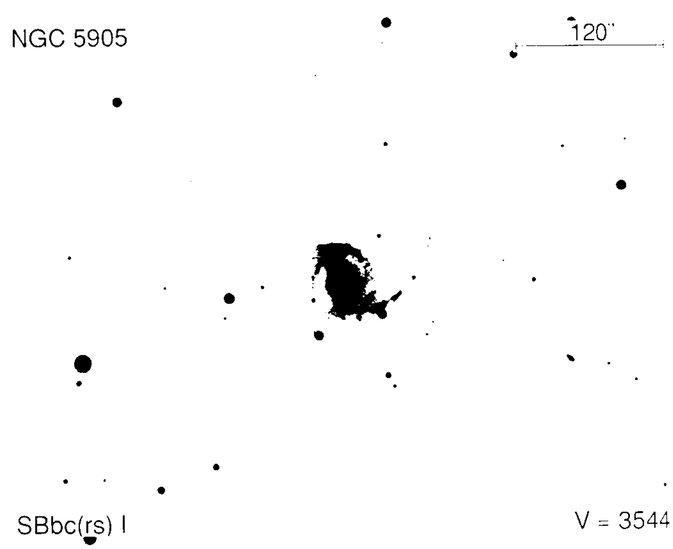
NGC 5905
120"
SBbc(rs) I
V = 3544

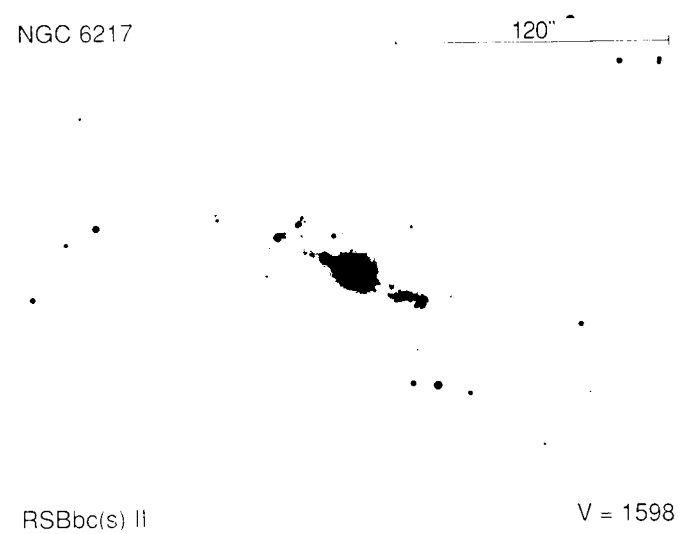
NGC 6217
120"
RSBbc(s) II
V = 1598

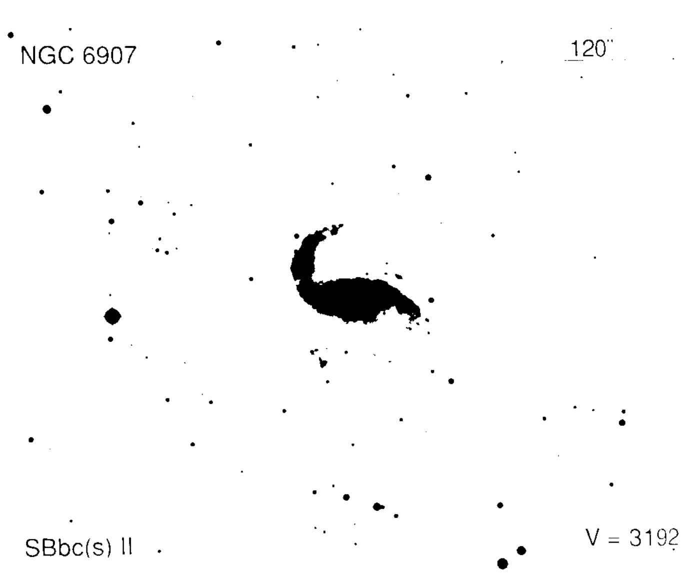
NGC 6907
120"
SBbc(s) II
V = 3192

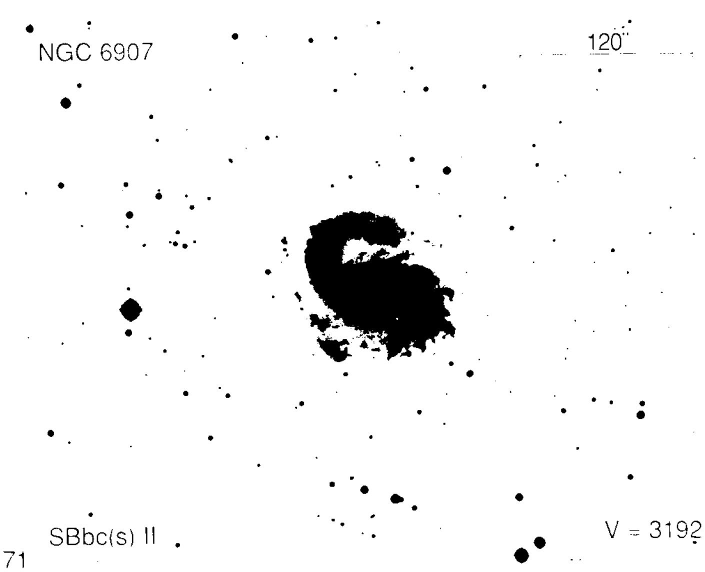
NGC 6907
120"
SBbc(s) II
V = 3192

NGC 7421 120"

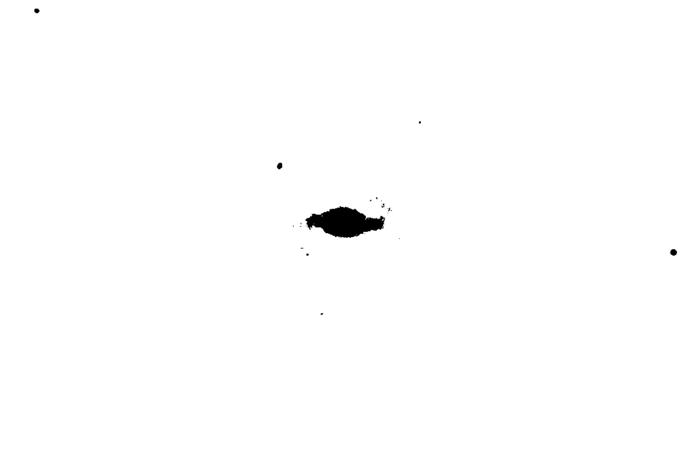

SBbc(rs) II-III V = 1838

NGC 7421 120"

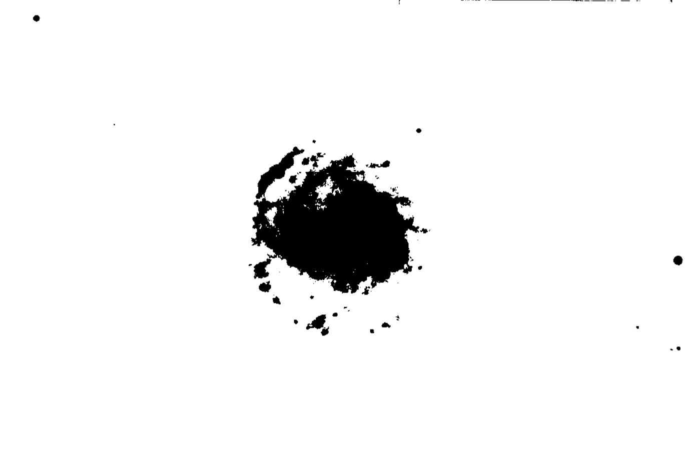

SBbc(rs) II-III V = 1838

NGC 7479 120"

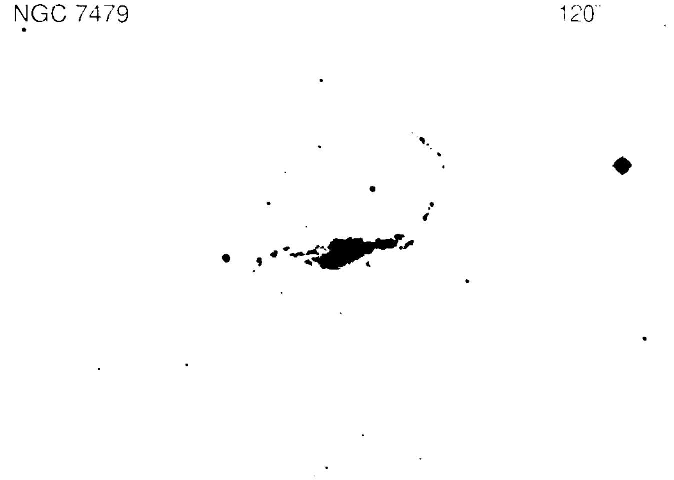

SBbc(s) I-II V = 2630

NGC 7678 120"

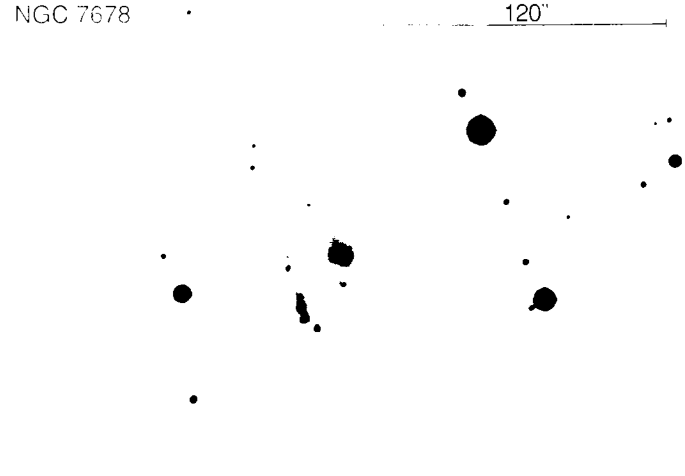

SBbc(s) I-II V = 3756

NGC 7755 120"

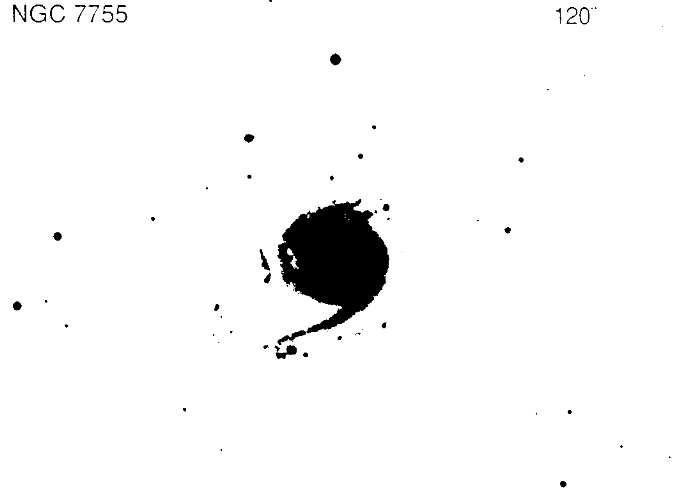

SBbc(r) Sbc(r) I-II V = 2969

IC 1953 120"

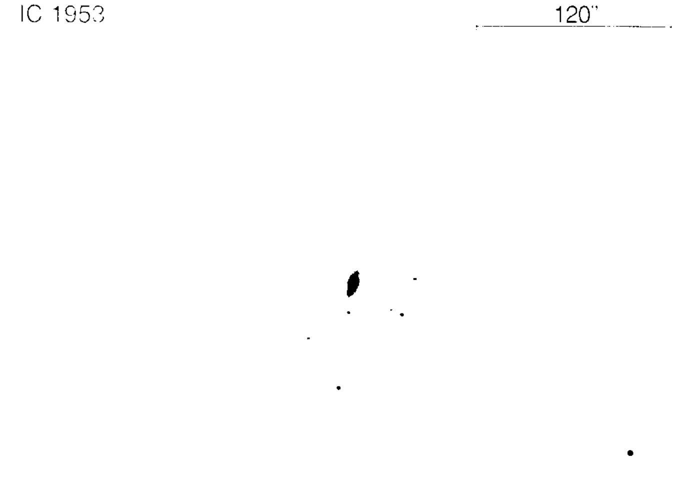

SBbc(rs) II V = 1856

NGC 428

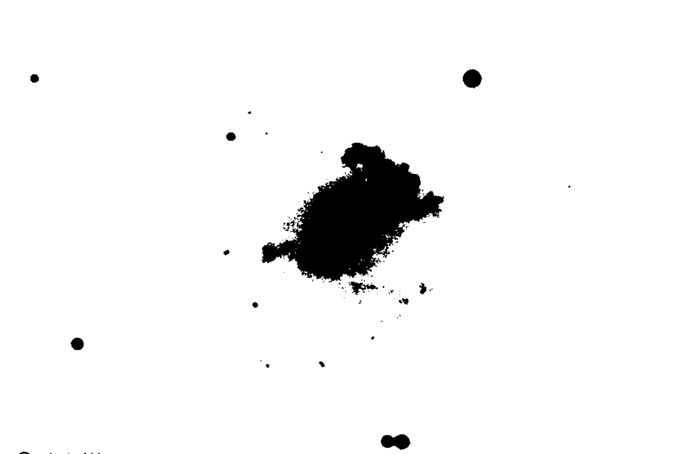

Sc(s) III

V = 1311

NGC 450

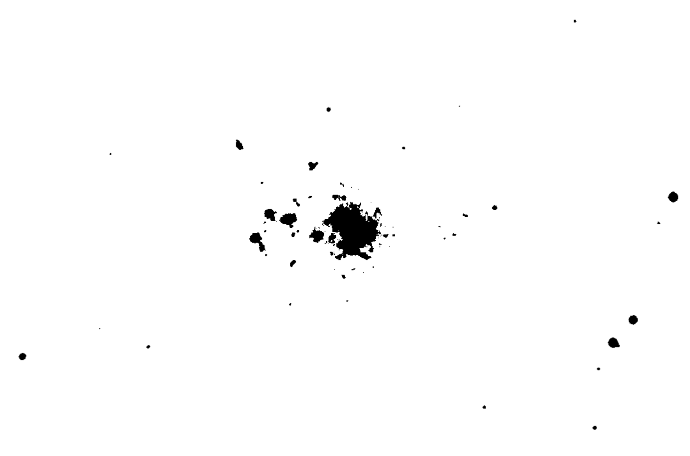

Sc(s) II.3

V = 1911

NGC 514

Sc(s) II

V = 2675

NGC 578

Sc(s) II

V = 1675

NGC 753

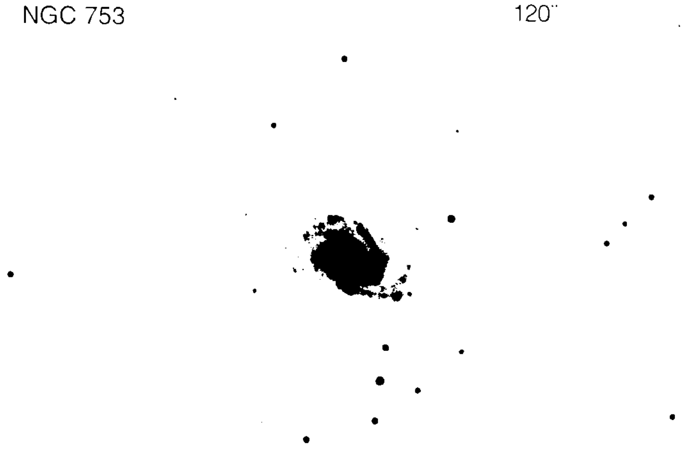

Sc(s) I-II

V = 5145

NGC 895

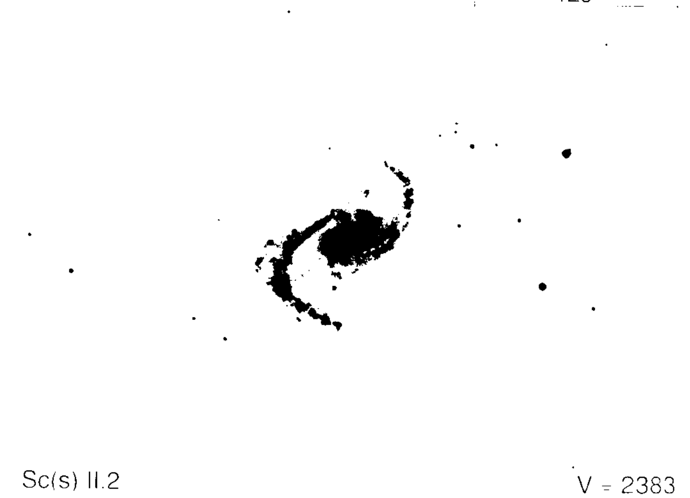

Sc(s) II.2

V = 2383

NGC 991 120"

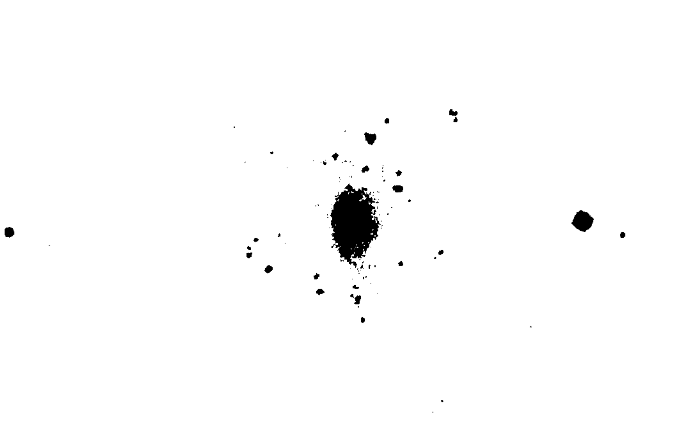

Sc(rs) II V = 1607

NGC 1042 120"

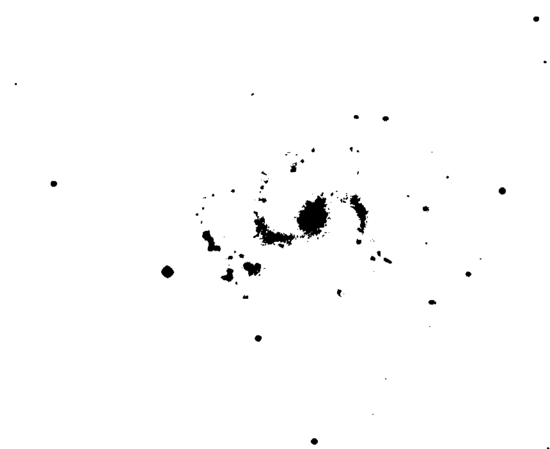

Sc(rs) I-II V = 1436

NGC 1058 120"

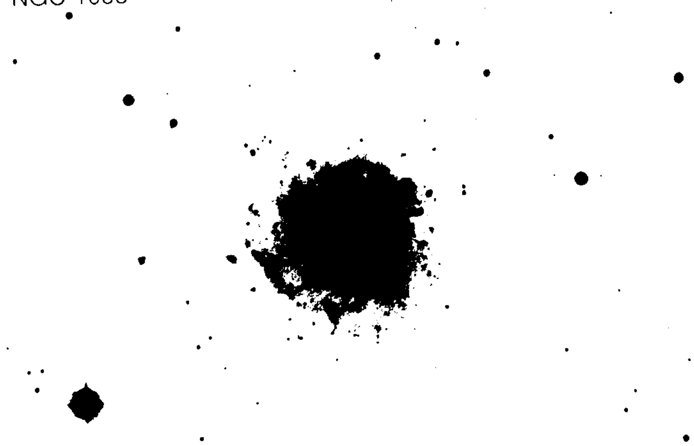

Sc(s) II-III V = 746

NGC 1087 120"

Sc(s) III.3 V = 1628

NGC 1232 120"

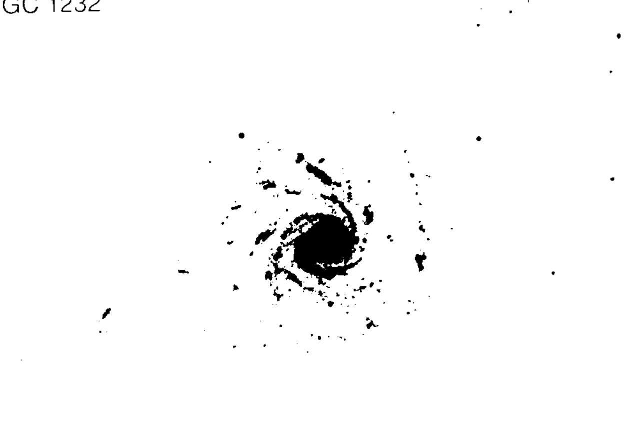

Sc(rs) I V = 1775

NGC 1337 120"

Sc(s) I II V = 1270

NGC 1359 120"

Sc(s) II-III V = 1972

NGC 1359 120"

Sc(s) II-III V = 1972

NGC 1448 120"

Sc(s) II V = 1038

NGC 2280 120"

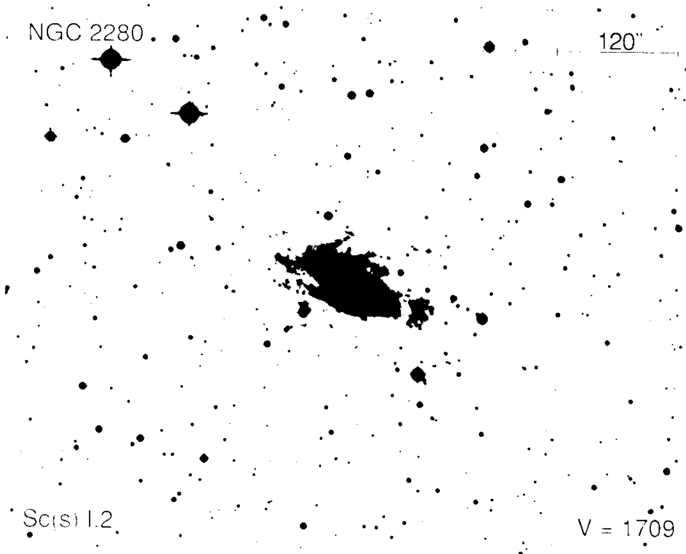

Sc(s) I.2 V = 1709

NGC 2763 120"

Sc(r) II V = 1658

NGC 2776 120"

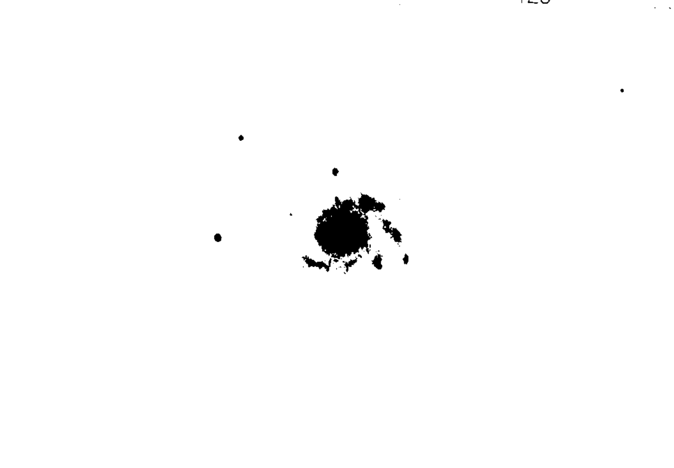

Sc(rs) I V = 2673

NGC 2848 120''

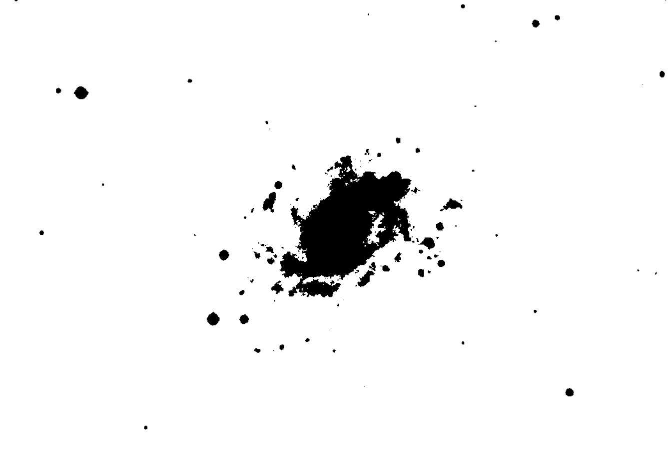

Sc(s) II V = 1795

NGC 2942 120''

Sc(s) I.3 V = 4399

NGC 2967 120''

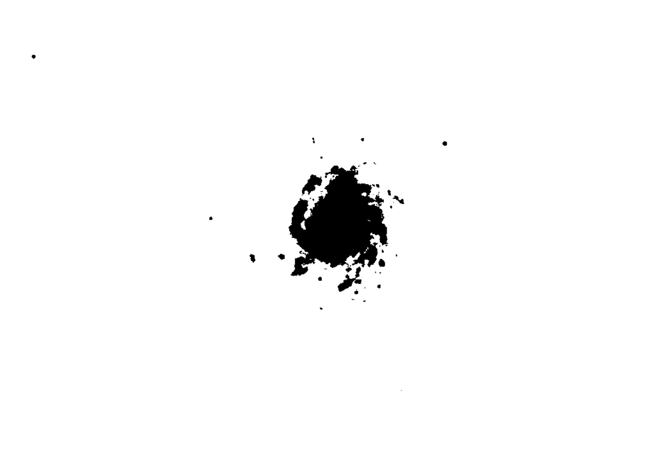

Sc(rs) I-II V = 2065

NGC 3041 120''

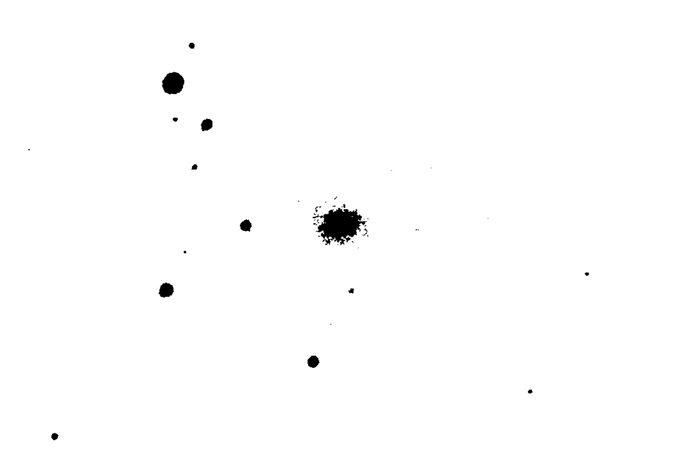

Sc(s) II V = 1296

NGC 3055 120''

Sc(s) II V 1747

NGC 3079 120''

Sc(s) II-III V = 1225

NGC 3198 120"

Sc(s) I-II V = 702

NGC 3464 120"

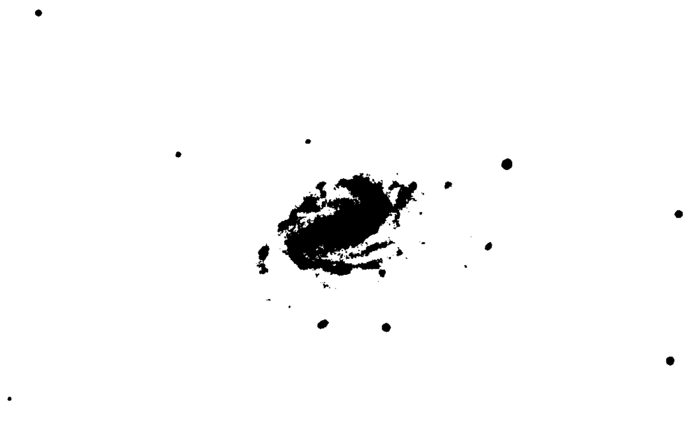

Sc(rs) I V = 3571

NGC 3511 120"

Sc(s) II.8 V = 951

NGC 3614 120"

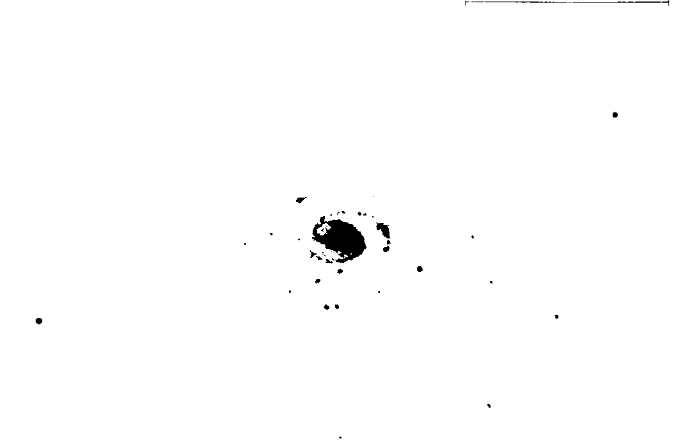

Sc(r) I V = 2362

NGC 3629 120"

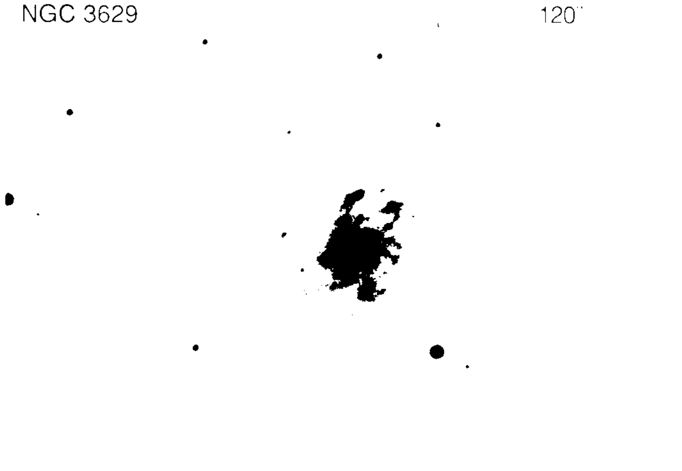

Sc(s) II.2 V = 1451

NGC 3684 120"

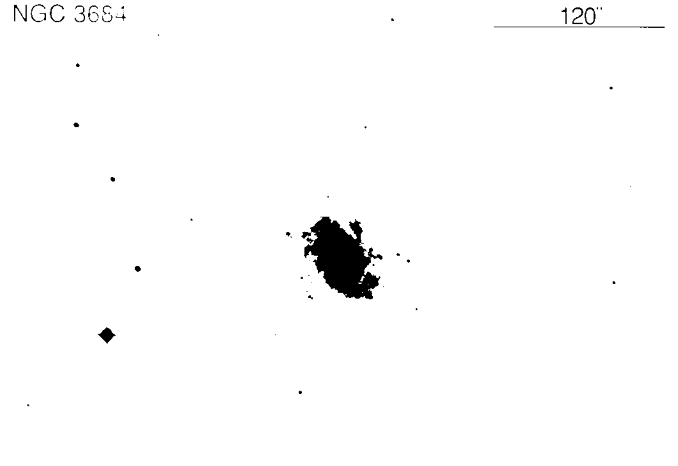

Sc(s) II V = 1065

NGC 3756 120"

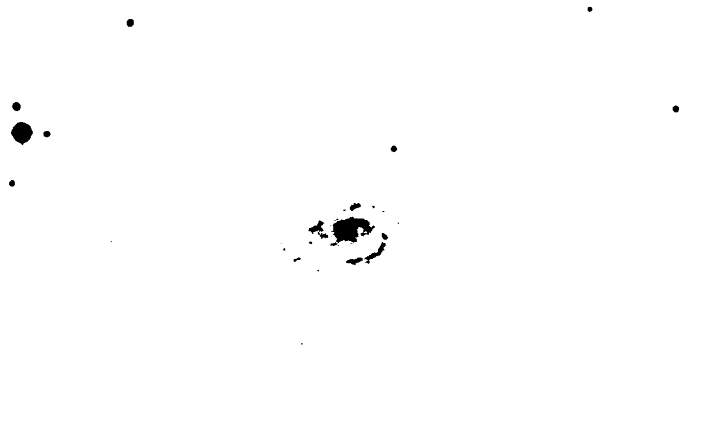

Sc(s) I-II V = 1372

NGC 3780 120"

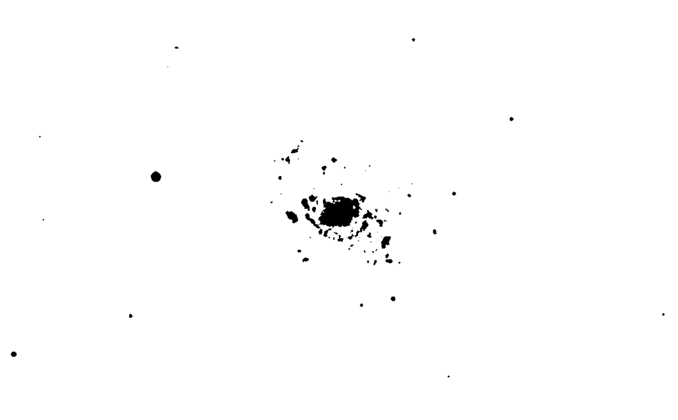

Sc(r) II.3 V = 2481

NGC 3810 120"

Sc(s) II V = 860

NGC 3893 120"

Sc(s) I.2 V = 1026

NGC 3995 120"

Sc (tides) V = 3327

NGC 4041 120"

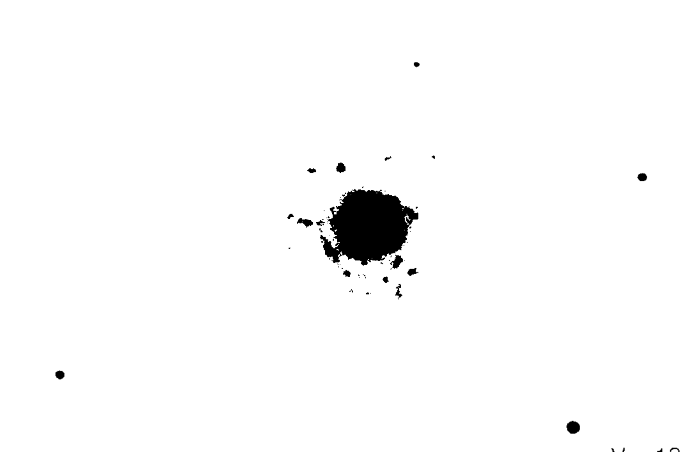

Sc(s) II-III V = 1361

NGC 4303

120"

Sc(s) I.2

V = 1404

NGC 4321

120"

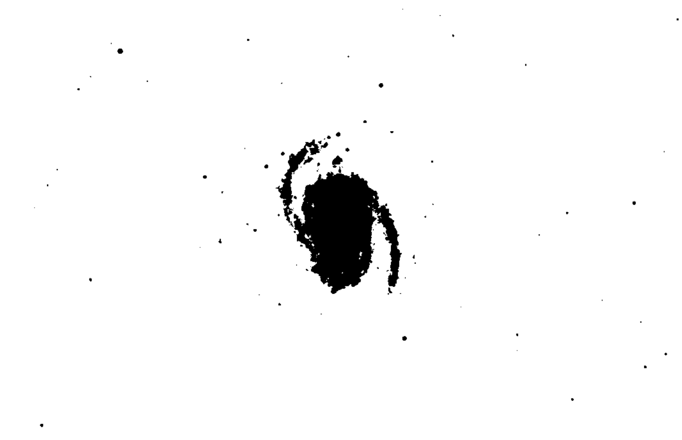

Sc(s) I

V = 1464

NGC 4414

120"

Sc(sr) II.2

V = 702

NGC 4536

120"

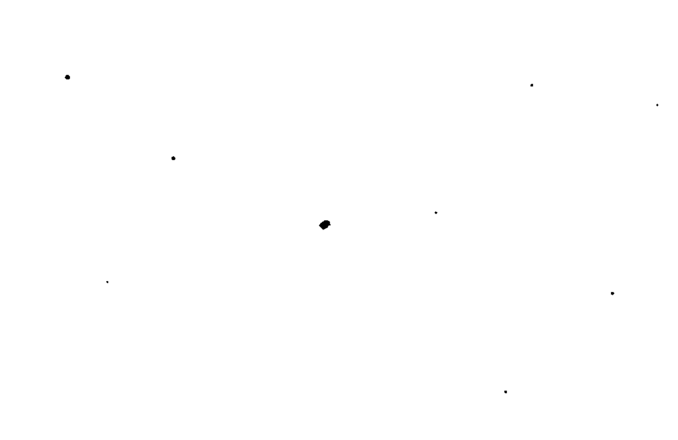

Sc(s) I

V = 1646

NGC 4651

120"

Sc(r) I.5

V = 723

NGC 4653

120"

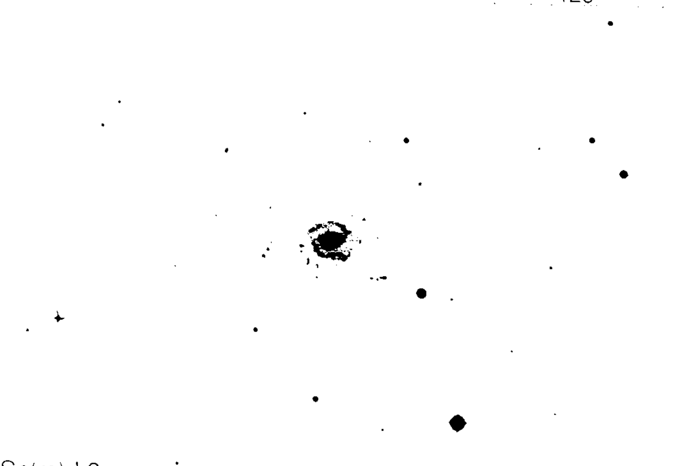

Sc(rs) I.3

V = 2433

NGC 4775 120"

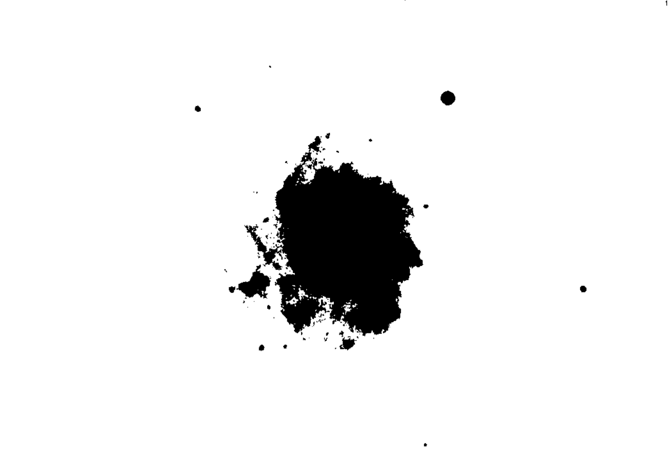

Sc(s) III V = 1375

NGC 4899 120"

Sc(s) I-II V = 2437

NGC 5085 120"

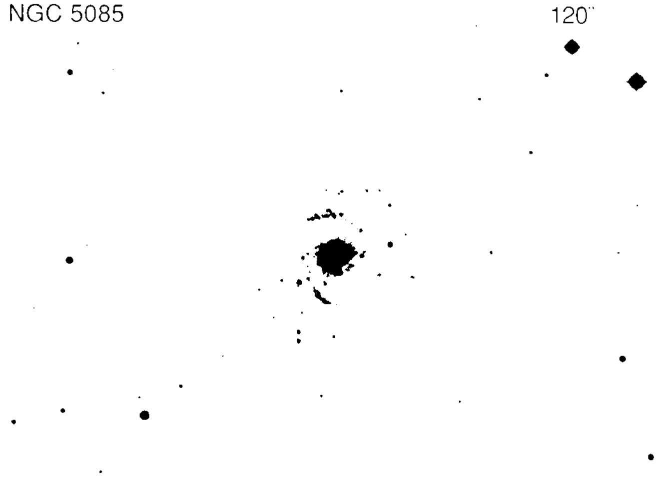

Sc(r) II V = 1720

NGC 5161 120"

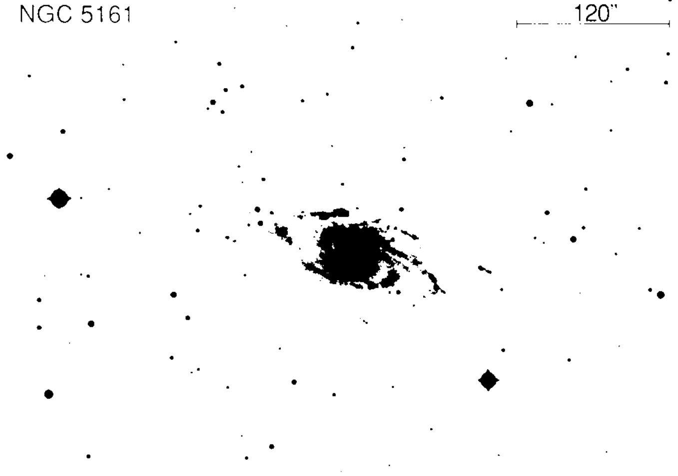

Sc(s) I V = 2113

NGC 5247 120"

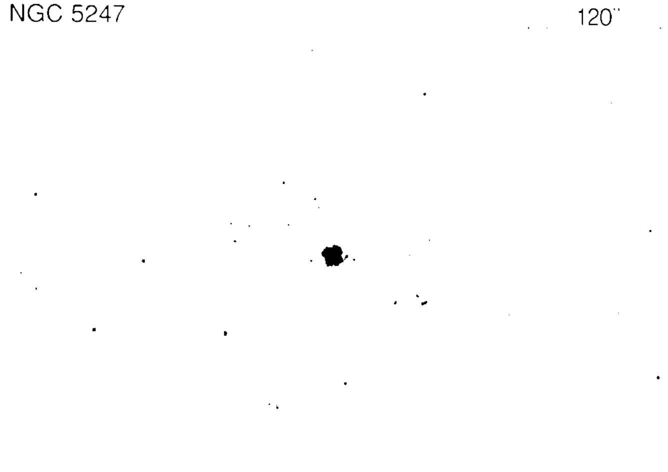

Sc(s) I-II V = 1143

NGC 5247 120"

Sc(s) I-II V = 1143

NGC 5364 120"

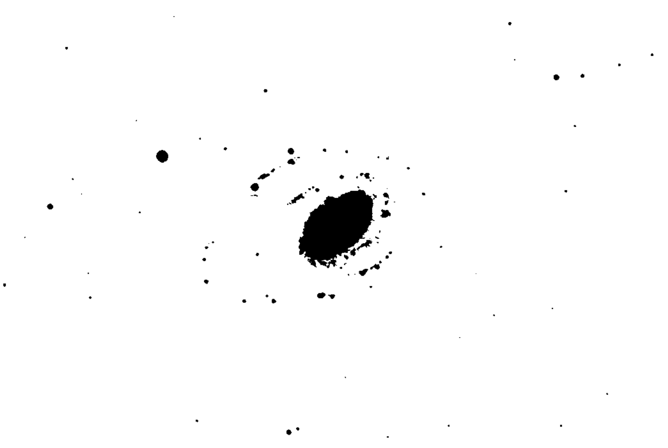

Sc(r) I V = 1140

NGC 5468 120"

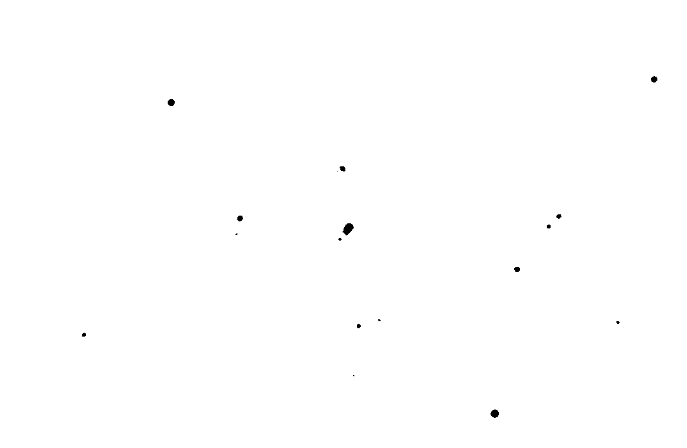

Sc(s) I.8 V = 2696

NGC 5494 120"

Sc(s) II V = 2461

NGC 5584 120"

Sc(s) I.8 V = 1518

NGC 5605 120"

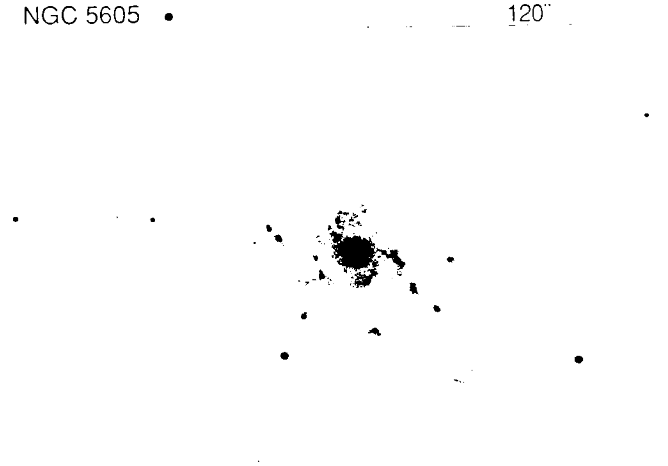

Sc(rs) II V = 3196

NGC 5660 120"

Sc(s) I.2 V = 2433

NGC 5668 120"

Sc(s) II-III V = 1491

NGC 5861 120"

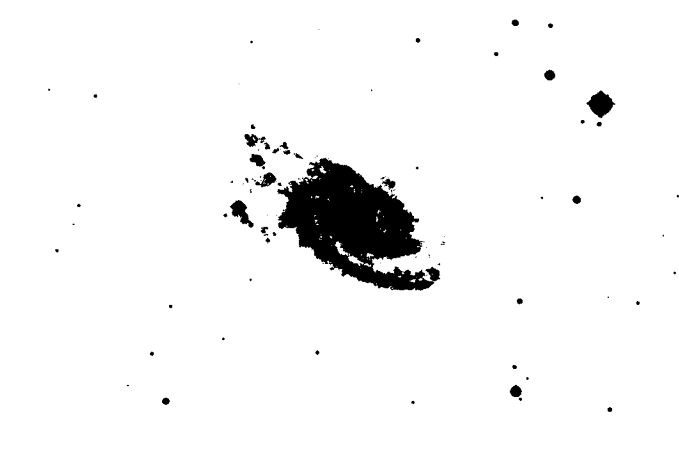

Sc(s) II V = 1725

NGC 6015 120"

Sc(s) II-III V = 1018

NGC 6070 120"

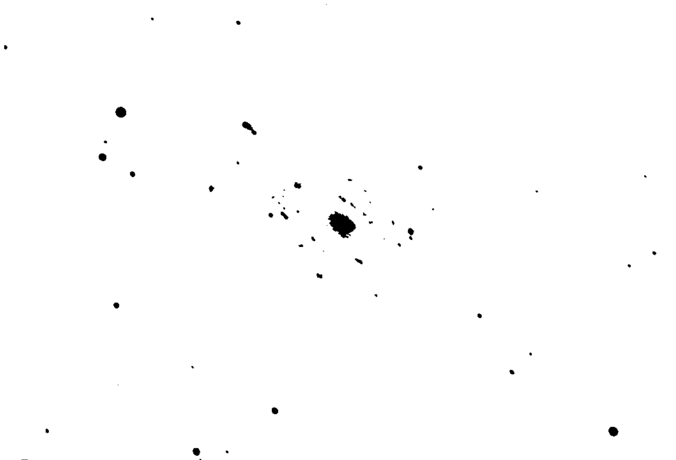

Sc(s) I-II V = 1979

NGC 6118 120"

Sc(s) I.3 V = 1535

NGC 6643 120"

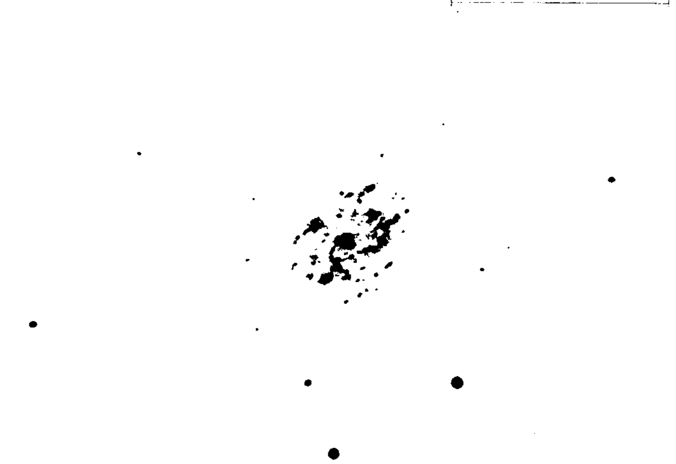

Sc(s) II V = 1743

NGC 7125 120"

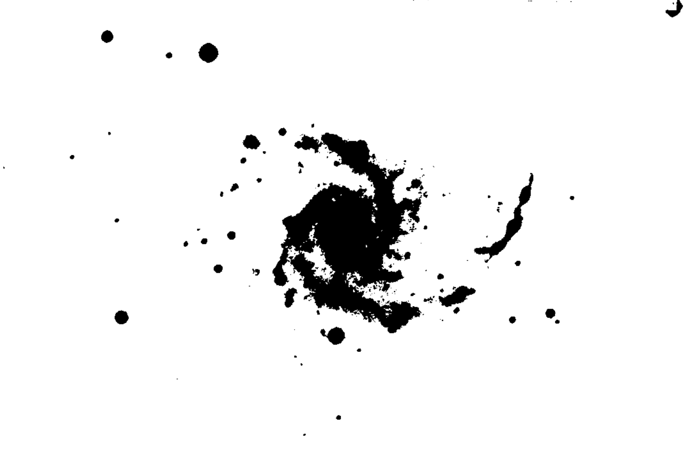

Sc(rs) I-II / SBc(s) I-II V = 2910

NGC 6836 120"

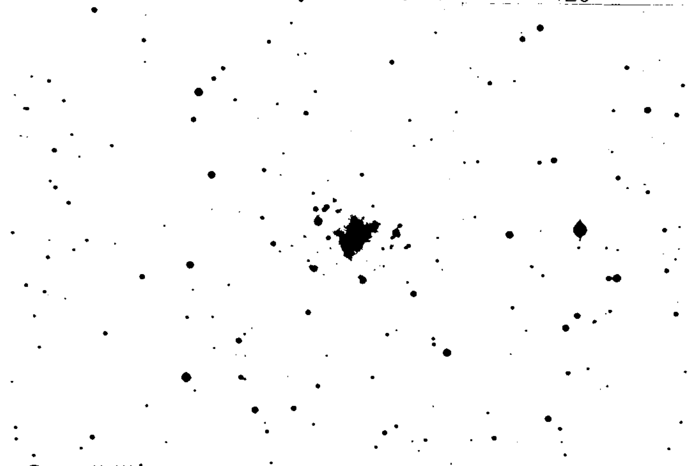

Sc(s) II-III V = 1628

NGC 7361 120"

Sc II-III V = 1276

NGC 7412 120"

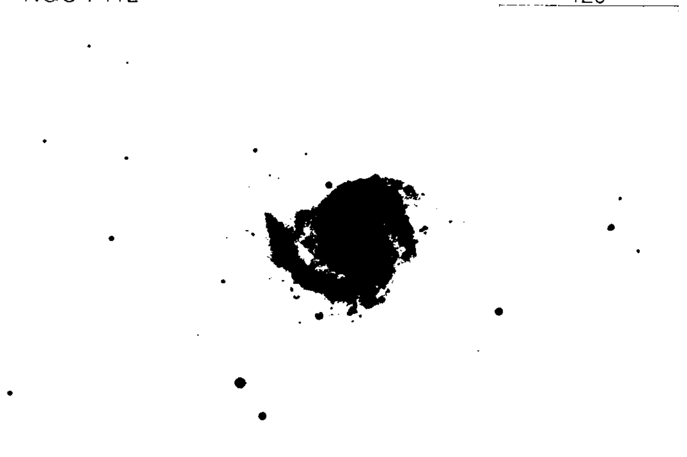

Sc(s) I-II V = 1691

NGC 7418 120"

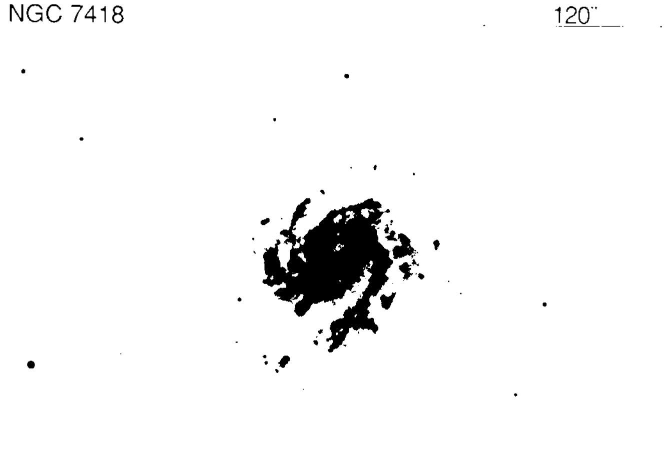

Sc(rs) I.8 V = 1451

NGC 7689 120"

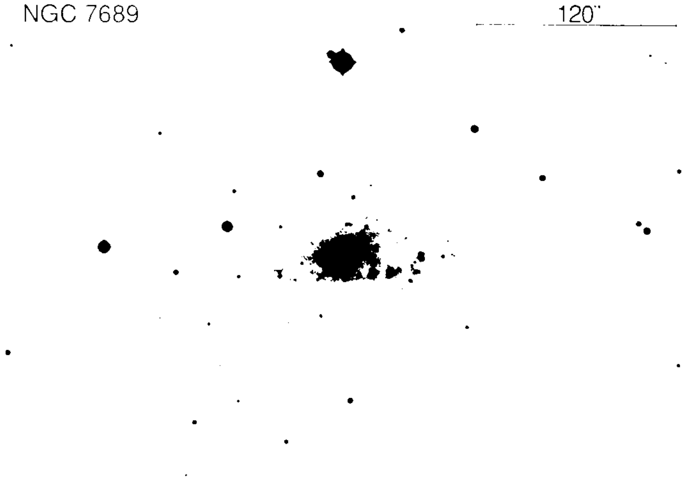

Sc(sr) II V = 1681

NGC 7713 120''

Sc(s) II-III V = 684

HA85-1 120''

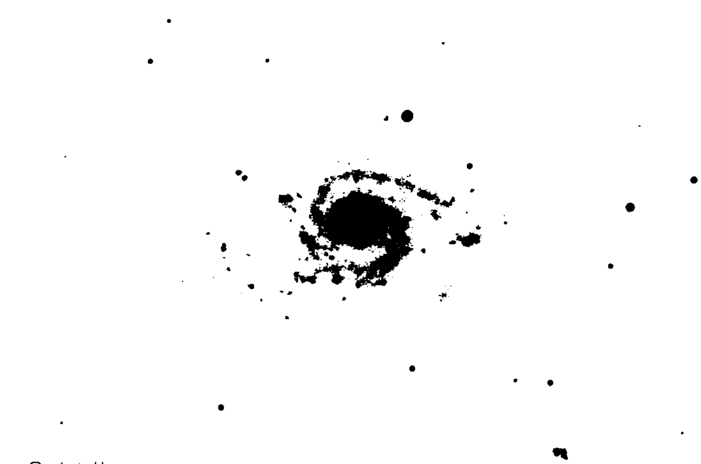

Sc(s) II V = 2063

IC 764 120''

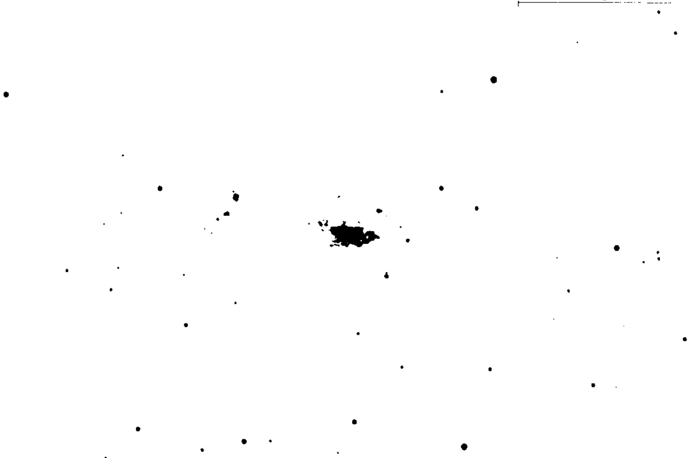

Sc(s) I.2 V = 1851

IC 764 120''

Sc(s) I.2 V = 1851

NEW 4 120''

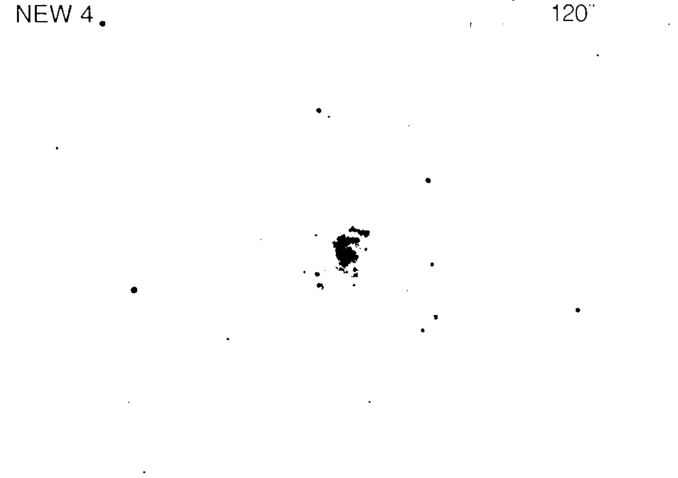

Sc(s) III V = 1160

F-703 120''

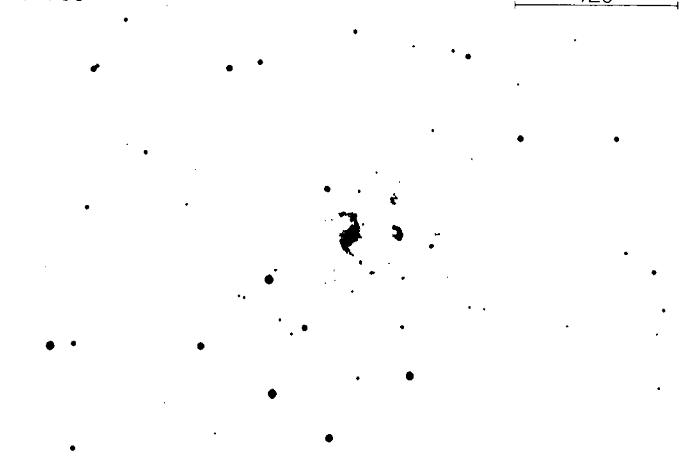

Sc(s) II.2 V = 2128

NGC 255 120"

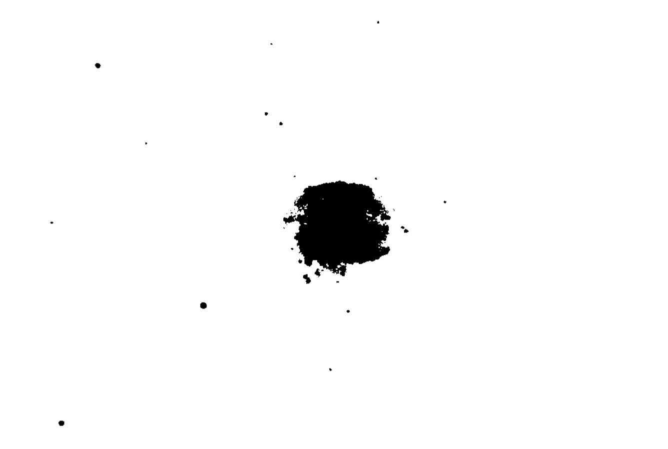

SBc(rs) II-III V = 1726

NGC 685 120"

SBc(rs) II V = 1306

NGC 1073 120"

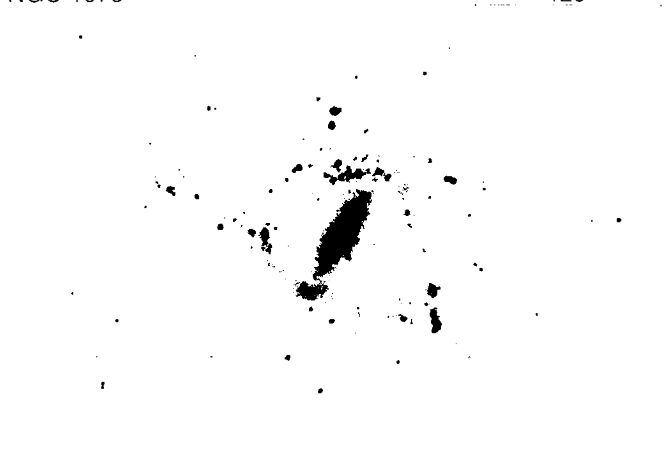

SBc(rs) II V = 1318

NGC 1179 120"

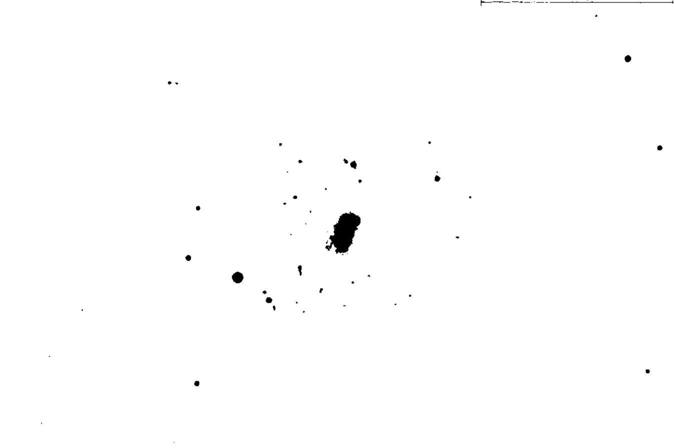

SBc(r) II.2 V = 1776

NGC 1493 120"

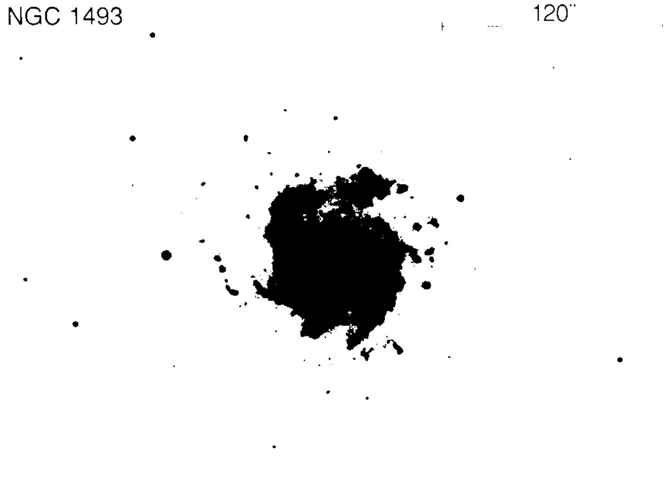

SBc(rs) III V = 910

NGC 3346 120"

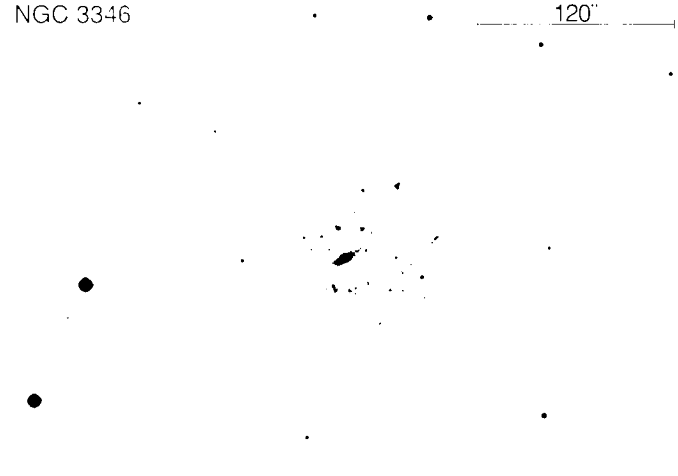

SBc(rs) II.2 V = 1138

NGC 5334 120''

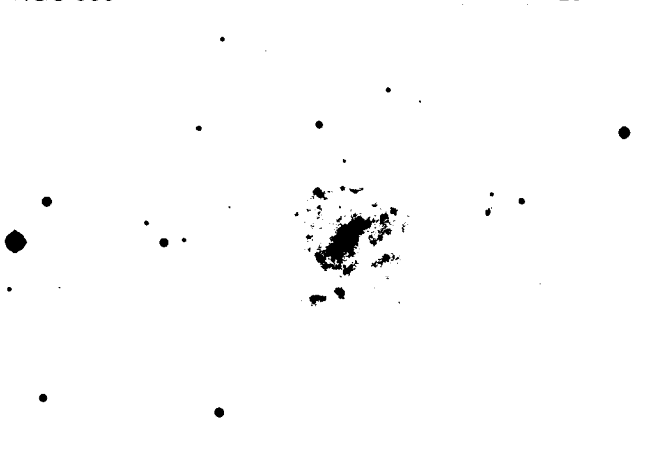

SBc(rs) II V = 1237

NGC 5556 120''

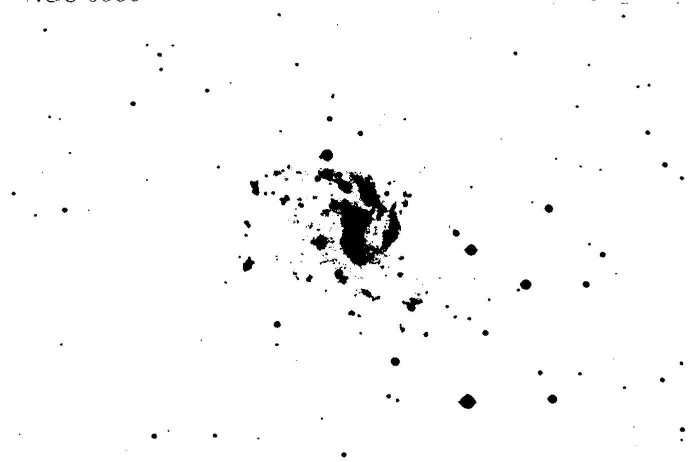

SBc(sr) II-III V = 1163

NGC5669 120''

Sc/SBc(r) I-II V = 1304

NGC 5885 120''

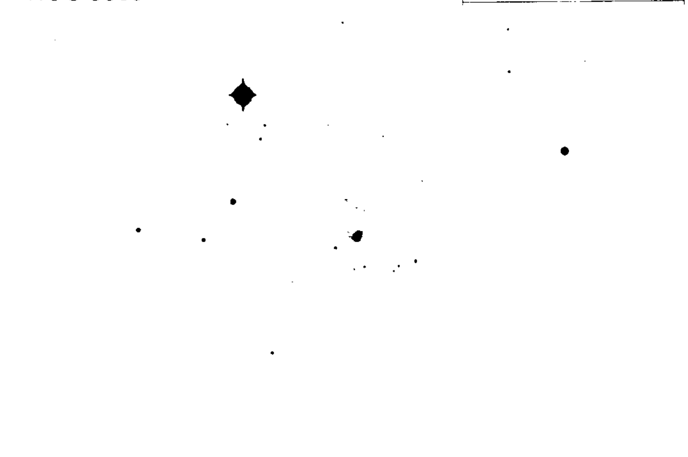

SBc(s) II V = 1879

NEW 1 120''

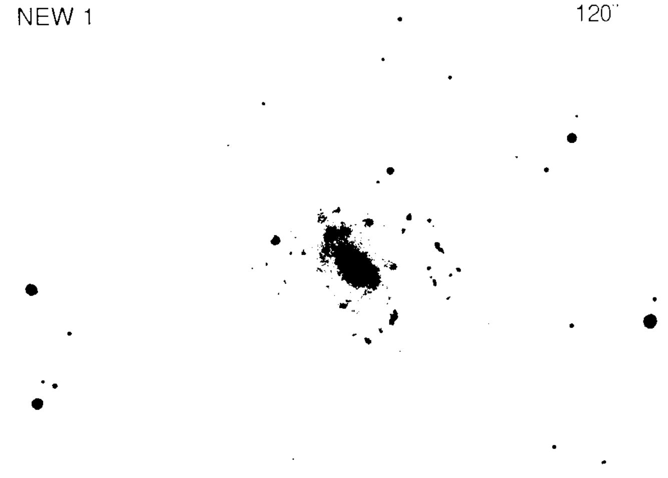

SBc(s) II.2 V = 1116

NGC 941 120''

Scd III V = 1717

NGC 1494 120"

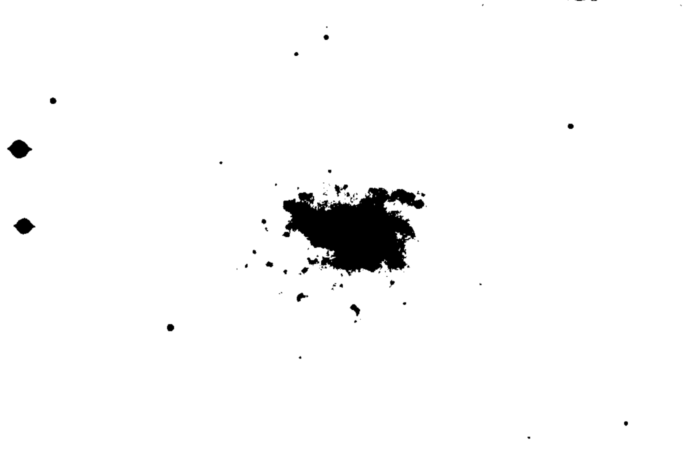

Scd(s) II V = 957

NGC 2188 120"

Scd III V = 555

NGC 4144 120"

Scd III V = 316

NGC 4592 120"

Scd III V = 903

NGC 4485 90 120"

S(tidal) Scd III pec V 817 601

NGC 4485 90 120"

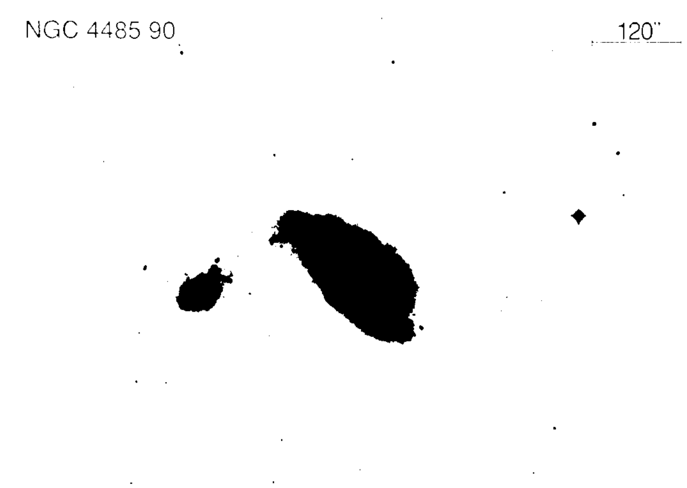

S(tidal) Scd III pec V - 817 601

Part IV

The 8 panels on atlas panels 88 to 95 illustrate the 75 galaxies in the 6° (radius) core of the Virgo Cluster listed in Table 4. The panels are ordered by the estimated ease of resolution.

NGC 4548 120" NGC 4571

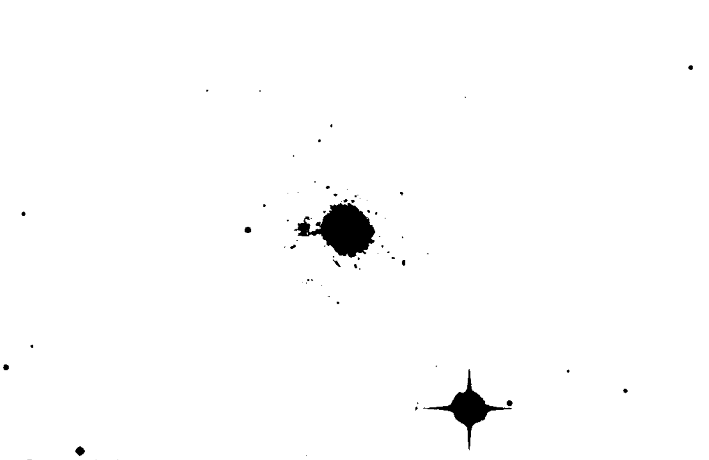

SBb(rs) I-II Sc(s) II-III

7 27 NGC 4496 A

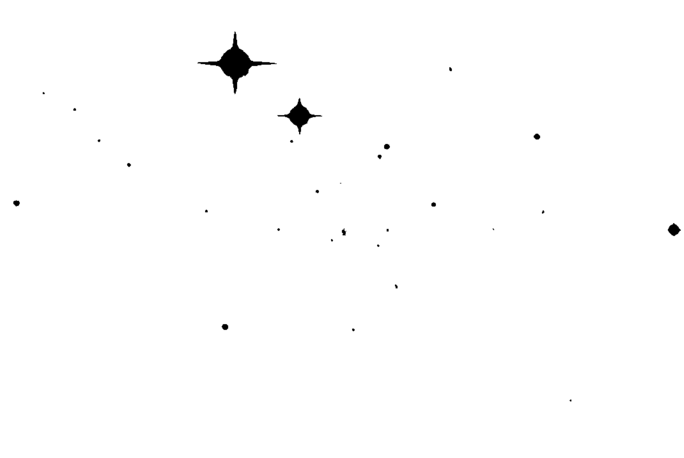

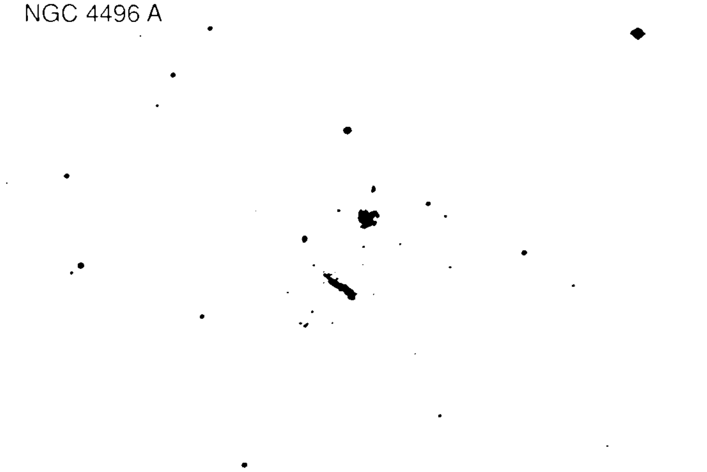

Scd(s) II SBc III-IV

NGC 4523 IC 3576

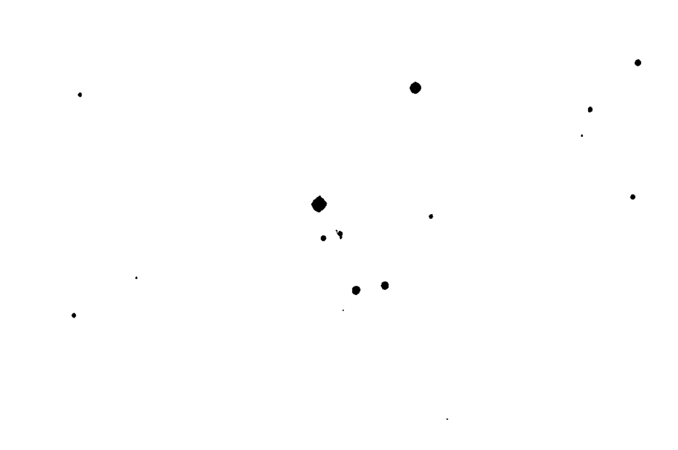

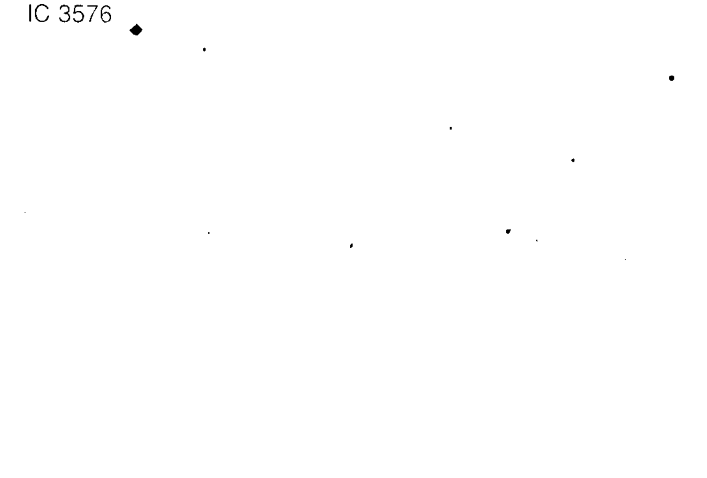

SBd(s) III SBd IV

120"

NGC 4535

SBc(s) I.3

NGC 4178

SBc(s) II

NGC 4394

SBb(sr) I-II

NGC 4519

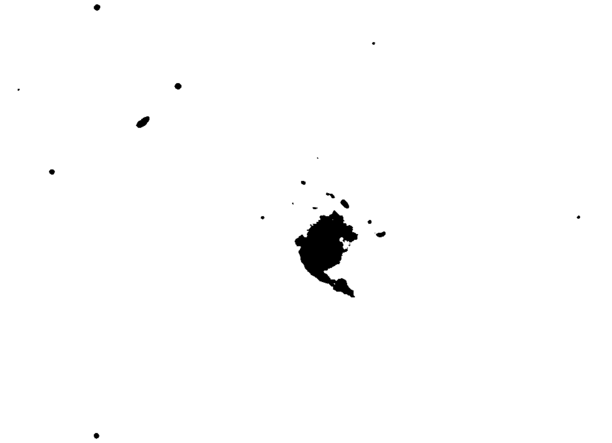

SBc(rs) II.2

NGC 4647

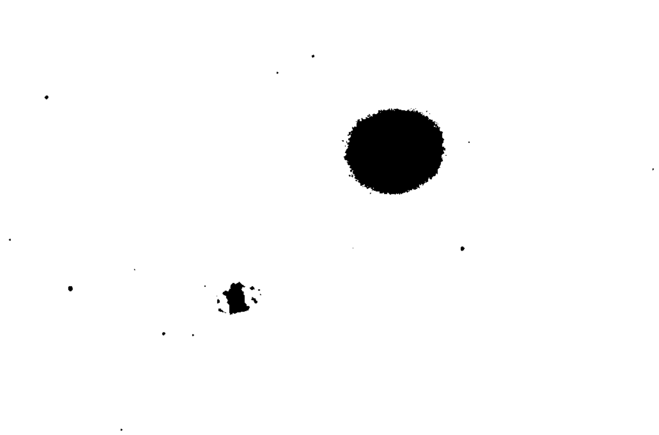

Sc(rs) III

NGC 4411 A + B

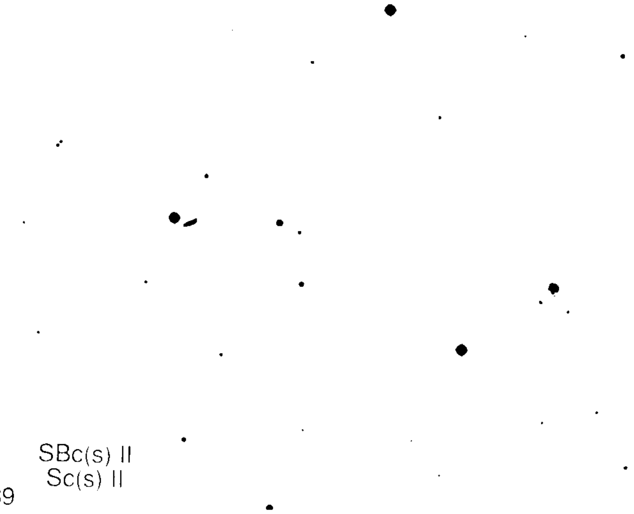

SBc(s) II
Sc(s) II

NGC 4654

120''

SBc(rs) II

NGC 4639 + A 1240.2

SBb(r) II
Im III

NGC 4689*

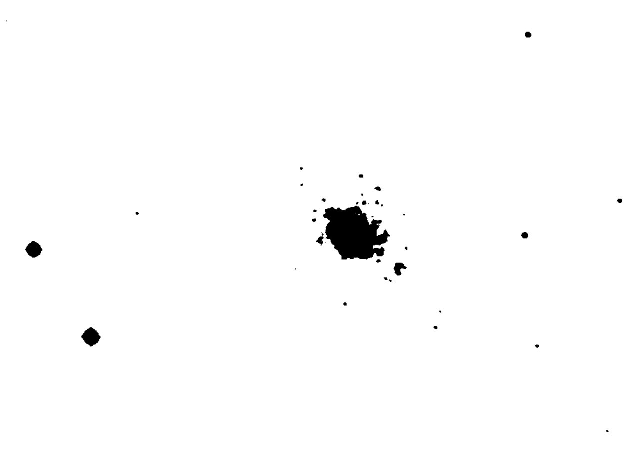

Sc(s) II.3

NGC 4430 + 4432

SBc(r) II + Sc(s) I-II

V = 1450
V = 6403

IC 776*

SBcd(s) III

IC 3365

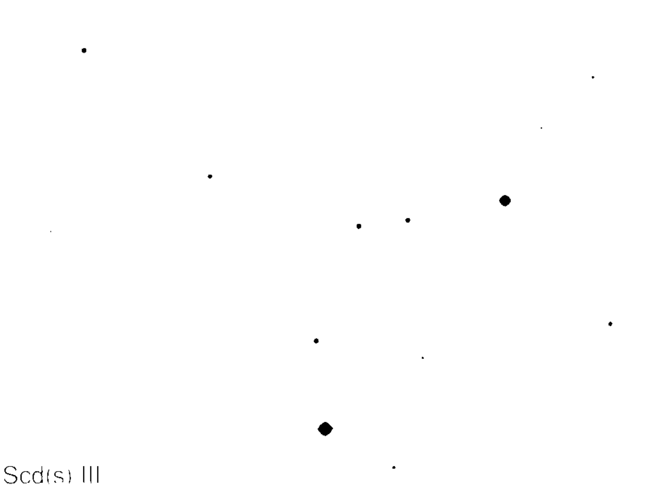

Scd(s) III

120"

NGC 4321

Sc(s) I

NGC 4536

Sc(s) I

NGC 4298 · 4302

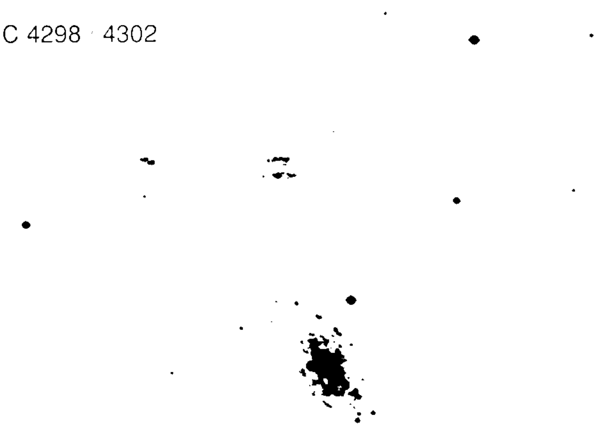

Sc(s) III
Sc(on edge)

NGC 4396

Sc(s) II

8 5

SBd IV

NGC 4498

SBc(s) II

120"

IC 3476

Sc(s) II.2

NGC 4390

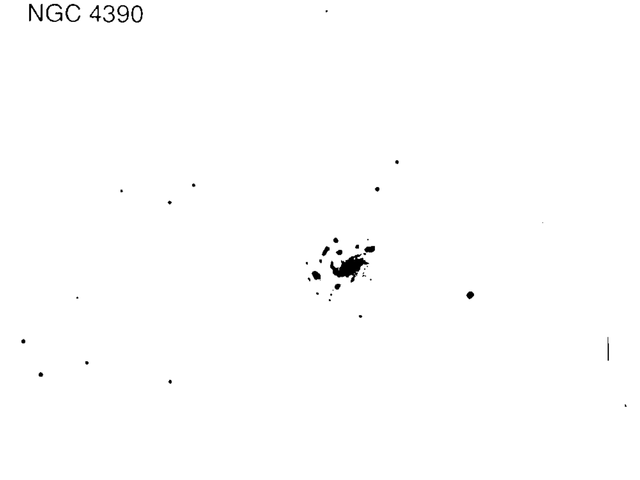

Sbc(s) II

NGC 4330

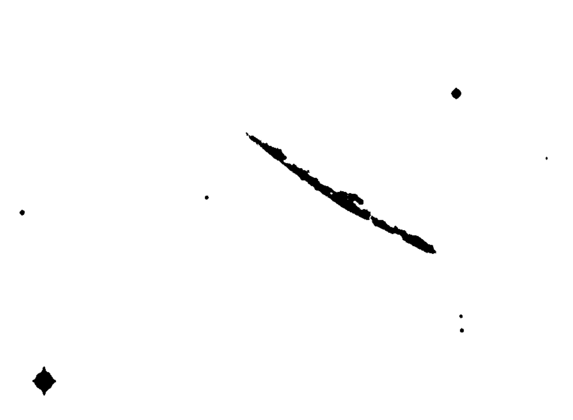

Sd(on edge)

IC 3258

Sc II.8

IC 3414

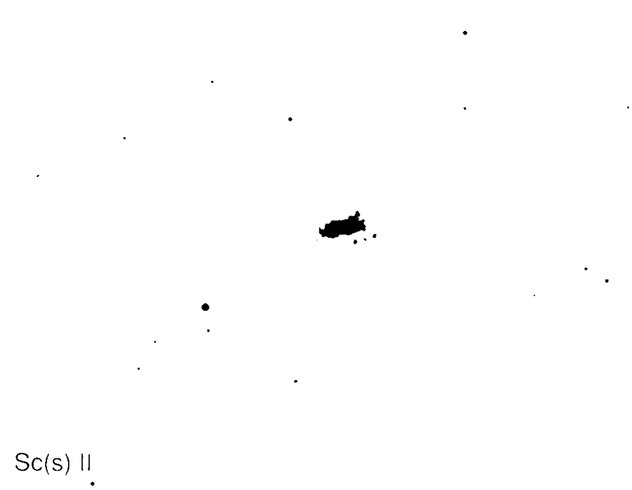

Sc(s) II

NGC 4633 + 4634

Scd(s)
Sc(on edge)

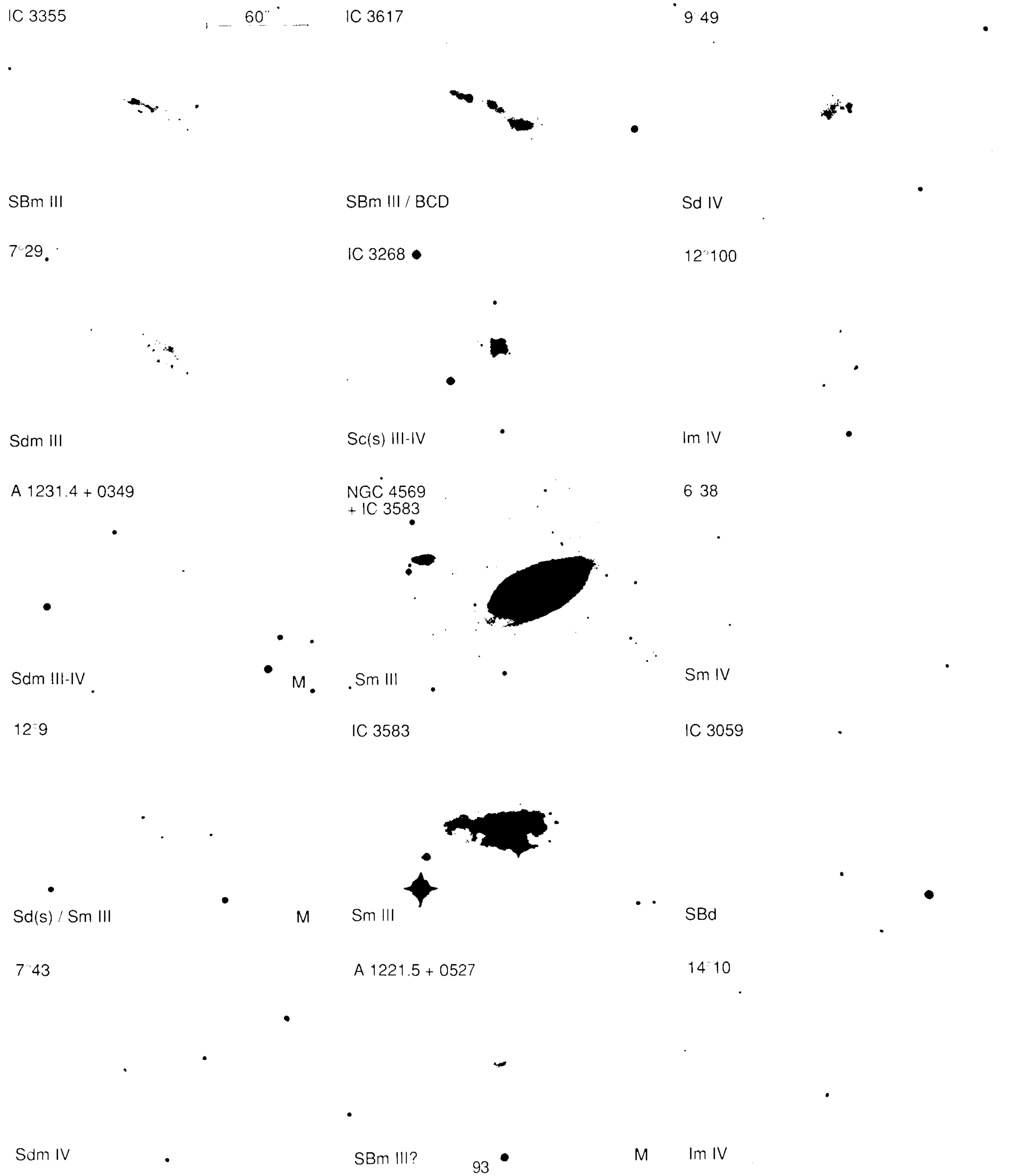
IC 3355
60''
SBm III
IC 3617
SBm III / BCD
9°49
Sd IV
7°29
Sdm III
IC 3268
Sc(s) III-IV
12°100
Im IV
A 1231.4 + 0349
Sdm III-IV
M
NGC 4569
+ IC 3583
Sm III
6°38
Sm IV
12°9
Sd(s) / Sm III
M
IC 3583
Sm III
IC 3059
SBd
7°43
Sdm IV
A 1221.5 + 0527
SBm III?
M
14°10
Im IV

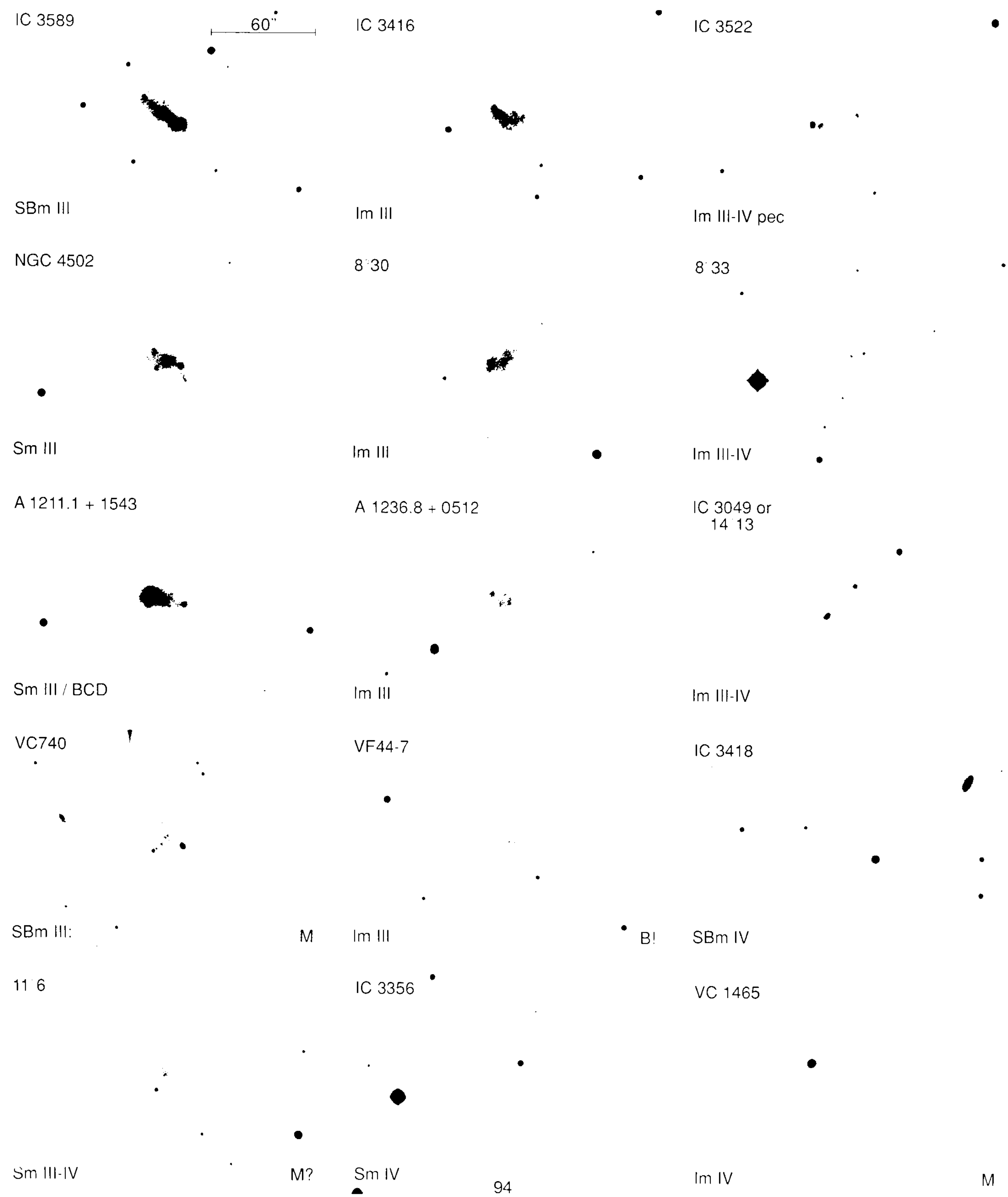
IC 3589
60"
SBm III
IC 3416
Im III
IC 3522
Im III-IV pec
NGC 4502
Sm III
8'30
Im III
8'33
Im III-IV
A 1211.1 + 1543
Sm III / BCD
A 1236.8 + 0512
Im III
IC 3049 or
14 13
Im III-IV
VC740
SBm III:
M
VF44-7
Im III
B!
IC 3418
SBm IV
11 6
Sm III-IV
M?
IC 3356
Sm IV
VC 1465
Im IV
M

A 1223.1 + 0226 (60")	14°31	IC 3475
Im IV M	Im? M?	Im IV or dE2
VC 260	13°29	A 1235.1 + 0850
Im IV	Im IV	Sm III / BCD
10°69	8°20	IC 3239
Im IV	Im IV-V	Sm III
VC 1468	9°4	IC 3412
Im IV M?	Im IV-V	Im III / BCD
10°22	11°34	10°71
Im IV, N?	Im IV-V:	Im III / BCD